4-15-2013 12:00 AM

Characterizing the contribution of the LXCXE binding cleft to pRB-mediated genome stability and tumor suppression

Courtney H. Coschi
The University of Western Ontario

Supervisor
Dr. Frederick A Dick
The University of Western Ontario

Graduate Program in Biochemistry
A thesis submitted in partial fulfillment of the requirements for the degree in Doctor of Philosophy

CHARACTERIZING THE CONTRIBUTION OF THE LXCXE BINDING CLEFT TO pRB-MEDIATED GENOME STABILITY AND TUMOR SUPPRESSION

Thesis format: Integrated Article

by

Courtney Heather Coschi

Graduate Program in Biochemistry

A thesis submitted in partial fulfillment
of the requirements for the degree of
Doctor of Philosophy

The School of Graduate and Postdoctoral Studies
The University of Western Ontario
London, Ontario, Canada

Abstract

Condensation and segregation of mitotic chromosomes are critical processes for cellular propagation and if compromised, can lead to genomic instability. Genomic instability is known to be an active contributor to tumorigenesis, rather than being a by-product of malignant progression. The retinoblastoma protein (pRB) is the prototypic tumor suppressor. Its tumor suppressive properties are linked to its ability to negatively regulate proliferation by inhibiting E2F target gene transcription. Using a gene targeted mouse model defective for interactions mediated by the pRB LXCXE binding cleft that is distinct from E2F binding ($Rb1^{\Delta L/\Delta L}$), I have demonstrated that LXCXE-interactions are an essential part of pRB-mediated tumor suppression. When these interactions are disrupted, cells exhibit chromosome condensation and mitotic defects that are unrelated to G1 to S-phase regulation by pRB. These defects contribute to earlier tumor formation and more aggressive pathology in $Trp53^{+/-}$ and $Trp53^{-/-}$ mouse models, revealing a new mechanism of tumor suppression, facilitated by pRB, whereby genome stability is maintained by the proper condensation of mitotic chromosomes. Subsequent study of the mechanism by which pRB facilitates genome stability suggests that a pRB-E2F1-Condensin II complex localizes to pericentromeric heterochromatin. In the absence of this complex, DNA double strand breaks are observed and persist into mitosis and the ensuing G1 phase of the cell division cycle. Moreover, haploinsufficiency of *Rb1* was enough to compromise loading of Condensin II at pericentromeric DNA and elicit the same defects. Significantly, $RB1^{+/-}$ fibroblasts from retinoblastoma patients also exhibit DNA damage and mitotic errors. And, in cancers of mesenchymal origin, $RB1^{+/-}$ cells exhibit as much genomic instability as $RB1^{-/-}$ cells. Finally, haploinsufficiency of the LXCXE binding cleft of pRB compromises pRB-mediated tumor suppression, resulting in tumors with increased chromosome gains and losses, comparable to $Rb1^{\Delta L/\Delta L}$ mutant mice. The data presented in this thesis change our understanding of the importance of genome stability as a tumor suppressive mechanism of the retinoblastoma protein and contrary to traditional thought, suggests that haploinsufficiency of *RB1* functionally contributes to tumorigenesis in humans.

Keywords

Retinoblastoma protein, E2F1, cancer, LXCXE, haploinsufficiency, genomic instability, condensin, replication, centromere.

Co-Authorship Statement

All Chapters were written by Courtney Coschi and edited by Dr. Fred Dick, with the exception of Chapter 2, which was written by Dr. Fred Dick and edited by Courtney Coschi.

All experiments in Chapter 2 were performed by Courtney Coschi with the exception of Figures 2.5, 2.6A, 2.8A, Table 2.2, and Appendix F-A, -B and -C, which were performed by Alison Martens, and Appendix E which was performed by Sarah Francis. Pathology review was provided by Dr. Subrata Chakrabarti. References to figures are modified from the original publication to fit formatting for this thesis.

All experiments in Chapter 3 were performed by Courtney Coschi with the exception of Figure 3.16A and Appendix K which were aided by Alison Martens. ChIP DNA for the experiment in Figure 3.7Ai was provided by Srikanth Talluri. Pathology review was provided by Dr. Ian Welch.

Dedication

For my Mom, the bravest person I know.
And for my Dad, whom I miss every day.

Acknowledgements

To my supervisor Dr. Fred Dick: I told you when I first interviewed with you that I wanted to learn how to think. Both you and this experience have certainly taught me how to do just that. You have also given me advice to apply not only in the lab, but in life as well, and I am grateful for it. Thank you for being an inspiring mentor, for challenging me to pursue research at the highest level, and for supporting me in my future endeavors.

Thank you to Dr. David Rodenhiser and Dr. Nathalie Bérubé, members of my advisory committee, for providing me with guidance, constructive criticism and thought provoking discussions over the years. Thank you as well to my examiners, Dr. Mellissa Mann, Dr. Dave Edgell, Dr. Kathleen Hill and Dr. Peter Whyte, for your probing questions, helpful critiques, and suggestions in the preparation of this final thesis.

To my fellow lab mates: thank you for being my family away from home, for commiserating with me, and celebrating with me. In your own way, each of you has made grad school an enjoyable and memorable experience. Thank you as well to my circle of friends both in and out of the lab, as well as old friends and those whom I met during grad school. You've given me unforgettable memories that I will always cherish. My life wouldn't be the same without each of you.

Finally, thank you to my family for your unconditional love and support. You were my reprieve from the lab when I needed it, and you were also my biggest champions; you have shaped who I am today. Lastly, and most importantly, thank you to my husband. You are my closest confidant and my best friend. Only you have seen everything that grad school and life has thrown at me. Thank you for being everything that I've needed, when I needed it. I couldn't have made it through grad school without your continued love, support and encouragement.

Abbreviations

^{o}C: degrees Celsius

α: anti

γH2AX: phosphorylation at serine 139 of the H2A variant H2AX

Δ: lacking

ΔL: ΔLXCXE

µg: microgram

µL: microliter

µm: micron

χ^2: chi squared test

129/B6: mouse with a mixed genetic background of 129 and C57BL/6

A: adenine (when referring to the nucleotide)

A: alanine (when referring to the amino acid)

aCGH: array comparative genomic hybridization

ADP: adenosine diphosphate

APC/C: anaphase promoting complex/ cyclosome

APC: Adenomatous polyposis coli protein

ATP: adenosine triphosphate

BAC: bacteria artificial chromosome

BCA: bicinchoninic acid

bp: base pair

BRCA1: breast cancer 1, early onset

BRCA2: breast cancer 2, early onset

BrdU: 5-bromo-2'-deoxyuridine

BRG1: Brahma-related gene 1

Brm: Brahma protein

BSA: bovine serum albumin

BubR1: budding uninhibited by benzimidazoles related 1

C > T: C to T transition

C: cortex (in Appendix F)

C: cytosine (when referring to the nucleotide)

***C. elegans*:** *Caenorhabditis elegans*

CAP- D2, D3, G, G2, H, H2: chromosome associated protein D2, D3, G, G2, H and H2 respectively

CD4: cluster of differentiation 4

CD8: cluster of differentiation 8

CDK: cyclin dependent kinase

CENPA: centromere protein A

ChIP: chromatin immunoprecipitation

CIN: chromosome instability

CIP: CDK interacting protein

CKI: cyclin dependent kinase inhibitor

c-myc: cellular-myelocytomatosis

CO_2: carbon dioxide

Abbreviations Continued

COSMIC: catalogue of somatic mutations in cancer

CRF: chromatin regulatory factor

C-terminal: carboxy terminal

DAPI: 4',6-Diamidino-2-Phenylindole

DBD: DNA binding domain

dCAP-D3: *Drosophila* CAP-D3

DHFR: dihydrofolate reductase

DMEM: Dulbecco's Modified Eagle Medium

DMZ: dimerization domain

DNA: deoxyribonucleic acid

DNMT1: DNA (cytosine-5-)-methyl transferase 1

dNTP: deoxyribonucleotide triphosphate

DP: Differentiation Related Transcription Factor-1 polypeptide-1

DREAM: DP, RB-like, E2F and MuvB

***Drosophila*:** *Drosophila melanogaster*

dsDNA: double stranded DNA

dup A: duplication of A

E: Embryonic day

E1A: early region 1A

E2F: E2 promoter binding factor

***E2f1*:** gene encoding the protein E2F1

E3: ubiquitin-protein ligase

E7: early protein 7

ELISA: enzyme-linked immune sorbent assay

Emi: early mitotic inhibitor 1

ESC: Embryonic stem cell

F: female

FBS: fetal bovine serum

FISH: fluorescence *in situ* hybridization

FITC: fluoresceini-sothiocyanat

G > C: G to C transversion

G > T: G to T transversion

G: guanine (when referring to the nucleotide)

G0: quiescence

G1: gap 1 phase of the cell division cycle

G2: gap 2 phase of the cell division cycle

GFP: green fluorescent protein

Glu: glutamic acid

GST: glutathione S-transferase

H&E: hematoxylin and eosin staining

H2A: histone 2A

H2B: histone 2B

H2BGFP: histone 2B tagged with GFP

Abbreviations Continued

H3: histone 3

H3-K9: histone 3- lysine 9 residue

H4: histone 4

H4-K20: histone 4- lysine 20 residue

HAT: histone acetyl transferase

hCAP-D3: human CAP-D3

HCl: hydrochloric acid

HDAC1/2: histone deacetylase 1 or 2

HEAT: huntington, elongation factor 3, protein phosphatase 2A, TOR1; four proteins that contain the HEAT repeat domain

hRAD21: double strand break repair protein rad21 homolog (*S. pombe*)

hSWI/SNF: human switch/sucrose nonfermentable

I: isoleucine

IB: immunoblot

IF: immunofluorescence

IgG: immunoglobulin G

IN: input

INK4: inhibitor of cyclin dependent kinase 4

IP: immunoprecipitation

kDa: kilodalton

KIP: kinase inhibitory protein

LacZ*α*: the alpha fragment of one β-galactosidase monomer

LOH: loss of heterozygosity

Luc: luciferase

LXCXE: leucine-any amino acid-cysteine-any amino acid-glutamate

M: male (in Appendices H and K)

M: medulla (in Appendix F)

M: methionine (when referring to the amino acid)

M: mitosis (when referring to the phases of the cell division cycle)

Mad2: mitotic arrest deficient 2

MB: marked box (in Figure 1.2)

MB: megabase

MCM7: minichromosome maintenance complex component 7

MEF: mouse embryonic fibroblast

$MgCl_2$: magnesium chloride

min: minutes

mL: milliliter

N: asparagine (when referring to the amino acid)

N: haploid ploidy (when referring to ploidy and DNA content)

N: normal (when referring to HCl concentration in Appendix O)

Abbreviations Continued

N or n: n-value (the number of samples)

N/A: not applicable

NES: nuclear export signal

ng: nanogram

NLS: nuclear localization signal

NS: not significant

N-terminal: amino terminal

(P): phosphorylation

***P*:** p value (estimated probability of rejecting the null hypothesis)

p107: protein encoded by *RBL1*

p130: protein encoded by *RBL2*

$p21^{CIP1}$: cyclin dependent kinase inhibitor 1

$p27^{KIP1}$: cyclin dependent kinase inhibitor 1B

p53: human and mouse *Tp53*/*Trp53* gene product

PARP: poly (ADP-ribose) polymerase

PBS: phosphate buffered saline

PBS-T: phosphate buffered saline-tween

PCNA: proliferating nuclear cell antigen

PCR: polymerase chain reaction

PGK: phosphoglycerate kinase

Plk1: polo-like kinase 1

PP1: protein phosphatase 1

PP2A: protein phosphatase 2A

pRB: retinoblastoma tumor suppressor protein

Pro: proline

q14: giemsa band 14 on the q arm of a chromosome

R or Arg: arginine

R654W: arginine to tryptophan missense mutation at residue 654

R661W: arginine to tryptophan missense mutation at residue 661

Ras: rat sarcoma

***RB1*:** human retinoblastoma tumor suppressor gene

***Rb1*:** mouse retinoblastoma tumor suppressor gene

***rbf1*:** *Drosophila* pRB family homolog (gene)

RBF1: *Drosophila* pRB family homolog (protein)

***RBL1*:** human retinoblastoma like 1 (gene)

***RBL2*:** human retinoblastoma like 2 (gene)

rDNA: ribosomal DNA

res: residue

RNA: ribonucleic acid

RNAi: RNA interference

RPA: replication protein A

Abbreviations Continued

S: DNA synthesis phase of the cell division cycle

***S. cerevisiae*:** *Saccharomyces cerevisiae*

***S. pombe*:** *Schizosaccharomyces pombe*

Scc2: sister chromatid cohesion protein 2

S-CIN: segmental chromosome instability

SDS-PAGE: sodium dodecyl sulfate polyacrylamide gel electrophoresis

sh: short hairpin

SMC: structural maintenance of chromosomes

SMC1, 2, 3, 4: structural maintenance of chromosomes protein 1, 2, 3 and 4 respectively

SP1: specificity protein 1

SSC: saline sodium citrate

Suv39h1: suppressor of variegation 3-9 homolog 1

T cell: lymphocyte maturing in the thymus

T: thymine

TA: transactivation domain

TAg: large T antigen

Taq: *Thermus aquaticus*

TCEP: tris (2-carboxyethyl) phosphine

TCR: T cell receptor

TGF-β: transforming growth factor β

***Tp53*:** human tumor protein 53 gene

tRNA: transfer RNA

***Trp53*:** mouse transformation-related protein 53 gene

Ub: ubiquitin

UV: ultraviolet

V(D)J: variable, diverse, joining gene recombination

W: tryptophan

WB: western blot

WCE: whole cell extract

W-CIN: whole chromosome instability

X: stop codon

Table of Contents

Abstract ii

Key Words ii

Co-Authorship Statement iiv

Dedication v

Acknowledgments vi

Abbreviations vii

Table of Contents xii

List of Tables xvi

List of Figures xviii

List of Appendices xx

Chapter 1 1

1 Introduction 1

1.1 The history of retinoblastoma and the retinoblastoma protein 1

1.1.1 Retinoblastoma and the discovery of the retinoblastoma protein 1

1.1.2 The retinoblastoma protein is a regulator of the cell division cycle 3

1.1.3 The pocket protein family 4

1.1.4 The current model of proliferative control by pocket proteins 6

1.1.5 pRB is unique among pocket proteins 10

1.2 Mouse models of *Rb1* 13

1.2.1 *Rb1* is dispensible for embryogenesis 13

1.2.2 A structure-function approach to investigating pRB's contribution to tumor suppression 14

1.3 The $Rb1^{\Delta L/\Delta L}$ mouse 17

1.3.1 The LXCXE binding cleft 17

1.3.2 *Rb1*$^{\Delta L/\Delta L}$ MEFs exhibit phenotypes independent of G1 to S-phase transition regulation 18

1.3.3 The *Rb1*$^{\Delta L/\Delta L}$ mouse exhibits no over tumor-suppressive phenotype 20

1.3.4 A non-canonical role for the LXCXE binding cleft of pRB 21

1.4 Condensins 21

1.4.1 The structural maintenance of chromosomes (SMC) family of complexes are integral for chromosome dynamics 21

1.4.2 Condensin I and Condensin II differentially contribute to mitotic chromosomes 24

1.4.3 Condensin II contributes to functions outside of mitotic chromosome condensation 27

1.4.4 Subunits of the Condensin complexes are mutated in cancer 28

1.5 Genomic instability 30

1.5.1 Types of genomic instability 30

1.5.2 Genomic instability in cancer 30

1.5.3 pRB and genomic instability 32

1.6 Objectives 34

1.7 References 35

Chapter 2 58

2 Mitotic chromosome condensation mediated by the retinoblastoma protein is tumor suppressive 58

2.1 Abstract 58

2.2 Introduction 58

2.3 Methods 61

2.3.1 Cell culture, viral infections and microscopy 61

2.3.2 Antibodies and protein detection 62

2.3.3 Mice 63

2.3.4 Thymic development 64

2.3.5 PCR, Southern blotting and aCGH 64

2.4 Results 65

2.4.1 Aberrant chromosome condensation and segregation in *Rb1*$^{\Delta L/\Delta L}$ mutant cells 65

2.4.2 The *Rb1*$^{\Delta L/\Delta L}$ mutation exacerbates tumorigenesis in *Trp53*$^{-/-}$ mice 74

2.4.3 Accelerated loss of heterozygosity in *Rb1*$^{\Delta L/\Delta L}$ mice 81

2.5 Discussion 84

2.6 References 86

Chapter 3 92

3 Haploinsufficiency of a pRB-E2F1-Condensin II complex causes genome instability and contributes to mesenchymal cancers 92

3.1 Abstract 92

3.2 Introduction 92

3.3 Methods 96

3.3.1 Cell culture, viral infections and microscopy 96

3.3.2 Antibodies and protein detection 97

3.3.3 GST pulldowns 98

3.3.4 Fluorescence *in situ* hybridization and immunofluorescence 98

3.3.5 Chromatin immunoprecipitation and real time PCR analysis 99

3.3.6 Tumor incidence in mice 99

3.3.7 PCR genotyping and array comparative genomic hybridization 100

3.3.8 Mutation detection in *RB1* patient fibroblasts 101

3.3.9 Analysis of instability in cancer cell lines 101

3.4 Results 101

3.4.1 Loss of *Rb1* causes double strand breaks at the centromere 101

3.4.2 E2F1, pRB and Condensin II form a complex at pericentromeric heterochromatin 110

3.4.3 DNA damage and recruitment of Condensin II to chromatin in *Rb1* gene dosage-dependent 112

3.4.4 Human *RB1*$^{+/-}$ cells exhibit DNA double strand breaks, mitotic defects and genomic instability 119

3.4.5 Haploinsufficiency of Rb1 compromises pRB-mediated tumor suppression 128

3.5 Discussion 132

3.6 References 134

Chapter 4 141

4 Discussion 141

4.1 A new model for pRB-mediated tumor suppression 141

4.2 Revisiting *RB1* haploinsufficiency 142

4.3 Impact on human cancer and cancer therapies 143

4.4 Remaining questions 145

4.5 Summary of findings 147

References 149

Appendices 156

Curriculum Vitae 166

List of Tables

Table 2.1: Summary of mitotic phenotypes observed in video microscopy experiments 70

Table 2.2: Summary of pathology from mice used in this study 76

Table 3.1: Summary of mitotic phenotypes observed in *Rb1* mutant MEF video microscopy experiments 114

Table 3.2: Summary of mitotic phenotypes observed in *Rb1*-ΔL mutant MEF video microscopy experiments 116

Table 3.3: Summary of sequencing results of retinoblastoma patient fibroblasts 120

Table 3.4: Summary of mitotic phenotypes observed in retinoblastoma patient fibroblast video microscopy experiments 123

Table 3.5: Summary of pathology from mice used in this study 130

List of Figures

Figure 1.1: There are multiple ways to acquire retinoblastoma 2

Figure 1.2: Structures of the pocket protein and E2F families of proteins 5

Figure 1.3: The current model of proliferative control by pocket proteins 7

Figure 1.4: Pocket proteins are differentially expressed during the cell division cycle 8

Figure 1.5: The pocket protein regulatory pathway 11

Figure 1.6: Spectrum of mutations of *RB1* in retinoblastoma patients 16

Figure 1.7: Disruption of protein-interaction sites on the retinoblastoma protein 19

Figure 1.8: Cohesin, Condensin I and Condensin II are complexes of the structural maintenance of chromosome (SMC) family 23

Figure 1.9: The SMC proteins are key chromosomal components for mitosis 25

Figure 2.1: $Rb1^{\Delta L/\Delta L}$ cells display centromere fusions 67

Figure 2.2: $Rb1^{\Delta L/\Delta L}$ cells display aberrant chromosome condensation and segregation 69

Figure 2.3: Defective loading of Condensin II complexes on $Rb1^{\Delta L/\Delta L}$ chromosomes 71

Figure 2.4: Mitotic phenotypes of CAP-D3 knock down MEFs mimic condensation and segregation defects in $Rb1^{\Delta L/\Delta L}$ MEFs 73

Figure 2.5: More aggressive tumors in $Rb1^{\Delta L/\Delta L}$; $Trp53^{-/-}$ mice 75

Figure 2.6: Non-bias selection of thymic lymphomas for subsequent analysis 79

Figure 2.7: Increased genomic instability in $Rb1^{\Delta L/\Delta L}$; $Trp53^{-/-}$ thymic lymphomas 80

Figure 2.8: Accelerated loss of heterozygosity in $Rb1^{\Delta L/\Delta L}$; $Trp53^{+/-}$ mice 83

Figure 3.1: *Rb1* homozygous mutant MEFs exhibit increased DNA double strand breaks 103

Figure 3.2: *Rb1* homozygous mutant MEFs accumulate DNA double strand breaks at pericentromeric DNA 104

Figure 3.3: Condensin II complex defective MEFs exhibit increased DNA double strand breaks 106

Figure 3.4: Condensin II complex defective MEFs accumulate DNA double strand breaks in pericentromeric regions of the genome 107

Figure 3.5: DNA damage in *Rb1* homozygous mutant MEFs and Condensin II complex defective MEFs persist into mitosis 108

Figure 3.6: $Rb1^{\Delta L/\Delta L}$ MEFs accumulate DNA damage in G1 109

Figure 3.7: pRB, E2F1 and Condensin II interact at pericentromeric heterochromatin 111

Figure 3.8: *Rb1* heterozygous mutants exhibit mitotic defects 113

Figure 3.9: DNA damage and recruitment of Condensin II is *Rb1* gene dosage-dependent 117

Figure 3.10: $Rb1^{\Delta L/+}$ MEFs accumulate DNA damage in G1 118

Figure 3.11: Retinoblastoma patient fibroblasts ($RB1^{+/-}$) exhibit increased DNA double strand breaks 121

Figure 3.12: Retinoblastoma patient fibroblasts ($RB1^{+/-}$) exhibit mitotic defects 122

Figure 3.13: Criteria for determining genome instability using copy number data from the COSMIC database 125

Figure 3.14: $RB1^{+/-}$ cancers exhibit as much genome instability as $RB1^{-/-}$ cancers 126

Figure 3.15: Verification of *RB1* genotype and functional pRB in mesenchymal cancer cell lines 127

Figure 3.16: Haploinsufficiency compromises pRB-mediated tumor suppression 129

Figure 3.17: Tumors from *Rb1*$^{\Delta L/+}$; *Trp53*$^{-/-}$ mice exhibit genomic instability..... 131

List of Appendices

Appendix A: Permission for publication by Cellular and Molecular Life Sciences..... 154

Appendix B: Permission for publication by Genes & Development..... 155

Appendix C: Investigation of chromosome fusions mediated by rDNA repeats..... 156

Appendix D: Equivalent, low level expression of H2B-GFP in *Rb1*$^{+/+}$ and *Rb1*$^{\Delta L/\Delta L}$ MEFs..... 157

Appendix E: *Rb1*$^{\Delta L/\Delta L}$ mice do not develop spontaneous tumors..... 158

Appendix F: Normal thymic development in *Rb1*$^{\Delta L/\Delta L}$ and *Rb1*$^{\Delta L/\Delta L}$; *Trp53*$^{-/-}$ mice..... 159

Appendix G: Some *Rb1*$^{\Delta L/\Delta L}$; *Trp53*$^{-/-}$ tumor DNA samples have an increased number of sub-chromosomal segment changes compared to controls..... 160

Appendix H: Histology and necropsy data of *Rb1*$^{\Delta L/\Delta L}$; *Trp53*$^{-/-}$, *Trp53*$^{-/-}$, *Rb1*$^{\Delta L/\Delta L}$; *Trp53*$^{+/-}$ and *Trp53*$^{+/-}$ mice in the Chapter 2 tumor study..... 161

Appendix I: Example of a whole chromosome loss from aCGH data..... 164

Appendix J: Example of a whole chromosome gain from aCGH data..... 165

Appendix K: Histology and necropsy data of *Rb1*$^{\Delta L/+}$; *Trp53*$^{-/-}$ mice in the Chapter 3 tumor study..... 166

Appendix L: List of plasmids..... 168

Appendix M: PCR conditions for genotyping..... 170

Appendix N: List of antibodies..... 171

Appendix O: Instructions for making and purifying anti-CAP-D3, -CAP-D2 and -SMC2 antibodies..... 173

Chapter 1

1 Introduction

1.1 The history of retinoblastoma and the retinoblastoma protein

1.1.1 Retinoblastoma and the discovery of the retinoblastoma protein

The childhood cancer retinoblastoma was first postulated to result from a dominant gene that arose by mutation and was selected against in normal individuals in the very generation in which it arose (Neel and Falls 1951). In essence, retinoblastoma was thought to be caused by an oncogene. However, careful study of the genetics of the disease revealed that it was loss of the q14 band on chromosome 13, and therefore loss of a tumor suppressive function, that was the source of retinoblastoma (Sparkes *et al* 1980, Sparkes *et al* 1983, Vogel 1979, Yunis and Ramsay 1978 among others). Finally, in 1986, the retinoblastoma gene was cloned through positional mapping and shown to be deleted in retinoblastomas and also osteosarcomas (Friend *et al* 1986).

Retinoblastoma can be inherited (germinal mutation) or can occur sporadically (somatic mutation) (Fig. 1.1; Falls and Neel 1951, Smith and Sorsby 1958, Schappert-Kimmijser *et al* 1966). In its inherited form, all cells in the developing foetus are hemizygous for the retinoblastoma gene (*RB1*), including germ cells. Patients with inherited retinoblastoma are often affected bilaterally (in both eyes), and a smaller proportion are affected unilaterally; rarely are these patients unaffected (Knudson 1971). If patients with inherited retinoblastoma survive, they pass the mutation on to approximately 50% of their offspring, consistent with Mendel's rule for dominant inheritance. Patients with non-inherited retinoblastoma acquire somatic mutations sequentially, leading to complete loss of *RB1* and retinoblastoma. These patients typically do not pass the mutation on to their offspring as the mutation is acquired in the somatic cells of the retina (Knudson 1971). In rare, non-inherited cases, the mutation is

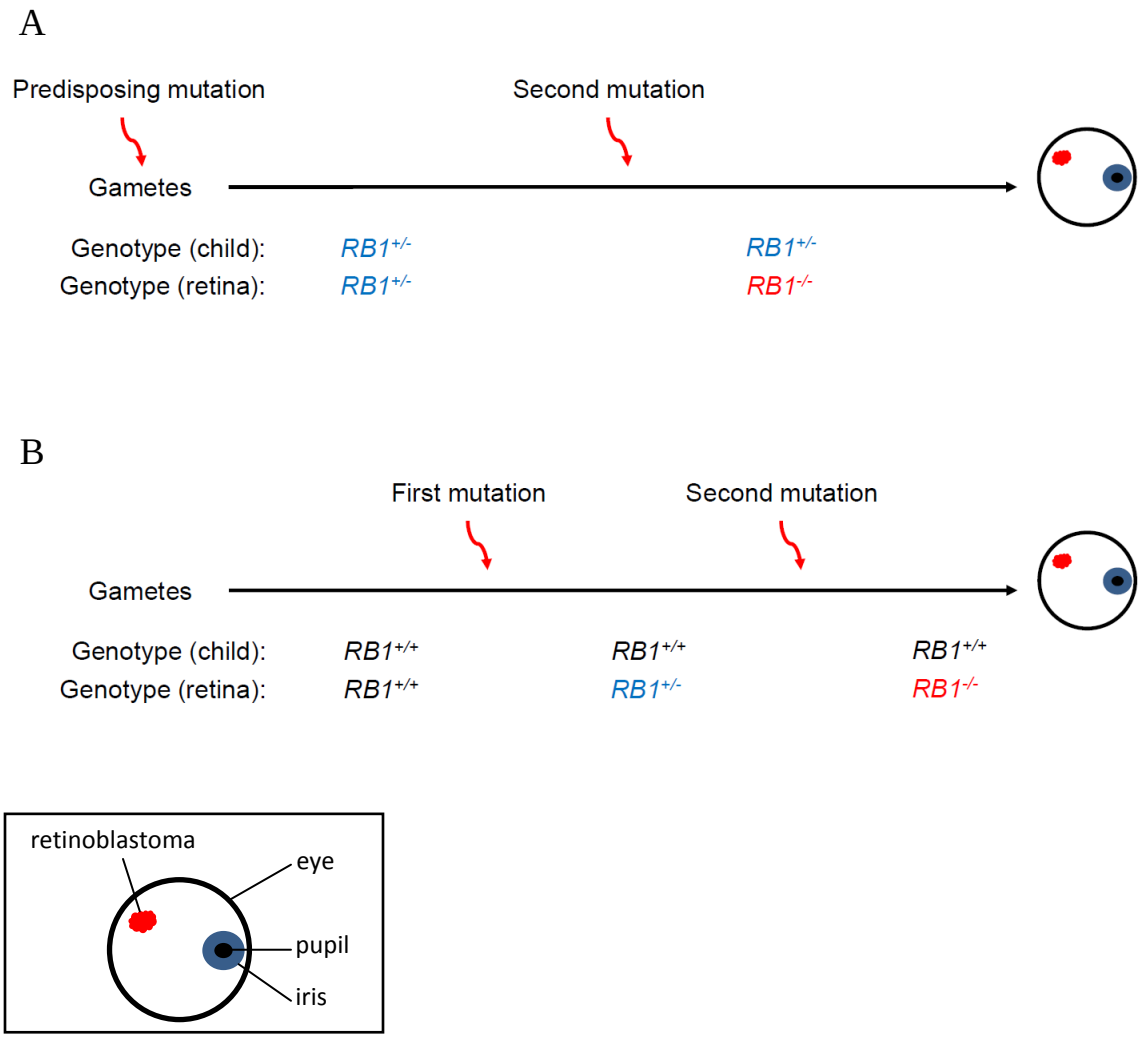

Figure 1.1: There are multiple ways to acquire retinoblastoma.

(A) Retinoblastoma can be inherited whereby one of the contributing gametes is *RB1*$^{-}$. All cells in the patient's body are subsequently hemizygous for *RB1*. A second somatic mutation in the retina results in retinoblastoma. **(B)** Retinoblastoma can occur sporadically, with two somatic hits in the retina often before three years of age. Retinoblastoma can also arise from a hit early in development, resulting in a patient wherein some cells have two wild type copies of *RB1*, and other cells have only one wild type copy of *RB1*, including those in the retina. A second somatic hit in the retina leads to retinoblastoma.

acquired early enough during embryogenesis that patients can pass the mutation on to their offspring.

In 1971, Knudson published a paper analyzing the mutation rate of *RB1* in both inherited and non-inherited retinoblastomas. He found that the mutation rate for loss of the first *RB1* gene in non-inherited cases, and the loss of the second *RB1* gene in both inherited and non-inherited cases was similar. From this study he proposed two key findings. The first is that retinoblastoma resulted from just two genetic events (germinal and somatic, or both somatic) resulting in loss of both copies of *RB1*. The second is that loss of the first *RB1* allele did not accelerate loss of the second *RB1* allele. Therefore hemizygosity of *RB1* did not create a haploinsufficiency, rather it recapitulated the wild type condition (Knudson 1971). As a result of this study, the retinoblastoma gene became known as the "prototypic tumor suppressor", in that its loss in retinoblastoma was the prototype to which other proposed tumor suppressor genes were compared (Murphree and Benedict 1984). To date, modeling *Rb1* loss in mouse models of cancer has supported Knudson's "two-hit" hypothesis (Jacks *et al* 1992, Vooijs *et al* 1998). However, data presented in this thesis suggest that certain aspects of pRB function exhibit haploinsufficiency when disrupted. In chapter three, I will discuss the applicability of extrapolating Knudson's hypothesis to other contexts of tumorigenesis.

1.1.2 The retinoblastoma protein is a regulator of the cell division cycle

Because loss of the retinoblastoma gene was found to be important for only a few tissues in hereditary cancer development (retina, bone), it was expected to have only a specialized role in these tissues. However, studies of the transforming activity of viral oncoproteins including the adenovirus E1A, simian virus 40 TAg and the human papilloma virus E7 oncoproteins, revealed that inactivation of the retinoblastoma protein (pRB) was required for transformation, suggesting that pRB might have a more broad tumor suppressive application (Whyte *et al* 1988, DeCaprio *et al* 1988, Dyson *et al* 1989).

Around the time of this discovery, loss of pRB function was found to be associated with loss of cellular proliferation control (Takahashi *et al* 1991, Bookstein *et al* 1990a, Huang *et al* 1988). For example, several studies demonstrated that adding back pRB to human cancer cells (bladder, prostate, osteosarcoma) significantly reduced their proliferative rate, their ability to form colonies in soft agar and reduced tumorigenicity in nude mice (Takahashi *et al* 1991, Bookstein *et al* 1990b, Huang *et al* 1988). Two regions, the "pocket" domain (res. 379-792) and the C-terminus of pRB (res. 793 – 928), were found to be responsible for its growth suppression properties (Fig. 1.2A; Qin *et al* 1992). These regions were also demonstrated to be required for pRB binding to the family of E2F transcription factors (Fig. 1.2B; Chellappan *et al* 1991, Bagchi *et al* 1991, Chittenden *et al* 1991, Bandara and La Thangue 1991).

The first human genes demonstrated to be regulated in an E2F dependent manner were c-myc and dihydrofolate reductase (DHFR), whose protein products are involved in cellular proliferation and DNA synthesis respectively (Hiebert *et al* 1989, Thalmeier *et al* 1989, Blake and Azizkhan 1989). Furthermore, these genes were shown to be regulated in a cell cycle-dependent manner (Hiebert *et al* 1989, Thalmeier *et al* 1989, Blake and Azizkhan 1989). In this way, a paradigm was formed in which the growth suppressive role of the retinoblastoma protein was mediated through inhibition of E2F target gene transcription, which in turn could be deregulated by viral oncoproteins (Nevins 1992). These and subsequent studies led to the understanding that pRB regulates the G1 to S-phase transition of the cell division cycle by binding to E2Fs and inhibiting E2F target gene transcription, and that this universal role for pRB in proliferation transcends all cell types (studies outlining this principle mechanism of cell cycle control are reviewed in Dyson 1998).

1.1.3 The pocket protein family

Based on sequence similarity and their ability to also be bound by viral oncoproteins, two other members of the pRB family were identified, *RBL1* and *RBL2*, producing the p107 and p130 proteins respectively (Fig. 1.2A; Ewen *et al* 1991, Zhu *et al* 1993, Mayol *et al* 1993, Cobrinik *et al* 1993, Li *et al* 1993, Hannon *et al* 1993). These proteins share many structural features including the "small pocket" region, which

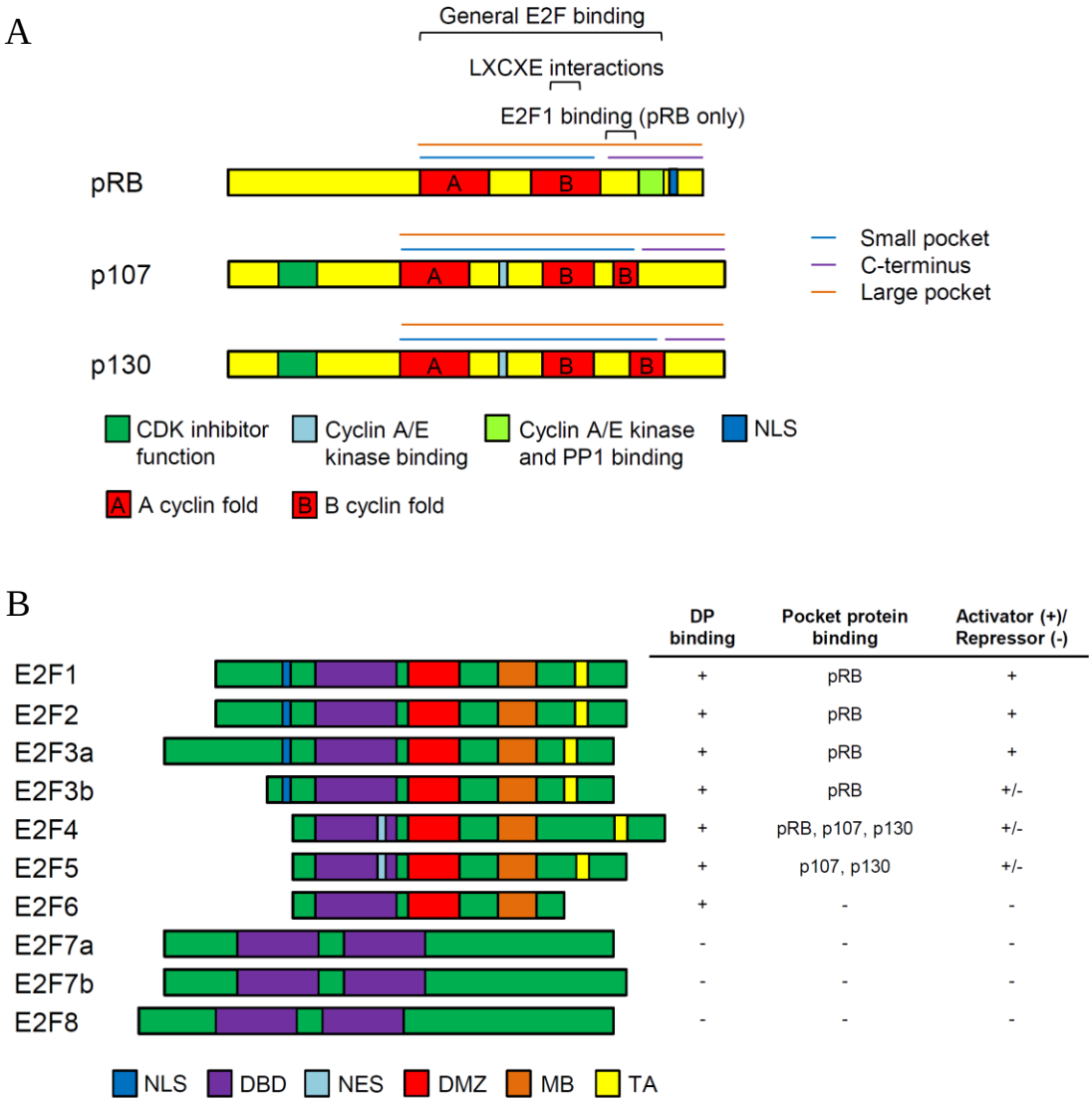

Figure 1.2: Structures of the pocket protein and E2F families of proteins.

(A) The pocket protein family is defined by the "small pocket" they all possess, into which viral oncoproteins bind. p107 and p130 are structurally more similar to each other than to pRB. CDK- cyclin-dependent kinase. NLS- nuclear localization signal. **(B)** The E2F family of transcription factors (E2Fs 1-8) mediate cell cycle advancement. E2Fs 1-6 heterodimerize with DP protein to bind to DNA. Activator E2Fs are bound by pRB, which prevents the transcription of genes required for S-phase progression. Repressor E2Fs either bind pRB, p107 or p130, or dimerize with atypical E2Fs (E2Fs 7 and 8) and recruit repressive complexes to DNA. NLS- nuclear localization signal. DBD- DNA binding domain. NES- nuclear export signal. DMZ- dimerization domain. MB- marked box. TA- transactivation domain. DP- Differentiation Related Transcription Factor-1 polypeptide-1.

is the most highly conserved region among the pocket protein family and across several species of pRB (Lee *et al* 1998). As these proteins all contain this "pocket domain", they are commonly called "pocket proteins". The small pocket contains an A and B domain, as well as a flexible linker that separates the two; each A and B domain contains a single cyclin fold, which interact to form the small pocket domain (Fig. 1.2A; Lee *et al* 1998). This small pocket is sufficient to repress transcription and interact with viral oncoproteins (Hu *et al* 1990, Sellers *et al* 1995, Chow and Dean 1996, Chow *et al* 1996). Crystallography has demonstrated that the LXCXE motif contained in viral oncoproteins makes contact with a shallow groove in the B domain of the small pocket (Fig. 1.2A; Lee *et al* 1998, Ewen *et al* 1989, Munger *et al* 1989, Whyte *et al* 1989, Dyson *et al* 1992). Indeed, several cellular proteins contain an LXCXE-like motif, or are otherwise able to bind in the LXCXE binding cleft, and thereby interact with the pocket protein family (summarized in Dick 2007). Many of the proteins that bind in the LXCXE binding cleft are chromatin remodeling proteins or components of complexes that have chromatin remodeling capabilities in order to effect transcriptional repression.

Pocket proteins also contain a C-terminal domain which, in conjunction with the small pocket, comprises the large pocket (Fig. 1.2A). As described above, this large pocket is the minimal growth suppressing domain and is sufficient to interact with the E2F family of transcription factors and inhibit E2F target gene transcription (Hiebert *et al* 1992, Qin *et al* 1992, Bremner *et al* 1995). Thus recruitment of pocket proteins by E2Fs to E2F target genes not only inhibits transactivation, but recruits transcriptionally repressive complexes to introduce histone modifications and further prevent E2F target gene transcription.

1.1.4 The current model of proliferative control by pocket proteins

pRB, p107 and p130 work in a concerted effort to mediate proliferative control (Fig. 1.3). This is aided by the differential expression and sub-cellular localization of pocket proteins during the cell division cycle, and their preference for binding to specific E2F transcription factors (Fig. 1-4, Fig. 1.2B).

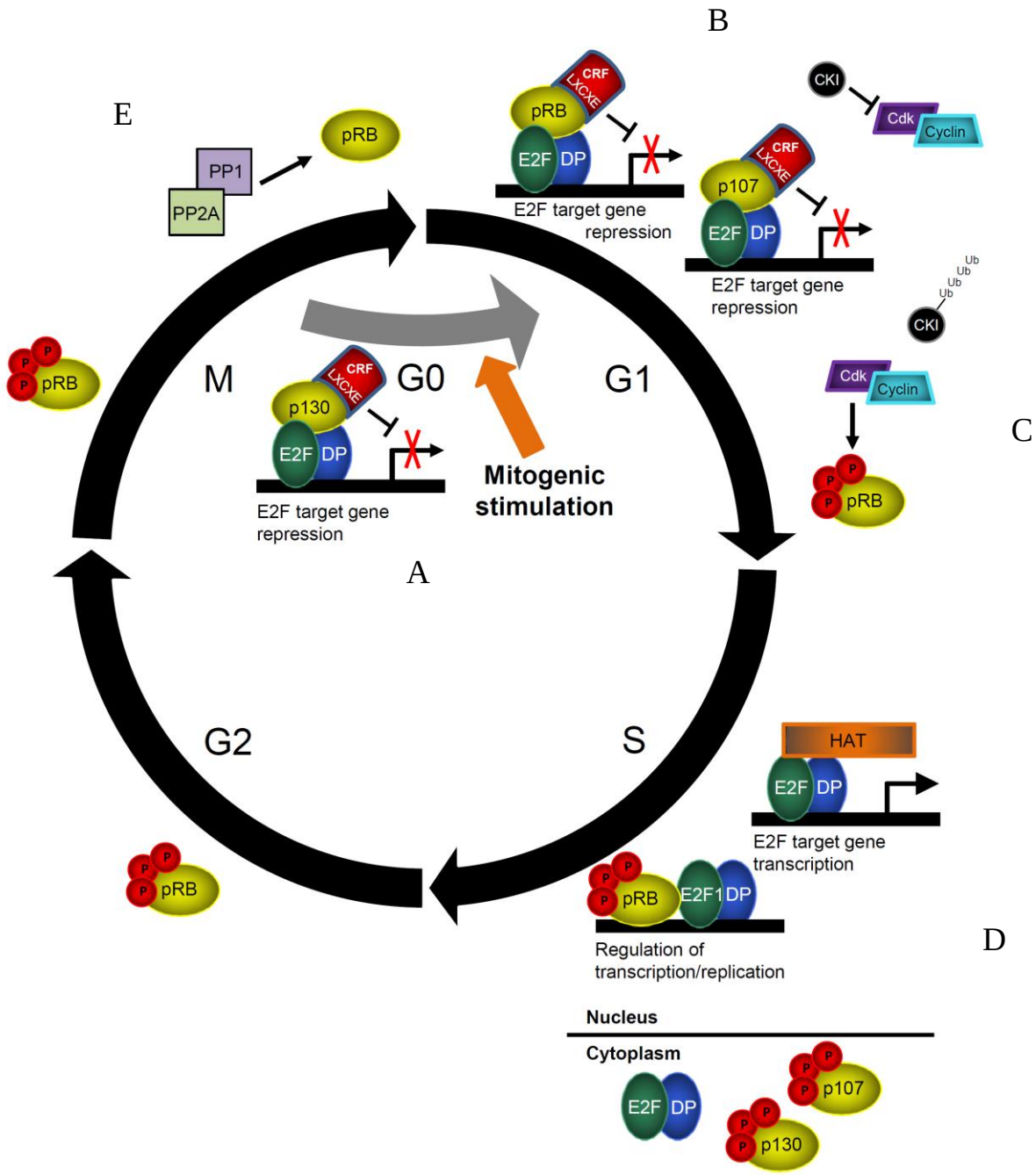

Figure 1.3: The current model of proliferative control by pocket proteins.

(A-B) Briefly, upon mitogenic stimulation, p107 replaces p130 at E2F target gene promoters and pRB-E2F complexes increase. CKIs inhibit the activity of cdks. **(C)** Upon a feed forward loop of increasing activity of cyclin-cdk complexes, pocket proteins become extensively hyperphosphorylated. **(D)** E2F target gene transcription occurs, and cells are committed to divide. p107 and p130 are exported from the nucleus and pRB can regulate the S-phase DNA damage checkpoint and DNA replication as needed. **(E)** At the end of mitosis, phosphatases PP1 and PP2A dephosphorylate pocket proteins.

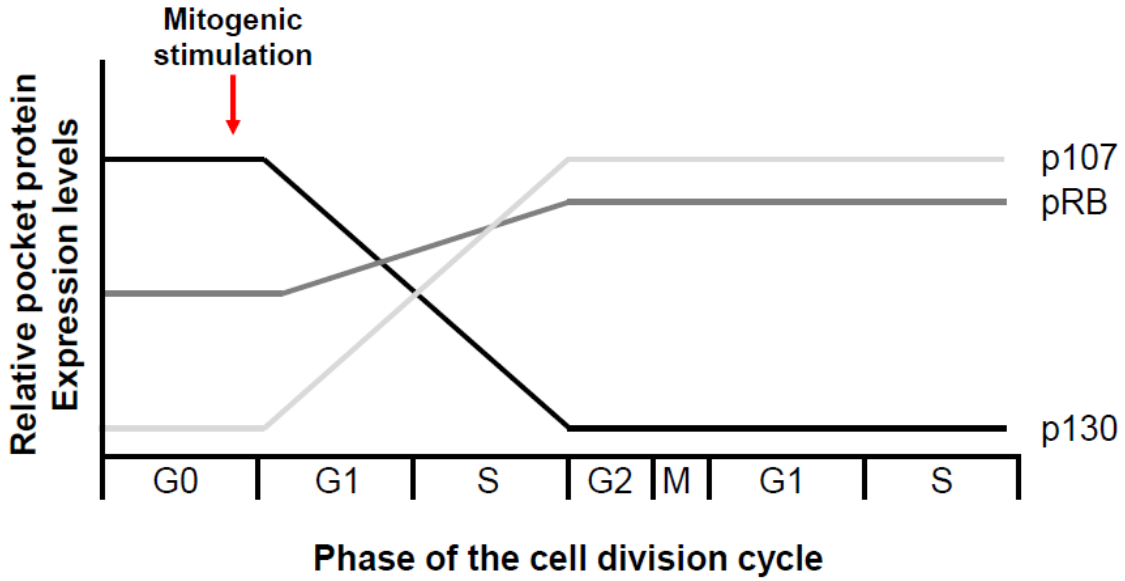

Figure 1.4: Pocket proteins are differentially expressed during the cell division cycle.

During quiescence (G0), p130 levels are high. p130 is found on chromatin bound to repressive E2Fs 4 and 5. pRB levels are moderate and p107 levels are negligible. Upon mitogenic stimulation, pRB and p107 levels rise and p130 levels decrease. p107 replaces p130 at E2F target genes and the amount of pRB-E2F complexes increases. As the cell cycle progresses, p107 and pRB levels peak and p130 levels are almost negligible. Levels then remain steady through the remainder of the cell division cycle and into the next cycle until cells re-enter quiescence (G0).

In brief, p130 binds to inhibitor E2Fs in G0 and recruits a transcriptionally repressive DREAM complex, mediating a reversible cell division cycle arrest called quiescence (Fig. 1.3A; Moburg *et al* 1996, Hurford *et al* 1997, Litovchick *et al* 2007). Upon mitogenic stimulation, cells enter G1 and p107 replaces p130 at E2F target genes (Takahashi *et al* 2000, Wells *et al* 2000). Expression of the retinoblastoma protein increases and pRB localizes to E2F target genes, inhibiting the transcriptional activity of activator E2Fs (Fig. 1.3B). This is mediated both by physically masking their transactivation domain, and by recruiting repressive chromatin remodeling complexes *via* the LXCXE binding cleft (Hiebert *et al* 1992, Schwarz *et al* 1993, Shirodkar *et al* 1992, Helin *et al* 1993, Flemington *et al* 1993, Zamanian and La Thangue1993).

E2F target genes that are regulated by pocket proteins include positive regulators of the cell division cycle and replication machinery, therefore E2F target gene transcription must be activated to progress from G1 into S-phase of the cell division cycle (Hurford *et al* 1997, Lavia and Jansen-Durr 1999, Takahashi *et al* 2000, Williams *et al* 2006). Activation of E2Fs is mediated by phosphorylation of pocket proteins in a cell cycle-dependent manner by cyclin/cyclin-dependent kinase (cdk) complexes (DeCaprio *et al* 1989, Sherr and Roberts 1999). This releases pocket proteins from binding to E2Fs allowing them to transactivate their target genes (Fig. 1.3C; Mudryj *et al* 1991, Chittenden *et al* 1993). The activation of cyclin/cdk complexes occurs in a feed-forward loop that is antagonized by cdk inhibitors (CKIs) (Fig. 1.3B; Sherr and Roberts 1999, Mittnacht 1998, Besson *et al* 2008). As a result of the cyclin-cdk feed forward loop that maximizes phosphorylation of pRB and inhibition of CKIs, cells are committed to irreversibly advance into S-phase.

At the end of mitosis, pocket proteins are dephosphorylated and once again bind to E2Fs and negatively regulate entry into the next cell division cycle. Protein phosphatases 1 and 2 are proposed to dephosphorylate either pRB or all pocket proteins respectively (Fig. 1.3E; Nelson *et al* 1997, Yan *et al* 1999, Dunaief *et al* 2002, Garriga *et al* 2004). Alternatively, pocket proteins are responsible for mediating the permanent cell cycle exit paradigms of both senescence and differentiation (Bruce *et al* 2000, Campisi and di Fagagna 2007, Sage *et al* 2003, Zhang *et al* 2007, Funayama *et al* 2006, Sage *et al*

2000, Dannenberg *et al* 2000, Peeper *et al* 2001, Gutierrez *et al* 2008, Berman *et al* 2008, Corbeil *et al* 1995, Zaksenhaus *et al* 1996, De Falco *et al* 2006, Korenjak and Brehm 2005, Herwig and Strauss 1997, Sellers *et al* 1998, Lee *et al* 1999, Thomas *et al* 2001 Nguyen and McCance 2005). The above discussion of the cell division cycle by pocket proteins is summarized in Figure 1.5.

It is clear that together, the pocket proteins are integral in mediating cell division cycle control, and permanent cell cycle arrest. These functions are tumor suppressive as in many human cancers, the activity of pocket proteins are disrupted (Sherr 1996). While deregulated cdks and CKIs lead to the inactivation of all pocket proteins, selective mutation of only the retinoblastoma protein in many human cancers distinguishes it from p107 and p130 (Harbour *et al* 1988, Horowitz *et al* 1989, Lee *et al* 1988, Malumbres and Barbacid 2001, Sherr 1996).

1.1.5 pRB is unique among pocket proteins

During S-phase, the retinoblastoma protein remains in the nucleus and has been proposed to be important for mediating cell cycle arrest and facilitating repair upon DNA damage by repressing E2F target gene transcription and suppressing further DNA synthesis (Fig. 1.3D; Knudsen *et al* 2000, Sever-Chroneos *et al* 2001, Wells *et al* 2003, Avni *et al* 2003). It is able to do so as its dephosphorylation can be induced upon DNA damage, followed by acetylation to inhibit subsequent hyperphosphorylation. The retinoblastoma protein can therefore remain active despite high levels of cdk activity to mediate this S-phase DNA damage checkpoint (Fig. 1.3D; Avni *et al* 2003, Markham *et al* 2006, Chan *et al* 2001).

pRB has also been indirectly implicated in events during mitosis. Certain E2F target genes including Emi, Mad2 and BubR1 are required for maintaining the mitotic checkpoint, preventing progression through mitosis if chromosomes are not properly attached to the mitotic spindle and lined up at the metaphase plate. If pRB is unable to repress transcription of these genes, their overexpression compromises mitosis, delaying its progression and resulting in aneuploidy (Hernando *et al* 2004, Margottin-Goguet *et al* 2003). As well, cells lacking pRB are more prone to re-replicate their DNA after they

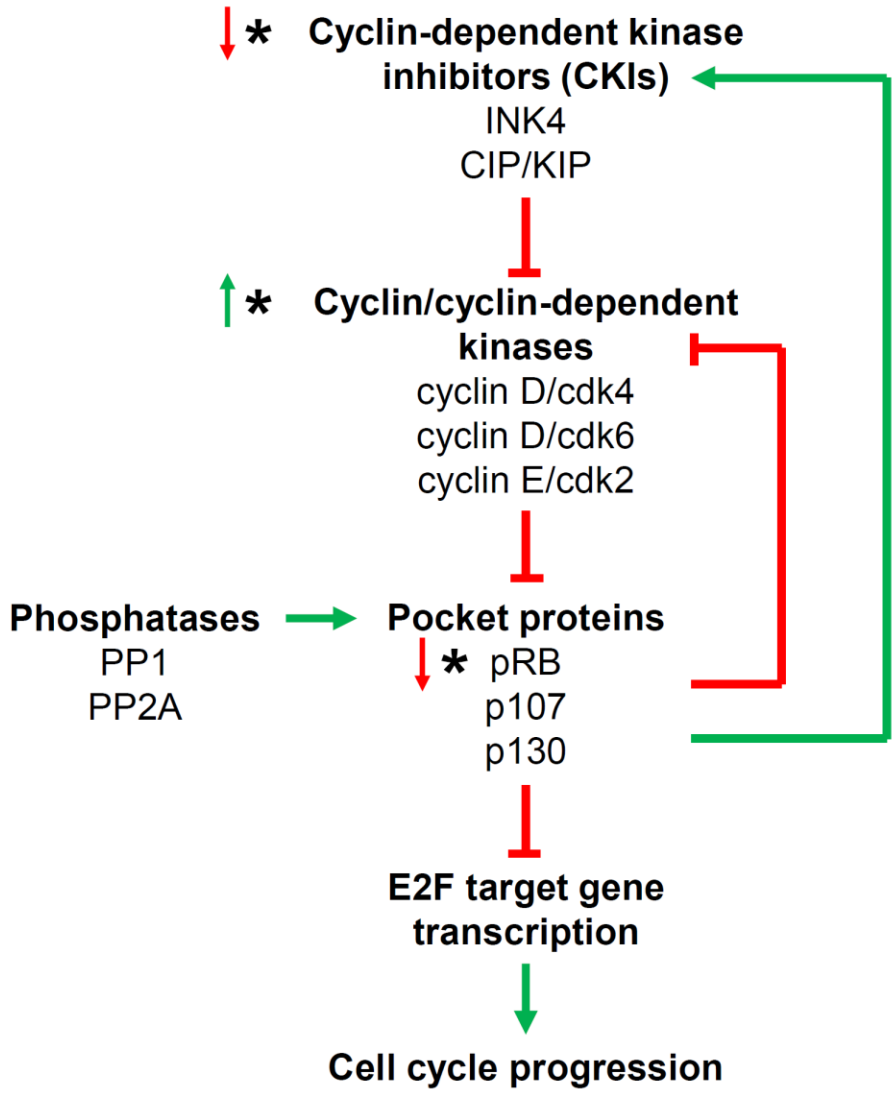

Figure 1.5: The pocket protein regulatory pathway.

Pocket proteins inhibit E2F target gene transcription, which in turn inhibits cell cycle progression. Pocket proteins are negatively regulated by cyclin-cdk complexes, and positively regulated by phosphatases. Activated CKIs inhibit cyclin-cdk complexes, restoring pocket protein activity. Pocket proteins can inhibit cyclin-cdk complexes and activate CKIs to maintain themselves in a hypophosphorylated state. (*) Indicates nodes in this regulatory pathway that are commonly mutated in cancer. (↑) Indicates upregulation/constitutive activation in cancers. (↓) Indicates loss or downregulation in cancers.

fail to progress through mitosis (Niculescu *et al* 1998, Srinivasan *et al* 2007). These cells persist in culture and can resume proliferating with aneuploidy.

In addition to pRB's role in the regulation of the cell division cycle, pRB plays regulatory rolls in both apoptosis and the DNA damage response (Dick and Dyson 2003, Julian *et al* 2008, Seifried *et al* 2008, Carnevale *et al* 2012, Cecchini and Dick 2011). It does this by binding to E2F1 specifically using the C-terminus of pRB (Fig. 1.2A; Dick and Dyson 2003). This specific interaction allows pRB to regulate E2F1-induced apoptosis, even when pRB is hyperphosphorylated and presumed inactive (Dick and Dyson 2003, Julian *et al* 2008, Seifried *et al* 2008, Carnevale *et al* 2012, Cecchini and Dick 2011). Moreover, pRB-E2F1 interactions are particularly important in mediating the DNA damage response, though this role appears to be context-dependent (Carnevale *et al* 2012). In addition to being unique from the other E2F transcription factors, the interaction between pRB and E2F1 is also unique amongst pocket proteins (Dick and Dyson 2003, Cecchini and Dick 2011, Julian *et al* 2008).

More recent data such as that presented in Chapters 2 and 3 of this thesis has begun to outline a unique role for pRB during mitosis that is independent of its regulation of E2F target gene transcription (Coschi *et al* 2010, Longworth *et al* 2008, Manning *et al* 2010, van Harn *et al* 2010). Importantly, this novel function contributes to pRB-mediated tumor suppression (Coschi *et al* 2010). Interestingly p107 and p130, whose sequences are more similar to each other than to pRB, contain structural features that are not found in pRB (Classon and Dyson 2001; Fig. 1.2A). This allows them to be differentially regulated and to accomplish different tasks (Lacy and Whyte 1997, Zhu *et al* 1995, Woo *et al* 1997, Moberg *et al* 1996). Conversely, structural features exclusive to pRB have yet to be discovered to explain the unique roles described above. Thus it has fallen to mouse models of the pocket proteins to describe the relative contributions of pRB, p107 and p130 to proliferation, cell cycle exit, and tumor suppression.

1.2 Mouse models of *Rb1*

1.2.1 *Rb1*$^{-/-}$ cells contribute to 'normal' tissues

The first models knocking out *Rb1* in mice were reported in 1992 from three different groups (Jacks *et al* 1992, Clarke *et al* 1992, Lee *et al* 1992). Each lab, using a different genetic strategy, generated homozygous mutant mice (*Rb1*$^{-/-}$) that died between embryonic days (E) 13 and 15, indicating that *Rb1* was required for embryogenesis, though surprisingly it was indespensible up to at least E13.

Mice heterozygous for *Rb1* were viable and fertile. Though humans hemizygous for *RB1* have a 90% likelihood of developing retinoblastoma by the age of three, *Rb1*$^{+/-}$ mice did not develop retinoblastomas or exhibit any precursor lesions (retinomas) (Matsunaga *et al* 1990; Jacks *et al* 1992, Lee *et al* 1992, Clarke *et al* 1992). One lab followed *Rb1*$^{+/-}$ mice long enough to discover a tumor phenotype (Jacks *et al* 1992). These mice succumbed to adenocarcinoma of the pituitary by ten months of age, and the majority of these tumors had lost the remaining wild type *Rb1* allele (LOH), seemingly consistent with Knudson's proposal that heterozygosity of the retinoblastoma gene was not functionally relevant to tumorigenesis (Jacks *et al* 1992).

A decade later it was reported that the most apparent defect in *Rb1*$^{-/-}$ mice was over-contribution of trophoblast cells to the placenta, creating an hypoxic environment for *Rb1*$^{-/-}$ embryos (Wu *et al* 2003). In fact, if the mutant placenta were replaced with wild type placenta, *Rb1*$^{-/-}$ embryos survived to birth with none of the neurological or erythropoietic defects previously reported (Jacks *et al* 1992, Clarke *et al* 1992, Lee *et al* 1992, Wu *et al* 2003). Instead, these mice died at birth with severe skeletal muscle dysplasia resulting in an inability of the diaphragm to work properly, preventing breathing (Wu *et al* 2003). The fact that the major defect in *Rb1*$^{-/-}$ mice was now reported to be in the trophoblast cells of the placenta, and that most other tissues appeared to develop normally, helped to explain why *Rb1*$^{-/-}$ cells in chimeric mice were found to contribute to a wide variety of what were described as 'normal' tissues (Williams *et al* 1994, Maandag *et al* 1994).

Several conditional knockout models of the *Rb1* gene have improved upon our understanding of the tissue-specific requirements of pRB. In general, knockout in certain tissues leads to increased proliferation and/or lack of proper differentiation though, with the exception of the pituitary, no spontaneous tumor development (Mayhew *et al* 2005, Ruiz *et al* 2004, Classon *et al* 2000, Hansen *et al* 2004, Vooijs *et al* 1998). Instead, this has been shown to require other complimentary mutations, such as disabling the p53 pathway (Wikenheiser-Brokamp 2004, Meuwissen *et al* 2003).

1.2.2 A structure-function approach to investigating pRB's contribution to tumor suppression

Generally, $Rb1^{-}$ alleles in mice have advanced our understanding of the role for pRB in different tissues and stages of development. Furthermore, lack of a tumor, or any overt phenotype, in both $p107^{-/-}$ and $p130^{-/-}$ mouse models has solidified pRB as unique among pocket proteins for mediating tumor suppression (Lee *et al* 1996, Cobrinik *et al* 1996). As described previously, there are currently three known binding surfaces on pRB that are distinct from one another and mediate binding to specific proteins. Knocking out pRB in mouse models disrupts all of its functions and therefore we are unable to attribute its tumor suppressive properties to one function or another. To this end, targeted mutation of certain binding sites on pRB would reveal their functional contribution to pRB-mediated tumor suppression. In the data chapters to follow, I will demonstrate how targeted mutation of the LXCXE binding cleft of pRB contributes to pRB-mediated tumor suppression, independently of E2F target gene transcription.

The advantage of a structure-function approach to investigating pRB function is supported by phenotypes observed in the $Rb1^{R654W}$ mouse. The arginine to tryptophan substitution at amino acid 654 (R654W) in the *Rb1* gene inhibits the ability of pRB to interact with E2Fs 1, 2 and 3, and thereby modulate their activity in a cell cycle-dependent manner (Sun *et al* 2006). This mutation has been modeled after the R661W mutation in the human *RB1* gene (Sun *et al* 2006, Lohmann *et al* 1994, Onadim *et al* 1992). $Rb1^{R654W/R654W}$ mice exhibit the same cell cycle defects as $Rb1^{-/-}$ embryos, however they survive two days longer than $Rb1^{-/-}$ mice *in utero,* and defects in erythropoiesis and liver macrophage differentiation are ameliorated (Sun *et al* 2006).

This suggests that pRB can have important contributions to differentiation that are unrelated to their ability to regulate E2F target gene transcription.

The idea that discrete interactions differentially contribute to pRB-mediated tumor suppression is supported by cancer mutation data in humans, suggesting that inactivation of the entire retinoblastoma gene is required to compromise pRB-mediated tumor suppression, and not just one discrete interaction surface. For example, tumor derived mutations of the *RB1* gene are inconsistent with the disruption of a single function of the retinoblastoma protein as there are thirty five known cancer-causing missense mutations in *RB1* from retinoblastoma patients, and most of these alleles have been reported only once (Fig. 1.6; Retinoblastoma genetics website). Additionally, the majority of these alleles are deletions or nonsense changes, abrogating complete pRB function (Lohmann 1999, Retinoblastoma genetics website). This is contrary to mutations in other oncogenes or tumor suppressors that cluster in regions based on functional importance as in Ras or p53 (Schubbert *et al* 2007, Joerger and Fersht 2007).

With evidence indicating that disrupting discrete pRB interactions with cellular proteins could help illuminate the contribution of that particular interaction to tumor suppression, the concept of a "structure-function" approach to study the retinoblastoma protein has been adopted. This was greatly aided by the publication of crystal structures of pRB's pocket showing which residues are on the surface of the protein, which are buried, and which are important for interacting with viral oncoproteins and E2Fs (Lee *et al* 1998, Rubin *et al* 2005, Xiao *et al* 2003). In this way, key residues mediating interactions between pRB and its binding partners were identified and could be used for targeted disruption. Indeed, substitution of amino acids required for pRB-E2F interactions in the small pocket of pRB eliminated pRB-mediated transcriptional repression of E2F target genes, and revealed a novel role for pRB in the regulation of apoptosis (Dick and Dyson 2003, Chau *et al* 2006).

Though there may be other, as yet undefined binding sites, at the current time, there are three well defined binding interfaces on the retinoblastoma protein that mediate binding to cellular proteins. These include i) the large pocket, which is the minimal

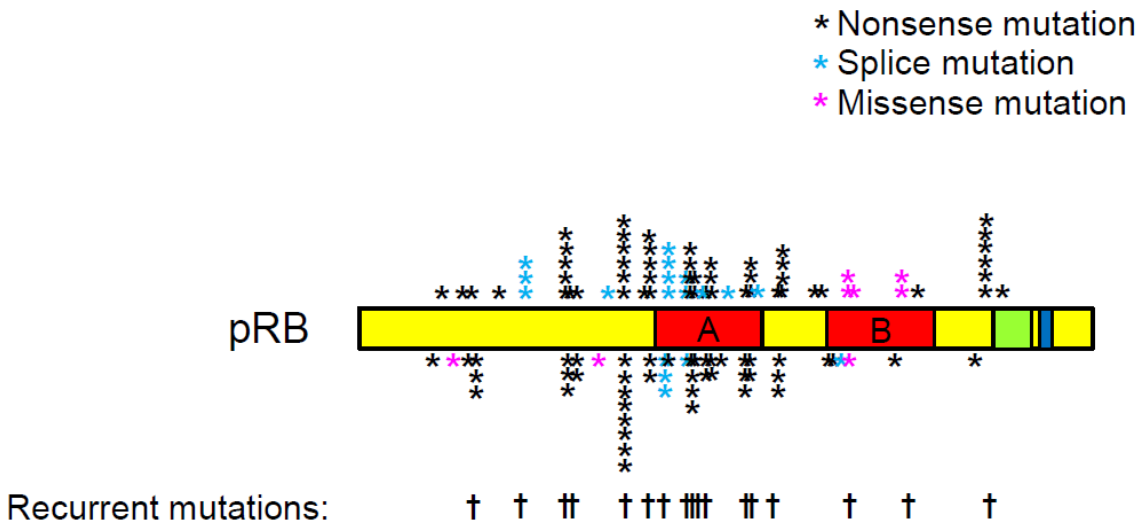

Figure 1.6: Spectrum of mutations of *RB1* in retinoblastoma patients.

Mutations of *RB1* in patients do not cluster within certain functional domains of the retinoblastoma protein. Most of the mutations are nonsense mutations, which inactivate the entire allele and not discrete functions of pRB. Few of these mutations are found more than once. Together, this indicates that all of pRB's functions are important for pRB-mediated tumor suppression. Each asterisk (*) is one mutation. Each cross (†) is one recurrent mutation. A- A cyclin fold. B- B cyclin fold.

sequence required for binding to E2F transcription factors, ii) the C-terminus, which binds specifically to E2F1, and iii) the LXCXE binding cleft, which is located in the B domain of the small pocket and mediates interactions with cellular proteins such as chromatin regulatory factors (Fig. 1.2A). The next several sub-sections of this introductory chapter will discuss the LXCXE binding cleft and the rationale for investigating the contribution of the LXCXE binding cleft to pRB-mediated tumor suppression.

1.3 The *Rb1*$^{\Delta L/\Delta L}$ mouse

1.3.1 The LXCXE binding cleft

As previously described, the LXCXE binding cleft is located in the B domain of the small pocket of pocket proteins (Lee *et al* 1998). Numerous cellular proteins are reported to bind pRB using this site (reviewed in Dick 2007). Many of these proteins can modify chromatin structure to induce heterochromatinization and thereby repression of gene transcription including HDAC1/2, Suv39h1, BRG1, Brm, DNMT1 and hSWI/SNF (Brehm *et al* 1998, Magnaghi *et al* 1998, Luo *et al* 1998, Lai *et al* 1999, Nielsen *et al* 2001, Dunaief *et al* 1994, Singh *et al* 1995, Robertson *et al* 2000, Zhang *et al* 2000). Other proteins function in transcriptional repression or DNA replication, or have no as yet known function. As previously discussed, binding of these proteins to the LXCXE binding cleft of pRB facilitates inhibition of E2F target gene transcription, thereby contributing to the inhibition of cell cycle progression.

Alternatively, using an LXCXE motif, viral oncoproteins bind in the LXCXE binding cleft to inactivate pRB, p107 and p130 (Lee *et al* 1998, Ewen *et al* 1989, Munger *et al* 1989, Whyte *et al* 1989, Dyson *et al* 1992). A study of amino acid sequence conservation has revealed that the LXCXE binding cleft is the most highly conserved region among pocket proteins and across several species of pRB (Lee *et al* 1998). As the LXCXE binding cleft on pRB renders it susceptible to viral oncoproteins, it raises the question as to why this site has remained so conserved over evolutionary time. Evidently, interactions between the LXCXE binding cleft of pRB and cellular proteins

must perform an essential function, though this is not reflected by its seemingly modest contribution to cell division cycle regulation.

Early efforts to address this conundrum began with the targeted disruption of LXCXE binding cleft interactions without compromising binding to E2Fs in the large pocket, or E2F1 in the C-terminus. These studies have revealed that while proliferative control remains intact, the ability of such a mutant pRB to mediate permanent cell cycle arrest is compromised (Dick *et al* 2000, Chan *et al* 2001, Chen and Wang 2000, Dahiya *et al* 2000). In order to further investigate the role of the LXCXE binding cleft of pRB in isolation, our lab has generated a mouse (*Rb1*$^{\Delta L/\Delta L}$) with alanine substitutions at three key amino acids in the LXCXE binding cleft that mediate important contacts with cellular proteins (I746A, N750A and M754A) (Fig. 1.7; Isaac *et al* 2006). The *Rb1*$^{\Delta L/\Delta L}$ mouse is viable, fertile and born at Mendelian ratios (Isaac *et al* 2006). Additionally, these mice do not acquire spontaneous tumors (Isaac *et al* 2006). The *Rb1*$^{\Delta L/\Delta L}$ mouse is described in detail below.

1.3.2 *Rb1*$^{\Delta L/\Delta L}$ MEFs exhibit phenotypes independent of G1 to S-phase transition regulation

Mouse embryonic fibroblasts from *Rb1*$^{\Delta L/\Delta L}$ mice reflect previous experiments in Saos2 and C33A cells in that they maintain proliferative control (E2F target genes are not upregulated), but fail to remain permanently arrested in senescence (Isaac *et al* 2006, Talluri *et al* 2010). In cycling *Rb1*$^{\Delta L/\Delta L}$ MEFs, there is an accumulation of a >4N DNA content peak, which is indicative of aneuploidy (Isaac *et al* 2006). They also exhibit a reduction in histone H4-K20 trimethylation, a mark of heterochromatin. Centromeres characterized by loss of this histone mark exhibit fusions leading to errors in mitosis (Isaac 2006). Finally, these cells also exhibit hypocondensation of chromatin. Taken together, genomic instability appears to be a hallmark of *Rb1*$^{\Delta L/\Delta L}$ MEFs.

In MEFs induced to senesce using oncogenic Ras, there is a reduction in the histone H3-K9 trimethylation mark at E2F target genes, which correlates with their upregulation. These cells also exhibit a striking inability to inactivate cell division cycle progression when challenged with Ras as *Rb1*$^{\Delta L/\Delta L}$ MEFs showed a significantly

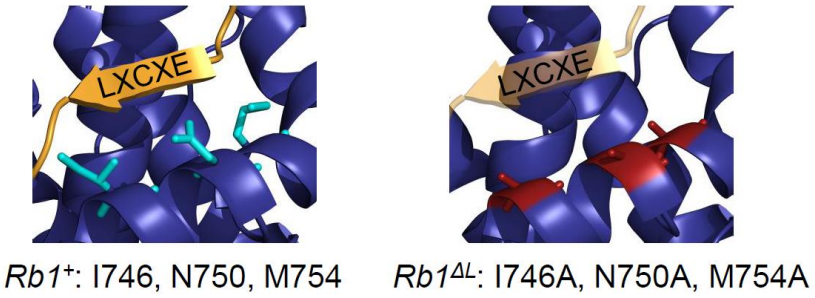

Figure 1.7: Disruption of protein-interaction sites on the retinoblastoma protein.

The LXCXE binding cleft of pRB contains three important contact residues with LXCXE motif-containing proteins, residues I746, N750 and M754 (*Rb1*$^{+}$). Mutation of these residues to alanine abrogates the ability of proteins to bind in the LXCXE binding cleft of pRB. This mutation is called the *Rb1*$^{\Delta L}$ mutation. The *Rb1*$^{\Delta L/\Delta L}$ mouse is defective for binding proteins in its LXCXE binding cleft, but maintains general and specific interactions with E2Fs. I- isoleucine. N- asparagine. M- methionine. A- alanine.

increased >4N DNA content compared to wild type. DNA content was often 8N or higher, indicating endoreduplication (Talluri *et al* 2010). Intriguingly, this is not observed in differentiation, a separate paradigm of permanent cell cycle arrest, suggesting that this is unique to pRB-mediated G1 arrest in response to oncogenic stress (Talluri *et al* 2010).

1.3.3 The *Rb1*$^{\Delta L/\Delta L}$ mouse exhibits no overt tumor-suppressive phenotype

As mentioned above, *Rb1*$^{\Delta L/\Delta L}$ mice are viable, fertile and born at the expected Mendelian ratios (Isaac *et al* 2006). These mice do not acquire spontaneous tumors, though they exhibit hyperplasia of the mammary gland ductal epithelium (Francis *et al* 2009). This hyperplasia was found to be a result of insensitivity to transforming growth factor β (TGF-β) growth inhibition (Francis *et al* 2009). Studies in MEFs were used to determine the mechanisms for this insensitivity and it was found that pRB-mediated repression of E2F target genes was compromised in response to TGF-β signalling, allowing for ectopic proliferation as measured by BrdU incorporation (Francis *et al* 2009).

In order to investigate the mechanism(s) by which the LXCXE binding cleft itself contributes to pRB-mediated tumor suppression, we crossed *Rb1*$^{\Delta L/\Delta L}$ mice into a *Trp53*$^{-/-}$ tumor prone mouse model. *Trp53*$^{-/-}$ mice reliably acquire thymic lymphomas that are karyotypically normal, and so this is an appropriate tumor phenotype for us to modify with the *Rb1*-ΔL mutation to observe whether its addition leads to increased genomic instability. Additionally, as mentioned previously, *Rb1*$^{\Delta L/\Delta L}$ MEFs are compromised for maintaining a G1 arrest in response to DNA damage and oncogene-induced senescence (Talluri *et al* 2010). Because p53 acts upstream of pRB in mediating such a G1 arrest, modification of the *Trp53*$^{-/-}$ tumor phenotype by pRB will be separate from its regulation of this G1 arrest mechanism. The results of this large tumor study are reported in Chapters 2 and 3 of this thesis.

1.3.4 A non-canonical role for the LXCXE binding cleft of pRB

The data described in this introductory chapter on the retinoblastoma protein have focused on the various ways in which it regulates proliferation, with the exception of its role in mediating E2F1-induced apoptosis, and the role of the LXCXE binding cleft in mediating genome stability. Recently, a paper published by Longworth *et al* described a role linking *Drosophila* pRB (RBF1) to the regulation of chromatin structure. This was mediated by an interaction between RBF1 and a subunit of the Condensin II complex, a member of the structural maintenance of chromosome (SMC) family of complexes that facilitates mitotic chromosome condensation (Longworth *et al* 2008).

Longworth *et al* report that this subunit, dCAP-D3, partially colocalizes with RBF1 on chromatin and that RBF1 is required for dCAP-D3 localization to chromatin (Longworth *et al* 2008). Mutants of *dCAP-D3* suppressed phenotypes induced by RBF1 overexpression and *rbf1* mutants exhibited significant defects in chromatin condensation during mitosis. Moreover in humans, adding wild type pRB to pRB-deficient cells increased hCAP-D3 loading on chromatin in a manner dependent on pRB's LXCXE binding cleft (Longworth *et al* 2008). This report provides a hint at the mechanism by which the LXCXE binding cleft was reported to mediate genome stability and contribute to pRB-mediated tumor suppression (Isaac *et al* 2006). In subsequent chapters I will describe the interaction of pRB with the Condensin II complex and will expand upon the mechanism by which this occurs in the context of pRB-mediated genome stability and tumor suppression.

1.4 Condensins

1.4.1 The structural maintenance of chromosomes (SMC) family of complexes are integral for chromosome dynamics

The structural maintenance of chromosome (SMC) family of complexes consists of the SMC5/6 complex, Cohesin (mitotic and meiotic), Condensin I and Condensin II (Fig. 1.8). The SMC proteins are conserved across the three phyla of life indicating that

chromosome organization is evolutionarily conserved (Cobbe and Heck 2004). SMC proteins always form a dimer and associate with regulatory subunits into a large holocomplex. SMC proteins have a "hinge" domain where the protein self-folds, and an ATP-binding cassette-like "head" domain separated by an antiparallel coiled-coil "arm" (Fig. 1.8A). Two of these SMC proteins associate *via* their hinge to produce a V-shaped dimer (Melby *et al* 1998, Anderson *et al* 2002, Haering *et al* 2002, Hirano and Hirano 2002) (Fig. 1.8A). It is predicted that ATP binding to, and hydrolysis at, the "head" domain facilitates engagement and disengagement respectively (Haering *et al* 2004, Lammens *et al* 2004, Hirano *et al* 2001, Hirano and Hirano 2004). Non-SMC regulatory subunits of SMC complexes include kleisins, HEAT-repeat containing proteins or other subunits (Fig. 1.8B). Kleisin subunits interact with the head domain of two SMC proteins through their N- and C-terminal domains to form a ring-like structure whereas HEAT-repeat containing proteins act as protein scaffolds to assemble cellular components and are proposed to direct SMC proteins to specific loci on DNA (Schleiffer *et al* 2003, Neuwald and Hirano 2000). HEAT-repeat regulatory subunits therefore greatly influence chromosome dynamics.

The SMC5/6 complex is sequentially divergent from the other SMC complexes and an understanding of its functions is reviewed elsewhere (Lehmann 2005, De Piccoli *et al* 2009). The mitotic Cohesin holocomplex is comprised of SMC1 and SMC3, the kleisin subunit hRAD21, and other subunits including a HEAT-repeat containing subunit Scc2 (Losada and Hirano 2005) (Fig. 1.8C). Condensins I and II both have SMC2 and SMC4 proteins, but differ in their regulatory subunits. Whereas Condensin I is composed of the kleisin subunit hCAP-H and two HEAT-repeat containing subunits hCAP-D2 and hCAP-G, Condensin II is comprised of the kleisin subunit hCAP-H2 and two HEAT-repeat containing subunits hCAP-D3 and hCAP-G2 (Fig. 1.8D, E respectively).

In general, Cohesin ensures proper resolution of sister chromatids while Condensins I and II facilitate sequential mitotic chromosome condensation (Fig. 1.9). Briefly, the Cohesin complex forms a ring-like structure around DNA that maintains sister chromatid cohesion as DNA is replicated in S-phase (Fig. 1.9A) (Gruber *et al* 2003,

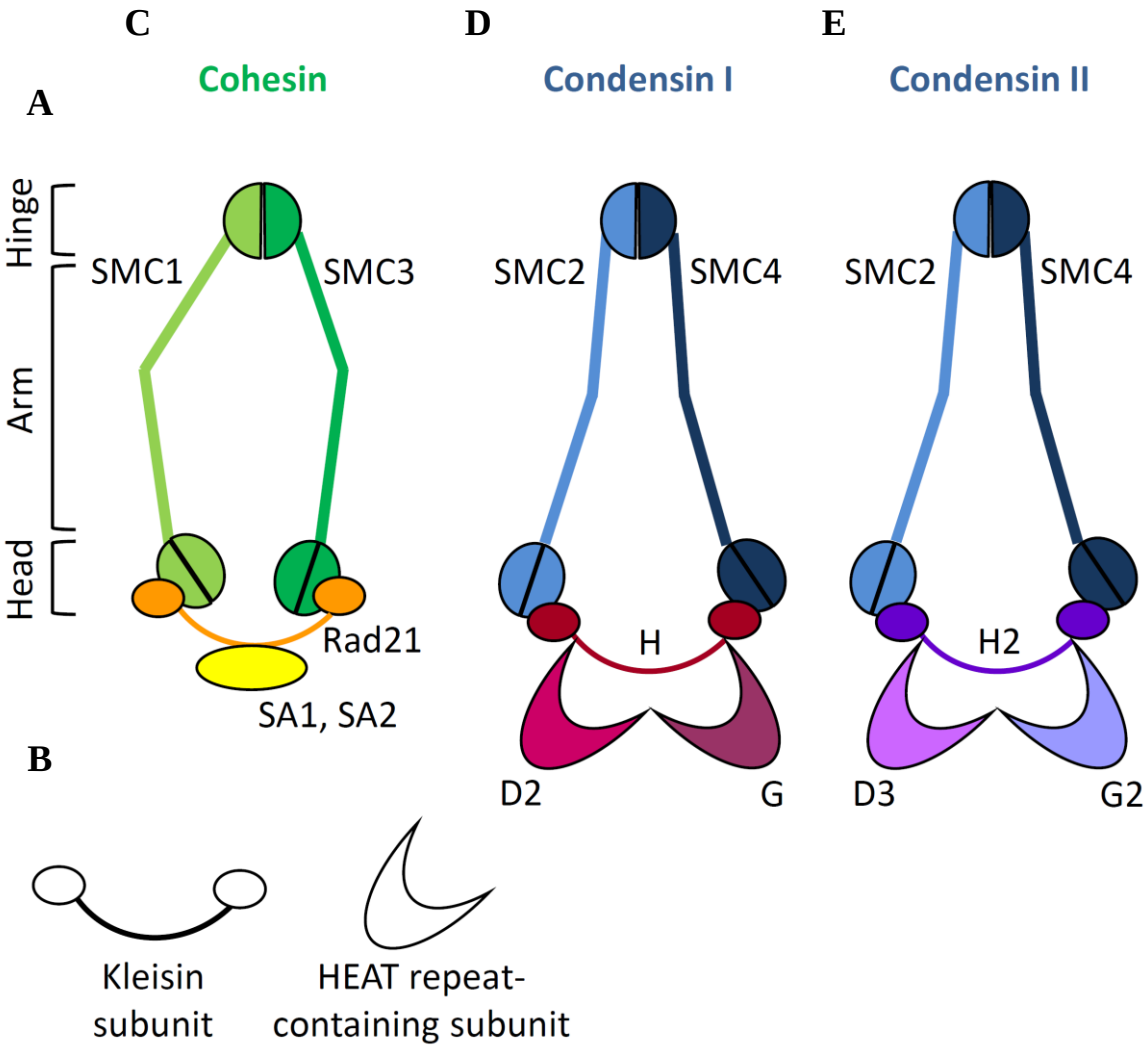

Figure 1.8: Cohesin, Condensin I and Condensin II are complexes of the structural maintenance of chromosome (SMC) family.

(A) Depiction of the domain organization of SMC proteins. Domains are organized by the folding back upon itself of the SMC protein. The hinge domain is globular and binds to the hinge domain of another SMC protein. The arms are coiled coils, and the head domain contains the N and C-terminus of the protein. **(B)** Depiction of the regulatory subunits of SMC proteins. **(C)** Cohesin facilitates sister chromatid resolution and is comprised of SMC1, SMC3, Rad21 and SA1 or SA2. **(D)** Condensin I is comprised of SMC2, SMC4, CAP-H, CAP-G and CAP-D2. **(E)** Condensin II is comprised of SMC2, SMC4, CAP-H2, CAP-G2 and CAP-D3. Adapted from Losada and Hirano, 2005.

Losada *et al* 2002). In prophase, mitotic Condensin II is loaded onto chromatin and facilitates condensation; this is accompanied by release of some Cohesin from chromosome arms (Losada *et al* 2002, Sumara *et al* 2002, Giménez-Abián *et al* 2004) (Fig. 1.9B). After nuclear envelop breakdown Condensin I, which is constitutively cytoplasmic, gains access to chromosomes and facilitates further mitotic chromosome condensation during prometaphase and metaphase (Fig. 1.9C). Again, this is accompanied by further release of Cohesin from chromosome arms. At this point, a small subset of Cohesin remains at pericentromeric chromatin and is protected from release by the protein shugoshin (Losada *et al* 2000, Clift *et al* 2009, Katis *et al* 2004, Kitajima *et al* 2004, Marston *et al* 2004). At anaphase onset, shugoshin is targeted for degradation and the kleisin subunit hRAD21 is cleaved by the separase enzyme, breaking its ring structure and triggering Cohesin dissociation from chromosomes (Fig. 1.9D). Mitotic chromosomes are then pulled to opposite poles of the cell (Gruber *et al* 2003, Losada and Hirano 2005). After chromosomes have reached opposite poles, Condensins are unloaded from chromatin (reviewed in Losada and Hirano 2005) (Fig. 1.9E).

1.4.2 Condensin I and Condensin II differentially contribute to mitotic chromosomes

Condensins are proposed to facilitate mitotic chromosome condensation by introducing supercoiling to DNA, or by associating with each other to create larger DNA loops, bringing distant sites on chromosomes together. While data in Chapters 2 and 3 report a unique interaction of pRB specifically with the Condensin II complex, Condensin I was the first discovered Condensin. As such, it has been extensively studied and what has been learned about Condensin I is inferred for the mechanisms of action of Condensin II. Condensin I has been shown to introduce positive supercoiling to double stranded DNA (dsDNA) in an ATP-dependent manner (Kimura and Hirano 1997, Strick *et al* 2004). This activity is stimulated by phosphorylation of the non-SMC subunits by Cyclin B-cdk1 (Kimura *et al* 1998, Kimura *et al* 1999, Strick *et al* 2004). Indeed, non-SMC subunit phosphorylation steadily increases from prophase to anaphase of the cell division cycle, and this correlates with increasing compaction of mitotic chromosomes (Kimura *et al* 1998). In accordance with this model, the hCAP-D3 subunit of Condensin

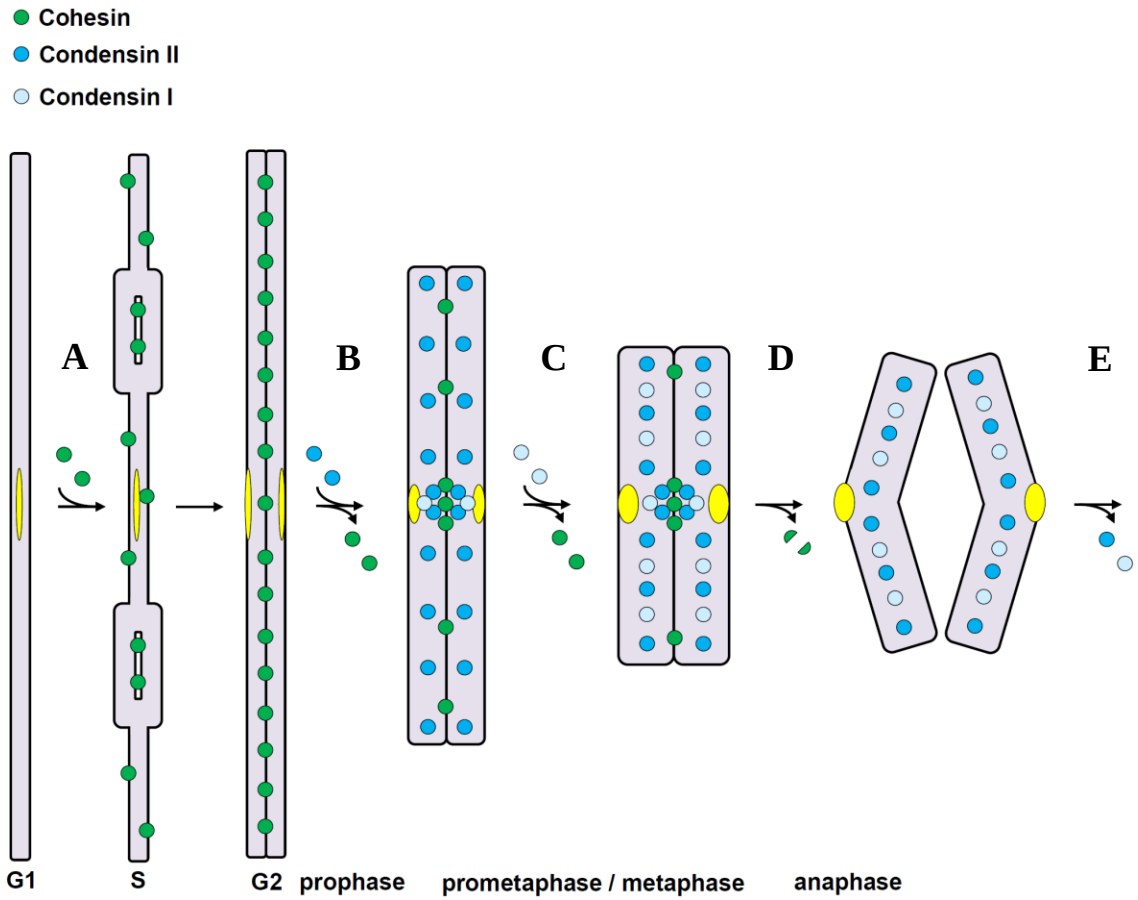

Figure 1.9: The SMC proteins are key chromosomal components for mitosis.

(A) As DNA is being replicated in S-phase, Cohesin is loaded onto chromosome arms to facilitate sister chromatid resolution. **(B)** In prophase, Condensin II is loaded onto chromosomes, facilitating partial chromosome condensation. Some cohesin is removed from chromosome arms. **(C)** After nuclear envelope breakdown, Condensin I is loaded onto chromosomes and further condenses mitotic chromosomes. The remaining Cohesin is removed from chromosomes except at centromeres and near telomeres. **(D)** At anaphase onset, the remaining Cohesin at centromeres is removed by separase-mediated cleavage of its kleisin subunit, and chromosomes are pulled apart by the mitotic spindle. **(E)** After chromosomes are pulled apart, mitotic Condensins I and II are unloaded from chromosomes. Adapted from Losada and Hirano, 2005.

II has been shown to be phosphorylated by Cyclin B-cdk1 to promote chromosome condensation early in mitosis (Abe *et al* 2011). In the same study, the Polo-like kinase 1 (Plk1) was proposed to cooperate with cdk1 to facilitate Condensin II-mediated chromosome condensation later in mitosis.

Despite having similar mechanisms of action, Condensins are differentially regulated, suggesting they differentially contribute to chromosome dynamics (Ono *et al* 2004, Lipp *et al* 2007, Takemoto *et al* 2006, Takemoto *et al* 2009, Yamashita *et al* 2011). Through numerous studies, Condensin I and Condensin II have been found to differentially and non-redundantly contribute to mitotic chromosome condensation as depletion of either complex alone leads to segregation errors and condensation defects (Hirota *et al* 2004, Ono *et al* 2003). Moreover, Condensin I and II do not colocalize on chromosomes, rather they alternate along the length of the chromosome arms (Ono *et al* 2003). Though Condensin I is involved in more primary organization of chromatin fibres around the mitotic spindle, Condensin II was found to be more architectural, determining the final chromosome shape by being more closely associated with the central mitotic chromosome axis.

While it is known that extensive phosphorylation of non-SMC complexes on chromatin facilitates mitotic chromosome condensation, few regulatory proteins such as those proposed above have been found to localize Condensins to chromatin and facilitate loading. For example, the Scc2 HEAT-repeat containing protein that associates with Cohesin has been shown to be necessary for Cohesin recruitment to chromatin, supposedly by facilitating ATP-hydrolysis of the SMC head domains, thereby stimulating opening of the ring to allow loading onto chromatin (Arumugam *et al* 2003). It is not known which proteins perform the same functions for Condensins, though the HEAT repeat-containing non-SMC subunits of both Condensin I and Condensin II would be natural candidates (Losada and Hirano 2005).

There must also be discriminatory mechanisms for loading Condensins onto chromatin though these mechanisms remain largely elusive. Cohesin, Condensin I and Condensin II are all localized to centromeres. Cohesin maintains sister chromatid

cohesion until anaphase onset, and Condensin I has been shown to be important for the rigidity of centromeric heterochromatin and its loss leads to abnormal orientation of sister chromatids (Losada *et al* 1998, Losada *et al* 2000, Katis *et al* 2004, Kitajima *et al* 2004, Marston *et al* 2004, Rabitsch *et al* 2004, Ono *et al* 2004, Oliveira *et al* 2005, Gerlich *et al* 2006, Ribeiro *et al* 2009). Condensin II also plays a particularly important role at centromeres. In *C. elegans*, which is holocentric with numerous centromeres assembled along the length of each chromosome, Condensin II predominates at centromeres and its loss leads to large merotelic attachments and segregation defects (Stear and Roth 2002). In humans and other animals, a specialized fraction of Condensin II is enriched at the inner kinetochore plate (Ono *et al* 2004, Shintomi and Hirano 2011, Savvidou *et al* 2005, Samoshkin *et al* 2009). Most recently, Condensin II has been proposed to be important for loading of the centromere-specific histone 3 variant CENPA, which is important for propagation of centromeric heterochromatin (Folco *et al* 2008, Samoshkin *et al* 2009).

1.4.3 Condensin II contributes to functions outside of mitotic chromosome condensation

In addition to their roles in mitotic chromosome condensation, Condensin II has been shown to mediate other cellular processes including gene regulation, recombination, and DNA damage response and repair. For example, in *Drosophila*, Condensin II has been shown to mediate resolution/disassembly of polytene chromosomes, a process that occurs during oogenesis in specialized ovarian nurse cells (Hartl *et al* 2008). Moreover, by resolving sister chromatids, Condensin II prevents homolog-homolog interactions from occurring, thereby preventing transvection (Hartl *et al* 2008). Similar to the resolution of polytene chromosomes in *Drosophila*, a recent report by Ono *et al*. also implicates the Condensin II complex in the resolution of sister chromatids following DNA replication in S-phase (Ono *et al* 2013).

Many studies investigating the roles of Condensins have been performed in yeast due to the ease of their genetic manipulation. Yeast contain only one Condensin complex, which more closely resembles Condensin I than Condensin II from higher eukaryotes (Losada and Hirano 2005). However, the non-mitotic functions of this single Condensin complex in yeast suggest that it may behave like Condensin II, especially as it

has access to chromosomes in the nucleus during interphase, which the higher eukaryotic Condensin I lacks (Losada and Hirano 2005). For example in yeast, Condensin plays a critical role in maintaining the copy number of rDNA repeats by preventing their expansion *via* recombination (Johzuka *et al* 2006, Clemente-Blanco *et al* 2009, Johzuka and Horiuchi 2007). As well, Condensin has been shown to promote clustering of yeast tRNA genes in the nucleolus (Thompson *et al* 2003, Haeusler *et al* 2008). In *S. pombe*, Condensin plays yet another role whereby it recruits Pol III genes to centromeres and thereby prevents their transcription (Iwasaki *et al* 2010). Interestingly, there appears to be a special requirement for these functions at repetitive DNA sequences.

Condensins have also been implicated in the DNA damage response and subsequent repair. In *S. cerevisiae*, loss of Condensin results in cells becoming sensitive to DNA damage as a result of compromised recombinational repair; these cells also exhibit genomic instability (Ide *et al* 2010). In *S. pombe*, loss of Condensin also compromises DNA damage repair (Akai *et al* 2011). Furthermore in humans, Condensin II was shown to be involved in DNA double strand break response and repair (Sakamoto *et al* 2011). This is supported by work showing that in meiosis in humans, Condensin II is important for resolving bivalent chromosomes, including chiasmata resolution (Lee *et al* 2011).

It is clear that Condensins play an important role in mediating chromosome dynamics outside of mitosis. Therefore the above-described non-mitotic functions of Condensin II are of particular interest in considering the data reported in Chapters 2 and 3 of this thesis where I propose a role for Condensin II at centromeres in S-phase that is mediated by the retinoblastoma protein.

1.4.4 Subunits of the Condensin complexes are mutated in cancer

Because Condensins exhibit a diverse array of functions, play an integral role in mediating mitotic chromosome condensation, and because defects with Condensins are associated with merotely, missegregation and hypocondensation, it is interesting to speculate that their proper function is important for preventing aneuploidy and genomic

instability. The SMC field is only beginning to utilize mouse models to explore this question, and whether it has any bearing on tumorigenesis.

Two mouse models have been published to date. The first mutant mouse was made with a mutation knocking out the HEAT repeat-containing CAP-G2 subunit of Condensin II; it was found to be embryonic lethal (Smith *et al* 2004, Xu *et al* 2006). This is perhaps not surprising as SMC2 and 4, and thereby Condensins I and II, have been found to be essential for mouse embryonic stem cell viability (Fazzio and Panning 2010). The second mouse was identified in a screen for recessive genes involved in T-cell development (Gosling *et al* 2007). This mutant mouse strain, referred to as *nessy*, carries a point mutation in CAP-H2, the kleisin subunit of Condensin II (Gosling *et al* 2007). Homozygous mice are viable, fertile, and exhibit no cancer phenotype. Instead, there is a specific defect in T-cell development and failure to initiate a normal immune response (Gosling *et al* 2008). Interestingly, the other functions of Condensin II appear uncompromised (Gosling *et al* 2008). One reason for this may be because it is a simple point mutation that may disrupt one function of the complex, but not others.

More promising data to support the importance of Condensins in tumor suppression can be found in the literature and cancer mutation databases. For example, several cases of pyothorax-associated lymphoma in humans have point mutations in SMC2 and SMC4 (Ham *et al* 2007). Additionally, mutation of the CAP-G subunit of Condensin I in zebrafish increases genomic imbalance (Seipold *et al* 2009). Finally, investigation of human cancer mutations using the Catalog Of Somatic Mutations In Cancer (COSMIC) database reveals several cancers containing missense and nonsense mutations in SMC and non-SMC subunits of both the Condensin I and Condensin II complexes (COSMIC database). Interestingly, nonsense mutations in these subunits are less common than missense mutations, indicating that some measure of proper Condensin function is still required by cancer cells to divide. It follows then, that point mutations disrupt minimal function and might serve to enable genomic instability, allowing the accumulation of mutations that promote or permit tumorigenesis.

1.5 Genomic instability

1.5.1 Types of genomic instability

Genome instability is a broad term used to describe the failure of a cell to accurately pass on a copy of its genome to its daughter cells. There are several mechanisms by which this can occur, and these have been grouped into three broad categories. Microsatellite instability is caused by defective mismatch repair that leaves DNA replication errors uncorrected (Grilley *et al* 1990, Ionov *et al* 1993, Thibodeau *et al* 1996). Nucleotide excision repair-related instability arises from defects that prevent removal and replacement of UV-damaged nucleotides (Sancar 1996, Wood 1997, Batty and Wood 2000). The third type of instability is chromosome instability (CIN), which can be further dissected into two types, whole chromosome instability (W-CIN) and segmental chromosome instability (S-CIN) (delineated by Geigl *et al* 2008). W-CIN arises through the gain and/or loss of whole chromosomes, which, if sustained through successive cell divisions, results in aneuploidy. Additionally, smaller regions of gain or loss, or changes in chromosome structure that do not result in copy number alterations, such as translocations or inversions, are broadly termed S-CIN (Geigl *et al* 2008). Over the years, genomic instability has been implicated, not surprisingly, in tumorigenesis. In the next few paragraphs I will describe the role of genomic instability in tumorigenesis, and how this relates to pRB.

1.5.2 Genomic instability in cancer

The concept that aneuploidy is a characteristic of malignant cells was first suggested by the work of von Hansemann and Boveri (Boveri 1912, Boveri 2008, Shirkhedkar Atul A *et al* 2009). However, this theory was not verified until the early 1950s, when Sajiro Makino, and Levan and Hauschka among others demonstrated that malignant cells have a unique chromosome compliment compared to their normal counterparts (Makino 1952, Makino and Nakahara 1952, Hauschka and Levan 1958, Hauschka 1953, Hauschka 1958). Since then, chromosome instability has been observed to be tolerated, and even selected for, in many malignant cell types (Hanahan and Weinberg 2000, Hanahan and Weinberg 2011). Originally, such chromosome instability

was thought to be a by-product, or a passenger that accompanied tumorigenesis. In other words, it was a cancer-associated phenotype, not a cancer-causing mechanism. However, in recent years, it has become evident that chromosome instability may exhibit a more causative role in the transformation of a normal cell into one that becomes cancerous. This shift in thought has been supported by several mouse models in which alterations of the spindle assembly checkpoint lead to higher than normal chromosome segregation errors, and offers proof of principle that chromosome instability alone can be the root cause of spontaneous tumors in mammals (reviewed in Schvartzman *et al* 2010, Bond *et al* 2004).

In addition, the combination of these spindle assembly defects with other genetic lesions can enhance tumorigenesis, further demonstrating that CIN can stimulate progression of the disease (Bond *et al* 2004). Moreover, chromosome instability phenotypes are caused by mutations in tumor suppressor genes whose primary function resides in maintaining genome stability through repair and damage checkpoints, and/or the spindle assembly checkpoint, such as BRCA1, BubR1, and others (Huen *et al* 2010, Joukov *et al* 2006, Stolz *et al* 2010, Choi and Lee 2008, Elowe *et al* 2010, Wei *et al* 2010). These tumor suppressors, along with recently reported massive chromosome rearrangements (chromothripsis) that are evident in initial disease, and even in relapse (Stephens *et al* 2011), further argue that defects in chromosome stability can be central to cancer pathogenesis.

In a manner similar to our shift towards viewing chromosome instability as an active contributor to cancer as opposed to being an associated phenotype, our understanding of many well-known oncogenes and tumor suppressors has followed a similar path. The adenomatous polyposis coli gene (APC), p53, and the retinoblastoma susceptibility gene (*RB1*) were all initially discovered to function in growth control (Su *et al* 1993, Rubinfeld *et al* 1993, Hinck *et al* 1994, Kastan *et al* 1991, Yonish-Rouach *et al* 1991, Lane 1992, Goodrich *et al* 1991). While this remains true, our expanding knowledge of these genes has revealed roles for them in the maintenance of genome stability and, in many cases, specifically in chromosome stability. In this way chromosome instability enhances the tumorigenic potential beyond deregulated

proliferation that is caused by loss of these tumor suppressors, or by gain of oncogenes. As a result, chromosome instability caused by common genetic lesions in cancer may be more central to the process of tumorigenesis than is currently estimated.

1.5.3 pRB and genomic instability

As described above, much attention has been focused on pRB's ability to regulate E2F transcription factors at the G1 to S-phase transition, as this regulates a cell's commitment to replicate its DNA and divide. There are two general divisions in which to categorize pRB's functions that maintain genome stability. The first is as a consequence of deregulated E2F transcription. As detailed above, the vast majority of cancers possess mutations that disrupt regulation of the pRB pathway, leading to uncontrolled E2F transcription. For this reason, missexpression of genes early in the cell cycle can result in chromosome re-replication or missegregation later, as is the case with deregulation of the E2F-target genes, cyclin E and MAD2, respectively (Spruck *et al* 1999, Hernando *et al* 2004). In addition, E2F-independent regulation of the chromatin structure of mitotic chromosomes has also emerged as a means by which the retinoblastoma protein contributes to the maintenance of genome stability and will be discussed in subsequent chapters (Coschi *et al* 2010, Manning *et al* 2010, van Harn *et al* 2010).

Among E2F transcriptional targets, a number stand out as known causes of chromosome instability when overexpressed. First, both cyclin E1 and E2 isoforms are E2F target genes; their stable overexpression leads to abnormally elevated cyclin-dependent kinase activity, ultimately leading to aneuploidy or polyploidy (Spruck *et al* 1999). Furthermore, a number of components of the spindle assembly checkpoint are E2F target genes, including Mad2 and BubR1, whose overexpression leads to enhanced checkpoint activity (Schvartzman *et al* 2010). This in turn delays progression through mitosis and manifests as chromosome segregation errors (Hernando *et al* 2004). These examples of deregulated E2F target gene-induced expression reveal how elevated levels of these gene products drive CIN, and offer a simple connection between loss of proliferation control and aneuploidy.

The first reports to suggest a role for pRB in maintaining a stable genome independently of E2Fs, and thereby G1 to S-phase regulation, demonstrated defects in chromosome structure or maintenance. In a study by Zheng *et al.* it was demonstrated that *Rb1*$^{+/-}$ and *Rb1*$^{-/-}$ mouse embryonic stem cells exhibit a high frequency of loss of a selectable chromosomal marker compared to wild-type (Zheng *et al* 2002). Furthermore, loss of drug resistance was due to complete absence of the selectable marker, implicating chromosomal loss or rearrangement as the explanation for genetic change (Zheng *et al* 2002). Similarly, it was also observed that cells deficient for all pRB family proteins display lengthened telomeres and centromere fusions (Gonzalo *et al* 2005, Felsher *et al* 2000). Metaphase spreads from these cells are characterized by chromosome fusions and tetraploidy (Gonzalo *et al* 2005).

Interestingly, similar centromere, aneuploidy, polyploidy, W-CIN, and S-CIN phenotypes have been observed in cells with defective Condensin I/II complex function (Ono *et al* 2003, Ono *et al* 2004, Samoshkin *et al* 2009, Ribeiro *et al* 2009, Vagnarelli *et al* 2006). The Condensin II complex facilitates chromosome condensation during prometaphase, and is important for maintaining chromosome structure and architecture during mitosis, particularly at the centromere (Ribeiro *et al* 2009, Yong-Gonzalez *et al* 2007, Hagstrom *et al* 2002). The association of the Condensin II complex with pRB occurs in an LXCXE-dependent manner (Longworth *et al* 2008). Defective Condensin II function offers an explanation for the observed hypocondensation at centromeres, centromere fusions, and increase in lagging chromosomes during mitosis in *Rb1*$^{\Delta L/\Delta L}$ MEFs (Isaac *et al* 2006). Presumably, defects in condensation lead to misshapen centromeres and merotelic attachments by spindle microtubules, which leads to missegregation of chromosomes without activating the spindle assembly checkpoint (Thompson *et al* 2008, Cimini *et al* 2001). Defects in S-CIN have also been reported in pRB family-deficient fibroblasts, suggesting that chromosome structure defects also occur elsewhere in the genome, rather than at centromeres alone (van Harn *et al* 2010).

Defects in E2F regulation lead to elevated levels of aneuploidy because of improper regulation of DNA replication and activation of the spindle assembly checkpoint (Spruck *et al* 1999, Hernando *et al* 2004). The connection between

chromosome instability caused by defective condensation in pRB mutants, and deregulated cell cycle control is less clear. For example, wild-type embryonic stem cells lack a pRB-dependent G1 arrest mechanism, but display CIN phenotypes caused by pRB deficiency (Frame and Balmain 1999, Zheng *et al* 2002). For this reason, it remains to be determined whether elevated cyclin-dependent kinase activity (the most common way of eliminating pRB function in cancer) compromises pRB's role in chromosome condensation, beyond causing aneuploidy through elevated E2F-mediated transcription.

As mentioned, heterozygous *Rb1*$^{+/-}$ mice are cancer prone and develop pituitary tumors by 1 year of age, the majority of which have lost the remaining wild-type *Rb1* allele (Jacks *et al* 1992); in this regard, they recapitulate the steps of the two-hit hypothesis quite faithfully. There are no reported attempts to evaluate CIN in these tumors, or any others created by conditional deletion of *Rb1* in a specific tissue. However, it would be difficult to discern the contribution of CIN to an *Rb1*-deficient cancer model in isolation from the effects of deregulated proliferation when using null alleles of *Rb1*. The recently generated mouse strain called *Rb1*-ΔL has demonstrated a connection between pRB-mediated chromosome condensation and tumor suppression and this will be explored in chapters to follow (Coschi *et al* 2010).

1.6 Hypothesis and objectives

As it has been introduced, the LXCXE binding cleft is the most highly conserved region among pocket proteins and across several species of retinoblastoma protein (Lee *et al* 1998). However, it is also targeted by viral oncoproteins, rendering the retinoblastoma protein non-functional and susceptible to degradation (Whyte *et al* 1988, DeCaprio *et al* 1988, Dyson *et al* 1989). If the LXCXE binding cleft was not uniquely important for overall protein function, it would not remain so conserved over evolutionary time, given its susceptibility to viral oncoproteins. It is possible that any unique roles of the LXCXE binding cleft are masked by loss of the entire protein when proliferative control is concomitantly lost (a phenotype which appears dominant over other more subtle ones). Therefore I hypothesize that the LXCXE binding cleft of pRB makes a unique

contribution to pRB-mediated tumor suppression by facilitating chromosome stability outside of regulating the G1- to S-phase transition. As such, the overall aims of this thesis are to determine the unique contribution of the LXCXE binding cleft to pRB-mediated tumor suppression, and the mechanism(s) by which it does so, utilizing the *Rb1*$^{\Delta L/\Delta L}$ mouse.

In Chapter 2, I describe a tumor study whereby we crossed *Rb1*$^{\Delta L/\Delta L}$ mice with both *Trp53*$^{-/-}$ and *Trp53*$^{+/-}$ mice to investigate the contribution of the LXCXE binding cleft to pRB-mediated tumor suppression (Coschi *et al* 2010). The addition of the *Rb1*$^{\Delta L}$ mutation to *Trp53*$^{+/-}$ tumor prone mice accelerated LOH of wild type *Trp53*. Moreover, there was a significant increase in whole-CIN in tumors from *Rb1*$^{\Delta L/\Delta L}$; *Trp53*$^{-/-}$ mice compared to *Trp53*$^{-/-}$ controls. Building on previously published data from our lab, I establish an interaction between pRB and the Condensin II complex which requires the LXCXE binding cleft of pRB. When this interaction is compromised, cells exhibit chromosome condensation and segregation defects (Coschi *et al* 2010). This critical role for pRB in chromosome condensation is therefore an essential aspect of pRB-mediated tumor suppression.

Data reported in Chapter 3 dissect the mechanism by which pRB interacts with the Condensin II complex and facilitates genome stability. I report a novel complex comprised of pRB, E2F1 and Condensin II which localizes to centromeres and prevents the accumulation of DNA damage following S-phase. This mechanism was found to be dependent upon the gene dosage of *Rb1*. Using cells from retinoblastoma patients (*RB1*$^{+/-}$), and copy number data from *RB1*$^{+/+}$, *RB1*$^{+/-}$ and *RB1*$^{-/-}$ cancer cell lines reported in the COSMIC database, I demonstrate that hemizygosity of *RB1* creates a haploinsufficiency that likely functionally contributes to tumorigenesis in humans.

1.7 References

Abe, S., Nagasaka, K., Hirayama, Y., Kozuka-Hata, H., Oyama, M., Aoyagi, Y., Obuse, C., Hirota, T. 2011. The initial phase of chromosome condensation requires Cdk1-mediated phosphorylation of the CAP-D3 subunit of condensin II. *Genes & Development* **25**(8): 863-74.

Akai, Y., Kurokawa, Y. Nakazawa, N., Tonami-Murakami, Y. Suzuki, Y., Yoshimura, S. H., Iwasaki, H., Shiroiwa, Y., Nakamura, T., Shibata, E., Yanagida, M. 2011. Opposing role of condensin hinge against replication protein A in mitosis and interphase through promoting DNA annealing. *Open Biology* **1**:110023.

Anderson, D. E., Losada, A., Erickson, H. O., Hirano, T. 2002. Condensin and cohesin display different conformations with characteristic hinge angles. *Journal of Cell Biology* **156**(3): 419-24.

Arumugam, P., Gruber, S., Tanaka, K., Haering, C. H., Mechtler, K., Nasmyth, K. 2003. ATP hydrolysis is required for cohesin's association with chromosomes. *Current Biology* **13**(22): 1941-53.

Avni, D., Yang, H., Martelli, F., Hofmann, F., El Shamy, W. M., Ganesan, S., Scully, R., Livingston, D. M. 2003. Active localization of the retinoblastoma protein in chromatin and its response to S phase DNA damage. *Molecular Cell* **12**(3): 735-46.

Bagchi, S., Weinmann, R., Raychaudhuri, P. 1991. The retinoblastoma protein copurifies with E2F-I, and E1A-regulated inhibitor of the transcription factor E2F. *Cell* **65**(6): 1063-72.

Bandara, L. R., La Thangue, N. B. 1991. Adenovirus-E1A prevents the retinoblastoma gene-product from complexing with a cellular transcription factor. *Nature* **351**(6326): 494-97.

Batty, D. P., Wood, R. D. 2000. Damage recognition in nucleotide excision repair of DNA. *Gene* **241**(2): 193-204.

Berman, S. D., Yuan, T. L., Miller, E. S., Lee, E. Y., Caron, A., Lees, J. A. 2008. The retinoblastoma protein tumor suppressor is important for appropriate osteoblast differentiation and bone development. *Molecular Cancer Research* **6**(9): 1440-51.

Besson, A., Dowdy, S. F., Roberts, J. M. 2008. CDK inhibtors: Cell cycle regulators and beyond. *Developmental Cell* **14**(2): 159-69.

Blake, M. C., Azizkhan, J. C. 1989. Transcription factor E2F is required for efficient expression of the hamster dihydrofolate-reductase gene *in vitro* and *in vivo*. *Molecular and Cellular Biology* **9**(11): 4994-5002.

Bond, G. L., Hu, W., Bond, E. E., Robins, H., Lutzker, S. G., Arva, N. C., Bargonetti, J., Bartel, F., Taubert, H., Wuerl, P., Onel, K., Yip, L., Hwang, S. J., Strong, L. C., Lozano, G., Levine, A. J. 2004. A single nucleotide polymorphism in the MDM2 promoter attenuates the p53 tumor suppressor pathway and accelerates tumor formation in humans. *Cell* **119**(5): 591-602.

Bookstein, R., Rio, P., Madreperla, S. A., Hong, F., Allred, C., Grizzle, W. E., Lee, W. H. 1990a. Promoter deletion and loss of retinoblastoma gene-expression in human prostate carcinoma. *PNAS USA* **87**(19): 7762-66.

Bookstein, R., Shew, J. Y., Chen, P. L., Scully, P., Lee, W. H. 1990b. Suppression of tumorigenicity of human prostate carcinoma-cells by replacing a mutated RB gene. *Science* **247**(4943): 712-15.

Boveri, T. 1912. Anton Dohbn. *Science* **36**(928): 453-68.

Boveri, T. 2008. Concerning the origin of malignant tumours by Theodor Boveri. Translated and annotated by Henry Harris. *Journal of Cell* Science **121**(Suppl 1): 1-84.

Brehm, A., Miska, E. A., McCance, D. J., Reid, J. L., Bannister, A. J., Kouzarides, T. 1998. Retinoblastoma protein recruits histone deacetylase to repress transcription. *Nature* **391**(6667): 597-601.

Bremner R., Cohen, B. L., Spota, M., Hamel, P. A., Ingles, C. J., Gallie, B. L., Phillips, R. A. 1995. Direct transcriptional repression by pRB and its reversal by specific cyclins. *Molecular and Cellular Biology* **15**(6): 3256-65.

Bruce, J. L., Hurford, R. K. J., Classon, M., Koh, J., Dyson, N. 2000. Requirements for cell cycle arrest by p16INK4a. *Molecular Cell* **6**(3): 737-42.

Campisi, J., di Fagagna, F. D. 2007. Cellular senescence: when bad things happen to good cells. *Nature Reviews Molecular Cell Biology* **8**(9): 729-740.

Carnevale, J., Palander, O., Seifried, L. A., Dick, F. A. 2012. DNA Damage Signals through Differentially Modified E2F1 Molecules To Induce Apoptosis. *Molecular and Cellular BiologyMolecular and Cellular Biology* **32**(5): 900-12.

Catalogue Of Somatic Mutations In Cancer (COSMIC) database- http://www.sanger.ac.uk/genetics/CGP/cosmic/

Cecchini, M. J., Dick, F. A. 2011. The biochemical basis of CDK phosphorylation-independent regulation of E2F1 by the retinoblastoma protein. *Biochemical Journal* **434**: 297-308.

Chan, H. M., Krstic-Demonacos, M., Smith, L., Demonacos, C., La Thangue, N. B. 2001. Acetylation control of the retinoblastoma tumor-suppressor protein. *Nature Cell Biology* **3**(7): 667-74.

Chan, H. M., Smith, L., La Thangue, N. B. 2001. Role of LXCXE motif-dependent interactions in the activity of the retinoblastoma protein. *Oncogene* **20**(43): 6152-63.

Chau, B. N., Pan, C. W., Wang, J. Y. J. 2006. Separation of Anti-Proliferation and Anti-Apoptotic Functions of Retinoblastoma Protein through Targeted Mutations of Its a/B Domain. *PLOS ONE* **1**(1): e82.

Chellappan, S. P., Hiebert, S., Mudryj, M., Horowitz, J. M., Nevins, J. R. 1991. The E2F transcription factor is a cellular target for the RB protein. *Cell* **65**(6): 1053-61.

Chen, T. T., Wang, J. Y. J. 2000. Establishment of irreversible growth arrest in myogenic differentiation requires the RB LXCXE-binding function. *Molecular and Cellular Biology* **20**(15): 5571-80.

Chittenden, T., Livingston, D. M., DeCAprio, J. A. 1993. Cell-cycle analysis of E2F in primary human T-cells reveals novel E2F complexes and biochemically distinct forms of free E2F. *Molecular and Cellular Biology* **13**(7): 3975-83.

Chittenden, T., Livingston, D. M., Kaelin, W. G. 1991. The T/E1A-binding domain of the retinoblastoma product can interact selectively with a sequence-specific DNA-binding protein. *Cell* **65**(6): 1073-82.

Choi, E., Lee, H. 2008. Chromosome damage in mitosis induces BubR1 activation and prometaphase arrest. *FEBS Letters* **582**(12): 1700-06.

Chow, J. N. B., Starostik, P., Dean, D. C., 1996. The rb family contains a conserved cyclin-dependent kinase-regulated transcriptional repressor motif. *Molecular and Cellular Biology***16**(12): 7173-81.

Chow, K. N. B., Dean, D. C. 1996. Domains A and B in the Rb pocket interact to form a transcriptional repressor motif. *Molecular and Cellular Biology***16**(9): 4862-68.

Cimini, D., Howell, B., Maddox, P., Khodjakov, A., Degrassi, F., Salmon, E. D. 2001. Merotelic kinetochore orientation is a major mechanism of aneuploidy in mitotic mammalian tissue cells. *Journal of Cell Biology* **153**(3): 517-27.

Clarke, A. R., Maandag, E. R., Vanroon, M., Vanderlugt, N. M. T., Vandervalk, M., Hooper, M. L., Berns, A., Riele, H. T. 1992. Requirement for a functional RB-1 gene in murine development. *Nature* **359**(6393): 328-30.

Classon, M., Dyson, N. 2001. p107 and p130: versatile proteins with interesting pockets. *Experimental Cell Research* **264**(1): 135-47.

Classon, M., Kennedy, B. K., Mulloy, R., Harlow, E. 2000. Opposing roles of pRB and p107 in adipocyte differentiation. *PNAS USA* **97**(20): 10826-31.

Clemente-Blanco, A., Mayan-Santos, M., Schneider, D. A., Machin, F., Jarmuz, A., Tschochner, H., Aragon, L. 2009. Cdc14 inhibits transcription by RNA polymerase I during anaphase. *Nature* **458**(7235): 219-22.

Clift, D., Bizzari, F., Marston, A. L. 2009. Shugoshin prevents cohesin cleavage by PP2A(Cdc55)-dependent inhibition of separase. *Genes & Development* **23**(6): 766, 780.

Cobbe, N., Heck, M. M. S. 2004. The evolution of SMC proteins: Phylogenetic analysis and structural implications. *Molecular Biology and Evolution* **21**(2): 332-47.

Cobrinik, D., Lee, M. H., Hannon, G., Mulligan, G., Bronson, R. T., Dyson, N., Harlow, E., Beach, D., Weinberg, R. A., Jacks, T. 1996. Shared role of the pRB-related p130 and p107 proteins in limb development. *Genes & Development* **10**(13): 1633-44.

Cobrinik, D., Whyte, P., Peeper, D. S., Jacks, T., Weinberg, R. R. 1993. Cell cycle-specific association of E2F with the p130 E1A-binding protein. *Genes & Development* **7**(12A): 2392-2404.

Corbeil, H. B., Whyte, P., Branton, P. E. 1995. Characterization of transcription factor E2F complexes during miscle and neuronal differentiation. *Oncogene* **11**(5): 909-20.

Coschi, C. H., Martens, A. L., Ritchie, K., Francis, S. M., Chakrabarti, S., Bérubé, N. G., Dick, F. A. 2010. Mitotic chromosome condensation mediated by the retinoblastoma protein is tumor-suppressive. *Genes & Development* **24**(13): 1351-63.

Dahiya, A., Gavin, M. R., Luo, R. X., Dean, D. C. 2000. Role of the LXCXE binding site in Rb function. *Molecular and Cellular Biology* **20**(18): 6799-6805.

Dannenberg, J. H., van Rossum, A., Schuijff, L., Riele, H. T. 2000. Ablation of the Retinoblastoma gene family deregulates G(1) control causing immortalization and increased cell turnover under growth-restricting conditions. *Genes & Development* **14**(23): 3051-64.

De Falco, G., Comes, F., Simone, C. 2006. pRB: master of differentiation. Coupling irreversible cell cycle withdrawal with induction of muscle-specific transcription. *Oncogene* **25**(38): 5244-49.

De Piccoli, G., Torres-Rosell, J., Aragon, L. 2009. The unnamed complex: what do we know about Smc5-Smc6? *Chromosome Research* **17**(2): 251-63.

DeCaprio, J. A., Ludlow, J. W., Figge, J., Shew, J. Y., Huang, C. M., Lee, W. H., Marsilio, E., Paucha, E., Livingston, D. M. 1988. SV40 large tumor-antigen forms a specific complex with the product of the retinoblastoma susceptibility gene. *Cell* **54**(2): 275-83.

DeCaprio, J. A., Ludlow, J. W., Lynch, D., Furukawa, Y., Griffin, J., Piwnicaworms, H., Huang, C. M., Livingston, D. M. 1989. The product of the retinoblastoma susceptibility gene has properties of a cell-cycle regulatory element. *Cell* **58**(6): 1085-95.

Dick F. A. 2007. Structure-function analysis of the retinoblastoma tumor suppressor protein- is the whole a sum of its parts? *Cell Division* **2**:26.

Dick, F. A., Dyson, N. 2003. pRB contains an E2F1-specific binding domain that allows E2F1-induced apoptosis to be regulated separately from other E2F activities. *Molecular Cell* **12**(3): 639-49.

Dick, F. A., Sailhamer, E., Dyson, N. J. 2000. Mutagenesis of the pRB pocket reveals that cell cycle arrest functions are separable from binding to viral oncoproteins. 2000. *Molecular and Cellular Biology* **20**(10): 3715-27.

Dunaief, J. L., King, A., Esumi, N., Eagen, M., Dentchev, T., Sung, C. H., Chen, S., Zack, D. J. 2002. Protein Phosphatase 1 binds strongly to the retinoblastoma protein but not to p107 or p130 *in vitro* and *in vivo*. *Current Eye Research* **24**(5): 392-96.

Dunaief, J. L., Strober, B. E., Guha, S., Khavari, P. A., Alin, K., Luban, J., Begemann, M., Crabtree, G. R., Goff, S. P. 1994. The retinoblastoma protein and BRG1 form a complex and cooperate to induce cell-cycle arrest. *Cell* **79**(1): 119-30.

Dyson, N. 1998. The regulation of E2F by pRB-family proteins. *Genes & Development* **12**(15): 2245-62.

Dyson, N., Guida, P., McCall, C., Harlow, E. 1992. Adenovirus-E1A makes 2 distinct contacts with the retinoblastoma protein. *Journal of Virology* **66**(7): 4606-11.

Dyson, N., Howley, P. M., Munger, K., Harlow, E. 1989. The human papilloma virus-16 E7-oncoprotein is able to bind to the retinoblastoma gene-product. *Science* **243**(4893): 934-37.

Elowe, S., Dulla, K., Uldschmid, A., Li, X., Dou, Z., Nigg, E. A. 2010. Uncoupling of the spindle-checkpoint and chromosome-congression functions of BubR1. *Journal of Cell Science* **123**(1): 84-94.

Ewen, M. E., Ludlow, J. W., Marsilio, E., DeCaprio, J. A., Millikan, R. C., Cheng, S. H., Paucha, E., Livingston, D. M. 1989. An N-terminal transformation-governing sequence of SV40 large T-antigen contributes to the binding of both P110RB and a 2nd cellular proteins, p120. *Cell* **58**(2): 257-67.

Ewen, M. E., Xing, Y. G, Lawrence, J. B., Livingston, D. M. 1991. Molecular-cloning, chromosomal mapping, and expression of the cDNA for p107, a retinoblastoma gene product-related protein. *Cell* **66**(6): 1155-64.

Falls H. F. and Neel, J. V. 1951. Genetics of retinoblastoma. *AMA Archives of Ophthalmology* **46**(4): 367-89.

Fazzio, T. G. and Panning, B. 2010. Condensin complexes regulate mitotic progression and interphase chromatin structure in embryonic stem cells. *Journal of Cell Biology* **188**(4): 491-503.

Felsher, D. W., Zetterberg, A., Zhu, J., Tlsty, T., Bishop, J. M. 2000. Overexpression of MYC causes p53-dependent G2 arrest of normal fibroblasts. *PNAS USA* **97**(19): 10544-48.

Flemington, E. K., Speck, S. H., Kaelin, W. G. Jr., 1993. E2F-1 mediated transactivation is inhibited by complex formation with the retinoblastoma susceptibility gene product. *PNAS USA* **90**(15): 6914-18.

Folco, H. D., Pidoux, A. L., Urano, T., Allshire, R. C. 2008. Heterochromatin and RNAi are required to establish CEMP-A chromatin at centromeres. *Science* **319**(5859): 94-97.

Frame, S., Balmain, A. 1999. Target genes and target cells in carcinogenesis. *British Journal of Cancer* **80**(Suppl 1): 28-33.

Francis, S. M., Bergsied, J., Isacac, C. E., Coschi, C. H., Martens, A. L., Hojilla, C. V., Chakrabarti, S., DiMattia, G. E., Khokha, R., Wang, J. Y. J., Dick, F. A. 2009. A Functional Connection between pRB and Transforming Growth Factor beta in Growth Inhibition and Mammary Gland Development. *Molecular and Cellular Biology* **29**(16): 4455-66.

Friend, S. H., Bernards, R., Rogelj, S., Weinberg, R. A., Rapaport, J. M., Albert, D. M., Dryja, T. P. 1986. A human DNA segment with properties of the gene that predisposes to retinoblastoma and osteosarcoma. *Nature* **323**(6089): 643-46.

Funayama, R., Saito, M., Tanobe, H., Ishikawa, F. 2006. Loss of linker histone H1 in cellular senescence. *Journal of Cell Biology* **175**(6): 869-80.

Garriga, J., Jayaraman, A. L., Limon, A., Jayadeva, G., Sotillo, E., Truongcao, M., Patsialou, A., Wadzinski, B. E., Grana, X. 2004. A dynamic equilibrium between CDKs and PP2A modulates phosphorylation of pRB, p107 and p130. *Cell Cycle* **2**(10): 1320-30.

Geigl, J. B., Obenauf, A. C., Schwarzbraun, T., Speicher, M. R. 2008. Defining 'chromosomal instability'. *Trends in Genetics* **24**(2): 64-69.

Gerlich, D., Hirota, T., Koch, B., Peters, J. M., Ellenberg, J. 2006. Condensin I stabilizes chromosomes mechanically through a dynamic interaction in live cells. *Current Biology* **16**(4): 333-44.

Giménez-Abián, J. F., Sumara, I., Hirota, T., Hauf, S., Gerlich, D., de la Torre, C., Ellenberg, J., Peters, J. M. 2004. Regulation of sister chromatid cohesion between chromosome arms. *Current Biology* **14**(13): 1187-93.

Gonzalo, S., Garcia-Cao, M., Fraga, M. F., Schotta, G., Peters, A. H., Cotter, S. E., Eguia, R., Dean, D. C., Esteller, M., Jenuwein, T., Blasco, M. A. 2005. Role of the RB1 family in stabilizing histone methylation at constitutive heterochromatin. *Nature Cell Biology* **7**(4): 420-28.

Goodrich, D. W., Wang, N. P., Qian, Y. W., Lee, E. Y., Lee, W. H. 1991. The retinoblastoma gene product regulates progression through the G1 phase of the cell cycle. *Cell* **67**(2): 293-302.

Gosling, K. M., Goodnow, C. C., Verma, N. K., Fahrer, A. M. 2008. Defective T-cell function leading to reduced antibody production in a kleisin-beta mutant mouse. *Immunology* **125**(2): 208-17.

Gosling, K. M., Makaroff, L. E., Theodoratos, A., Kim, Y. H., Whittle, B., Rui, L. X., Wu, H., Hong, N. A., Kennedy, g. G., Fritz, J. A., Yates, A. L., Goodnow, C. C., Fahrer, A. M. 2007. A mutation in a chromosome condensin II subunit, kleisin beta, specifically disrupts T cell development. *PNAS USA* **104**(30): 12445-50.

Grilley, M., Holmes, J., Yashar, B., Modrich, P. 1990. Mechanisms of DNA-mismatch correction. *Mutation Research* **236**(2): 253-67.

Gruber, S., Haering, C. H., Nasmyth, K. 2003. Chromosomal cohesin forms a ring. *Cell* **112**(6): 765-77.

Gutierrez, G. M., Kong, E., Sabbagh, Y., Brown, N. E., Lee, J. S., Demay, M. B., Thomas, D. M., Hinds, P. W. 2008. Impaired bone development and increased mesenchymal progenitor cells in calvaria of *RB1*$^{-/-}$ mice. *PNAS USA* **105**(47): 18402-07.

Haering, C. H., Lowe, J., Hochwagen, A., Nasmyth, K. 2002. Molecular architecture of SMC proteins and the yeast cohesin complex. *Molecular Cell* **9**(4): 773-88.

Haering, C. H., Schoffnegger, D., Nishino, T., Helmhart, W., Nasmyth, K., Lowe, J. 2004. Structure and stability of cohesin's Smc1-kleisin interaction. *Molecular Cell* **15**(6): 951-64.

Haeusler, R. A., Pratt-Hyatt, M., Good, P. D., Gipson, T. A., Engelke, D. R. 2008. Clustering of yeast tRNA genes is mediated by specific association of condensin with tRNA gene transcription complexes. *Genes & Development* **22**(16): 2204-14.

Hagstrom, K. A., Holmes, V. F., Cozzarelli, N. R., Meyer, B. J. 2002 C. elegans condensin promotes mitotic chromosome architecture, centromere organization, and sister chromatid segregation during mitosis and meiosis. *Genes & Development* **16**(6): 729-42.

Ham, M. F., Takakuwa, T., Rahadiani, N., Tresnasari, K., Nakajima, H., Aozasa, K. 2007. Condensin mutations and abnormal chromosomal structures in pyothorax-associated lymphoma. *Cancer Science* **98**(7): 1041-47.

Hanahan, D., Weinberg, R. A. 2000. The hallmarks of cancer. *Cell* **100**(1): 57-70

Hanahan, D., Weinberg, R. A. 2011. Hallmarks of cancer: the next generation. *Cell* **144**(5): 646-74.

Hannon, G. J., Demetrick, D., Beach, D. 1993. Isolation of the RB-related p130 through its interaction with CDK2 and cyclins. *Genes & Development***7**(12A):2378-2391.

Hansen, J. B., Jorgensen, C., Petersen, R. K., Hallenborg, P., De Matteis, R., Boye, H. A., Petrovic, N., Enerback, S., Nedergaard, J., Cinti, S., te Rielet, H., Kristiansen, K. 2004. Retinoblastoma protein functions as a molecular switch determining white versus brown adipocyte differentiation. *PNAS USA* **101**(12):4112-17.

Harbour, J. W., Lai, S. L., Whangpeng, J., Gazdar, A. F., Minna, J. D., Kaye, F. J. 1988. Abnormalities in structure and expression of the human retinoblastoma gene in SCLC. *Science* **241**(4863): 353-57.

Hartl, T. A., Smith, H. F., Bosco, G. 2008. Chromosome Alignment and Transvection Are Antagonized by Condensin II. *Science* **322**(5906): 1384-87.

Hauschka, T. S. 1953. Cell population studies on mouse ascites tumors. *Transactions of the New York Academy of Sciences* **16**(2): 64-73.

Hauschka, T. S. 1958. Correlation of chromosomal and physiologic changes in tumors. *Journal of Cellular Physiology Supplement* **52**(Supp 1): 197-233.

Hauschka, T. S., Levan, A. 1958. Cytologic and functional characterization of single cell clones isolated from the Krebs-2 and Ehrlich ascites tumors. *Journal of the National Cancer Institute* **21**(1): 77-135.

Helin, K., Harlow, E., Fattaey, A. 1993. Inhibition of E2F-1 transactivation by direct binding of the retinoblastoma protein. *Molecular and Cellular Biology* **13**(10): 6501-08.

Hernando, E., Nahle, Z., Juan, G., Diaz-Rodriguez, E., Alaminos, M., Hemann, M., Michel, L., Mittal, V., Gerald, W., Benezra, R., Lowe, S. W., Cordon-Cardo, C. 2004. Rb inactivation promotes genomic instability by uncoupling cell cycle progression from mitotic control. 2004. *Nature* **430**(7001): 797-802.

Herwig, S., Strauss, M. 1997. The retinoblastoma protein: a master regulator of cell cycle, differentiation and apoptosis. *European Journal of Biochemistry* **246**(3): 581-601.

Hiebert, S. W., Chellappan, S. P., Horowitz, J. M., Nevins, J. R. 1992. The interaction of RB with E2F coincides with an inhibition of the transcriptional activity of E2F. *Genes & Development* **6**(2): 177-85.

Hiebert, S. W., Lipp, M., Nevins, J. R. 1989. E1A-dependent trans-activation of the human myc promoter is mediated by the E2F factor. *PNAS USA* **86**(10): 3594-98.

Hinck, L., Nathke, I. S., Papkoff, J., Nelson, W. J. 1994. Dynamics of cadherin/catenin complex formation: novel protein interactions and pathways of complex assembly. *Journal of Cell Biology* **125**(6): 1327-40.

Hirano, M., Anderson, D. E., Erickson, H. P., Hirano, T. 2001. Bimodal activation of SMC ATPase by intra- and inter-molecular interactions. *EMBO Journal* **20**(12): 3238-50.

Hirano, M., Hirano, T. 2002. Hinge-mediated dimerization of SMC protein is essential for its dynamic interaction with DNA. *EMBO Journal* **21**(21): 5733-44.

Hirano, M., Hirano, T. 2004. Positive and negative regulation of SMC-DNA interactions by ATP and accessory proteins. *EMBO Journal* **23**(13): 2664-73.

Hirota, T., Gerlich, D., Koch, B., Ellenberg, J., Peters, J. M. 2004. Distinct functions of condensin I and II in mitotic chromosome assembly. *Journal of Cell Science* **117**(26): 6435-45.

Horowitz, J. M., Yandell, D. W., Park, S. H., Canning, S., Whyte, P., Buchkovich, K., Harlow, E., Weinberg, R. A., Dryja, T. P. 1989. Point mutational inactivation of the retinoblastoma antioncogene. *Science* **243**(4893): 937-40.

Hu, Q. J., Dyson, N., Harlow, E. 1990. The regions of the retinoblastoma protein needed for binding to adenovirus-E1A or adenovirus-SV40 large T-antigen are common sites for mutations. *EMBO Journal* **9**(4): 1147-55.

Huang, H. J. S., Yee, J. K., Shew, J. Y., Chen, P. L., Bookstein, R., Friedmann, T., Lee, E. Y. H. P., Lee, W. H. 1988. Suppression of the neoplastic phenotype by replacement of the RB gene in human cancer-cells. *Science* **242**(4885): 1563-66.

Huen, M. S., Sy, S. M., Chen, J. 2010. BRCA1 and its toolbox for the maintenance of genome integrity. *Nature Reviews Molecular Cell Biology* **11**(2): 138-48.

Hurford, R. K. Jr., Cobrinik, D., Lee, M. H., Dyson, N. 1997. pRB and p107/p130 are required for the regulated expression of different sets of E2F responsive genes. *Genes & Development* **11**(11): 1447-63.

Ide, S., Miyazaki, T., Maki, H., Kobayashi, T. 2010. Abundance of Ribosomal RNA Gene Copies Maintains Genome Integrity. *Science* **327**(5966): 693-96.

Ionov, Y., Peinado, M. A., Malkhosyan, S., Shibata, D., Perucho, M. 1993. Ubiquitous somatic mutations in simple repeated sequences reveal a new mechanism for colonic carcinogenesis. *Nature* **363**(6429): 558-61.

Isaac, C. E., Francis, S. M., Martens, A. L., Julian, L. M., Seifried, L. A., Erdmann, N., Binne, U. K., Harrington, L., Sicinski, P., Bérubé, N. G., Dyson, N. J., Dick, F. A. 2006. The retinoblastoma protein regulates pericentric heterochromatin. *Molecular and Cellular Biology* **26**(9): 3659-71.

Iwasaki, O., Tanaka, A., Tanizawa, H., Grewal, S. I. S., Noma, K. 2010. Centromeric Localization of Dispersed Pol II Genes in Fission Yeast. *Molecular Biology of the Cell* **21**(2): 254-65.

Jacks, T., Fazeli, A., Schmitt, E. M., Bronson, R. T., Goodell, M. A., Weinberg, R. A. 1992. Effects of an Rb mutation in the mouse. *Nature* **359**(6393): 295-300.

Joerger, A. A., Fersht, A. R. 2007. Structural biology of the tumor suppressor p53 and cancer-associated mutants. *Advances in Cancer Research* **97**: 1-23.

Johzuka, K., Horiuchi, T. 2007. RNA polymerase I transcription obstructs condensin association with 35S rRNA coding regions and can cause contraction of long repeat in Saccharomyces cerevisiae. *Genes to Cells* **12**(6): 759-71.

Johzuka, K., Terasawa, M., Ogawa, H., Ogawa, T., Horiuchi, T. 2006. Condensin loaded onto the replication fork barrier site in the rRNA gene repeats during S phase in a FOB1-dependent fashion to prevent contraction of a long repetitive array in Saccharomyces cerevisiae. *Molecular and Cellular Biology* **26**(6): 2226-36.

Joukov, V., Groen, A. C., Prokhorova, T., Gerson, R., White, E., Rodriguez, A., Walter, J. C., Livingston, D. M. 2006. The BRCA1/BARD1 heterodimer modulates ran-dependent mitotic spindle assembly. *Cell* **127**(3): 539-52.

Julian, L. M., Palander, O., Seifried, L. A., Foster, J. E. G., Dick, F. A. 2008. Characterization of an E2F1-specific binding domain in pRB and its implications for apoptotic regulation. *Oncogene* **27**(11): 1572-79.

Kastan, M. B., Onyekwere, O., Sidransky, D., Vogelstein, B., Craig, R. W. 1991. Participation of p53 protein in the cellular response to DNA damage. *Cancer Res*earch **51**(23): 6304-11.

Katis, V. L., Galova, M., Rabitsch, K. P., Gregan J., Nasmyth, K. 2004. Maintenance of cohesin at centromeres after meiosis I in budding yeast requires a kinetochore-associated protein related to MEI-S332. *Current Biology* **14**(7): 560-72.

Kimura, K. and Hirano, T. 1997. ATP-dependent positive supercoiling of DNA by 13S condensin: A biochemical implication for chromosome condensation. *Cell* **90**(4): 625-34.

Kimura, K., Hirano, M., Kobayashi, R., Hirano, T. 1998. Phosphorylation an activation of 13S condensin by Cdc2 *in vitro*. *Science* **282**(5388): 487-90.

Kimura, K., Rybenkov, V. V., Crisona, N. J., Hirano, T., Cozzarelli, N. R. 1999. 13S condensin actively reconfigures DNA by introducing global positive writh: Implications for chromosome condensation. *Cell* **98**(2): 239-48.

Kitajima, T. S., Kawashima, S. A., Watanabe, Y. 2004. The conserved kinetochore protein shugoshin protects centromeric cohesin during meiosis. *Nature* **427**(6974): 510-17.

Knudsen, K. E., Booth, D., Naderi, S., Sever-Chroneos, Z., Fribourg, A. F., Hunton, I. C., Feramisco, J. R., Wang, J. Y., Knudsen E. S. 2000. RB-dependent S-phase response to DNA damage. *Molecular and Cellular Biology* **20**(20): 7751-63.

Knudson, A. G. 1971. Mutation and cancer- Statistical study of retinoblastoma. *PNAS USA* **68**(4):820-823.

Korenjak, M., Brehm, A. 2005. E2F-Rb complexes regulating transcription of genes important for differentiation and development. *Current Opinion in Genetics & Development* **15**(5): 520-27.

Lacy, S., Whyte, P. 1997. Identification of a p130 domain mediating interactions with cyclin A/cdk2 and cyclin E/cdk2 complexes. *Oncogene* **14**(20): 2395-2406.

Lai, A., Lee, J. M., Yang, W. M., DeCaprio, J. A., Kaelin, W. G. Jr., Seto, E., Branton, P. E. 1999. RBP1 recruits both histone deacetylase-dependent and –independent repression activities to retinoblastoma family proteins. *Molecular and Cellular Biology* **19**(10): 6632-41.

Lammens, A., Schele, A., Hopfner, K. P. 2004. Structural biochemistry of ATP-driven dimerization and DNA-stimulated activation of SMC ATPases. *Current Biology* **14**(19): 1778-82.

Lane, D. P. 1992. Cancer. p53, guardian of the genome. *Nature* **358**(6381): 15-16.

Lavia, P., Jansen-Durr, P. 1999. E2F target genes and cell-cycle checkpoint control. *Bioessays* **21**(3): 221-30.

Lee, E. Y. H. P., Chang, C. Y., Hu, N. P., Wang, Y. C. J., Lai, C. C., Herrup, K., Lee, W. H., Bradley, A. 1992. *Nature* **359**(6393): 288-94.

Lee, E. Y. H. P., To, H., Shew, J. Y., Bookstein, R., Scully, P., Lee, W. H. 1988. Inactivation of the retinoblastoma susceptibility gene in human-breast cancers. *Science* **241**(4862): 218-221.

Lee, J., Ogushi, S., Saitou, M., Hirano, T. 2011. Condensins I and II are essential for construction of bivalent chromosome in mouse oocytes. *Molecular Biology of the Cell* **22**(18): 3465-77.

Lee, K. Y., Ladha, M. H., McMahon, C., Ewen, M. E. 1999. The retinoblastoma protein is linked to the activation of Ras. *Molecular and Cellular Biology* **19**(11): 7724-32.

Lee, M. H., Williams, B. O., Mulligan, G., Mukai, S., Bronson, R. T., Dyson, N., Harlow, E., Jacks, T. 1996. Targeted disruption of p107: Functional overlap between p107 and Rb. *Genes & Development* **10**(13): 1621-32.

Lee. J. O., Russo, A. A., Pavletich, N. P. 1998. Structure of the retinoblastoma tumor-suppressor pocket domain bound to a peptide from HPV E7. *Nature***391**(6670: 859-65.

Lehman, A. R. 2005. The role of SMC proteins in the responses to DNA damage. *DNA Repair* **4**(3): 309-14.

Li, Y., Craham, C., Lacy, S., Duncan, A. M. V., Whyte, P. 1993. The adenovirus-E1A-associated 130-KD protein is encoded by a member of the retinoblastoma gene family and physically interacts with cyclin-A and cyclin-E. *Genes & Development* **7**(12A): 2366-77.

Lipp J. J., Hirota, T., Poser, I., Peters, J. M. 2007. Aurora B controls the association of condensin I but not condensin II with mitotic chromosomes. *Journal of Cell Science* **120**(7): 1245-55.

Litovchick, L., Sadasivam, S., Florens, L., Zhu, X., Swanson, S. K., Velmurugan, S., Chen, R., Washburn, M. P., Lie, X. S., DeCaprio, J. A. 2007. Evolutionarily conserved multisubunit RBL2/p130 and E2F4 protein complex represses human cell cycle-dependent genes in quiescence. *Molecular Cell* **26**(4): 539-51.

Lohmann, D. R. 1999. RB1 gene mutations in retinoblastoma. *Human Mutation* **14**(4): 283-88.

Lohmann, D. R., Brandt, B., Hopping, W., Passarge, E., Horsthemke, B. 1994. Distinct RB-1 gene-mutations with low penetrance in hereditary retinoblastoma. *Human Genetics* **94**(4): 249-54.

Longworth, M. S., Herr, A., Ji, J. Y., Dyson, N. J. 2008. RBF1 promotes chromatin condensation through a conserved interaction with the Condensin II protein dCAP-D3. *Genes & Development* **22**(8): 1011-1024.

Losada, A., Hirano, M., Hirano, T. 2002. Cohesin release is required for siter chromatid resolution, but not for condensin-mediated compaction, at the onset of mitosis. *Genes & Development* **16**(23): 3004-16.

Losada, A., Hirano, T. 2005. Dynamic molecular linkers of the genome: the first decade of SMC proteins. *Genes & Development* **19**(11): 1269-87.

Losada, A., Yokochi, T., Kobayashi, R., Hirano, T. 2000. Identification and characterization of SA/Scc3p subunits in the Xenopus and human cohesin complexes. *Journal of Cell Biology* **150**(3): 405-16.

Luo, R. X., Postigo, A. A., Dean, D. C. 1998. Rb interacts with histone deacetylase to repress transcription. *Cell* **92**(4): 463-73.

Maandag, E. C. R., Vandervalk, M., Vlaar, M., Feltkamp, C., O'Brien, J., Vanroon, M., Vanderlugt, N., Berns, A., Teriele, H. 1994. Developmental rescue of an embryonic-lethal mutation in the retinoblastoma gene in chimeric mice. *EMBO Journal* **13**(18): 4260-68.

Magnaghi-Jaulin, L., Groisman, R., Naguibneva, I., Robin, P., Lorain, S., Le Villain, J. P., Troalen, F., Trouche, D., Harel-Bellan, A.1998. Retinoblastoma protein represses transcription by recruiting a histone deacetylase. *Nature* **391**(6667): 601-605.

Makino, S. 1952. Cytological studies on cancer. III. The characteristics and individuality of chromosomes in tumor cells of the Yoshida sarcoma which contribute to the growth of the tumor. *Gan* **43**(1): 17-34.

Makino, S., Nakahara, H. 1952. Observations on cell division in living tumor cells of ascites-sarcomas of rats. *Gan* **43**(2-3): 302.

Malumbres, M., Barbacid, M. 2001. To cycle or not to cycle: A critical decision in cancer. *Nature Reviews Cancer* **1**(3): 222-31.

Manning, A. L., Longworth, M. S., Dyson, N. J. 2010. Loss of pRB causes centromere dysfunction and chromosomal instability. *Genes & Development* **24**(13): 1364-76.

Margottin-Goguet, F., Hsu, J. K., Loktev, A., Hsieh, H. M., Reiman, J. D., Jackson, P. K. 2003. Prophase destruction of Emi1 by the SCF(betaTrCP/Slimb) ubiquitin ligase activates the anaphase promoting complex to allow progression beyond prometaphase. *Developmental Cell* **4**(6): 813-26.

Markham, D., Munro, S., Soloway, J., O'Connor, D. P., La Thangue, N. B. 2006. DNA-damage-responsive acetylation of pRB regulates binding to E2F-1. *EMBO Reports* **7**(2): 192-98.

Marston, A. L., Tham, W. H., Shah, H., Amon, A. 2004. A genome-wise screen identifies genes required for centromeric cohesion. *Science* **303**(5662): 1367-70.

Matsunaga, E., Minoda, K., Sasaki, M. S. 1990. Parental age and seasonal-variation in the births of children with sporadic retinoblastoma- a mutation-epidemiologic study. *Human Genetics* **84**(2): 155-158.

Mayhew, C. N., Bosco, E. E., Fox, S. R., Okaya, T., Tarapore, P., Schwemberger, S. J., Babcock, G. F., Lentsch, A. B., Fukasawa, K., Knudsen, E. S. 2005. Liver-specific pRB loss results in ectopic cell cycle entry and aberrant ploidy. *Cancer Research* **65**(11): 4568-77.

Mayol, X., Grana, X., Baldi, A., Sang, N. L., Hu, Q. J., Giordano, A. 1993. Cloning of a new member of the retinoblastoma gene family (PRB2) which binds to the E1A transforming domain. *Oncogene* **8**(9): 2561-66.

Melby, T. E, Ciampaglio, C. N., Briscoe, G., Erickson, H. P. 1998. The symmetrical structure of structural maintenance of chromosomes (SMC) and MukB proteins: Long, antiparallel coiled coils, folded at a flexible hinge. *Journal of Cell Biology* **142**(6): 1595-1604.

Meuwissen, R., Linn, S. C., Linnoila, R. I., Zevenhoven, J., Mooi, W. J., Berns, A. 2003. Induction of small cell lung cancer by somatic inactivation of both Trp53 and Rb1 in a conditional mouse model. *Cancer Cell* **4**(3): 181-89.

Mittnacht, S. 1998. Control of pRB phosphorylation. *Current Opinion in Genetics & Development* **8**(1): 21-27.

Moberg, K., Starz, M. A., Lees, J. A. 1996. E2F-4 switches from p130 to p107 and pRB in response to cell cycle reentry. *Molecular and Cellular Biology* **16**(4): 1436-49.

Mudryj, M., Devoto, S. H., Hiebert, S. W., Hunter, T., Pines, J., Nevins, J. R. 1991. Cell –cycle regulation of the E2F transcription factor involves an interaction with cyclin-A. *Cell* **65**(7): 1243-53.

Munger, K., Weness, B. A., Dyson, N., Phelps, W. C., Harlow, E., Howley, P. M. 1989. Complex-formation of human papillomavirus-E7 proteins with the retinoblastoma tumor suppressor gene-product. *EMBO Journal* **8**(13): 4099-4105.

Murphree, A. L., Benedict, W. F. 1984. Retinoblastoma- Clues to human oncogenes. *Science* **223**(4640): 1028-1033.

Neel, J. V. and Falls, H. F. 1951. The rate of mutation of the gene responsible for retinoblastoma in man. *Science* **114**(2964): 419-422.

Nelson, D. A., Krucher, N. A., Ludlow, J. W. 1997. High molecular weight protein phosphatase type 1 dephosphorylates the retinoblastoma protein. *Journal of Biological Chemistry* **272**(7): 4528-35.

Neuwald, A. F., Hirano, T. 2000. HEAT repeats associated with condensins, cohesins, and other complexes involved in chromosome-related functions. *Genome Research* **10**(10): 1445-52.

Nevins, J. R. 1992. E2F- A link between the RB tumor suppressor protein and viral oncoproteins. *Science* **258**(5081): 424-29.

Nguyen, D. X., McCance, D. J. 2005. Role of the retinoblastoma tumor suppressor protein in cellular differentiation. *Journal of Cellular Biochemistry* **94**(5): 870-79.

Niculescu, A. B. III., Chen, X., Smeets, M., Hengst, L., Prives, C., Reed, S. I. 1998. Effects of p21 Cip1/Waf1 at both the G1/S and G2/M cell cycle transitions: pRB is a critical determinant in blocking DNA replication and in preventing endoreduplication. *Molecular and Cellular Biology* **18**(1): 629-43.

Nielson, S. J., Schneider, R., Bauer, U. M., Bannister, A. J., Morrison, A., O;Carroll, D., Firestein, R., Cleary, M., Jenuwein, T., Herrera, R. E., Zouzarides, T. 2001. Rb targets histone H3 methylation and HP1 to promoters. *Nature* **412**(6846): 561-65.

Oliveira, R. A., Coelho, P. A., Sunkel, C. E. 2005. The condensin I subunit Barren/CAP-H is essential for the structural integrity of centromeric heterochromatin during mitosis. *Molecular and Cellular Biology* **25**(20): 8971-84.

Onadim, Z., Hogg, A., Baird, P. N., Cowell, J. K. 1992. Oncogenic point mutations in exon-20 of the RB1 gene in families showing incomplete penetrance and mild expression of the retinoblastoma phenotype. *PNAS USA* **89**(13): 6177-81.

Ono, T., Fang, Y., Spector, D. L., Hirano, T. 2004. Spatial and temporal regulation of condensin I and II in mitotic chromosome assembly in human cells. *Molecular Biology of the Cell* **15**(7): 3296-3308.

Ono, T., Losada, A., Hirano, M., Myers, M. P., Neuwald, A. F., Hirano, T. 2003. Differential contributions of condensin I and condensin II to mitotic chromosome architecture in vertebrate cells. *Cell* **115**(1): 109-21.

Ono, T., Yamashita, D., Hirano, T. 2013. Condensin II initiates sister chromatid resolution during S phase. *Journal of Cell Biology* **200**(4): 429-41.

Peeper, D. S., Dannenberg, J. H., Douma, S., Riele, H. T., Bernards, R. 2001. Escape from premature senescence is not sufficient for oncogenic transformation by Ras. *Nature Cell Biology* **3**(2): 198-203.

Qin, X. Q., Chittenden, T., Livingston, D. M., Kaelin, W. G. 1992. Identification of a growth suppression domain within the retinoblastoma gene-product. *Genes & Development* **6**(6): 953-64.

Rabitsch, K. P., Gregan, J., Schleiffer, A., Javerzat, J. P., Eisenhaber, F., Nasmyth, K. 2004. Two fission yeast homologs of Drosophila Mei-S332 are required for chromosome segregation during meiosis I and II. *Current Biology* **14**(4): 287-301.

Ribeiro, S. A., Gatlin, J. C., Dong, Y. M., Joglekar, A., Cameron, L., Hudson, D. F., Farr, C. J., McEwen, B. F., Salmon, E. D., Earnshaw, W. C., Vagnarelli, P. 2009. Condensin Regulates the Stiffness of Vertebrate Centromeres. *Molecular Biology of the Cell* **20**(9): 2371-80.

Robertson, K. D., Ait-Si-Ali, S., Yokochi, T., Wade, P. A., Jones, P. L., Wolffe, A. P. 2000. DNMT1 forms a complex with Rb, E2F1 and HDAC and represses transcription from E2F-responsive promoters. *Nature Genetics* **25**(3): 338-42.

Rubin, S. M., Call, A. L., Zheng, N., Pavletich, N. P. 2005. Structure of the RbC-terminal domain bound to E2F1-DP1: A mechanism for phosphorylation-induced E2F release. *Cell* **123**(6): 1093-1106.

Rubinfeld, B., Souza, B., Albert, I., Muller, O., Chamberlain, S. H., Masiarz, F. R., Munemitsu, S., Polakis, P. 1993. Association of the APC gene product with beta-catenin. *Science* **262**(5140): 1731-34.

Ruiz, S., Santos, M., Sagrelles, C., Leis, H., Jorcano, J. L., Berns, A., Paramio, J. M., Vooijs, M. 2004. Unique and overlapping functions of pRB and p107 in the control of proliferation and differentiation in epidermis. *Development* **131**(11): 2737-48,

Sage, J., Miller, A. L., Perez-Mancera, P. A., Mysocki, J. M., Jacks, T. 2003. Acute mutation of retinoblastoma gene function is sufficient for cell cycle re-entry. *Nature* **424**(6945): 223-228.

Sage, J., Mulligan, G. J., Attardi, L. D., Miller, A., Chen, S. Q., Williams, B., Theodorou, E., Jacks, T. 2000. Targeted disruption of the three Rb-related genes leads to loss of G(1) control and immortalization. *Genes & Development* **14**(23): 3037-50.

Sakamoto, T., Inui, Y. T., Uraguchi, S., Yoshizumi, T., Matsunaga, S., Mastui, M., Umeda, M., Fukui, K., Fukiwara, T. 2011. Condensin II Alleviates DNA Damage and Is Essential for Tolerance of Boron Overload Stress in Arabidopsis. *Plant Cell* **23**(9): 3533-46.

Samoshkin, A., Arnaoutov, A., Jansen, L. E. T., Ouspenski, I., Dye, L., Karpova, T., McNally, J., Dasso, M., Cleveland, D. W. Strunnikov, A. 2009. Human Condensin Function Is Essential for Centromeric Chromatin Assembly and Proper Sister Kinetochore Orientation. *PLOS ONE* **4**(8): e6831.

Sancar, A. 1996. DNA excision repair. *Annual Review of Biochemistry* **65**: 43-81.

Savvidou, E., Cobbe N. Steffensen, S., Cotterill, S., Heck, M. M. S. 2005. Drosophila CAP-D2 is required for condensin complex stability and resolution of sister chromatids. *Journal of Cell Science* **118**(11): 2529-43.

Schappert-Kimmijser, J., Hemmes, G. D., Nijland, R. 1966. Heredity of retinoblastoma. *Ophthalmologica*. **151**(2): 197-213.

Schleiffer, A. ,Kaitna, S., Maurer-Stroh, S., Glotzer, M., Nasmyth, K., Eisenhaber, F. 2003. Kleisins: A superfamily of bacterial and eukaryotic SMC protein partners.*Molecular Cell* **11**(3): 571-75.

Schubbert, S., Bollag, G., Lyubynska, N., Nguyen, H., Kratz, C. P., Zenker, M., Niemeyer, C. M., Molven, A., Shannon, K. 2007. Biochemical and functional characterization of germ line KRAS mutations. *Molecular and Cellular Biology* **27**(22): 7765-70.

Schvartzman, J. M., Sotillo, R., Benezra, R. 2010. Mitotic chromosomal instability and cancer: mouse modelling of the human disease. *Nature Reviews Cancer* **10**(2): 102-15.

Schwarz, J. K., Devoto, S. H., Smith, E. J., Chellappan, S. P., Jakoi, L., Nevins J. R. 1993. Interactions of the p107 and RB proteins with E2F during the cell-proliferation response. *EMBO Journal***12**(3): 1013-20.

Seifried, L. A., Talluri, S., Cecchini, M., Julian, L. M., Mymryk, J. S., Dick, F. A. 2008. PRB-E2F1 complexes are resistant to adenovirus E1A-mediated disruption. *Journal of Virology* **82**(9): 4511-20.

Seipold, S., Priller, F. C., Goldsmith, P., Harris, W. A., Baier, H., Abdelilah-Seyfried, S. 2009. Non-SMC condensin I complex proteins control chromosome segregation and survival of proliferating cells in the zebrafish neural retina. *BMC Developmental Biology* **9**: 40.

Sellers, W. R., Novitch, B. G., Miyake, S., Heith, A., Otterson, G. A., Kaye, F. J., Lassar, A. B., Kaelin, W. G. 1998. Stable binding to E2F is not required for the retinoblastoma protein to activate transcription, promote differentiation, and suppress tumor cell growth. *Genes & Development* **12**(1): 95-106.

Sellers, W. R., Rodgers, J. W., Kaelin, W. G. 1995. A potent transrepression domain in the retinoblastoma protein induces a cell-cycle arrest when bound to E2F sites. *PNAS USA* **92**(25): 11544-48.

Sever-Chroneos, Z., Angus, S. P., Fribourg, A. F., Wan, H., Todorov, I., Knudsen, K. E., Knudsen, E. S. 2001. Retinoblastoma tumor suppressor protein signals through inhibition of cyclin-dependent kinase 2 activity to disrupt PCNA function in S-phase. *Molecular and Cellular Biology* **21**(12): 4032-45.

Sherr, C. J. 1996. Cancer cell cycles. *Science* **274**(5293): 1672-77.

Sherr, C. J., Roberts, J. M. 1999. CDK inhibitors: positive and negative regulators of G(1)- phase progression. *Genes & Development* **13**(12): 1501-12.

Shintomi, K., Hirano, T. 2011. The relative ratio of condensin I to II determines chromosome shapes. *Genes & Development* **25**(14): 1464-69.

Shirkhedkar Atul A, Bhirud Charushila H, Surana Sanjay J. 2009. Application of UV-spectrophotometric methods for estimation of tenofovir disoproxil fumarate in tablets. *Pakistan Journal of Pharmaceutical Sciences* **22**(1): 27-29.

Shirodkar, S., Ewen, M., DeCaprio, J. A., Morgan, J., Livingston, D. M., Chittenden, T. 1992. The transcription factor E2F interacts with the retinoblastoma product and a p107-cyclin-A complex in a cell cycle-regulated manner. *Cell* **68**(1): 157-66.

Singh, P., Coe, J., Hong, W. J. 1995. A role for retinoblastoma protein in potentiating transcriptional activation by the glucocorticoid receptor. 1995. *Nature* **374**(6522): 562-65.

Smith, E. D., Xu, Y., Tomson, B. N., Leung, C. G., Fujiwara, Y., Orking, S. H., Crispino, J. D. 2004. *More than blood,* a Novel Gene Required for Mammalian Postimplantation Development. *Molecular and Cellular Biology* **24**(3): 1168-73.

Smith, S. M., Sorsby, A. 1958. Retinoblastoma- Some genetic aspects. *Annals of Human Genetics* **23**(1):50-58.

Sparkes, R. S., Murphree, A. L., Lingua, R. W., Sparkes, M. C., Funderburk, S. J., Benedict, W. F. 1983. *Science* **219**(4587): 971-973.

Sparkes, R.S., Sparkes, M. C., Wilson, M.G., Towner, J. W., Benedict, W., Murphree, A. L., Yunis, J. J. 1980. Regional assignment of genes for human esterase-D and retinoblastoma to chromosome band 13Q14. *Science* **208**(4447): 1042-44.

Spruck, C. H., Won, K. A., Reed, S. I. 1999. Deregulated cyclin E induces chromosome instability. *Nature* **401**(6750): 297-300.

Srinivasan, S. V., Mayhew, C. N., Schwemberger, S., Zagorski, W., Knudsen, E. S. 2007. RB loss promotes aberrant ploidy by deregulating levels and activity of DNA replication factors. *Journal of Biological Chemistry* **282**(33): 23867-77.

Stear, J. H., Roth, M. B. 2002. Characterization of HCP-6, a C-elegans protein required to prevent chromosome twisting and merotelic attachment. *Genes & Development* **16**(12): 1498-1508.

Stephens, P. J., Greenman, C. D., Fu, B., Yang, F., Bignell, G. R., Mudie, L. J., Pleasance, E. D., Lau, K. W., Beare, D., Stebbings, L. A., McLaren, S., Lin, M. L., McBride, D. J., Varela, I., Nik-Zainal, S., Leroy, C., Jia, M. M., Menzies, A., Butler, A. P., Teague, J. W., Quail, M. A., Burton, J., Swerdlow, H., Carter, N. P., Morsberger, L. A., Iacobuzio-Donahue, C., Follows, G. A., Green, A. R., Flanagan, A. M., Futreal, P. A., Campell, P. J. 2011. Massive genomic rearrangement acquired in a single catastrophic event during cancer development. *Cell* **144**(1): 27-40.

Stolz, A., Ertych, N., Kienitz, A., Vogel, C., Schneider, V., Fritz, B., Jacob, R., Dittmar, G., Weichert, W., Petersen, I., Bastians, H. 2010. The CHK2-BRCA1 tumour suppressor pathway ensures chromosomal stability in human somatic cells. *Nature Cell Biology* **12**(5): 492-99.

Strick T. R., Kawaguchi, T., Hirano, T. 2004. Real-time detection of single-molecule DNA compaction by condensin I. *Current Biology* **14**(10): 874-80.

Su, L. K., Vogelstein, B., Kinzler, K. W. 1993. Association of the APC tumor suppressor protein with catenins. *Science* **262**(5140): 1734-37.

Sumara, I., Vorlaufer, E., Stukenberg, P. T., Kelm, O., Redemann, N., Nigg, E. A., Peters, J. M. 2002. The dissociation of cohesin from chromosomes in prophase is regulated by polo-like kinase. *Molecular Cell* **9**(3): 515-25.

Sun, H. F., Chang, Y. J., Schweers, B., Dyer, M. A., Zhang, X. J., Hayward, S. W., Goodrich, D. W. 2006. An E2F binding-deficient Rb1 protein partially rescues developmental defects associated with Rb1 nullizygosity. *Molecular and Cellular Biology* **26**(4): 1527-37.

Takahashi, R., Hashimoto, T., Xu, H. J., Hu, S. X., Matsui, T., Miki, T., Bigomarshall, H., Aaronson, S. A., Benedict, W. F. 1991. The Retinoblastoma gene functions as a growth and tumor suppressor in human bladder-carcinoma cells. *PNAS USA* **88**(12): 5257-61.

Takahashi, Y., Rayman, J., Dynlacht, B. 2000. Analysis of promoter binding by the E2F and pRB families *in vivo*: distinct E2F proteins mediate activation and repression. *Genes & Development* **14**(7): 804-16.

Takemoto, A., Kimura, K., Yanagisawa, J., Yokoyama, S., Hanaoka, F. 2006. Negative regulation of condensin I by CK2-mediated phosphorylation. *EMBO Journal* **25**(22): 5339-48.

Takemoto, A., Maeshima, K., Ikehara, T., Yamaguchi, K., Murayama, A., Imamura, S., Imamoto, N., Yokoyama, S., Hirano, T., Watanabe, Y., Hanaoka, F., Yanagisawa, J., Kimura, K. 2009. The chromosomal association of condensin II is regulated by a noncatalytic function of PP2A. *Nature Structural & Molecular Biology* **16**(12): 1302-08.

Talluri, S., Isaac, C. E., Ahmad, M., Henley, S. A., Francis, S. M., Martens, A. L., Bremner, R., Dick, F. A. 2010. A G(1) Checkpoint Mediated by the Retinoblastoma Protein That Is Dispensable in Terminal Differentiation but Essential for Senescence. *Molecular and Cellular Biology* **30**(4): 948-60.

Thalmeier, K., Synovzik, H., Mertz, R., Winnacker, E. L., Lipp, M. 1989. Nuclear factor E2F mediates basic transcription and trans-activation by E1A of the human myc promoter. *Genes & Development* **3**(4): 527-36.

The retinoblastoma genetics website- www.verandi.de/joomla

Thibodeau, S. N., Bren, G., Schaid, D. 1993. Microsatellite instability in cancer of the proximal colon. *Science* **260**(5109): 816-19.

Thomas, D. M., Carty, S. A., Piscopo, D. M., Lee, J. S., Wang, W. F., Forrester, W. C., Hinds, P. W. 2001. The retinoblastoma protein acts as a transcriptional coactivator required for osteogenic differentiation. *Molecular Cell* **8**(2): 303-16.

Thompson, M., Haeusler, R. A., Good, P. D., Engelke, D. R. 2003. Nucleolar clustering of dispersed tRNA genes. *Science* **302**(5649): 1399-1401.

Thompson, S. L., Compton, D. A. 2008. Examining the link between chromosomal instability and aneuploidy in human cells. *Journal of Cell Biology* **180**(4): 665-72.

Vagnarelli, P., Hudson, D. F., Ribeiro, S. A., Trinkle-Mulcahy, L., Spence, J. M., Lai, F., Farr, C. J., Lamond, A.I., Earnshaw, W. C. 2006. Condensin and Repo-Man-PP1 co-operate in the regulation of chromosome architecture during mitosis. *Nature Cell Biology* **8**(10): 1133-42.

van Harn, T., Foijer, F., van Vugt, M., Banerjee, R., Yang, F. T., Oostra, A., Joenje, H., te Riele, H. 2010. Loss of Rb proteins causes genomic instability in the absence of mitogenic signaling. *Genes & Development* **24**(13): 1377-88.

Vogel, F. 1979. Genetics of retinoblastoma. *Human Genetics* **52**(1): 1-54.

Vooijs, M., van der Valk, M., te Riele, H., Berns, A. 1998. Flp-mediated tissue-specific inactivation of the retinoblastoma tumor suppressor gene in the mouse. *Oncogene* **17**(1):1-12.

Wei, L., Liang, X. W., Zhang, Q. H., Li, M., Yuan, J., Li, S., Sun, S. C., Ouyang, Y. C., Schatten, H., Sun, Q. Y. 2010. BubR1 is a spindle assembly checkpoint protein regulating meiotic cell cycle progression of mouse oocyte. *Cell Cycle* **9**(6): 1112-21.

Wells, J., Boyd, K., Fry, C., Bartley, S., Farnham, P. 2000. Target gene specificity of E2F and pocket protein family members in living cells. *Molecular and Cellular Biology* **20**(16): 5797-5807.

Wells, J., Yan, P. S., Cechvala, M., Huang, T., Farnham, P. J. 2003. Identification of novel pRB binding sites using CpG microarrays suggests that E2F recruits pRB to specific genomic sites during S-phase. *Oncogene* **22**(10): 1445-60.

Whyte, P., Buchkovich, K. J., Horowitz, J. M., Friend, S. H., Raybuck, M., Weinberg, R. A., Harlow, E. 1988. Association between an oncogene and an anti-oncogene- The adenovirus E1A proteins bind to the retinoblastoma gene-product. *Nature* **334**(6178): 124-29.

Whyte, P., Williamson, N. M., Harlow, E. 1989. Cellular targets for transformation by the adenocirus E1A proteins. *Cell* **56**(1): 67-75.

Wikenheiser-Brokamp, K. A. 2004. Rb family proteins differentially regulate distinct cell lineages during epithelial development. *Development* **131**(17): 4299-4310.

Williams, B. O., Schmitt, E. M., Remington, L., Bronson, R. T., Albert, D. M., Weinberg, R. A., Jacks, T. 1994. Extensive contribution of Rb-deficient cells to adult chimeric mice with limited histopathological consequences. *EMBO Journal* **13**(18): 4251-49.

Williams, J. P., Stewart, T., Li, B., Mulloy, R. Dimova, D., Classon, M. 2006. The retinoblastoma protein is required for Ras-induced oncogenic transformation. *Molecular and Cellular Biology* **26**(4): 1170-82.

Woo, M. S-A., Sanchez, I., Dynlacht, B. D. 1997. p130 and p107 use a conserved domain to inhibit cellular cyclin-dependent kinase activity. *Molecular and Cellular Biology* **17**(7): 3566-79.

Wood, R. D. 1997. Nucleotide excision repair in mammalian cells. *Journal of Biological Chemistry* **272**(38): 23465-68.

Wu, L. Z., de Bruin, A., Saavedra, H. I., Starovic, M., Trimboli, A., Yang, Y., Opavska, J., Wilson, P., Thompson, J. C., Ostrowski, M. C., Rosol, T. J., Woollett, L. A., Weinstein, M., Cross, J. C., Robinson, M. L., Leone, G. 2003. Extra-embryonic function of Rb is essential for embryonic development and viability. *Nature* **421**(6926): 942-47.

Xiao, B., Spencer, J., Clements, A., Ali-Khan, N., Mittnacht, S., Broceno, C., Burghammer, M., Perrakis, A., Marmorstein, R., Gamblin, S. J. 2003. Crystal structure of the retinoblastoma tumor suppressor protein bound to E2F and the molecular basis of its regulation. *PNAS USA* **100**(5): 2363-68.

Xu. Y, Leung, C. G., Lee, D. C., Kennedy, B. K., Crispino, J. D. 2006. MTB, the murine homolog of condensin II subunit CAP-G2, represses transcription and promotes erythroid cell differentiation. *Leukemia* **20**(7): 1261-69.

Yamashita, D., Shintomi, K., Ono, T., Gavvovidis, I., Schindler, D., Neitzel, H., Trimborn, M., Hirano, T. 2011. MCPH1 regulates chromosome condensation and shaping as a composite modulator of condensin II. *Journal of Cell Biology* **194**(6): 841-54.

Yan, Y., Mumby, M. C. 1999. Distinct roles for PP1 and PP2A in phosphorylation of the retinoblastoma protein. PP2a regulates the activities of G(1) cyclin-dependent kinases. *Journal of Biological Chemistry* **274**(45): 31917-24.

Yong-Gonzalez, V., Wang, B. D., Butylin, P., Ouspenski, I., Strunnikov, A. 2007. Condensin function at centromere chromatin facilitates proper kinetochore tension and ensures correct mitotic segregation of sister chromatids. *Genes to Cells* **12**(9): 1075-90.

Yonish-Rouach, E., Resnitzky, D., Lotem, J., Sachs, L., Kimchi, A., Oren, M. 1991. Wild-type p53 induces apoptosis of myeloid leukaemic cells that is inhibited by interleukin-6. *Nature* **352**(6333): 345-47.

Yunis, J. J., Ramsay, N. 1978. Retinoblastoma and subband deletion of chromosome-13. *American Journal of Diseases of Children* **132**(2): 161-63.

Zacksenhaus, E., Jiang, Z., Chung, D., Marth, J. D., Phillips, R. A., Gallie, B. L. 1996. pRB controls proliferation, differentiation, and death of skeletal muscle cells and other lineages during embryogenesis. *Genes & Development* **10**(23):3051-64.

Zamanian, M., La Thangue, N. B., 1993. Transcriptional repression by the Rb-related protein p107. *Molecular Biology of the Cell* **4**(4): 389-96.

Zhang, H. S., Gavin, M., Dahiya, A., Postigo, A. A., Ma, D. D., Luo, R. X., Harbour, J. W., Dean, D. C. 2000. Exit from G1 and S phase of the cell cycle is regulated by repressor complexes containing HDAC-Rb-hSWI/SNF and Rb-hSWI/SNF. *Cell* **101**(1): 79-89,

Zhang, R., Chen, W., Adams, P. D. 2007. Molecular dissection of formation of senescence-associated heterochromatin foci. *Molecular and Cellular Biology* **27**(6): 2343-58.

Zheng, L., Flesken-Nikitin, A., Chen, P. L., Lee, W. H. 2002. Deficiency of Retinoblastoma gene in mouse embryonic stem cells leads to genetic instability. *Cancer Res*earch **62**(9): 2498-2502.

Zhu, L., Harlow, E., Dynlacht, B. D. 1995. P107 uses a $p21^{CIP1}$-related domain to bind cyclin/cdk2 and regulate interactions with E2F. *Genes & Development* **9**(14): 1740-52.

Zhu, L., van den Heuvel, S., Helin, K., Fattaey, A., Ewen, M., Livingston, D. Dyson, N., Harlow, E. 1993. Inhibition of cell-proliferation by p107, a relative of the retinoblastoma protein. *Genes & Development* **7**(7A): 1111-25.

Chapter 2

2 Mitotic chromosome condensation mediated by the retinoblastoma protein is tumor suppressive

2.1 Abstract

Condensation and segregation of mitotic chromosomes is a critical process for cellular propagation and in mammals, mitotic errors can contribute to the pathogenesis of cancer. In this report we demonstrate that the retinoblastoma protein (pRB), a well-known regulator of progression through the G1 phase of the cell cycle, plays a critical role in mitotic chromosome condensation that is independent of G1 to S-phase regulation. Using gene targeted mutant mice, we studied this aspect of pRB function in isolation and demonstrate that it is an essential part of pRB-mediated tumor suppression. Cancer prone *Trp53*$^{-/-}$ mice succumb to more aggressive forms of cancer when pRB's ability to condense chromosomes is compromised. Furthermore, we demonstrate that defective mitotic chromosome structure caused by mutant pRB accelerates loss-of-heterozygosity, leading to earlier tumor formation in *Trp53*$^{+/-}$ mice. These data reveal a new mechanism of tumor suppression, facilitated by pRB, in which genome stability is maintained by proper condensation of mitotic chromosomes.

2.2 Introduction

The compaction of the mammalian genome into mitotic chromosomes, and their faithful segregation to recipient daughter cells in mitosis, is a critical event for eukaryotic cells. This stage of the cell division cycle carries considerable risk as there is no opportunity to reverse the effects of missegregated or damaged chromosomes in daughter cells. For these reasons, understanding mitosis is of vital importance because changes in genome integrity can lead to cancer.

The processes of chromosome condensation and segregation are intimately linked, as insufficient condensation of chromosome arms can prevent their proper separation in anaphase (Belmont 2006). Of chief importance in facilitating proper chromosome

structure is the mitotic chromosome scaffold, upon which mitotic chromosomes are condensed. These scaffolds are composed largely of topoisomerase 2 and Condensins (Maeshima and Laemmli 2003). While the enzymatic activity of topoisomerases suggests a mechanism by which they participate in chromosome compaction, the precise role of Condensins has been less clear. There are two types of condensin complexes (I and II) that are structurally very similar. Each is comprised of an SMC2 and SMC4 subunit that interact to form the coiled-coil arms of their ring like structures (Losada and Hirano 2005). In addition, each condensin complex also contains distinct subunits, CAP-H, -D2, and -G in Condensin I and CAP-H2, -D3, and -G2 in Condensin II (Losada and Hirano 2005). Surprisingly, depletion of individual components of these complexes by RNA interference does not prevent outright chromosome condensation (Ono *et al* 2003; Hirota *et al* 2004). Instead each complex appears to offer a unique contribution to the architecture of mitotic chromosomes. This may be in part due to differences in the timing of their loading onto chromosomes, with Condensin II being present on chromatin in interphase, and Condensin I being loaded only after nuclear envelope breakdown (Ono *et al* 2003; Hirota *et al* 2004). Additionally, differences in subunit composition imply that they may have different functional or regulatory properties (Losada and Hirano 2005). Importantly, defects and delays in chromatid condensation are manifested as lagging chromosomes during anaphase that impede mitotic progression resulting in aneuploidy (Hirota *et al* 2004; Ono *et al* 2004; Samoshkin *et al* 2009). However, there is limited evidence connecting condensin proteins and chromosome condensation to cancer (Ham *et al* 2007; Lapointe *et al* 2008).

In addition to condensation defects leading to segregation errors, faithful chromosome segregation can also be affected by mitotic spindle abnormalities. This includes the mitotic spindle checkpoint, which serves to detect unattached kinetochores at metaphase (Nasmyth 2005, Musacchio and Salmon 2007). Signals that emanate from a complex containing MAD2 and BUBR1 at unattached kinetochores prevent the E3-ubiquitin ligase complex APC/C from triggering the degradation of cyclin B1 and securin. Once this checkpoint is satisfied, mitotic cyclin dependent kinase activity drops and a securin associated protease called separase is free to cleave cohesins, allowing sister chromatid separation (Nasmyth 2005, Musacchio and Salmon 2007). Experimental

models in which spindle assembly checkpoint components are misexpressed show errors in chromosome segregation (Pei and Melmed 1997, Hernando *et al* 2004, Vader and Lens 2008). Thus, defects in either chromosome condensation, or spindle assembly checkpoints, can lead to segregation errors, aneuploidy, and potentially contribute to cancer pathogenesis. A number of examples of spindle assembly checkpoint defects contributing to cancer incidence in genetically modified mice have been reported (reviewed in Schvartzman *et al* 2010). Conversely, even though defects in chromosome condensation cause similar mitotic errors, there are no reports using gene-targeted mouse models to confirm a role for Condensins as tumor suppressors.

The retinoblastoma tumor suppressor protein (pRB) is best known for its role in regulating the G1 to S-phase transition early in the cell cycle (reviewed in Burkhart and Sage 2008). Its ability to negatively regulate transcription of DNA replication machinery through E2F transcription factors creates a mechanism by which it can inhibit cell cycle entry. More recently, pRB has been shown to influence both chromosome condensation and mitotic checkpoint function (Longworth and Dyson 2010, Schvartzman *et al* 2010). Components of the spindle assembly checkpoint, such as MAD2, are regulated by E2F transcription factors (Ren *et al* 2002, Hernando *et al* 2004). For this reason loss of E2F regulation by pRB, which is almost ubiquitous in cancer, leads to genome instability (Mayhew *et al* 2007, Schvartzman *et al* 2010). Conversely, the ability of pRB to influence mitotic chromosome condensation has emerged as an E2F independent function and loss of pRB function can influence chromosome loss irrespective of proliferation (Zheng *et al* 2002, Gonzalo *et al* 2005, Isaac *et al* 2006, Longworth *et al* 2008). To date, evidence for pRB's involvement in chromosome condensation has been largely genetic. Mouse fibroblasts deficient for all pRB family proteins, or a knock in mutation that partially inactivates pRB, have abnormal centromeric heterochromatin, leading to chromosome fusions and aneuploidy (Gonzalo *et al* 2005, Isaac *et al* 2006). Further analyses that combine the use of *Drosophila* genetics and mammalian cell culture suggest that pRB can interact with the Condensin II subunit CAP-D3, and that this interaction is necessary for chromosome compaction in mitosis (Longworth *et al* 2008). While studies of spindle checkpoint components such as MAD2 have offered explanations for why their deregulation in cancer can be traced back to pRB function, the importance for pRB's role

in chromosome condensation is less well understood, and has not yet been connected to a cancer phenotype (Schvartzman *et al* 2010).

In this report, we investigate the mechanism used by pRB to facilitate mitotic chromosome condensation. We rely on a viable, gene targeted mouse strain in which pRB is mutated to block LXCXE dependent interactions, such as those with viral oncoproteins and chromatin remodeling enzymes like histone deacetylases (Isaac *et al* 2006). Cells from these mice have limited proliferative control defects, except for the responsiveness to TGF-β and senescence inducing stimuli (Francis *et al* 2009, Talluri *et al* 2010). We demonstrate that pRB interacts with the Condensin II complex to establish proper chromosome structure. Our experiments reveal that condensation defects caused by a deficiency in pRB-LXCXE interactions occur before metaphase, and are unrelated to the ability to regulate G1 to S-phase progression. We used $Rb1^{\Delta L/\Delta L}$; $Trp53^{-/-}$ mice, as well as $Trp53^{-/-}$ controls, both of which are uniformly defective in their response to G1 arrest stimuli such as DNA damage and oncogene induced senescence, to study pRB's role in chromosome condensation in isolation. $Rb1^{\Delta L/\Delta L}$; $Trp53^{-/-}$ mice succumb to much more aggressive forms of cancer than p53 deficient controls, and their tumors are characterized by elevated levels of chromosome instability. Furthermore, we demonstrate that defective chromosome condensation caused by mutant pRB can accelerate loss of heterozygosity and cancer onset in $Trp53^{+/-}$ mice. This study reveals that participation in mitotic chromosome condensation is an integral aspect of pRB's function as a tumor suppressor protein.

2.3 Methods

2.3.1 Cell culture, viral infections and microscopy

Primary mouse embryonic fibroblasts (MEFs) were prepared and cultured according to standard methods as reported previously (Hurford *et al* 1997). Embryonic stem cells (ESCs) were prepared by intercrossing $Rb1^{\Delta L/+}$ mice and harvesting day 3.5 blastocysts for culture. The inner cell mass was dissociated and colonies were picked and expanded for genotyping as described (Hogan *et al* 1994). Mitotic chromosome spreads

were prepared from MEFs by treating cells with 50 ng/mL of colcemid for three hours before harvesting, swelling, and fixing. ESC chromosome spreads were generated similarly after treating cultures with 10 µg/mL of colchicine for three hours. Chromosome spreads were stained with a major satellite pericentromeric probe as before (Isaac *et al* 2006). Staining of rDNA repeats and the probes used were as described (Grummt *et al* 1979; Romanova *et al* 2006). Fluorescent microscopic images were captured on a Zeiss axioskop 40 microscope using a Spotflex camera and EyeImage software.

To introduce H2B-GFP into MEFs, we created a pBABE retroviral vector that expresses H2B-GFP by cloning the gene from pBOS-H2B-GFP. Short hairpin retroviral vectors targeting CAP-D3 were purchased from Open Biosystems and were cloned into the pLMP plasmid along with the H2B-GFP gene. Viral vectors were packaged into ecotropic retroviruses using Bosc23 cells and subsequently used to infect MEFs as described (Pear *et al* 1993).

Live cell microscopy was carried out by plating early passage, H2B-GFP transduced MEFs onto glass-bottom tissue culture dishes (MatTek) containing phenol-free DMEM and 5% FBS supplemented with penicillin, streptomycin, and glutamine. During imaging, cells were maintained at 37°C with 5% CO_2 using a stage mounted environment chamber (Neue Biosciences) and were monitored with an automated inverted microscope (DMI 6000b, Leica). Phase contrast and fluorescent images were collected every 3 minutes over a 15 hour timecourse using Openlab Software automation (Ritchie *et al* 2008). Measurements of metaphase plate dimensions were made using Volocity software.

Stained tissue sections were examined microscopically on a Zeiss axioskop 40 microscope and photographed using a Spotflex camera and EyeImage software.

2.3.2 Antibodies and protein detection

The following antibodies were used to detect or precipitate proteins in this study. Rabbit anti-histone H2B (07-371, Upstate), goat anti-GFP (G095, Clontech), rabbit anti-

CAP-H (a kind gift of Kyoko Yokomori, UC-Irvine) (Heale *et al* 2006), rabbit anti-CAP-H2 (a generous gift of Tatsuya Hirano, Riken, Japan)(Ono *et al* 2003), rabbit anti-SMC1 (A300-055A, Bethyl Laboratories), anti-pRB (G3-245, BD-Pharmingen), anti-BubR1: C-20 (sc-16195, Santa Cruz), anti-PCNA: PC10 (sc-56, Santa Cruz), anti-MCM7: 141.2 (sc-9966, Santa Cruz), anti-E2F3: C-18 (sc-878, Santa Cruz), and anti-E2F3 clone PG37 (05-551, Upstate). Antibodies to CAP-D3 were raised against a GST fusion protein containing amino acids 1243-1506 of CAP-D3. CAP-D2 antibodies were raised against a GST fusion containing amino acids 943-1132. Rabbits were immunized in a commercial facility (PTG Labs, Chicago). Antibodies were affinity purified by adsorbing to a His-tagged version of the same protein coupled to a Sulfolink column (Pierce), eluted in low pH, and neutralized.

Cell extracts for western blotting were prepared by freeze-thaw lysis as described previously (Hurford *et al* 1997). Chromatin fractions were prepared by low salt wash of nuclei followed by nuclease treatment to solubilize chromatin bound proteins (Mendez and Stillman 2000). MEFs were synchronized using a two-step method of confluence arrest and aphidicolin, followed by wash out and collection of cells when the mitotic index is greatest (Isaac *et al* 2006). Nuclease prepared chromatin fractions were used for immunoprecipitation experiments where they were pre-cleared with mouse IgG and protein-G magnetic beads before precipitation using anti-pRB antibodies. Proteins in all experiments were resolved by SDS-PAGE followed by western blotting using standard techniques.

2.3.3 Mice

The *Rb1*$^{\Delta L}$ mutant strain carries three amino acid substitutions in its *Rb1* encoded protein (I746A, N750A, and M754A) that disrupt interactions with LXCXE motif containing proteins, but not E2F transcription factors (Dick *et al* 2000; Isaac *et al* 2006); details of its construct and initial characterization have been previously published (Isaac *et al* 2006; Francis *et al* 2009; Talluri *et al* 2010). The *Trp53*$^{-/-}$ mice were purchased from Jackson Labs and were intercrossed with *Rb1*$^{\Delta L}$ mutants to produce the required genotypes for this study. All animals were maintained in a mixed 129/B6 background. Mice were housed and maintained according to the guidelines of the Canadian Council

on Animal Care. Animals were followed throughout their lives for signs of tumor burden and were euthanized when tumors became visible, or the animal experienced sudden weight loss or became lethargic. All animals were subjected to a thorough necropsy and abnormal tissues, organs, or tumors were fixed in formalin and processed for histological assessment. Portions of tumors were also snap frozen and used to prepare genomic DNA. Tissues were embedded, sectioned, and stained with hematoxylin and eosin according to standard methods and photographed as described above. See Appendix H for synopsis of histopathology for all animals used in this study.

2.3.4 Thymic development

To investigate thymic development and proliferation we isolated thymi from six to eight week old animals. Tissue was either fixed and frozen for cryosectioning, or dissociated and stained for flow cytometry. Fluorescently labeled antibodies against CD4 (553650) and CD8 (553032) were purchased from BD Pharmingen. CD4/CD8 flow cytometry was carried out essentially as described (Bruins *et al* 2004). To detect proliferation, mice were injected with 200 µL of 16 mg/mL BrdU in DMEM one hour before euthanasia. BrdU labeled thymi were fixed, sectioned, and stained with anti-BrdU antibodies (347580, BD Biosciences) and photographed under fluorescent optics as described above.

2.3.5 PCR, Southern blotting and aCGH

High molecular weight DNA was extracted from frozen tumor samples using standard DNA isolation procedures and used in the following analyses. DNA from thymic lymphomas was analyzed for T-cell receptor V(D)J recombination patterns using nested PCR. In brief, the $D_{\beta 12}$ and $J_{\beta 12}$ region was characterized using primer pairs and PCR conditions as described by Whitehurst (Whitehurst *et al* 1999). Loss of heterozygosity of *Trp53* in tumors from *Trp53*$^{+/-}$ mice was determined by Southern blotting. Genomic DNA was digested with EcoRI and StuI and resolved, transferred, and hybridized using standard methods. The probe was a genomic DNA clone encompassing intron seven to intron nine. Band intensities were measured on a Molecular Dynamics

Storm scanner phosphorimager and densitometry analysis was performed using AlphaEase FC software.

For array CGH experiments, DNA was extracted from livers of five male and female wild type animals to create pools of control DNA. Same sex control vs. control, control male vs. control female, and tumor DNA vs. the appropriate sex control hybridizations were performed by NimbleGen on a mouse whole genome array (design 2006-07-26-MM8-WG-CGH). Segmentation analysis described by Olshen was performed and was used to infer changes in copy number (Olshen *et al* 2004). A segment was defined as a group of adjacent data points whose $\log_2$ ratio values were not statistically different. To determine cut-off values, indicating normal copy number, the mean $\log_2$ ratio for all data points of individual chromosomes from the control hybridization was determined. A range of +/- one standard deviation from this mean was determined to encompass the $\log_2$ ratio from 99.8% of all segments from the control hybridization, suggesting that it was a reliable range that captures the vast majority of normal copy number chromosomal segments. This range was calculated for each individual chromosome from the control hybridization. Segments from individual chromosomes from each tumor hybridization were then compared to the appropriate range for their chromosome to determine if they were of a normal copy number. This allowed us to assess, on a chromosome-by-chromosome basis, the copy number status of each segment. Using this approach, we interpreted whole chromosome gains or losses based on the chromosomal locations of each constituent segment, and their associated copy number status (See Appendices I and J).

2.4 Results

2.4.1 Aberrant chromosome condensation and segregation in *Rb1*$^{\Delta L/\Delta L}$ mutant cells

A number of recent reports have indicated that cells deficient for pRB family proteins have chromosomal abnormalities, and we have demonstrated centromere fusions and lagging anaphase chromosomes in cells from *Rb1*$^{\Delta L/\Delta L}$ mice (Gonzalo *et al* 2005,

Longworth *et al* 2008, Isaac *et al* 2006). One interpretation of altered chromosome numbers in these cells is that they are a consequence of deregulated E2F transcriptional control in G1 leading to inappropriate proliferation. In this way, alterations in transcriptional control or commitment to enter S-phase early in the cell cycle, are manifested in subsequent mitotic errors. To investigate this possibility with $Rb1^{\Delta L/\Delta L}$ mutant cells, we compared chromosomal abnormalities found in homozygous mouse embryonic fibroblasts (MEFs) with embryonic stem cells (ESCs). Since MEFs have a pronounced G1 phase regulated by pRB, and ESCs lack the ability to arrest in G1, we reasoned that chromosomal abnormalities found in both are unlikely to be a consequence of unregulated cell cycle advancement (Herrera *et al* 1996, Harrington *et al* 1998, Aladjem *et al* 1998). Figure 2.1A shows representative chromosome spreads from each cell type for both wild type and $Rb1^{\Delta L/\Delta L}$ mutants. Chromosomes were stained with DAPI and a major satellite DNA probe to visualize contacts between centromeres from different chromosomes. In both cell types, a statistically significant increase in centromere interactions was detected in the mutant $Rb1^{\Delta L/\Delta L}$ genotype, suggesting an increase in chromosome fusions (Fig. 2.1A, inlays; χ2-test, $P<0.05$ for each comparison in Fig. 2.1B left, middle). Interestingly, there was also an increase in the number of centromeres interacting in $Rb1^{\Delta L/\Delta L}$ ESCs compared to wild type (χ2-test, $P<0.05$; Fig. 2.1A inlay, Fig. 2.1B right). In addition to its contribution to centromere structure, pRB is also known to silence transcription at nearby rDNA repeats (Cavanaugh *et al* 1995, Hannan *et al* 2000, Ciarmatori *et al* 2001). Therefore, we also investigated their involvement in these fusions as they are found on the p-arms of mouse chromosomes 12, 15, 16, 17, 18, and 19, and are therefore in close proximity to the centromere (Appendix C-A). These chromosomes are not over-represented in $Rb1^{\Delta L/\Delta L}$ fusion events, further suggesting that loss of transcriptional regulation early in the cell cycle does not contribute to this phenotype (Appendix C-B, C). These data support a specific role for pRB in regulating chromatin structure at the centromeric repeat sequences of mitotic chromosomes that is independent of pRB's ability to regulate the G1 to S-phase transition in these cells.

In order to better understand the origin of defective chromosomal compaction in $Rb1^{\Delta L/\Delta L}$ mutant cells and its effect on mitosis, we established a video microscopy assay

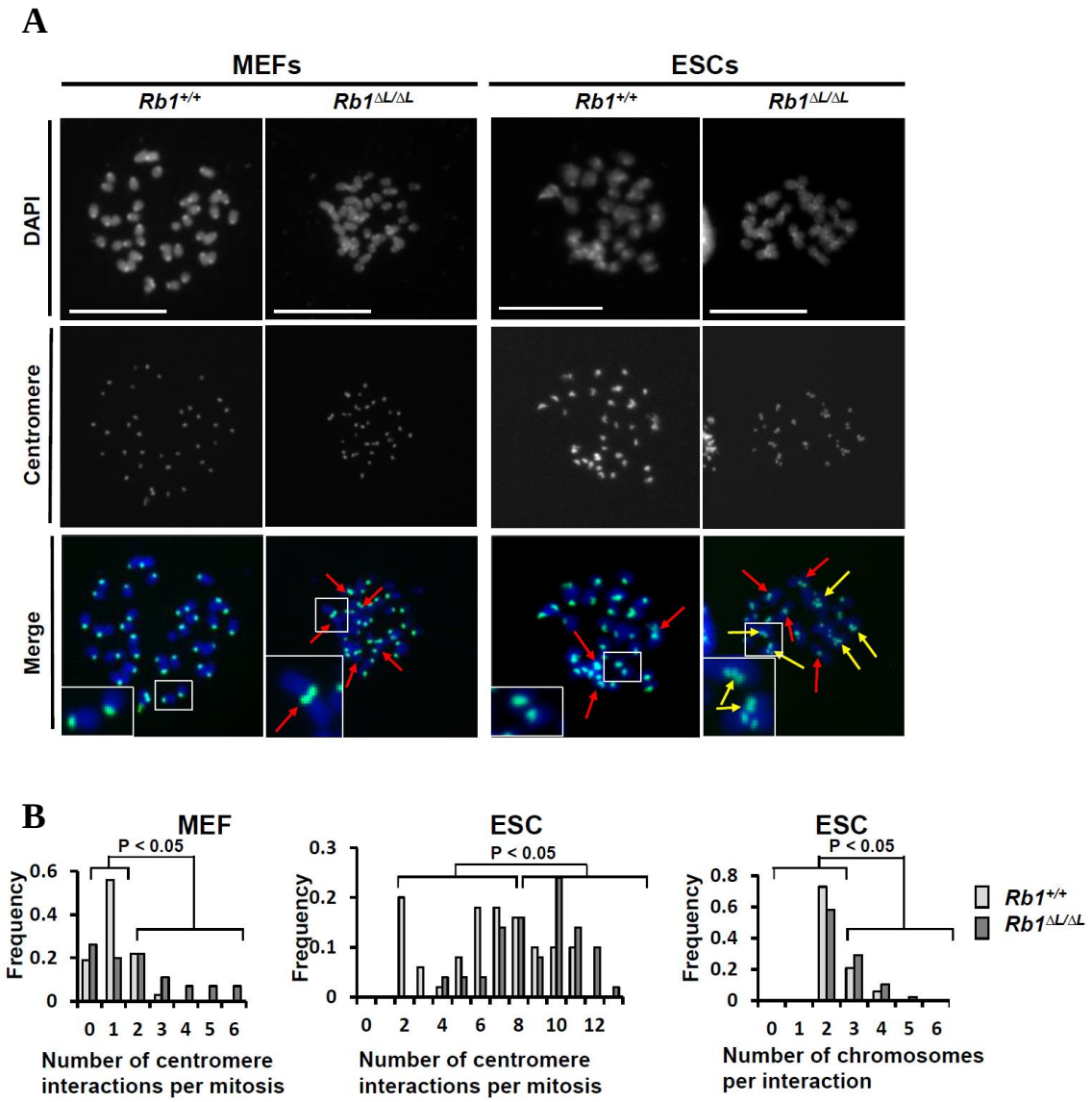

Figure 2.1: *Rb1*$^{\Delta L/\Delta L}$ cells display centromere fusions.

(A) Metaphase chromosome spreads were prepared from mouse embryonic fibroblasts (MEFs) or embryonic stem cells (ESCs) of the indicated genotypes. Chromosomes were stained with DAPI (blue) and a probe for major satellite repeats (green) to mark centromeres. Red arrows indicate contact between centromeres from different chromosomes, yellow arrows indicate centromere contact involving three or more chromosomes. Inlays highlight expanded views of select chromosomes. The scale bars are 25 µm. **(B)** The frequency of centromere interactions per mitosis is plotted for each genotype (*Rb1*$^{\Delta L/\Delta L}$ and *Rb1*$^{+/+}$) and cell type (MEF and ESC). In addition, the number of centromeres involved in each interaction was determined for ESC metaphase spreads and is displayed as the frequency of multiple chromosome interactions (right-most graph).

to observe cell division in MEFs. Early passage MEFs were transduced with an H2B-GFP expressing retrovirus. This led to equivalent expression of the H2B-GFP fusion in both genotypes. Importantly, expression of this fusion protein was very low and did not lead to a detectable increase in total H2B levels in these cells (Appendix D-A). H2B-GFP expressing cells were monitored microscopically under phase contrast and fluorescent optics to visualize chromosome condensation, metaphase alignment, anaphase, and cytokinesis. Images from three representative movies are shown in Figure 2.2. Typically, mutant cells took longer to progress from the onset of chromosome condensation to the point at which the metaphase plate is most tightly aligned (Table 2.1). Furthermore, the metaphase plate in mutant mitoses was less compact than wild type (Table 2.1). To determine whether these phenotypes are associated with defects later in mitosis, we observed sister chromatid separation in anaphase, and found that lagging chromosomes occurred more frequently in mutant cells (Table 2.1). Lagging chromosomes resulted in a prolonged anaphase that was often resolved abruptly, suggesting either chromosomal breaks or missegregation of whole chromosomes (Fig. 2.2, middle). Alternatively, some cells failed to complete mitosis and became binucleated (Fig. 2.2, bottom). In summary, mitosis in $Rb1^{\Delta L/\Delta L}$ cells is characterized by delayed chromosome condensation, an abnormal metaphase plate, and lagging chromosomes that lead to aneuploidy.

The preceding experiments are consistent with previous reports of defects in condensation and/or cohesion of mitotic chromosomes (Ono *et al* 2004). For these reasons we investigated the levels of the Condensin and Cohesin protein complexes that were present on chromatin in $Rb1^{\Delta L/\Delta L}$ cells. Protein extracts were prepared from cell cultures that were synchronized in S-phase, released and harvested at their maximal mitotic index (M-phase enriched), or that were asynchronous. SDS-PAGE and western blotting were used to analyze the chromatin fractions from these lysates using histone proteins as a marker for this fraction (Fig. 2.3A, Appendix D-B). Since Cohesins and Condensins are multiprotein complexes, we chose representative subunits to measure their presence on chromatin. The SMC1 subunit was used as a surrogate for the levels of the Cohesin complex; CAP-H and CAP-D2 were used similarly for Condensin I, and

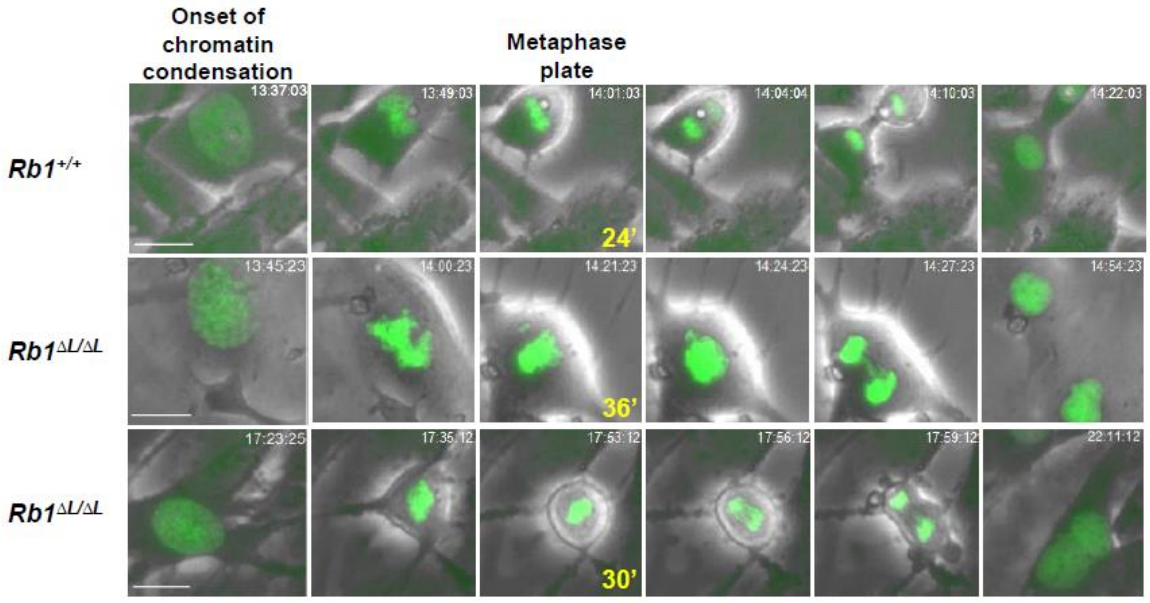

Figure 2.2: *Rb1*$^{\Delta L/\Delta L}$ cells display aberrant chromosome condensation and segregation.

Video microscopy was performed on MEFs expressing an H2B-GFP reporter by capturing phase contrast and GFP images every three minutes over a 15 hour time course. The images shown begin with the onset of chromatin condensation in prophase as the left most panel. The last image of the metaphase plate before the onset of anaphase is indicated along with the elapsed time since the onset of prophase (in minutes). The right most image shows resolved daughter (or binucleated) cells. Scale bars are 50 µm.

Table 2.1: Summary of mitotic phenotypes observed in video microscopy experiments.

Genotype[a]	N-value	Lagging Chromosomes[b]	N-value	Average time from onset of condensation to onset of anaphase (min)	Average metaphase plate width (μm)[c]
Rb1$^{+/+}$	57	14	43	27.95	4.99
Rb1$^{\Delta L/\Delta L}$	37	19[d]	27	33.89[e]	6.22[e]
Rb1$^{+/+}$ shLuc	38	11	37	33.92	4.77
Rb1$^{+/+}$ sh63	41	34[d]	43	107.07[e]	5.04
Rb1$^{+/+}$ sh64	10	8[d]	11	186.5[e]	7.96[e]
Rb1$^{+/+}$ sh66	27	18[d]	27	121.4[e]	7.03[e]

[a]For all statistical tests, *Rb1*$^{\Delta L/\Delta L}$ is compared with wild type, and all shRNAs directed against CAP-D3 were compared with shLuc.
[b]Includes mitoses where the metaphase plate never visually divided, chromatin decondensed and cells became tetraploid.
[c]Five equally spaced cross-sections for each metaphase plate were measured from the last image before the initiation of anaphase.
[d]A difference from controls that is above 95% confidence interval (χ^2 test, $P < 0.05$).
[e]Above 95% confidence interval (*t*-test, $P < 0.05$).

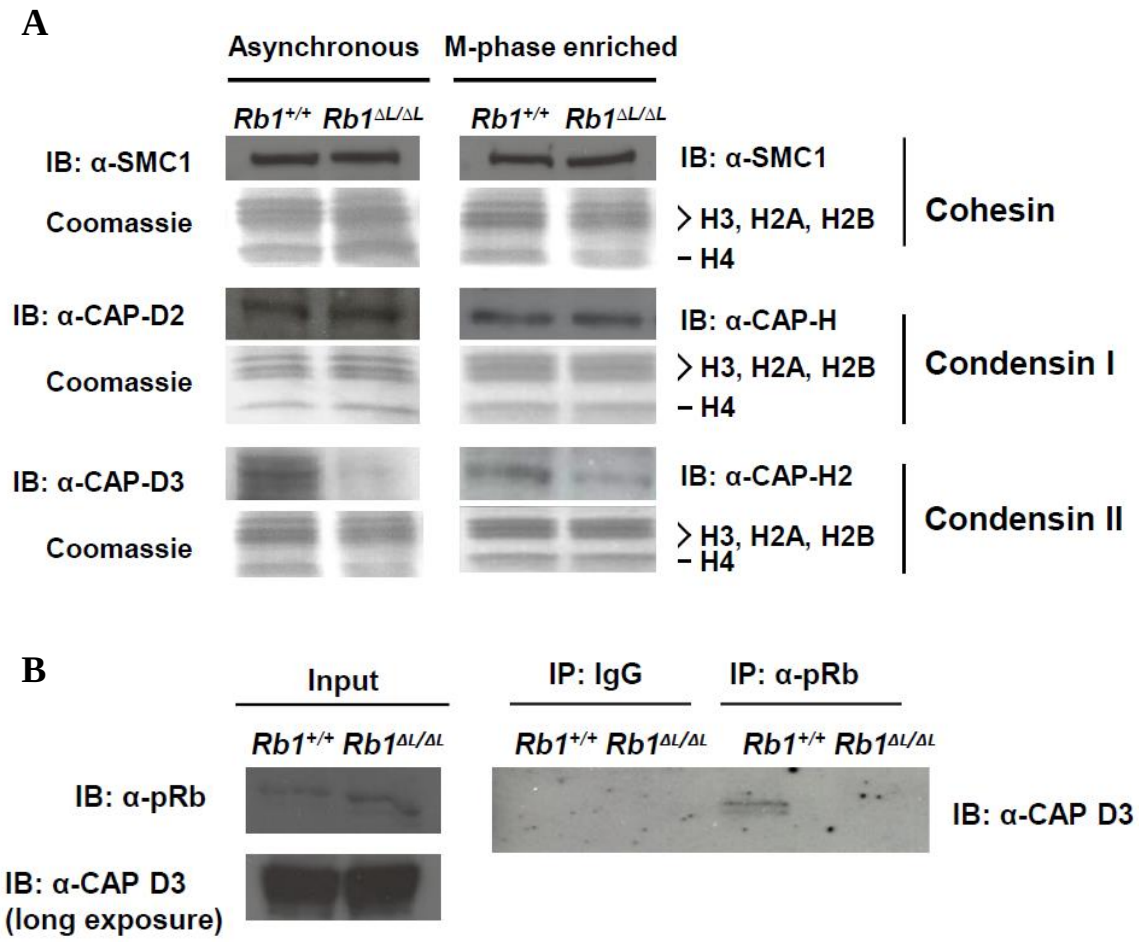

Figure 2.3: Defective loading of Condensin II complexes on *Rb1*$^{\Delta L/\Delta L}$ chromosomes.

(A) Chromatin fractions were prepared from MEFs that were either proliferating asynchronously or enriched for M-phase cells. Protein content in these fractions was analyzed by SDS-PAGE followed by coomassie staining for histone proteins, or western blotting for the indicated components of the Cohesin and Condensin complexes. **(B)** Extracts were prepared from MEFs of the indicated genotypes. Chromatin fractions from these cells were then subject to immunoprecipitation with anti-pRB antibodies. The relative amount of CAP-D3 precipitated with wild type and mutant pRB, was detected by western blotting. Input levels of relevant proteins from chromatin fractions are shown and the CAP-D3 blot is overexposed to demonstrate that Condensin II complexes are present in the *Rb1* mutant input.

CAP-H2 and CAP-D3 were used to detect Condensin II. This analysis revealed reduced levels of Condensin II on chromatin derived from *Rb1*$^{\Delta L/\Delta L}$ cells while the overall levels of Condensin I and Cohesin were unchanged. To ensure that the reduction in Condensin II loading on chromatin is not due to overall reduction of the protein, we probed for levels in whole cell extracts and determined that Condensin II protein is expressed at wild type levels in *Rb1*$^{\Delta L/\Delta L}$ fibroblasts (Appendix D-C).

Depletion of the Condensin II subunit CAP-D3 by RNAi delays progression from the onset of condensation to anaphase and results in lagging chromosomes in pRB deficient HeLa cells (Hirota *et al* 2004). Furthermore, a recent report indicates that GST-RB can bind to Condensin II complexes using its LXCXE binding cleft region (Longworth *et al* 2008). For this reason we investigated the role of CAP-D3 in more detail using video microscopy so that the mitotic defects in *Rb1*$^{\Delta L/\Delta L}$ fibroblasts could be directly compared with CAP-D3 deficiency in primary cells. To this end, we generated retroviruses expressing short hairpin RNAs against CAP-D3, along with an H2B-GFP reporter, and used them to infect wild type MEFs. Figure 2.4A demonstrates the degree of knock down obtained from each shRNA construct. We used the partial knock down of sh63, and the more extensive depletion of the others, to investigate the impact of different levels of CAP-D3 expression on mitosis in MEFs. Video microscopy revealed that partial knock down using sh63 resulted in a delay in reaching anaphase that was longer than in *Rb1*$^{\Delta L/\Delta L}$ cells, it also caused lagging chromosomes, but little widening of the metaphase plate (Fig. 2.4B middle, Table 2.1). Extensive depletion of CAP-D3, shown by sh64 (and sh66) caused a proportionately longer delay from chromosome condensation to anaphase than in sh63, but a similar frequency of lagging chromosomes (Fig. 2.4B bottom, Table 2.1). Interestingly, these depleted cells had a wider metaphase plate akin to *Rb1*$^{\Delta L/\Delta L}$ fibroblasts (Table 2.1). We interpret this to mean that the earliest defect in mitosis in *Rb1*$^{\Delta L/\Delta L}$ MEFs is similar to the delayed condensation that results from CAP-D3 depletion, but is less pronounced. Since RNAi depletion of CAP-D3 has been shown to reduce sister chromosome cohesion, this is a likely explanation for the broader metaphase plate in both *Rb1*$^{\Delta L/\Delta L}$ and CAP-D3 depleted MEFs (Hirota *et al* 2004). Lastly, CAP-D3 depleted, and *Rb1*$^{\Delta L/\Delta L}$ mutant cells, both exhibit lagging chromosomes in anaphase as a result of these chromosomal abnormalities. To ensure that the similarity of

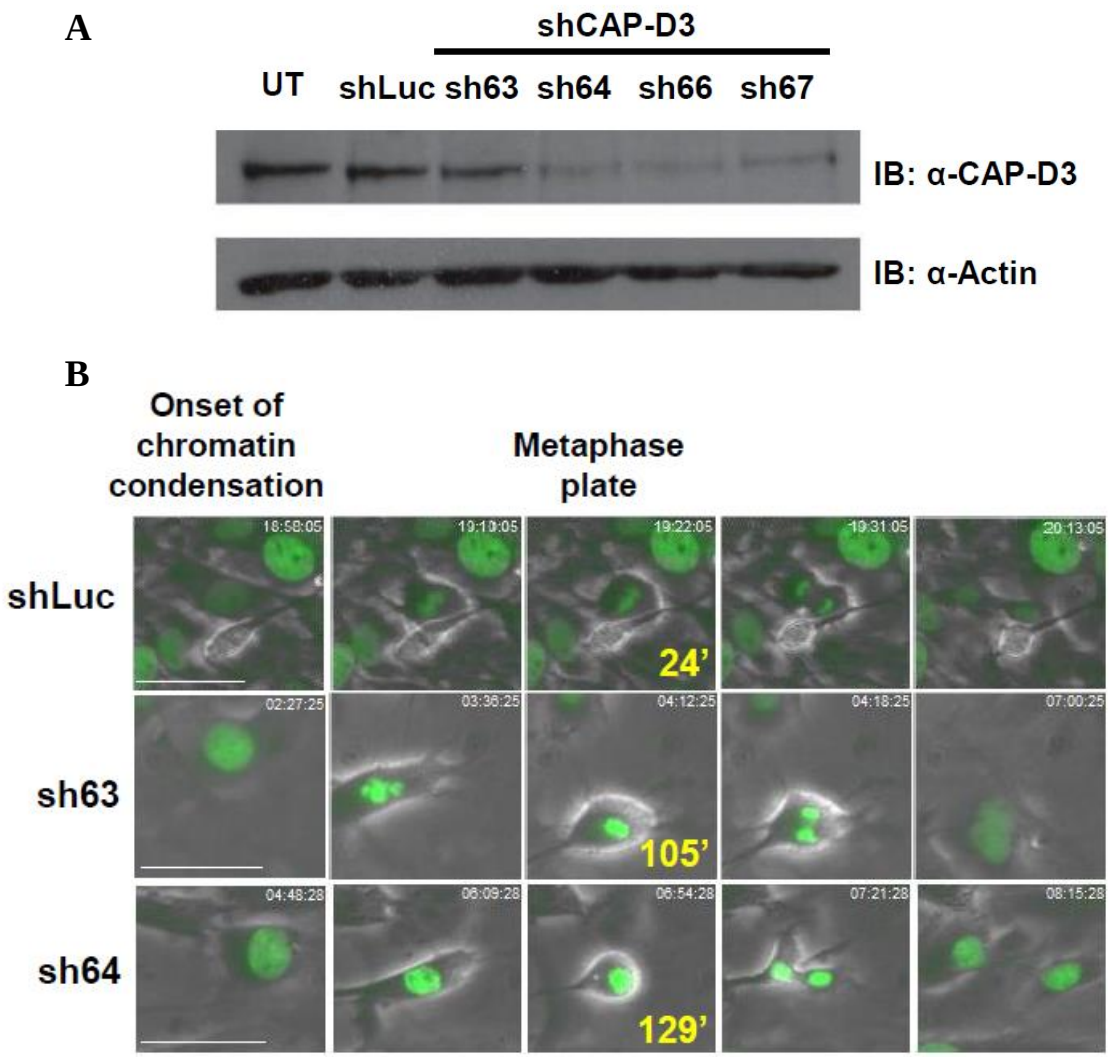

Figure 2.4: Mitotic phenotypes of CAP-D3 knock down MEFs mimic condensation and segregation defects in *Rb1*$^{\Delta L/\Delta L}$ MEFs.

(A) Wild type MEFs were transduced with retroviruses expressing the indicated shRNAs and H2B-GFP. Cell extracts were analyzed by western blotting for CAP-D3 and Actin. UT indicates untransduced cells. **(B)** Video microscopy was performed on cells expressing either a control luciferase shRNA, or shRNAs directed against CAP-D3 (sh63 and sh64). Phase contrast and GFP images were taken every three minutes for 15 hours. Representative pictures include the onset of prophase in the left most panel, and the last view of the metaphase plate before anaphase along with the time elapsed from prophase. The last frame on the right shows the cells either after cytokinesis (shLuc), or failure to resolve as two daughter cells resulting in binucleation (sh63), or as persistent anaphase bridges (sh64). The scale bars are 50 μm.

phenotype between *Rb1*$^{\Delta L/\Delta L}$ cells and CAP-D3 depleted cells is not a coincidence, we investigated the physical interaction between pRB and the Condensin II complex. Immunoprecipitation of pRB followed by western blotting for CAP-D3 reveals that pRB interacts with the Condensin II complex in the chromatin fraction of wild type, but not *Rb1*$^{\Delta L/\Delta L}$ MEFs (Fig. 2.3B). Western blots reveal the input levels of each of the relevant proteins and that CAP-D3 is present in this fraction. Furthermore, control immunoprecipitations were performed to detect pRB-E2F3 interactions to confirm the specificity of this interaction defect (Appendix D-D).

Therefore, these experiments reveal a role for pRB outside of the regulation of E2F target genes in the G1 phase of the cell cycle. We demonstrate that endogenous pRB interacts with Condensin II to compact mitotic chromosomes. Furthermore, a deficiency in this process causes a specific defect in condensation during prophase that manifests as lagging anaphase chromosomes in a primary cell culture system.

2.4.2 The *Rb1*$^{\Delta L}$ mutation exacerbates tumorigenesis in *Trp53*$^{-/-}$ mice

Since chromosome instability is commonly thought to contribute to tumorigenesis by facilitating the acquisition of malignant characteristics, we sought to investigate how the *Rb1*$^{\Delta L}$ mutation impacts cancer pathogenesis. Since we have shown that the *Rb1*$^{\Delta L}$ mutation compromises G1 cell cycle arrest in response to negative growth signals from DNA damage and oncogene induced senescence, we chose to cross *Rb1*$^{\Delta L/\Delta L}$ mice into a *Trp53*$^{-/-}$ background as *Trp53*$^{-/-}$ mice are known to be defective for the G1 arrest response from DNA breaks and senescence (Talluri *et al* 2010, Lowe *et al* 1993, Serrano *et al* 1997, Braig *et al* 2005, Post *et al* 2010). Consequently, comparing *Rb1*$^{\Delta L/\Delta L}$*; Trp53*$^{-/-}$ mice with *Trp53*$^{-/-}$ controls eliminates G1 to S-phase regulation in response to these stimuli in both cohorts of mice, and allows pRB's role in mitosis to be studied in relative isolation. Interestingly, *Rb1*$^{\Delta L/\Delta L}$*; Trp53*$^{-/-}$ mice succumb to cancer in a significantly shorter time than *Trp53*$^{-/-}$ controls (log rank test, P=0.0067; Fig. 2.5A). *Trp53*$^{-/-}$ mice have been reported to develop mainly thymic lymphomas with rare metastases and our data is no exception (Table 2.2). However, in addition to earlier tumor onset in *Rb1*$^{\Delta L/\Delta L}$*; Trp53*$^{-/-}$ mice, we also see a trend towards more aggressive tumors, increased numbers of

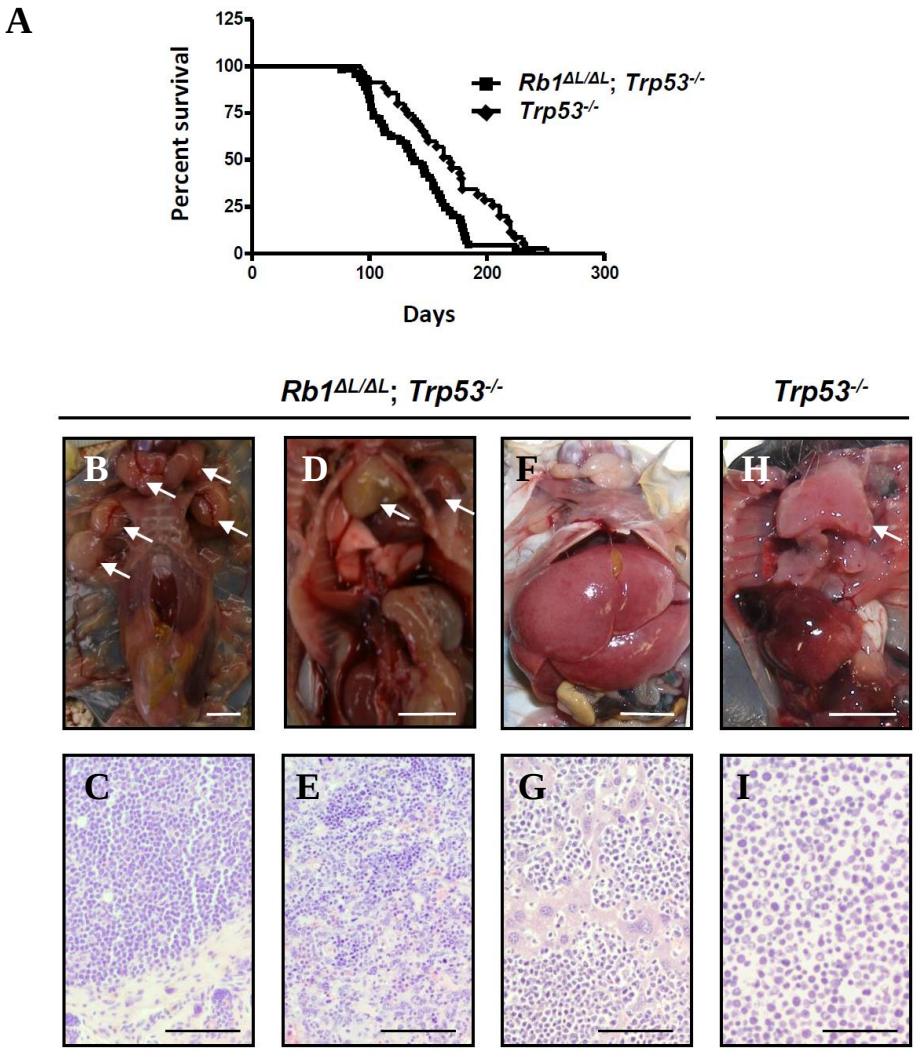

Figure 2.5: More aggressive tumors in *Rb1*$^{\Delta L/\Delta L}$; *Trp53*$^{-/-}$ mice.

(A) Kaplan-Meier survival proportions are shown for *Rb1*$^{\Delta L/\Delta L}$; *Trp53*$^{-/-}$ (n=45) and *Trp53*$^{-/-}$ (n=35) mice. **(B-I)** Representative images of cancers found in *Trp53*$^{-/-}$ control and *Rb1*$^{\Delta L/\Delta L}$; *Trp53*$^{-/-}$ compound mutants. **(B)** This necropsy reveals lymphoma with multiple affected lymph nodes as indicated by arrows. **(C)** H&E staining of a tissue section from one of the affected lymph nodes from B. **(D)** Mouse with thymic lymphoma and a sarcoma near its left forelimb, both are indicated by arrows. **(E)** Histological analysis of the sarcoma in D reveals extensive infiltration of this tumor by cells from the neighboring lymphoma. **(F)** Necropsy demonstrates an enlarged liver in this *Rb1*$^{\Delta L/\Delta L}$; *Trp53*$^{-/-}$ mutant mouse. **(G)** Histology of the liver in F reveals extensive infiltration by lymphocytes indicative of metastasis. **(H)** Necropsy of a *Trp53*$^{-/-}$ control mouse shows an enlarged thymus that is typical of these mice. **(I)** This micrograph shows H&E staining of a thymic lymphoma from a *Trp53*$^{-/-}$ mouse. Scale bars in B, D, F and H are 1 cm, and scale bars in C, E, G and I are 100 µm.

Table 2.2: Summary of pathology from mice used in this study.

Genotype	Lymphoma[a]	Sarcoma	Carcinoma	Multiple types[b]	Metastases	N-value
Trp53$^{-/-}$	33	3	0	1	7	35
Rb1$^{\Delta L/\Delta L}$;*Trp53*$^{-/-}$	31	27	3	15[c]	18[d]	45
Trp53$^{+/-}$	17	16	1	9	12	25
Rb1$^{\Delta L/\Delta L}$;*Trp53*$^{+/-}$	18	18	1	13	13	24

[a]Includes thymic lymphoma and other lymphomas.
[b]An individual mouse had more than one tumor in the categories on the left.
[c]A difference from controls that is above 95% confidence interval (χ^2 test, $P = 0.0019$).
[d]Above 90% confidence interval (χ^2 test, $P = 0.094$).

animals with multiple tumors, and more frequent metastases in *Rb1*$^{\Delta L/\Delta L}$*; Trp53*$^{-/-}$ compound mutant mice (Table 2.2). Examples of this aggressive cancer phenotype are shown in Figure 2.5. Figure 2.5B shows a mouse with lymphoma affecting at least five major lymph nodes in the thoracic and cervical regions. Panel C shows an H&E stained tissue section from one of these lymph nodes, revealing densely packed cells in immediate contact with the underlying epidermis, with no resemblance of normal lymph node structure. The mouse pictured in Panel D had both thymic lymphoma and a sarcoma associated with its left forelimb. The accompanying histology in Figure 2.5E shows that the sarcoma is being invaded by lymphocytes from the nearby thymic lymphoma. Figure 2.5F shows striking distension of the liver in a mouse that is caused by metastasis. Histology of this liver in Figure 2.5G shows islands of hepatocytes amid abundant invading lymphocytes. Lastly, the image in Figure 2.5H shows a typical, enlarged thymus from a *Trp53*$^{-/-}$ control. Histology of these lymphomas was typically characterized by larger cells, suggesting that *Trp53*$^{-/-}$ lymphomas are of a lower grade than those in C, E, and G (Fig. 2.5H). From this analysis it is clear that *Rb1*$^{\Delta L/\Delta L}$*; Trp53*$^{-/-}$ mice succumb to cancer more rapidly than *Trp53*$^{-/-}$ controls, and that the characteristics of disease in compound mutant animals indicates that these cancers are more aggressive than those found in *Trp53*$^{-/-}$ mice.

In order to make direct comparisons between *Rb1*$^{\Delta L/\Delta L}$*; Trp53*$^{-/-}$ and *Trp53*$^{-/-}$ derived tumors, we decided to focus on thymic lymphomas. These tumors have been extensively studied in *Trp53*$^{-/-}$ animals and have been shown to be near diploid with rare chromosomal translocations (Liao *et al* 1998, Artandi *et al* 2000, Braig *et al* 2005). In this way, they offered an ideal starting point for investigating the effects caused by the *Rb1*$^{\Delta L}$ mutation on chromosome instability. To ensure that the comparison between these tumors was appropriate, we sought to investigate whether the *Rb1*$^{\Delta L}$ mutation affects thymic development in a way that could bias this analysis. First, defects caused by the *Rb1*$^{\Delta L}$ mutation alone are not sufficient to cause cancer in this, or any other organ in these mice (Appendix E). Secondly, gross histological analysis of thymi from *Rb1*$^{\Delta L/\Delta L}$ and *Rb1*$^{\Delta L/\Delta L}$*; Trp53*$^{-/-}$ animals did not reveal any obvious abnormalities (Appendix F-A). Furthermore, analysis of CD4 and CD8 positive cells revealed no alterations in T-cell development, and rates of proliferation were unaltered by the *Rb1*$^{\Delta L}$ mutation (Appendix

F-B, C). Finally, E2F target gene expression was not deregulated in thymi from these mice (Appendix F-D). From these experiments we conclude that differences in *Rb1*$^{\Delta L/\Delta L}$*; Trp53*$^{-/-}$ and *Trp53*$^{-/-}$ thymic lymphomas are unlikely to be explained by differences in either development, or the basal proliferation rate of cells in this organ.

Examining the survival proportions of the animals that succumbed to thymic lymphoma alone revealed that the *Rb1*$^{\Delta L/\Delta L}$*; Trp53*$^{-/-}$ mice have a shorter latency before tumor formation compared with *Trp53*$^{-/-}$ controls (log rank test, P=0.0198; Fig. 2.6A). One possibility to explain the difference in aggressiveness of these tumors is that compound mutant lymphomas may arise from many initiating thymocytes resulting in a polyclonal tumor, whereas the *Trp53*$^{-/-}$ controls may be mono or oligoclonal. To address this question we used a PCR assay to detect individual T-cell receptor recombination events to estimate the number of individual thymocytes that have become transformed and populate each lymphoma (Fig. 2.6B, C). This revealed that tumors of both genotypes were rarely monoclonal, and both showed a similar range of clonality, suggesting that clonality does not bias our comparison between the thymic lymphomas found in animals of these two genotypes.

To investigate the effects of the *Rb1*$^{\Delta L}$ mutation on chromosome instability, we used array comparative genomic hybridization (aCGH) to compare the genomes of thymic lymphoma cells from *Rb1*$^{\Delta L/\Delta L}$*; Trp53*$^{-/-}$ and *Trp53*$^{-/-}$ mice. Figure 2.7A shows representative Log_2 ratio plots from male versus female control hybridizations as well as from selected *Rb1*$^{\Delta L/\Delta L}$*; Trp53*$^{-/-}$ and *Trp53*$^{-/-}$ tumors hybridized against same sex control DNA. Using male versus male, and male versus female control hybridizations as a guide for normal copy number and whole chromosome gains, we inferred changes in chromosome copy number present in these tumors. Since these lymphomas are polyclonal, the gain or loss of a single chromosome in one clone can be a relatively modest change when the whole thymus is analyzed as one. For this reason we searched for chromosomes that were statistically different than control, and did not try to distinguish if these represent single or multiple chromosome gains. Satisfyingly, the average number of gains and losses in our *Trp53*$^{-/-}$ lymphoma controls (4.2) was similar to the frequency of chromosome number changes reported by karyotyping in other

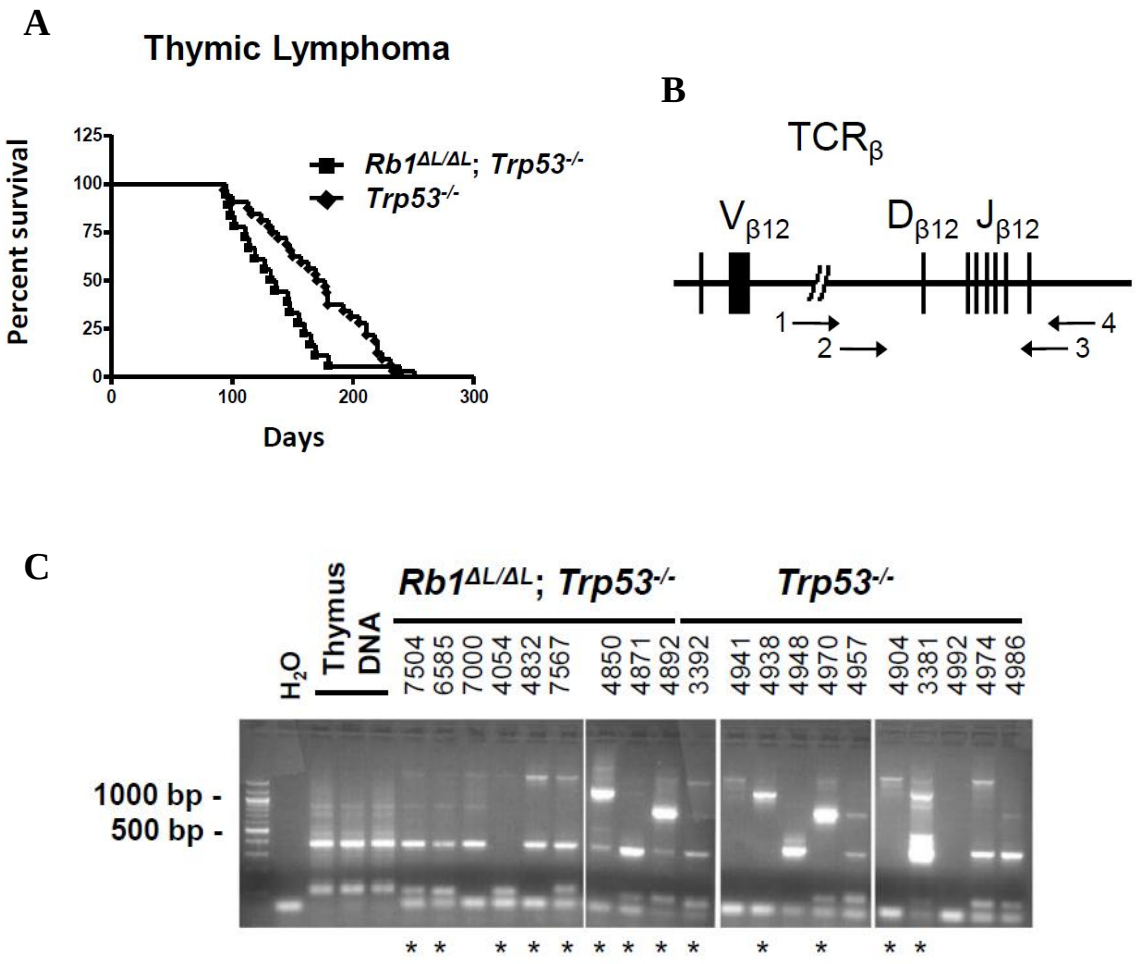

Figure 2.6: Non-bias selection of thymic lymphomas for subsequent analysis.

(A) Kaplan-Meier survival proportions are shown for *Rb1*$^{\Delta L/\Delta L}$; *Trp53*$^{-/-}$ (n=18) and *Trp53*$^{-/-}$ (n=32) mice that succumbed to thymic lymphoma. **(B)** Schematic diagram of the T-cell receptor β (TCR_β) locus that was PCR amplified to assess clonality of thymic lymphomas. Primer pairs 1 and 4, and 2 and 3 were used in a nested strategy to amplify rearranged forms of this gene found in tumor samples as described in materials and methods. **(C)** Agarose gel electrophoresis of TCR_β PCR, including a water only negative control, and three normal thymus samples as positive controls. Four digit numbers correspond to ear tag numbers for individual mice and are present to allow correlations with pathology data in Appendix H. The asterisks indicate samples that were used for aCGH analysis.

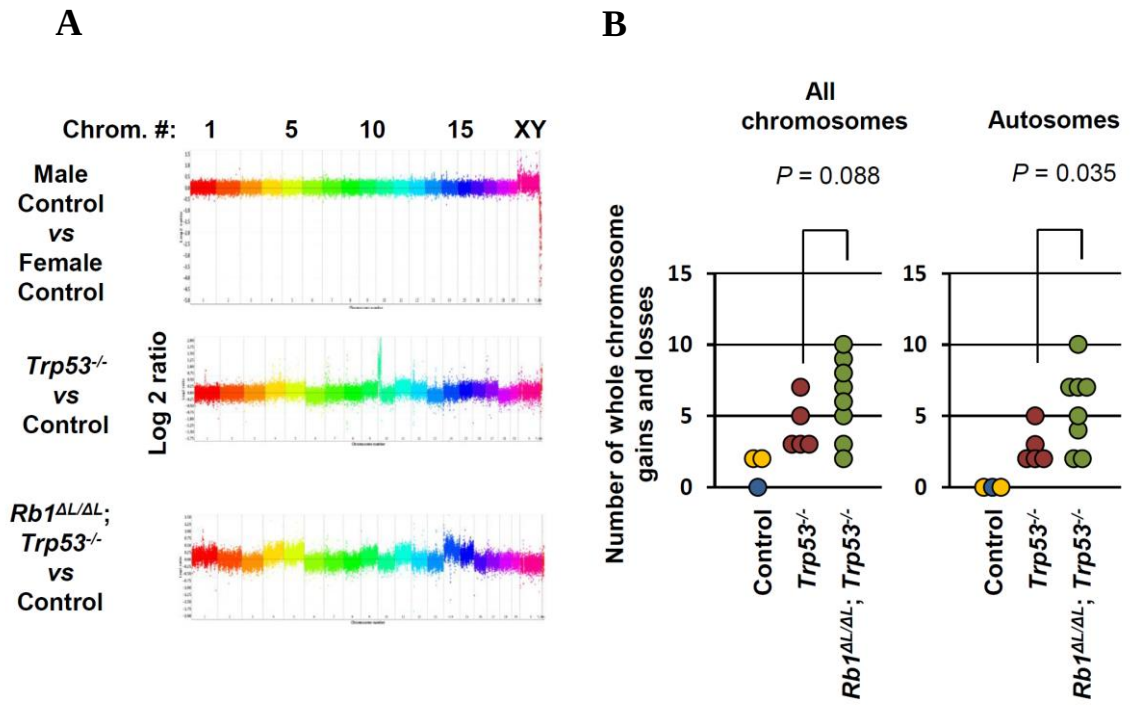

Figure 2.7: Increased genomic instability in *Rb1*$^{\Delta L/\Delta L}$; *Trp53*$^{-/-}$ thymic lymphomas.

(A) Control, or tumor DNA versus control, was used for hybridization to whole genome arrays to determine regions of gain or loss in thymic lymphoma samples. Representative graphs depicting Log_2 ratio values plotted against chromosome number are shown. Data points from individual chromosomes are shown in different colors. **(B)** Whole chromosome gains and losses were inferred by differences in an entire chromosome and compared with controls. The number of whole chromosome changes for each tumor is plotted against their genotypes. The control male versus control male hybridization is shown in blue, the male versus female hybridizations are shown in yellow, and *Trp53*$^{-/-}$ and *Rb1*$^{\Delta L/\Delta L}$; *Trp53*$^{-/-}$ samples are denoted by red and green respectively. The analysis of all chromosomes, or autosomes alone, are shown. The mean number of changes was compared between genotypes using a *t*-test.

studies of *Trp53* deficient lymphomas in which these cancers typically have chromosome counts in the low forties (Liao *et al* 1998, Artandi *et al* 2000, Braig *et al* 2005). Our analysis revealed that whole chromosome gains or losses were more prevalent in $Rb1^{\Delta L/\Delta L}$; $Trp53^{-/-}$ lymphomas than in $Trp53^{-/-}$ controls (Fig. 2.7B). Because not all tumors originate from mice of the same sex, and this creates unequal opportunities to gain and lose sex chromosomes, we have displayed this data in graphs for all chromosomes and for autosomes. This suggests that whole chromosome instability may be the underlying mechanism that increases cancer susceptibility in $Rb1^{\Delta L/\Delta L}$; $Trp53^{-/-}$ animals compared with $Trp53^{-/-}$ mice, an interpretation that is consistent with centromere fusions observed in metaphase spreads and lagging chromosomes in anaphase that were observed in our videos (Fig. 2.1A, Fig. 2.2). We note that the quantity of copy number segments (local regions of gain or loss relative to adjacent chromosomal sequences) are also elevated in most $Rb1^{\Delta L/\Delta L}$; $Trp53^{-/-}$ thymic lymphomas (Appendix G). This implies that smaller genomic rearrangements also take place and this is consistent with resolution of lagging chromosomes in Figure 2.2 (middle) occurring by chromosomal breakage. Therefore, both forms of chromosomal instability may be caused by the $Rb1^{\Delta L}$ mutation and contribute to the increase in cancer susceptibility that we observe.

Our analysis of the $Rb1^{\Delta L}$ allele's effects on cancer reveal that it causes a dramatic increase in susceptibility, and $Rb1^{\Delta L/\Delta L}$; $Trp53^{-/-}$ mice are characterized by more aggressive tumors than the $Trp53^{-/-}$ controls. Furthermore, characterization of genomic abnormalities found in $Rb1^{\Delta L/\Delta L}$ tumors demonstrates that they are consistent with the chromosomal and mitotic abnormalities in primary cultures that we observed in Figure 2.2 by video microscopy. These data strongly suggest that pRB facilitates mitotic chromosome condensation as part of its function as a tumor suppressor.

2.4.3 Accelerated loss of heterozygosity in $Rb1^{\Delta L/\Delta L}$ mice

Thus far, our work suggests that failure to condense and properly segregate mitotic chromosomes because of defective pRB-LXCXE interactions leads to chromosome instability and exacerbates cancer pathogenesis. In order to test this more directly, we generated cohorts of $Rb1^{\Delta L/\Delta L}$; $Trp53^{+/-}$ and $Trp53^{+/-}$ control animals. It is known that $Trp53^{+/-}$ mice develop a broad spectrum of tumors, including thymic

lymphomas, after a considerably longer latency period than *Trp53*$^{-/-}$ mice (Jacks *et al* 1994, Purdie *et al* 1994, Donehower *et al* 1995). Loss of heterozygosity, that eliminates the remaining wild type allele, is reported with high frequency in tumors from *Trp53*$^{+/-}$ mice strongly suggesting that it is the rate limiting step for tumor formation since it can cause the same types of cancer found in *Trp53*$^{-/-}$ animals (Jacks *et al* 1994). For this reason use of *Trp53*$^{+/-}$ mice has emerged as an assay for genome instability effects on cancer (Kuperwasser *et al* 2000, Smith *et al* 2006, Baker *et al* 2009). We followed these animals over approximately two years and discovered that the *Rb1*$^{\Delta L/\Delta L}$*; Trp53*$^{+/-}$ compound mutants succumbed to cancer at a significantly younger age than *Trp53*$^{+/-}$ controls (log rank test, P=0.0105; Fig. 2.8A). Consistent with previous reports we found that these animals were susceptible to a broad range of cancer types in both *Rb1*$^{\Delta L/\Delta L}$*; Trp53*$^{+/-}$ and control genotypes (Table 2.2). In this cross, the best evidence for increased aggressiveness in the compound mutants was the earlier age of cancer incidence. The histopathology of these tumors was similar, reinforcing the validity of comparing these two cohorts for their mechanism of tumor initiation (Appendix H). To search for loss of heterozygosity, DNA was extracted from tumors and subjected to Southern blot analysis to measure the relative abundance of wild type and null alleles of *Trp53*. This revealed that the wild type allele was reduced in abundance in tumor samples derived from all animals (Fig. 2.8B); the existence of residual wild type *Trp53* is consistent with the presence of *Trp53*$^{+/-}$ stroma in these tumor samples. Since these data reveal loss of the wild type *Trp53* locus in all of the tumors we analyzed, and *Rb1*$^{\Delta L/\Delta L}$*; Trp53*$^{+/-}$ mice develop cancer earlier, this suggests that the rate-limiting step for tumor formation, namely loss of heterozygosity, has taken place more rapidly and was facilitated by the *Rb1*$^{\Delta L}$ mutation in these mice (Fig. 2.8C).

This analysis of loss of heterozygosity in tumors from *Rb1*$^{\Delta L/\Delta L}$*; Trp53*$^{+/-}$ mice offers evidence that cells bearing the *Rb1*$^{\Delta L}$ mutation are more prone to chromosomal instability. Based on this experiment, and the analysis of *Rb1*$^{\Delta L/\Delta L}$*; Trp53*$^{-/-}$ lymphomas, our study reveals that chromosome condensation mediated by pRB is likely an important component of its role as a tumor suppressor.

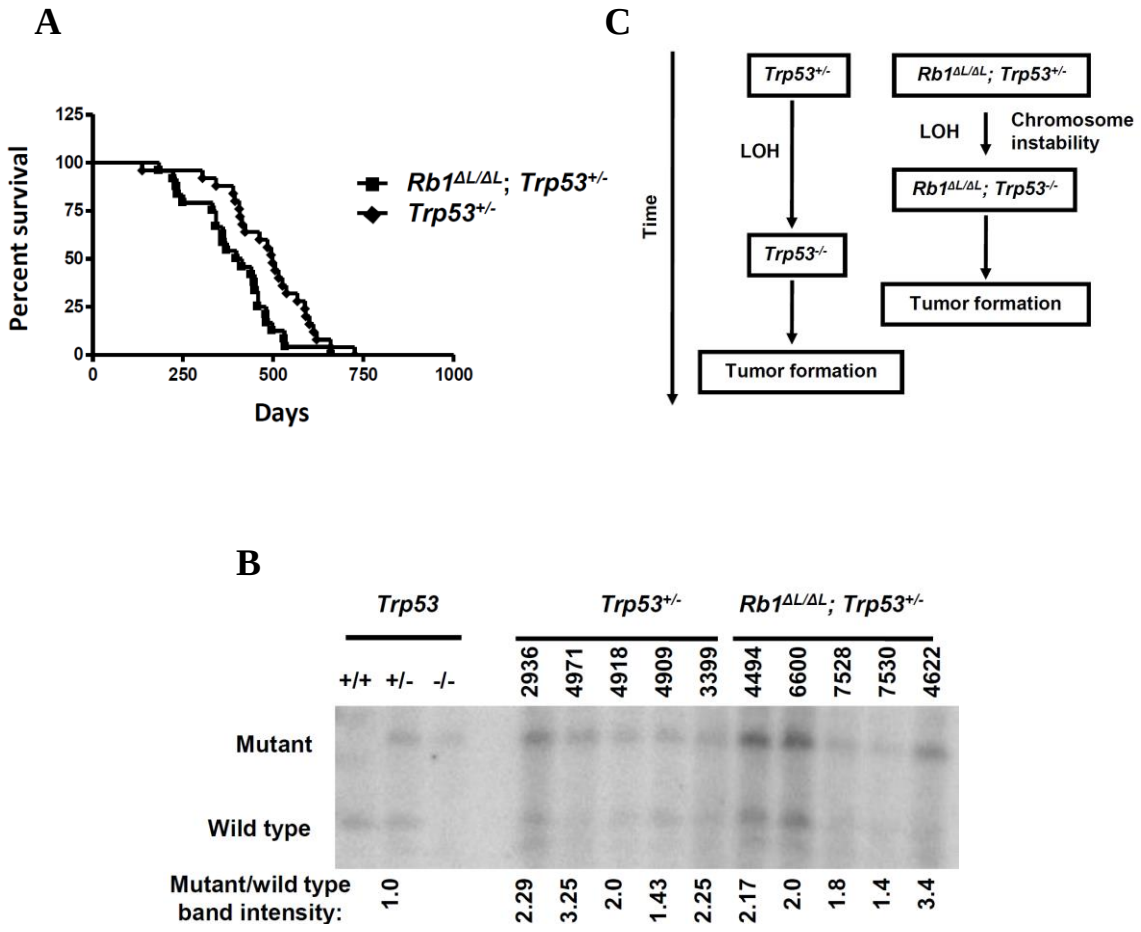

Figure 2.8: Accelerated loss of heterozygosity in *Rb1$^{\Delta L/\Delta L}$; Trp53$^{+/-}$* mice.

(A) Kaplan-Meier survival proportions are shown for *Rb1$^{\Delta L/\Delta L}$; Trp53$^{+/-}$* (n= 24) and *Trp53$^{+/-}$* (n=25) mice that succumbed to detectable cancers. **(B)** Southern blot analysis of tumors from *Rb1$^{\Delta L/\Delta L}$; Trp53$^{+/-}$* and *Trp53$^{+/-}$* mice was performed to assess the relative abundance of wild type and null *Trp53* alleles. Four digit numbers correspond to ear tags for individual mice to allow correlation with pathology data in Appendix G. The ratio of mutant to wild type allele abundance was determined by phosphorimaging and is displayed below each lane. **(C)** Model of the *Rb1$^{\Delta L}$* mutation's role in cancer susceptibility of these mice. Prior reports establish that *Trp53$^{+/-}$* mice succumb to cancer after a long latency and that it is accompanied by loss of heterozygosity at the *Trp53* locus. The age at which cancer initiates in *Rb1$^{\Delta L/\Delta L}$; Trp53$^{+/-}$* mice and the loss of the wild type *Trp53* locus in these tumors suggests that chromosome instability, caused by the *Rb1$^{\Delta L}$* mutation, induces loss of heterozygosity more rapidly, causing an earlier onset of cancer.

2.5 Discussion

This report investigates the role of the retinoblastoma protein in mitotic chromosome condensation. Our data indicate that this is a mechanism by which pRB acts as a tumor suppressor. The novelty of this tumor suppressive mechanism relies extensively on the ability to separate the mitotic specific functions of pRB from cell cycle entry control in our cancer prone mice. The analysis of thymic lymphomas in *Rb1*$^{\Delta L/\Delta L}$*; Trp53*$^{-/-}$ mice allows us to distinguish between the effects of the *Rb1*$^{\Delta L}$ mutation at these different points in the cell cycle. First, the response to DNA damage, or other stress inducing stimuli that activate p53, leads to increased p21/CIP1 expression, this in turn inhibits cyclin dependent kinases, and leads to pRB activation during G1 and cell cycle arrest (Campisi and d'Adda di Fagagna 2007). Since we have previously demonstrated that *Rb1*$^{\Delta L/\Delta L}$ cells are defective for a G1 arrest in response to γ-irradiation or oncogene induced senescence (Talluri *et al* 2010), including p53 deficiency in both cohorts of our tumor study prevents these *Rb1*$^{\Delta L}$ defects from confounding our interpretations. In addition to these defects, we have also determined that *Rb1*$^{\Delta L/\Delta L}$ cells are resistant to the growth inhibitory effects of transforming growth factor β (TGF-β) (Francis *et al* 2009). This growth inhibitory cytokine has been shown to play a key role in peripheral T-cell regulation. In particular, transgenic mice expressing a dominant negative TGF-β type II receptor in CD8 positive T-cells are prone to develop lymphoproliferative disease, and ultimately lymphoma (Lucas *et al* 2000, Lucas *et al* 2004). Interestingly, the phenotype of these animals is very different from *Rb1*$^{\Delta L/\Delta L}$*; Trp53*$^{-/-}$ mice, with extensive expansion of T cells in the periphery, but not the thymus. In fact, these studies suggest that TGF-β signaling may have very little function in the thymus. Since, *Rb1*$^{\Delta L/\Delta L}$ mice do not display any lymphoproliferative characteristics in their lifetime (Appendix F), it is unlikely that defective TGF-β growth control can explain the cancer phenotype of *Rb1*$^{\Delta L/\Delta L}$*; Trp53*$^{-/-}$ mice. There is no evidence of aberrant proliferation, or alterations in thymic development or morphology in *Rb1*$^{\Delta L/\Delta L}$*; Trp53*$^{-/-}$ mice. Furthermore, E2F target genes are regulated normally in this tissue. Because there is evidence of elevated chromosomal instability in these thymic lymphomas, our conclusion that pRB can function as a tumor suppressor by facilitating chromosome condensation is the most appropriate interpretation of these data.

The physical interaction between pRB and Condensin II offers a logical explanation for how pRB can participate in mitotic chromosome condensation. The phenotypes seen in video microscopy experiments of $Rb1^{\Delta L/\Delta L}$ cells suggest an acute defect in condensation during prophase. However, the extensive reduction in Condensin II levels on chromatin in asynchronously proliferating $Rb1^{\Delta L/\Delta L}$ MEFs suggests that pRB participates in chromatin loading earlier in the cell cycle, as these cultures contain only a small proportion of mitotic cells. In addition, Condensin II is known to be present on chromatin in interphase nuclei (Hirota *et al* 2004). These observations suggest that pRB's role in chromosome condensation may take place earlier in the cell cycle, perhaps in G1 where it is relatively unphosphorylated and already thought to regulate chromatin structure. Immunoprecipitation and western blotting experiments demonstrate that wild type pRB interacts with Condensin II in chromatin fractions, but this interaction was absent from $Rb1^{\Delta L/\Delta L}$ chromatin. Because Condensin II is underrepresented in this fraction in the first place, the lack of interaction may not reflect a need for the pRB-LXCXE binding cleft to mediate physical contact with Condensin II, but may indicate that this aspect of pRB is more important for Condensin II to be loaded on chromatin. It will be important in future studies to determine precisely how pRB uses LXCXE type interactions to exert its regulatory role over Condensin II function. At this point we have no evidence to indicate that it must be direct. In similar studies from the Dyson and te Riele labs, pRB is shown to also participate in chromosome cohesion at the centromere. In their studies, Cohesin complexes are reduced at centromeres. We cannot rule out that a similar biochemical defect may be present in $Rb1^{\Delta L/\Delta L}$ cells. However, Condensin complexes are also well known to be concentrated at centromeric heterochromatin (Ono *et al* 2004, Oliveira *et al* 2005, Vagnarelli *et al* 2006). Taken together, this suggests that future studies to understand pRB's role in mitosis will need to focus more closely on its ability to regulate chromatin at centromeric regions as this is likely where it acts to ensure proper chromosome architecture and segregation in mitosis.

This study reveals a novel mechanism of tumor suppression by pRB. While other reports have indicated that defective pRB is associated with chromosomal abnormalities (Hernando *et al* 2004, Gonzalo *et al* 2005, Iovino *et al* 2006, Isaac *et al* 2006, Longworth *et al* 2008, Amato *et al* 2009), our work demonstrates that this manifests in more rapid

tumor formation. This raises the question, how important is this aspect of tumor suppression by pRB relative to its well characterized role in regulating E2F transcription factors and entry into S-phase? The lack of spontaneous tumors in our *Rb1*$^{\Delta L/\Delta L}$ mice may suggest that it is less important. We favor a more cautious view of this question. The inability to arrest proliferation in G1 because of a pRB deficiency is also accompanied by deregulation of activator E2Fs, and this creates an intrinsic pro-growth signal. This is inherently a stronger oncogenic event than diminished chromosome condensation because it combines the loss of negative growth regulation with the gain of a growth promoting signal. Defective chromosome condensation on the other hand, creates the opportunity for genetic change that can contribute to cancer pathogenesis, but it does not provide an inappropriate growth promoting signal. For these reasons, experiments designed to equalize the loss of safeguards with gain of proliferative advantages will be necessary to appropriately compare these aspects of tumor suppression by pRB. Only through this type of investigation will it be possible to fully comprehend what makes the retinoblastoma gene such a critical factor in cell cycle regulation and cancer.

2.6 References

Aladjem, M.I., Spike, B.T., Rodewald, L.W., Hope, T.J., Klemm, M., Jaenisch, R., and Wahl, G.M. 1998. ES cells do not activate p53-dependent stress responses and undergo p53-independent apoptosis in response to DNA damage. *Curr Biol* **8**: 145-155.

Amato, A., Lentini, L., Schillaci, T., Iovino, F., and Di Leonardo, A. 2009. RNAi mediated acute depletion of retinoblastoma protein (pRB) promotes aneuploidy in human primary cells via micronuclei formation. *BMC Cell Biol* **10**: 79.

Artandi, S.E., Chang, S., Lee, S.L., Alson, S., Gottlieb, G.J., Chin, L., and DePinho, R.A. 2000. Telomere dysfunction promotes non-reciprocal translocations and epithelial cancers in mice. *Nature* **406**: 641-645.

Baker, D.J., Jin, F., Jeganathan, K.B., and van Deursen, J.M. 2009. Whole chromosome instability caused by Bub1 insufficiency drives tumorigenesis through tumor suppressor gene loss of heterozygosity. *Cancer Cell* **16**: 475-486.

Belmont, A.S. 2006. Mitotic chromosome structure and condensation. *Curr Opin Cell Biol* **18**: 632-638.

Braig, M., Lee, S., Loddenkemper, C., Rudolph, C., Peters, A.H., Schlegelberger, B., Stein, H., Dorken, B., Jenuwein, T., and Schmitt, C.A. 2005. Oncogene-induced senescence as an initial barrier in lymphoma development. *Nature* **436**: 660-665.

Bruins, W., Zwart, E., Attardi, L.D., Iwakuma, T., Hoogervorst, E.M., Beems, R.B., Miranda, B., van Oostrom, C.T., van den Berg, J., van den Aardweg, G.J., Lozano, G., van Steeg, H., Jacks, T., and de Vries, A. 2004. Increased sensitivity to UV radiation in mice with a p53 point mutation at Ser389. *Mol Cell Biol* **24**: 8884-8894.

Burkhart, D.L. and Sage, J. 2008. Cellular mechanisms of tumour suppression by the retinoblastoma gene. *Nat Rev Cancer* **8**: 671-682.

Campisi, J. and d'Adda di Fagagna, F. 2007. Cellular senescence: when bad things happen to good cells. *Nat Rev Mol Cell Biol* **8**: 729-740.

Cavanaugh, A.H., Hempel, W.M., Taylor, L.J., Rogalsky, V., Todorov, G., and Rothblum, L.I.e. 1995. Activity of RNA polymerase I transcription factor UBF blocked by Rb gene product [see comments]. *Nature* **374**: 177-180.

Ciarmatori, S., Scott, P.H., Sutcliffe, J.E., McLees, A., Alzuherri, H.M., Dannenberg, J.H., te Riele, H., Grummt, I., Voit, R., and White, R.J. 2001. Overlapping functions of the pRB family in the regulation of rRNA synthesis. *Mol Cell Biol* **21**: 5806-5814.

Dick, F.A., Sailhamer, E., and Dyson, N.J. 2000. Mutagenesis of the pRB pocket domain reveals that cell cycle arrest functions are separable from binding to viral oncoproteins. *Mol Cell Biol* **20**: 3715-3727.

Donehower, L.A., Harvey, M., Vogel, H., McArthur, M.J., Montgomery, C.A.J., Park, S.H., Thompson, T., Ford, R.J., and Bradley, A. 1995. Effects of genetic background on tumorigenesis in p53-deficient mice. *Mol Carcinog* **14**: 16-22.

Francis, S.M., Bergsied, J., Isaac, C.E., Coschi, C.H., Martens, A.L., Hojilla, C.V., Chakrabarti, S., Dimattia, G.E., Khoka, R., Wang, J.Y., and Dick, F.A. 2009. A functional connection between pRB and transforming growth factor beta in growth inhibition and mammary gland development. *Mol Cell Biol* **29**: 4455-4466.

Gonzalo, S., Garcia-Cao, M., Fraga, M.F., Schotta, G., Peters, A.H., Cotter, S.E., Eguia, R., Dean, D.C., Esteller, M., Jenuwein, T., and Blasco, M.A. 2005. Role of the RB1 family in stabilizing histone methylation at constitutive heterochromatin. *Nat Cell Biol* **7**: 420-428.

Grummt, I., Soellner, C., and Scholz, I. 1979. Characterization of a cloned ribosomal fragment from mouse which contains the 18S coding region and adjacent spacer sequences. *Nucleic Acids Res* **6**: 1351-1369.

Ham, M.F., Takakuwa, T., Rahadiani, N., Tresnasari, K., Nakajima, H., and Aozasa, K. 2007. Condensin mutations and abnormal chromosomal structures in pyothorax-associated lymphoma. *Cancer Sci* **98**: 1041-1047.

Hannan, K.M., Hannan, R.D., Smith, S.D., Jefferson, L.S., Lun, M., and Rothblum, L.I. 2000. Rb and p130 regulate RNA polymerase I transcription: Rb disrupts the interaction between UBF and SL-1. *Oncogene* **19**: 4988-4999.

Harrington, E.A., Bruce, J.L., Harlow, E., and Dyson, N. 1998. pRB plays an essential role in cell cycle arrest induced by DNA damage. *Proc Natl Acad Sci U S A* **95**: 11945-11950.

Heale, J.T., Ball, A.R., Jr., Schmiesing, J.A., Kim, J.S., Kong, X., Zhou, S., Hudson, D.F., Earnshaw, W.C., and Yokomori, K. 2006. Condensin I interacts with the PARP-1-XRCC1 complex and functions in DNA single-strand break repair. *Mol Cell* **21**: 837-848.

Hernando, E., Nahle, Z., Juan, G., Diaz-Rodriguez, E., Alaminos, M., Hemann, M., Michel, L., Mittal, V., Gerald, W., Benezra, R., Lowe, S.W., and Cordon-Cardo, C. 2004. Rb inactivation promotes genomic instability by uncoupling cell cycle progression from mitotic control. *Nature* **430**: 797-802.

Herrera, R.E., Sah, V.P., Williams, B.O., Makela, T.P., Weinberg, R.A., and Jacks, T. 1996. Altered cell cycle kinetics, gene expression, and G1 restriction point regulation in Rb-deficient fibroblasts. *Mol Cell Biol* **16**: 2402-2407.

Hirota, T., Gerlich, D., Koch, B., Ellenberg, J., and Peters, J.M. 2004. Distinct functions of condensin I and II in mitotic chromosome assembly. *J Cell Sci* **117**: 6435-6445.

Hogan, B., Beddington, R., Costantini, F., and Lacy, E. 1994. *Manipulating The Mouse Embryo:a laboratory manual*. Cold Spring Harbor Press, Plainview.

Hurford, R., Cobrinik, D., Lee, M.-H., and Dyson, N. 1997. pRB and p107/p130 are required for the regulated expression of different sets of E2F responsive genes. *Genes Dev* **11**: 1447-1463.

Iovino, F., Lentini, L., Amato, A., and Di Leonardo, A. 2006. RB acute loss induces centrosome amplification and aneuploidy in murine primary fibroblasts. *Mol Cancer* **5**: 38.

Isaac, C.E., Francis, S.M., Martens, A.L., Julian, L.M., Seifried, L.A., Erdmann, N., Binne, U.K., Harrington, L., Sicinski, P., Berube, N.G., Dyson, N.J., and Dick, F.A. 2006. The retinoblastoma protein regulates pericentric heterochromatin. *Mol Cell Biol* **26**: 3659-3671.

Jacks, T., Remington, L., Williams, B.O., Schmitt, E.M., Halachmi, S., Bronson, R.T., and Weinberg, R.A. 1994. Tumor spectrum analysis in p53-mutant mice. *Curr Biol* **4**: 1-7.

Kuperwasser, C., Hurlbut, G.D., Kittrell, F.S., Dickinson, E.S., Laucirica, R., Medina, D., Naber, S.P., and Jerry, D.J. 2000. Development of spontaneous mammary tumors in BALB/c p53 heterozygous mice. A model for Li-Fraumeni syndrome. *Am J Pathol* **157**: 2151-2159.

Lapointe, J., Malhotra, S., Higgins, J.P., Bair, E., Thompson, M., Salari, K., Giacomini, C.P., Ferrari, M., Montgomery, K., Tibshirani, R., van de Rijn, M., Brooks, J.D., and Pollack, J.R. 2008. hCAP-D3 expression marks a prostate cancer subtype with favorable clinical behavior and androgen signaling signature. *Am J Surg Pathol* **32**: 205-209.

Liao, M.J., Zhang, X.X., Hill, R., Gao, J., Qumsiyeh, M.B., Nichols, W., and Van Dyke, T. 1998. No requirement for V(D)J recombination in p53-deficient thymic lymphoma. *Mol Cell Biol* **18**: 3495-3501.

Longworth, M.S. and Dyson, N.J. 2010. pRB, a local chromatin organizer with global possibilities. *Chromosoma* **119**: 1-11.

Longworth, M.S., Herr, A., Ji, J.Y., and Dyson, N.J. 2008. RBF1 promotes chromatin condensation through a conserved interaction with the Condensin II protein dCAP-D3. *Genes Dev* **22**: 1011-1024.

Losada, A. and Hirano, T. 2005. Dynamic molecular linkers of the genome: the first decade of SMC proteins. *Genes Dev* **19**: 1269-1287.

Lowe, S.W., Schmitt, E.M., Smith, S.W., Osborne, B.A., and Jacks, T. 1993. p53 is required for radiation-induced apoptosis in mouse thymocytes. *Nature* **362**: 847-849.

Lucas, P.J., Kim, S.J., Melby, S.J., and Gress, R.E. 2000. Disruption of T cell homeostasis in mice expressing a T cell-specific dominant negative transforming growth factor beta II receptor. *J Exp Med* **191**: 1187-1196.

Lucas, P.J., McNeil, N., Hilgenfeld, E., Choudhury, B., Kim, S.J., Eckhaus, M.A., Ried, T., and Gress, R.E. 2004. Transforming growth factor-beta pathway serves as a primary tumor suppressor in CD8+ T cell tumorigenesis. *Cancer Res* **64**: 6524-6529.

Maeshima, K. and Laemmli, U.K. 2003. A two-step scaffolding model for mitotic chromosome assembly. *Dev Cell* **4**: 467-480.

Mayhew, C.N., Carter, S.L., Fox, S.R., Sexton, C.R., Reed, C.A., Srinivasan, S.V., Liu, X., Wikenheiser-Brokamp, K., Boivin, G.P., Lee, J.S., Aronow, B.J., Thorgeirsson, S.S., and Knudsen, E.S. 2007. RB loss abrogates cell cycle control and genome integrity to promote liver tumorigenesis. *Gastroenterology* **133**: 976-984.

Mendez, J. and Stillman, B. 2000. Chromatin association of human origin recognition complex, cdc6, and minichromosome maintenance proteins during the cell cycle: assembly of prereplication complexes in late mitosis. *Mol Cell Biol* **20**: 8602-8612.

Musacchio, A. and Salmon, E.D. 2007. The spindle-assembly checkpoint in space and time. *Nat Rev Mol Cell Biol* **8**: 379-393.

Nasmyth, K. 2005. How do so few control so many? *Cell* **120**: 739-746.

Oliveira, R.A., Coelho, P.A., and Sunkel, C.E. 2005. The condensin I subunit Barren/CAP-H is essential for the structural integrity of centromeric heterochromatin during mitosis. *Mol Cell Biol* **25**: 8971-8984.

Olshen, A.B., Venkatraman, E.S., Lucito, R., and Wigler, M. 2004. Circular binary segmentation for the analysis of array-based DNA copy number data. *Biostatistics* **5**: 557-572.

Ono, T., Fang, Y., Spector, D.L., and Hirano, T. 2004. Spatial and temporal regulation of Condensins I and II in mitotic chromosome assembly in human cells. *Mol Biol Cell* **15**: 3296-3308.

Ono, T., Losada, A., Hirano, M., Myers, M.P., Neuwald, A.F., and Hirano, T. 2003. Differential contributions of condensin I and condensin II to mitotic chromosome architecture in vertebrate cells. *Cell* **115**: 109-121.

Pear, W.S., Nolan, G.P., Scott, M.L., and Baltimore, D. 1993. Production of high-titre helper-free retroviuses by transient transfection. *Proc Natl Acad Sci* **90**: 8392-8396.

Pei, L. and Melmed, S. 1997. Isolation and characterization of a pituitary tumor-transforming gene (PTTG). *Mol Endocrinol* **11**: 433-441.

Post, S.M., Quintas-Cardama, A., Terzian, T., Smith, C., Eischen, C.M., and Lozano, G. 2010. p53-dependent senescence delays Emu-myc-induced B-cell lymphomagenesis. *Oncogene* **29**: 1260-1269.

Purdie, C.A., Harrison, D.J., Peter, A., Dobbie, L., White, S., Howie, S.E., Salter, D.M., Bird, C.C., Wyllie, A.H., Hooper, M.L., and Clarke, A.R. 1994. Tumour incidence, spectrum and ploidy in mice with a large deletion in the p53 gene. *Oncogene* **9**: 603-609.

Ren, B., Cam, H., Takahashi, Y., Volkert, T., Terragni, J., Young, R.A., and Dynlacht, B.D. 2002. E2F integrates cell cycle progression with DNA repair, replication, and G(2)/M checkpoints. *Genes Dev.* **16**: 245-256.

Ritchie, K., Seah, C., Moulin, J., Isaac, C., Dick, F., and Berube, N.G. 2008. Loss of ATRX leads to chromosome cohesion and congression defects. *J Cell Biol* **180**: 315-324.

Romanova, L., Korobova, F., Noniashvilli, E., Dyban, A., and Zatsepina, O. 2006. High resolution mapping of ribosomal DNA in early mouse embryos by fluorescence in situ hybridization. *Biol Reprod* **74**: 807-815.

Samoshkin, A., Arnaoutov, A., Jansen, L.E., Ouspenski, I., Dye, L., Karpova, T., McNally, J., Dasso, M., Cleveland, D.W., and Strunnikov, A. 2009. Human condensin function is essential for centromeric chromatin assembly and proper sister kinetochore orientation. *PLoS One* **4**: e6831.

Schvartzman, J.M., Sotillo, R., and Benezra, R. 2010. Mitotic chromosomal instability and cancer: mouse modelling of the human disease. *Nat Rev Cancer* **10**: 102-115.

Serrano, M., Lin, A.W., McCurrach, M.E., Beach, D., and Lowe, S.W. 1997. Oncogenic ras provokes premature senescence associated with accumulation of p53 and p16. *Cell* **88**: 593-602.

Smith, A.P., Henze, M., Lee, J.A., Osborn, K.G., Keck, J.M., Tedesco, D., Bortner, D.M., Rosenberg, M.P., and Reed, S.I. 2006. Deregulated cyclin E promotes p53 loss of heterozygosity and tumorigenesis in the mouse mammary gland. *Oncogene* **25**: 7245-7259.

Talluri, S., Isaac, C.E., Ahmad, M., Henley, S.A., Francis, S.M., Martens, A.L., Bremner, R., and Dick, F.A. 2010. A G1 checkpoint mediated by the retinoblastoma protein that is dispensable in terminal differentiation but essential for senescence. *Mol Cell Biol* **30**: 948-960.

Vader, G. and Lens, S.M. 2008. The Aurora kinase family in cell division and cancer. *Biochim Biophys Acta* **1786**: 60-72.

Vagnarelli, P., Hudson, D.F., Ribeiro, S.A., Trinkle-Mulcahy, L., Spence, J.M., Lai, F., Farr, C.J., Lamond, A.I., and Earnshaw, W.C. 2006. Condensin and Repo-Man-PP1 co-operate in the regulation of chromosome architecture during mitosis. *Nat Cell Biol* **8**: 1133-1142.

Whitehurst, C.E., Chattopadhyay, S., and Chen, J. 1999. Control of V(D)J recombinational accessibility of the D beta 1 gene segment at the TCR beta locus by a germline promoter. *Immunity* **10**: 313-322.

Zheng, L., Flesken-Nikitin, A., Chen, P.L., and Lee, W.H. 2002. Deficiency of Retinoblastoma gene in mouse embryonic stem cells leads to genetic instability. *Cancer Res* **62**: 2498-2502.

Chapter 3

3 Haploinsufficiency of a pRB-E2F1-Condensin II complex causes genome instability and contributes to mesenchymal cancers

3.1 Abstract

Genomic instability is a characteristic of malignant cells, however, evidence for its role as an active contributor to tumorigenesis has been enigmatic. In this study we demonstrate that a complex containing the retinoblastoma protein, E2F1, and condensin II localizes to pericentromeric repeat regions. In its absence, DNA double strand breaks ensue and persist through mitosis and into the next G1 phase. Surprisingly, loss of even one copy of the retinoblastoma gene (*RB1*) was sufficient to cause DNA breaks and reduce recruitment of Condensin II to pericentromeric repeats. We further investigated DNA damage and mitotic errors in hemizygous *RB1* mutant fibroblasts from retinoblastoma patients, these cells also exhibited DNA breaks and lagging chromosomes in anaphase. We subsequently determined that *RB1* mutation status correlated with copy number variation, chromosomal gains and losses, as well as rearrangements, in cancers of mesenchymal origin. Importantly, the magnitude of these changes was indistinguishable between $RB1^{+/-}$ and $RB1^{-/-}$ tumors, demonstrating the haploinsufficiency of *RB1* hemizygosity. Lastly, using gene-targeted mice we determine that mutation of just one copy of the murine *Rb1* gene causes sarcomas that are accompanied by chromosomal abnormalities comparable to homozygous *Rb1* mutants. In sum, our study identifies a chromatin regulating complex whose abundance directly impacts genome stability and cancer pathogenesis.

3.2 Introduction

Fidelity of DNA replication and cell division are critical processes in multicellular organisms. Errors that go unrepaired can be passed on to daughter cells and contribute to the genetic changes that are essential for cancer (Lukas *et al* 2011). A general principal

of cell cycle regulation is that damaged DNA signals the cell cycle to arrest, and repair is undertaken before advancement into mitosis. Recent evidence suggests that there may be exceptions to this principle, as DNA breaks observed before mitosis have been shown to be transmitted through M-phase and result in residual damage in the ensuing G1 phase of daughter cells (Torres-Rosell *et al* 2007, Lukas *et al* 2011). These DNA lesions are often associated with replication stress that occurs in fragile or repetitive regions of the genome (Lukas *et al* 2011, Aguilera and Gomez-Gonzalez 2008). The ability of these damaged sites to evade checkpoints suggests their impact on genomic instability and cancer may be significant.

Replication fork stalling in fragile or repetitive sequences can lead to a state known as under replication (Dulev *et al* 2009). Under replication can create short gaps in sequence, or unresolved replication intermediates that persist beyond S-phase (Dulev *et al* 2009). Much of the evidence for under replication has been demonstrated using repetitive elements in yeast such as the rDNA locus, a genomic region that is known to require condensin complex function for replication and accurate segregation in mitosis (Dulev *et al* 2009, Johzuka *et al* 2006, Johzuka and Horiuchi 2007, Clemente-Blanco *et al* 2009, Ide *et al* 2010). Mammals contain two condensin complexes, but only Condensin II is constitutively nuclear, suggesting it can play roles in both replication and condensation during the cell cycle (Losada and Hirano 2005, Hirota *et al* 2004). In addition to its canonical role in facilitating mitotic chromosome condensation, chromosome shape, and controlling recombination, Condensin II has been implicated in both DNA replication and DNA damage repair (Wood *et al* 2008, Wang *et al* 2005). In particular, Condensin II functions in the resolution of sister chromatids immediately following replication in S-phase (Ono *et al* 2013). Despite these roles for Condensin II in S-phase and mitosis, we still know little about the fundamentals of how it is recruited to specific genomic locations, such as repetitive sequences, to carry out these functions.

The retinoblastoma protein (pRB) is generally thought of as a regulator of the G1 to S-phase transition through its control of E2F transcription factors (Dyson 1998). However, loss of pRB function leads to many of the same phenotypes as defects in Condensin II (Coschi *et al* 2010, Longworth *et al* 2008, Manning *et al* 2010). pRB is

implicated in an S-phase checkpoint to repair DNA breaks and it facilitates chromosome condensation in mitosis (Knudsen *et al* 2000, Sever-Chroneos *et al* 2001, Wells *et al* 2003, Avni *et al* 2003, Coschi *et al* 2010, Longworth *et al* 2008). On a molecular level it has been demonstrated to interact with E2F1 in S-phase on chromatin, and a number of reports have implicated such a complex in regulating the initiation of DNA replication (Knudsen *et al* 2000, Wells *et al* 2003, Avni *et al* 2003). Phenotypically, pRB deficient cells have been demonstrated to have increased levels of spontaneous DNA breaks and to undergo chromosome missegregation in mitosis (Pickering and Kowalik 2006, Hernando *et al* 2004, Mayhew *et al* 2007, Knudsen *et al* 2000). In particular, pRB loss alters the structure and function of the pericentromeric and centromeric regions of mitotic chromosomes, a location known to be enriched in Condensin II complexes (Isaac *et al* 2006, Coschi *et al* 2010, Stear and Roth 2002, Ono *et al* 2004, Shintomi *et al* 2011, Savvidou *et al* 2005, Samoshkin *et al* 2009). An obvious connection between pRB and Condensin II deficient phenotypes is their physical interaction, however there are a plethora of competing models for how loss of pRB can cause these genomic abnormalities. Altered regulation of E2F transcription has been implicated in shifts in intermediary metabolism, missexpression of spindle assembly checkpoint genes, as well as imbalances in nucleotide pools (Nicolay *et al* 2013, Reynolds *et al* 2013, Hernando *et al* 2004, Margottin-Goguet *et al* 2003, Nisculescu *et al* 1998, Srinivasan *et al* 2007). Thus, a clear mechanism of pRB function in genome stability has yet to emerge, in part because these altered phenotypes are not necessarily mutually exclusive, and complete loss of pRB function may cause each of them simultaneously.

Coordination of DNA replication is a complex process and many factors can alter replisome progression leading to replication stress. This suggests that signals to trigger the initiation of replication must be tightly regulated and factors involved in the replication process must be available in the appropriate abundance to avoid replication stress. Notably, under replication is reported to be caused by insufficient supplies of replication machinery (Dulev *et al* 2009). Haploinsufficiency occurs when a single functional copy of a gene fails to recapitulate the wild type condition. Given the importance of supplying replication machinery in S-phase, it is surprising that examples of haploinsufficiency for these factors are unreported. The CKI $p27^{Kip1}$ inhibits

cyclin/cdks whose overactivation can cause replication stress. While deficiency for the cyclin dependent kinase inhibitor $p27^{Kip1}$ has yet to be reported to cause replication stress, it is noteworthy that murine $p27^{Kip1}$ has been demonstrated to exhibit a haploinsufficient tumor suppressor phenotype when challenged with DNA damage-inducing γ-irradiation or chemical carcinogens. Importantly, these $p27^{+/-}$ mice develop tumors that retain the wild type allele (Fero *et al* 1998). It is unclear whether pRB exhibits a truly haploinsufficient phenotype. In humans, the retinoblastoma gene (*RB1*) is lost in the majority of retinoblastomas and small cell lung cancers, and is sporadically eliminated in other cancers (Sherr 1996, Knudson 1971, Harbour *et al* 1988, Hensel *et al* 1990). The canonical way in which *RB1* function is lost occurs *via* the classic 'two hit' model proposed by Knudson to explain the incidence of retinoblastoma in children (Knudson 1971). Because loss of heterozygosity was the rate-limiting step in retinoblastoma genesis, Knudson concluded that heterozygosity of *RB1* did not create a haploinsufficiency, and therefore did not functionally contribute to tumorigenesis. This premise is largely recapitulated in $Rb1^{+/-}$ mice that develop pituitary tumors characterized by loss of heterozygosity (Jacks *et al*1992). On the contrary, crosses between *Rb1* and *Trp53* deficient mice revealed that $Rb1^{+/-}$; $Trp53^{-/-}$ mice develop more rapid thymic lymphomas than $Trp53^{-/-}$ controls (Williams *et al* 1994). In most cases, these tumors were not accompanied by LOH to eliminate the remaining *Rb1* allele (Williams *et al* 1994). Compound homozygous mutant mice from this cross are inviable thus preventing a direct comparison of hemizygosity of *Rb1* with homozygous null, which would truly determine if this is an example of haploinsufficiency. Therefore while the majority of data investigating the role of the retinoblastoma gene in cancer indicates that only LOH completely eliminates its function, this may not be true for all contexts of *RB1* loss in tumorigenesis.

In this study we describe a complex composed of pRB, E2F1, and Condensin II that localizes to pericentromeric repeats. Cells that are unable to assemble this complex display increased DNA breaks at pericentromeric regions, γH2AX foci that persist through mitosis into the ensuing G1, and lagging anaphase chromosomes that are evident in mitosis. Our data are highly suggestive that the genomic instability associated with loss of this novel complex result from replication stress. Importantly, these phenotypes

were recapitulated in *Rb1*$^{+/-}$ and *Rb1*$^{\Delta L/+}$ fibroblasts, indicating that this genome instability phenotype is gene-dosage dependent. Similarly, we demonstrate that fibroblasts from retinoblastoma patients (*RB1*$^{+/-}$) exhibit mitotic defects and increased DNA damage, akin to our mutant fibroblasts from mice. Using genotype and copy number variation data from the catalogue of somatic mutations in cancer (COSMIC) database, we demonstrate that *RB1*$^{+/-}$ lymphoma and sarcoma cancer cell lines exhibit as much genomic instability as *RB1*$^{-/-}$ cell lines (COSMIC database). Finally, using gene targeted mice bearing a single mutant allele that is defective for recruiting Condensin II to pericentromeric DNA (*Rb1*$^{\Delta L}$), we demonstrate that *Rb1*$^{\Delta L/+}$*; Trp53*$^{-/-}$ mice have a significantly reduced survival compared to *Trp53*$^{-/-}$ controls that is indistinguishable from *Rb1*$^{\Delta L/\Delta L}$; *Trp53*$^{-/-}$ mice. This provides proof of principle that dosage sensitivity of a pRB-E2F1-Condensin II complex compromises the maintenance of genome stability and plays a causative role in cancer.

3.3 Methods

3.3.1 Cell culture, viral infections and microscopy

Primary mouse embryonic fibroblasts (MEFs) were prepared and cultured according to standard methods as reported previously for the following genotypes: *Rb1*$^{+/+}$, *Rb1*$^{+/-}$, *Rb1*$^{-/-}$, *Rb1*$^{\Delta L/+}$, *Rb1*$^{\Delta L/\Delta L}$, *E2f1*$^{+/+}$, *E2f1*$^{-/-}$ (Hurford *et al* 1997). Mitotic chromosome spreads were prepared from MEFs by treating cells with 50 ng/mL of colcemid for three hours before harvesting, swelling, and fixing. Chromosome spreads were stained with Vectashield mounting media with DAPI. Fluorescent microscopic images were captured on a Zeiss axioskop 40 microscope using a Spotflex camera and EyeImage software.

To introduce H2B-GFP into MEFs, we utilized the pBABE-H2BGFP vector (Coschi *et al* 2010). Viral vectors were packaged into ecotropic retroviruses using Bosc23 cells and subsequently used to infect MEFs as described (Pear *et al* 1993).

Primary patient fibroblasts (GM_01123, GM_01408, GM_06418) were obtained from the Coriell Institute for Medical Research and cultured in DMEM supplemented with 15% FBS and 1X Glutamine-Penicillin-Streptomycin (Fisher Scientific Cat. # SV 30082.01). IMR90 fetal lung fibroblasts from ATCC (Cat. # CCL-186), WI-38 fetal lung fibroblasts from ATCC (Cat. # CCL-75) and BJ foreskin fibroblasts from ATCC (Cat. # CRL-2522) were cultured in DMEM supplemented with 10% FBS and 1X Glutamine-Penicillin-Streptomycin (Fisher Scientific Cat. # SV 30082.01).

To introduce H2B-GFP into human fibroblasts, we created a FUtdTW lentiviral vector that expresses H2BGFP by cloning the gene from the pBOS-H2BGFP. This lentiviral vector, along with the PMD2.G and PAX2 vectors were packaged into lentiviruses using Phoenix cells and subsequently used to infect human fibroblasts according to Coschi *et* al and Pear *et al*, with the necessary precautions for lentiviral work (Coschi *et al* 2010, Pear *et al* 1993).

Cancer cell lines, SK-PN-DW (Cat. # CRL-2139), RD (Cat. #CCL-136) and T1-73 (Cat. # CRL-7943) from ATCC were cultured in DMEM supplemented with 10% FBS. Cancer cell lines MES-SA (Cat. #CRL-1976) and SK-LMS (Cat. # HTB-88) from ATCC were cultured in McCoy's 5A and EMEM media respectively, supplemented with 10% FBS.

Live cell microscopy was carried out as described previously (Coschi *et al* 2010).

Stained tissue sections were examined microscopically on a Zeiss axioskop 40 microscope and photographed using a Spotflex camera and EyeImage software.

3.3.2 Antibodies and protein detection

The following antibodies were used to detect or precipitate proteins in this study: mouse anti-pRB (G3-245, BD-Pharmingen), rabbit anti-pRB (sc-7905, Santa Cruz), mouse anti-Phospho histone H2A.X Ser139 (05-636, Millipore), rabbit anti-Phospho H2A.X Ser139 (07-164 Millipore), mouse anti-digoxigenin (11 333062910, Roche), rabbit anti E2F1 (C-20) (sc-193, Santa Cruz), rabbit anti-CAP-D3 (previously described

Coschi *et al* 2010), goat anti-mouse Alexa fluor 488 (A11029, Invitrogen), goat-anti-rabbit Alexa fluor 594 (A11012, Invitrogen).

3.3.3 GST pulldowns

Nuclear extracts from cell lines and GST-pulldowns were obtained as previously described (Dick *et al* 2000). Eluted protein from each sample was used to immunoblot for pRB and the nuclear loading control SP1. Eluted protein was also run on an SDS-PAGE gel and stained with Coomassie to detect levels of GST and GST-E7.

3.3.4 Fluorescence *in situ* hybridization (FISH) and immunofluorescence (IF)

Asynchronously cycling cells were grown on glass cover slips and processed as follows. For FISH, cells were fixed in 3% formaldehyde in 1X PBS. Cells were washed and permeabilized in 0.5% Triton in 1X PBS, dehydrated in an ethanol series, followed by denaturation in 50% formamide in 2X SSC. Cells were then rinsed in ice cold 2X SSC and hybridized over night with denatured probe at 37^{o}C in a humidified chamber. BAC probes were purchased from The Centre for Applied Genomics and include: RP23-342L13, RP23-191E3. Cells were rinsed three times with 50% formamide in 2X SSC, and three times with 2X SSC at 42^{o}C followed by blocking in 0.2% tween/5% BSA in 4X SSC at room temperature. Cells were subjected to two, one-hour long incubations with mouse anti-digoxigenin antibody, and goat anti-mouse Alexafluor 488 respectively, with washing in 2X SSC between incubations. Cells were then washed in 2X SSC and mounted in Vectashield with DAPI. Cells were examined on an Olympus Fluoview FV1000 confocal microscope system, and z stacks at intervals of 7 μm were collected using the Olympus Fluoview FV1000 Viewer. Collapsed images as viewed using Volocity software were used to count the number of FISH foci per cell.

For IF, cells were fixed in 3:1 ratio of 100% ethanol:methanol, washed, and permeabilized in 0.5% Triton in 1X PBS. Cells were blocked in 0.2% tween, 5% horse serum and 5% goat serum in 1X PBS. Cells were incubated for one hour in indicated primary antibodies and the appropriate anti-mouse or anti-rabbit Alexa fluor secondary antibody. Cells were washed three times in PBS-T, and once in PBS followed by

mounting in Vectashield with DAPI. Cells were examined on an Olympus Fluoview FV1000 confocal microscope system, and z stacks at intervals of 7µm were collected using the Olympus Fluoview FV1000 Viewer. Collapsed and 3D rendered images using Volocity software were used to determine if colocalization of DNA damage foci coincided with pericentromeric DNA. Colocalization was determined if fluorescence signals overlapped in the X, Y and Z planes.

3.3.5 Chromatin immunoprecipitation (ChIP) and real time PCR analysis

Asynchronously cycling cells were fixed in 1% formaldehyde in 1X PBS followed by neutralization with glycine to a final concentration of 0.125M. ChIP was performed as described (Thillainadesan *et al* 2008). Immuno-precipitated DNA was diluted 1:2000 in pGEM4Z-E18-1 plasmid containing murine cyclin E1. Real-time PCR was performed using the iQSYBRGreen master mix on a BioRad CFX Connect Real-Time System machine using the CFX Manager software for analysis. Target and cyclin E1 sequences were amplified with the following primers: Major satellite repeats (For: GACGACTTGAAAAATGACGAAATC , Rev: CATATTCCAGGTCCTTCAGTGTGC), Cyclin E1 (For: AAGGGAACTTCCGGGGTACT, Rev: CTAGGTTCGGTCCCAACAGG). Cyclin E was used as a technical control for normalization to ensure the same amount of DNA was pipetted into each reaction. ChIPs were performed in triplicate and reported as 'percent of input'.

3.3.6 Tumor incidence in mice

The $Rb1^{\Delta L}$ mutant strain carries three amino acid substitutions in its *Rb1* encoded protein (I746A, N750A, and M754A) that disrupt interactions with LXCXE motif containing proteins, but not E2F transcription factors (Dick *et al* 2000; Isaac *et al* 2006); details of its construction and initial characterization have been previously published (Isaac *et al* 2006). The $Trp53^{-/-}$ mice were purchased from Jackson Labs and were intercrossed with $Rb1^{\Delta L}$ mutants to produce the required genotypes for this study. All animals were maintained in a mixed 129/B6 background. Mice were housed and

maintained according to the guidelines of the Canadian Council on Animal Care. Animals were followed throughout their lives for signs of tumor burden and were euthanized when tumors became visible, or the animal experienced sudden weight loss or became lethargic. All animals were subjected to a thorough necropsy and abnormal tissues, organs, or tumors were fixed in formalin and processed for histological assessment. Portions of tumors were snap frozen and used to prepare genomic DNA. Tissues were embedded, sectioned, and stained with hematoxylin and eosin according to standard methods and photographed as described above. See Appendix K for a synopsis of histopathology for all animals used in this study.

3.3.7 PCR genotyping and array comparative genomic hybridization (aCGH)

High molecular weight DNA was extracted from frozen tumor samples using standard DNA isolation procedures and used in the following analyses.

To determine whether the remaining wild type allele of pRB was maintained in tumors from *Rb1*$^{\Delta L/\Delta L}$ mice, DNA extracted from tumors was subjected to PCR amplification that detected both the knock-in allele and the wild type allele. Tail DNA of the same mouse from which the tumor was taken was PCR amplified in parallel and used for comparison. PCR amplification used standard conditions and the following primers: Genotyping (For: AGCTTCATACAGATAGTTGGG, Rev: CACACAAATCCCCATACCTATG).

For array CGH experiments, DNA was extracted from livers of five male and female wild type animals to create pools of control DNA. Control male vs. control female, and tumor DNA vs. the appropriate sex control hybridizations were performed by NimbleGen on a mouse whole genome array (design 2006-07-26-MM8-WG-CGH). Segmentation analysis described by Olshen was performed and was used to infer changes in copy number (Olshen *et al* 2004). Analysis of segmented data was performed as previously reported (Coschi *et al* 2010).

3.3.8 Mutation detection in *RB1* patient fibroblasts

Sequencing was performed by Retinoblastoma Solutions (www.retinoblastomasolutions.org), (now Impact Genetics Inc.- www.impactgenetics.com). The sequencing results are summarized in Table 3.3. Briefly, cell lines were analyzed for copy number and allele-specific PCR of recurrent mutations in the *RB1* gene. Chromatographs of mutant and control sequence for comparison were supplied by Retinoblastoma Solutions.

3.3.9 Analysis of instability in cancer cell lines

Data were obtained from the COSMIC database (Cancer Cell Line Project- Copy Number Analysis) for cancer cell lines SK-PN-DW, RD, T1-73, MES-SA, SK-LMS and Saos2. Statistical analysis, segmentation, whole chromosome changes and chromothriptic regions were determined using criteria outlined in Figure 3.13 for the following mesenchymal cell lines: $RB1^{+/+}$ (ES1, H-EMC-SS, CADO-ES1, TI-73, ES4, EW13, A673, A204, G402, MES-SA, SW982, TE-441-T, BL-70, CESS, HT), $RB1^{+/-}$ (KMS-12-PE, BALL-1, SK-MM-2, IM9, CML-T1, CMK, SK-LMS-1, RD, ES3, NY), $RB1^{-/-}$ (Saos2, SK-PN-DW, HUO9, HUO-3N1, SK-UT-1, H9, BC-3, CTV-1, GR-ST, KMOE-2, MONO-MAC-6, U266).

3.4 Results

3.4.1 Loss of *Rb1* causes double strand breaks at the centromere

In normal human fibroblasts, loss of the retinoblastoma protein results in spontaneous DNA double strand breaks (Pickering and Kowalik 2006). The cause of these double strand breaks in *RB1* deficient cells is unknown as complete loss of *RB1* has multiple effects on cell physiology. To investigate the mechanism by which loss of the retinoblastoma protein leads to the accumulation of DNA double strand breaks, we compared DNA double strand break accumulation between $Rb1^{+/+}$ and $Rb1^{-/-}$ mouse embryonic fibroblasts (MEFs). γH2AX was used as a marker of DNA damage, and cells were counterstained with DAPI to visualize DNA. There was a significant increase in the

number of cells with three or more DNA double strand break foci in *Rb1*$^{-/-}$ MEFs compared to wild type (Fig. 3.1A, B). DAPI counterstain produces punctate foci at pericentromeric and centromeric regions because it is a large, highly heterochromatinized structure. We observed a bias in the location of DNA double strand breaks in *Rb1*$^{-/-}$ MEFs; double strand break accumulation was more frequent at DAPI rich spots in *Rb1*$^{-/-}$ MEFs compared to wild type controls (Fig. 3.2B). Colocalization was determined using confocal microscopy and ensuring DAPI-rich foci coincided with γH2AX foci in all three planes (Fig. 3.2A).

Previous data have implicated the retinoblastoma protein as having a unique role at centromeric and pericentromeric heterochromatin (Isaac *et al* 2006, Coschi *et al* 2010, Manning *et al* 2010). Specifically, homozygosity of a mutant *Rb1* allele that lacks the ability to bind proteins in its LXCXE binding cleft (*Rb1*$^{\Delta L}$) results in centromere fusions, congression and condensation defects and missegregation in mitosis (Isaac *et al* 2006, Coschi *et al* 2010). Therefore, we investigated whether the LXCXE binding cleft was required to prevent DNA double strand break accumulation. *Rb1*$^{\Delta L/\Delta L}$ MEFs exhibit a significant increase in the number of cells with three or more DNA double strand break foci compared to wild type controls (Fig. 3.1A, B). Moreover, upon examination of confocal microscopy images, more *Rb1*$^{\Delta L/\Delta L}$ MEFs demonstrated colocalization of DAPI-rich foci with DNA damage foci (Fig. 3.2 A, B).

To confirm the colocalization of DNA damage foci at pericentromeres, chromatin immunoprecipitation (ChIP) was performed using an antibody against γH2AX, and precipitated chromatin was quantified using real time PCR amplification of pericentromeric repeat DNA. There was a significant increase in DNA double strand breaks at pericentromeric DNA in both *Rb1*$^{-/-}$ and *Rb1*$^{\Delta L/\Delta L}$ MEFs compared to wild type (Fig. 3.2Ci, Cii). Therefore increased DNA double strand breaks are caused by the absence of pRB. Furthermore, loss of just pRB-LXCXE interactions in isolation was sufficient to cause DNA breaks.

Previous work has implicated pRB-LXCXE interactions in the loading of Condensin II complexes on chromatin as a means to maintain genome stability

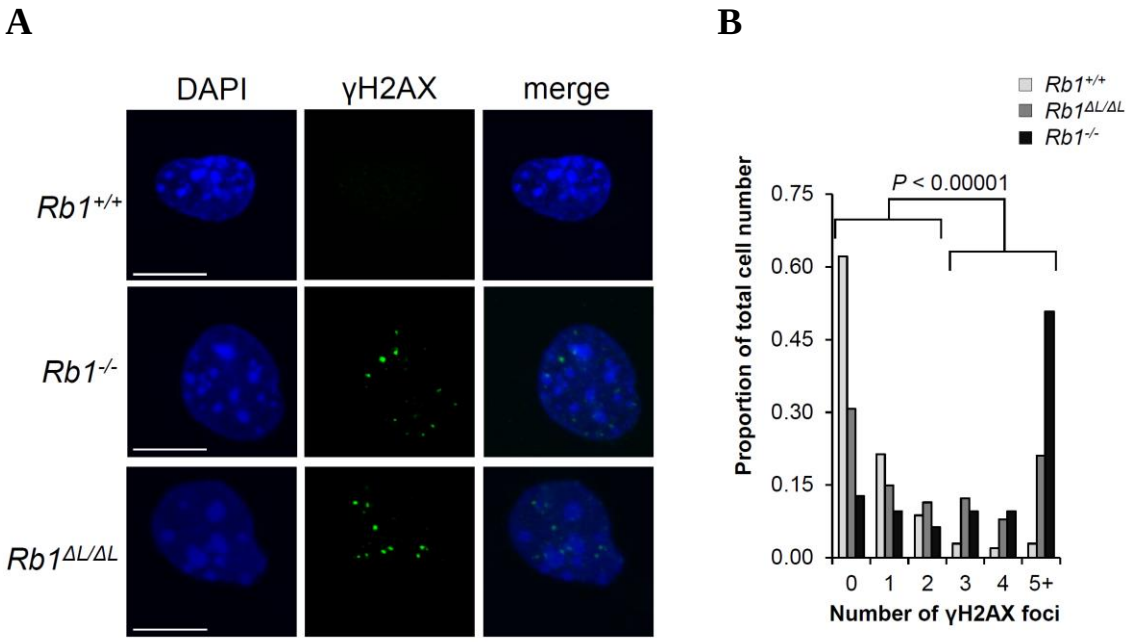

Figure 3.1: *Rb1* homozygous mutant MEFs exhibit increased DNA double strand breaks.

(A) Immunofluorescence in $Rb1^{+/+}$, $Rb1^{-/-}$ and $Rb1^{\Delta L/\Delta L}$ MEFs to detect DNA double strand breaks using γH2AX as representative of damage (green). MEFs were counterstained with DAPI (blue). **(B)** Quantitation of DNA damage foci in MEFs. The number of cells with two or less foci was compared for $Rb1^{+/+}$ controls (n = 103) and $Rb1^{-/-}$ (n = 63) and $Rb1^{\Delta L/\Delta L}$ (n = 114) MEFs using a χ^2 test.

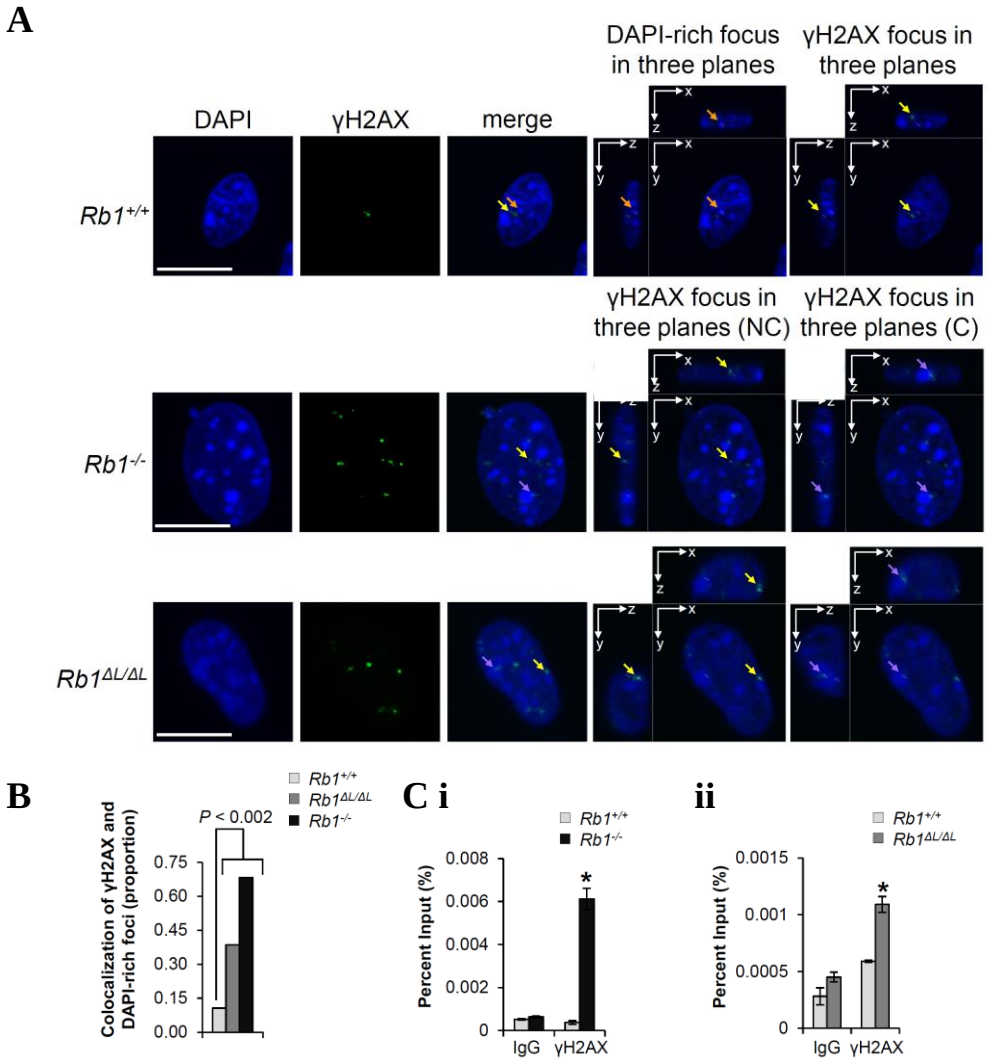

Figure 3.2: *Rb1* homozygous mutant MEFs accumulate DNA double strand breaks at pericentromeric DNA.

(A) Immunofluorescence of γH2AX foci (green) and DAPI counterstain (blue). 3D rendering of the cells in the two rightmost panels allows visualization of colocalization of DNA damage foci with DAPI-rich foci. Orange arrows- DAPI-rich focus absent of DNA damage; Yellow arrows- DNA damage foci that do not colocalize with DAPI-rich foci; Purple arrows- DNA damage foci colocalizing with DAPI-rich foci. NC- no colocalization. C- colocalization. Scale bars are 10μm. **(B)** The proportion of cells with DNA damage foci colocalizing with DAPI-rich foci for $Rb1^{+/+}$ controls (n = 103) and $Rb1^{-/-}$ (n = 63) and $Rb1^{\Delta L/\Delta L}$ (n = 114) MEFs was compared using a χ^2 test. **(C)** Chromatin immunoprecipitation investigating DNA damage at pericentromeric DNA. ChIP for γH2AX was followed by real time PCR amplification of major satellite repeat DNA. Data are reported as a percent of the chromatin input into the ChIP. **(Ci)** ChIP with a γH2AX antibody and IgG control was performed in $Rb1^{+/+}$ and $Rb1^{-/-}$ MEFs; n = 3. **(Cii)** ChIP with a γH2AX antibody and IgG control was performed in $Rb1^{+/+}$ and $Rb1^{\Delta L/\Delta L}$ MEFs; n = 3. ***P* < 0.05 using a t-test.

(Longworth *et al* 2008, Coschi *et al* 2010, Manning *et al* 2010). Based on these data we investigated whether loss of Condensin II function could cause DNA double strand breaks at a similar genomic location. MEFs transduced with a short hairpin targeting Luciferase (control) or CAP-D3 (a Condensin II complex subunit) were subjected to fluorescence confocal microscopy. Only cells successfully transduced (expressing H2BGFP) were investigated for the number and genomic location of DNA double strand break foci. There was a significant increase in the number of CAP-D3 depleted cells exhibiting three or more DNA damage foci compared with the Luciferase control (Fig. 3.3A, B). Furthermore, γH2AX foci colocalized with DAPI-rich foci more frequently in MEFs transduced with short hairpins targeting CAP-D3 than those of the Luciferase control (Fig. 3.4A, B). This strongly implicates the Condensin II complex in the ability of pRB to prevent DNA double strand break accumulation at pericentromeres and to maintain genome stability.

Over the course of the above-described immunofluorescence microscopy experiments, we noted that DNA damage foci were also present in prometaphase and metaphase of *Rb1* mutant MEFs (Fig. 3.5A). Similarly, MEFs depleted of Condensin II function also exhibit DNA damage foci in mitosis (Fig. 3.5B). For these reasons we sought to identify the stages in the cell cycle where these foci are present and determine when they first arise. In $Rb1^{\Delta L/\Delta L}$ MEFs, the proportion of cells in G1 with three or greater DNA damage foci was significantly increased over cells in other stages of the cell division cycle with comparable numbers of DNA damage foci ($P < 0.05$; Fig. 3.6A, B). The prominence of DNA damage foci in mitosis and the extensive accumulation in G1 is highly reminiscent of replication stress that occurs at fragile or repetitive sequences in late S-phase and is transmitted through mitosis and into the next G1-phase. For these reasons, our data are consistent with DNA breaks arising in late S-phase and contributing to defects in chromosome structure at the pericentromere and interfering with accurate chromosome segregation in mitosis.

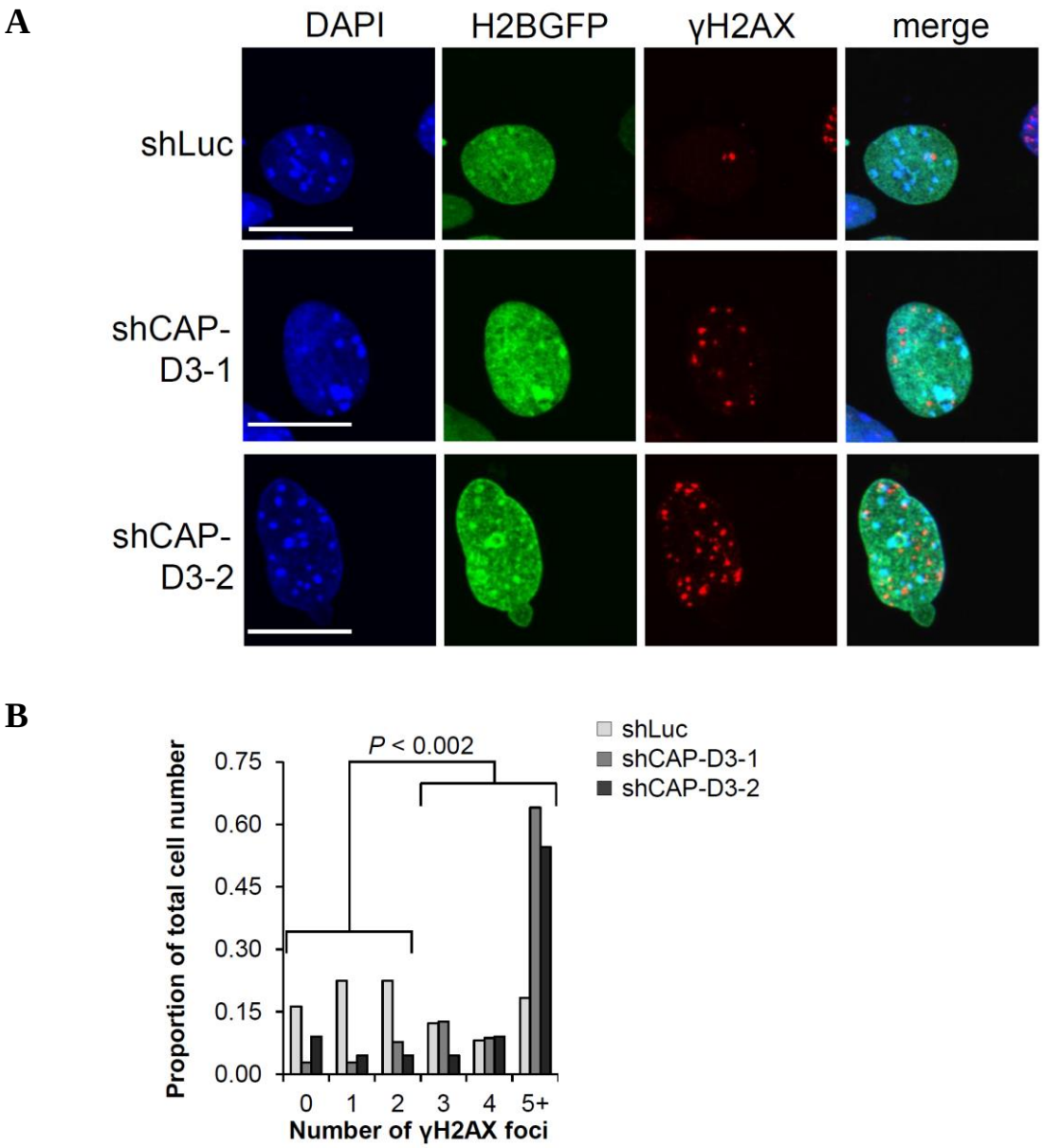

Figure 3.3: Condensin II complex defective MEFs exhibit increased DNA double strand breaks.

(A) Immunofluorescence in *Rb1*$^{+/+}$ MEFs transduced with short hairpins targeting CAP-D3 (shCAP-D3-1, shCAP-D3-2) or Luciferase as a control to detect DNA damage. Successfully transduced MEFs express H2BGFP (green). γH2AX was used as representative of damage (red). MEFs were counterstained with DAPI (blue). **(B)** Quantitation of DNA damage foci in transduced MEFs. The number of cells with two or less foci was compared between CAP-D3 knock down cells (shCAP-D3-1, n = 103; shCAP-D3-2, n = 22) and the Luciferase control (n = 49) using a χ^2 test.

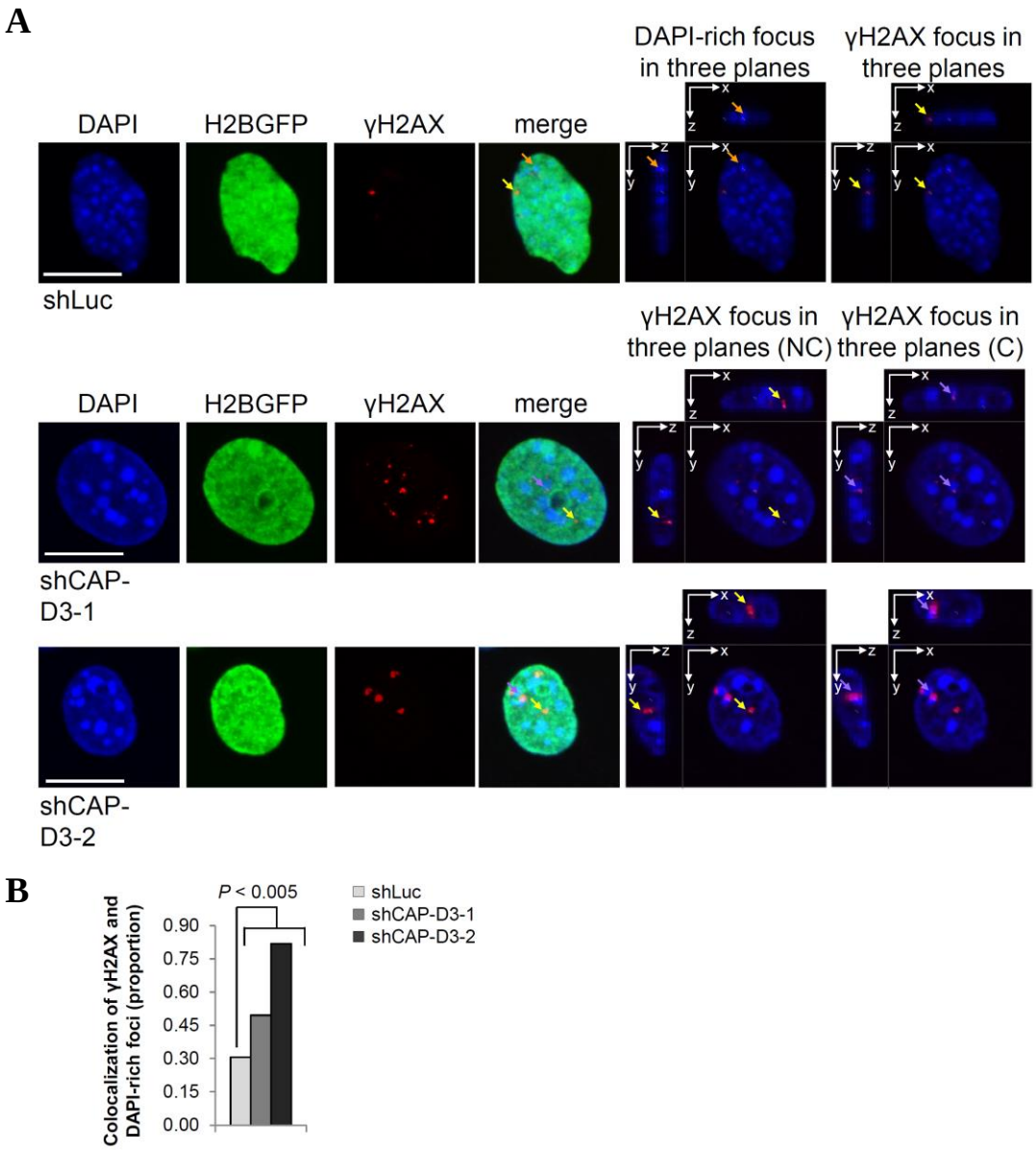

Figure 3.4: Condensin II complex defective MEFs accumulate DNA double strand breaks in pericentromeric regions of the genome.

(A) Immunofluorescence of MEFs transduced with control (Luciferase) or target (CAP-D3) short hairpins showing γH2AX foci (red), H2BGFP (green) and DAPI counterstain (blue). 3D rendering of the cells in the two rightmost panels allows visualization of colocalization of DNA damage foci with DAPI-rich foci. Orange arrows- DAPI-rich focus absent of DNA damage; Yellow arrows- DNA damage foci that do not colocalize with DAPI-rich foci; Purple arrows- DNA damage foci colocalizing with DAPI-rich foci. NC- no colocalization. C- colocalization. Scale bars are 10μm. **(B)** The proportion of CAP-D3 knock down (shCAP-D3-1, n = 103; shCAP-D3-2, n = 22) and Luciferase control (n = 49) cells with DNA damage foci colocalizing with DAPI-rich foci was compared using a χ^2 test.

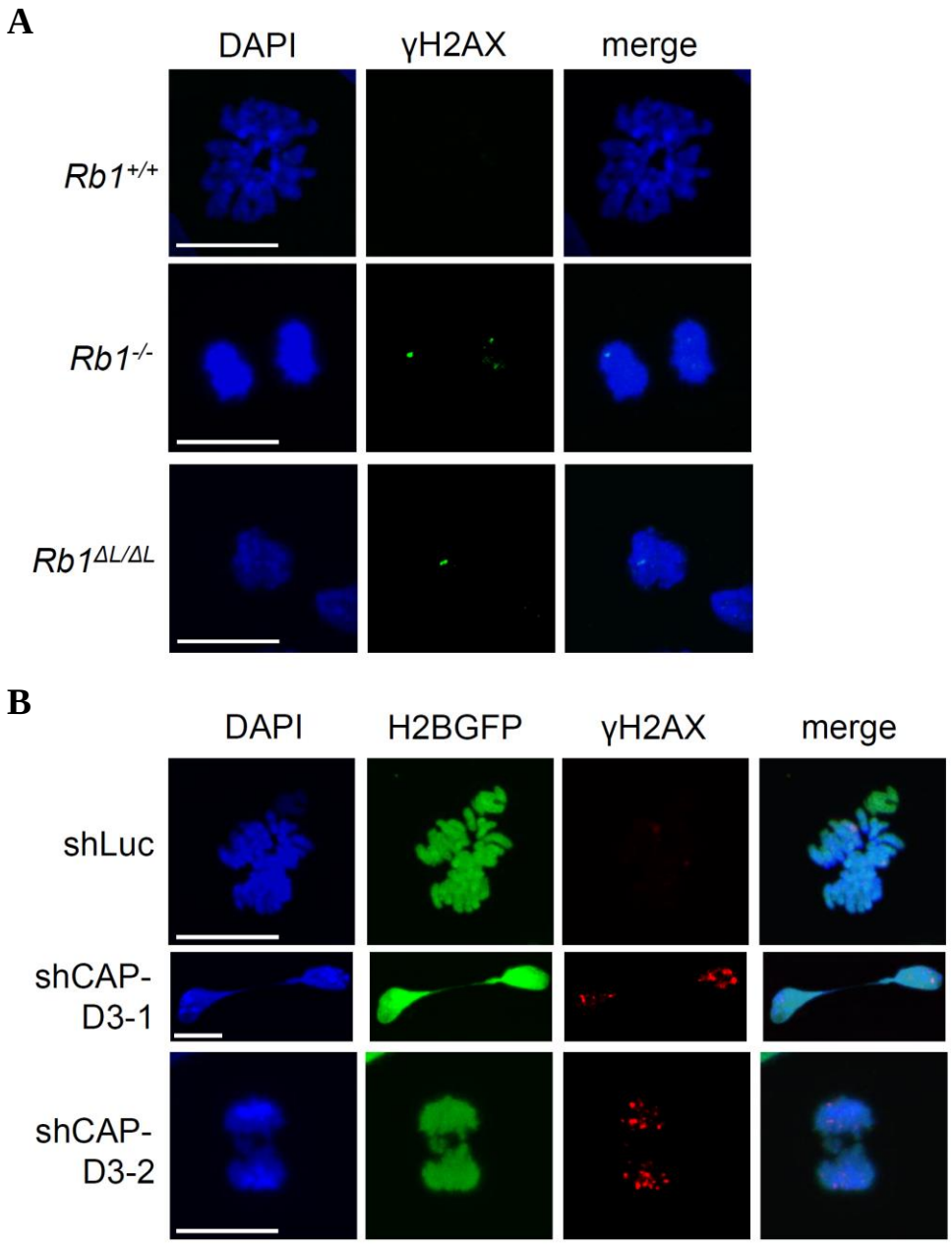

Figure 3.5: DNA damage in *Rb1* homozygous mutant MEFs and Condensin II complex defective MEFs persists into mitosis.

(A) Immunofluorescence of MEFs with the indicated genotypes in various stages of mitosis. DNA damage is marked by γH2AX (green) and DNA is counterstained with DAPI (blue). Scale bars at 10μm. **(B)** Immunofluorescence of MEFs transduced with either a Luciferase short hairpin control or one of two short hairpins against CAP-D3 (sh-CAP-D3-1, shCAP-D3-2) in various stages of mitosis. Successfully transduced MEFs express H2BGFP (green), DNA damage is marked by γH2AX (red) and DNA is counterstained with DAPI (blue). Scale bars at 10μm.

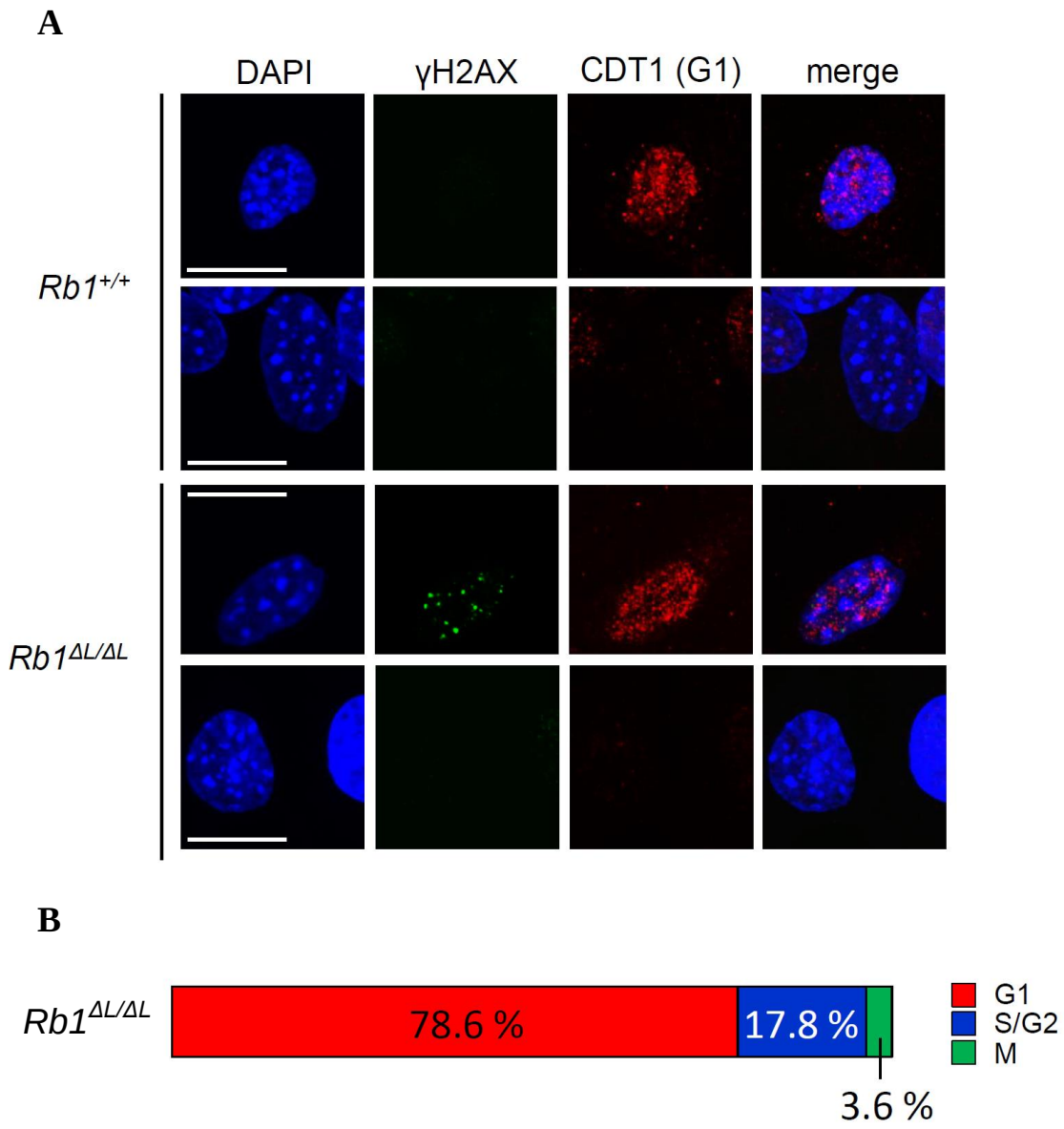

Figure 3.6: *Rb1*$^{\Delta L/\Delta L}$ MEFs accumulate DNA damage in G1.

(A) Immunofluorescence of MEFs of the indicated genotypes. DNA double strand breaks are marked by γH2AX (green) and cells in G1 are marked by CDT1 expression (red). DNA is counter-stained with DAPI (blue). Scale bars are 10μm. **(B)** Representation of the proportion of cells in G1, S/G2 and M phases of the cell division cycle with three or greater DNA damage foci in *Rb1*$^{\Delta L/\Delta L}$ MEFs (n = 148).

3.4.2 E2F1, pRB and Condensin II form a complex at pericentromeric heterochromatin

Since DNA damage found in mitosis is associated with replication stress at repetitive DNA, pericentromeric heterochromatin may be particularly sensitive to DNA breaks. We therefore proceeded to investigate whether pRB or the Condensin II complex localizes to pericentromeric heterochromatin. Chromatin immunoprecipitation followed by real time PCR amplification of pericentromeric repeats demonstrated that both pRB and the Condensin II complex (represented by its subunit CAP-D3) localize to pericentromeric heterochromatin (Fig. 3.7Ai, Aii respectively). In order to confirm that these proteins form a complex at pericentromeric heterochromatin, we performed the following chromatin immunoprecipitation experiments in *Rb1* mutant MEFs. First we demonstrated that localization of CAP-D3 to pericentromeric heterochromatin is dependent upon pRB, as CAP-D3 localizes to pericentromeric heterochromatin in $Rb1^{+/+}$ MEFs, but fails to localize to pericentromeres in $Rb1^{-/-}$ MEFs (Fig. 3.7Bi). Moreover, CAP-D3 localization to pericentromeric repeats was dependent upon interactions with pRB's LXCXE binding cleft as CAP-D3 loading at pericentromeric heterochromatin was significantly reduced in $Rb1^{\Delta L/\Delta L}$ MEFs (Fig. 3.7Bii).

Interestingly, pRB and E2F1 have been shown to interact at sites of replication in S-phase while pRB is hyperphosphorylated and cannot bind to the other E2Fs (Wells *et al* 2003, Korenjak *et al* 2012, Mendoza-Maldonado *et al* 2010, Barbie *et al* 2004, Cecchini and Dick 2011, Dyson 1998). For these reasons, we wondered whether E2F1 recruits the retinoblastoma protein, and in turn the Condensin II complex, to pericentromeric heterochromatin. Chromatin immunoprecipitation in wild type MEFs demonstrates that E2F1 localizes to pericentromeric heterochromatin (Fig. 3.7Ci). In order to demonstrate that E2F1 recruits pRB and the Condensin II complex to chromatin, we performed ChIP in $E2f1^{-/-}$ MEFs. In $E2f1^{+/+}$ controls, CAP-D3 localizes to pericentromeric heterochromatin while in $E2f1^{-/-}$ MEFs, CAP-D3 fails to localize to this genomic region (Fig. 3.7Cii).

Pericentromeric repeats do not contain the consensus E2F DNA binding motif, which led us to investigate the mechanism by which E2F1 is recruited to pericentromeric

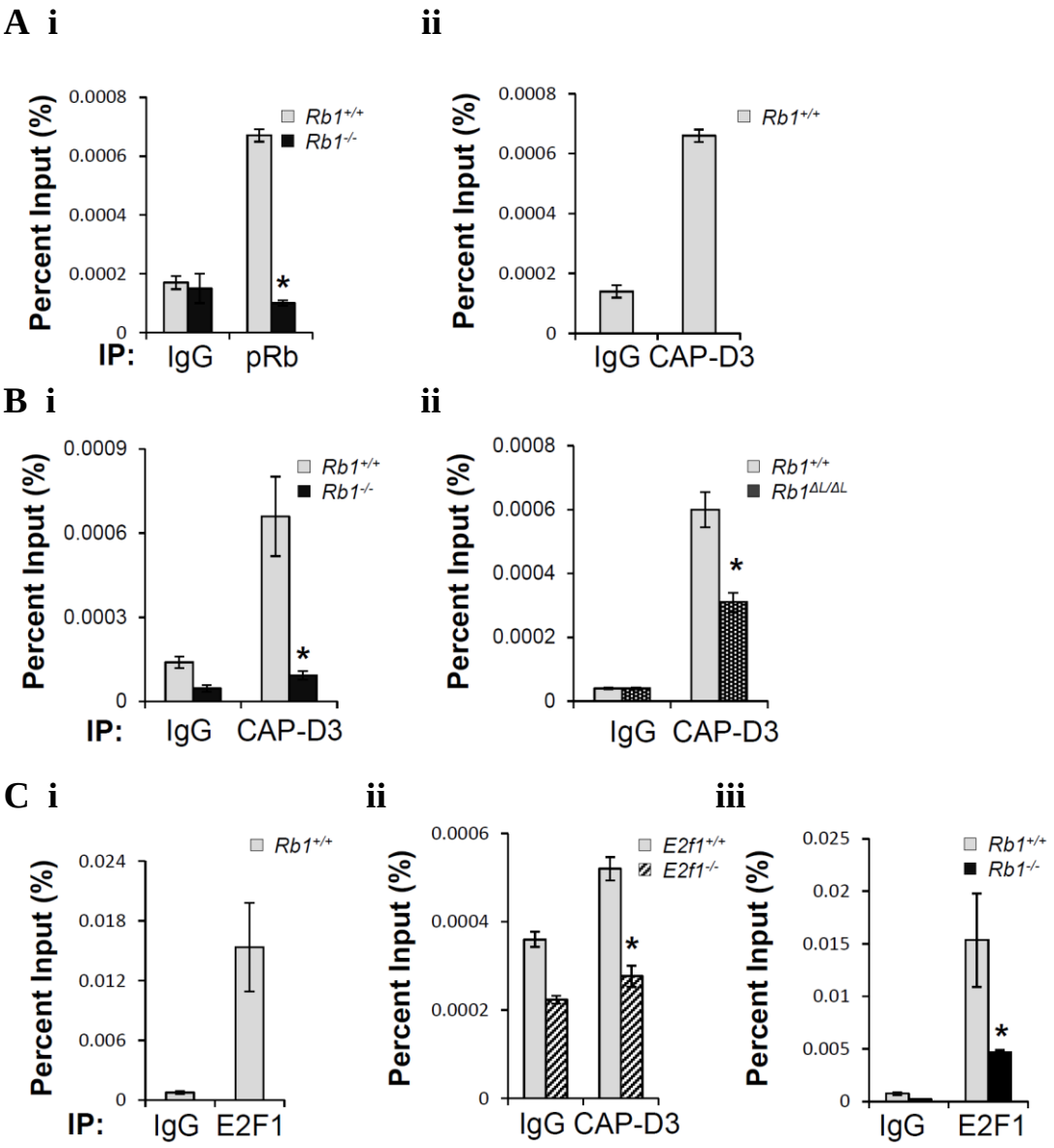

Figure 3.7: pRB, E2F1 and Condensin II interact at pericentromeric heterochromatin.

(A-C) Chromatin immunoprecipitation using the indicated antibodies was followed by real time PCR amplification of major satellite repeat DNA at pericentromeric heterochromatin. Data are reported as percent of input. **(Ai)** ChIP using an antibody against pRB in *Rb1*$^{+/+}$ and *Rb1*$^{-/-}$ MEFs; n = 3. **(Aii)** ChIP using a CAP-D3 antibody in wild type MEFs; n = 3. **(Bi-ii)** ChIP using a CAP-D3 antibody to represent the Condensin II complex in *Rb1*$^{+/+}$, *Rb1*$^{-/-}$ and *Rb1*$^{\Delta L/\Delta L}$ MEFs; n = 3. **(Ci)** ChIP using an E2F1 antibody in wild type MEFs; n = 3. **(Cii)** ChIP using a CAP-D3 antibody to represent the Condensin II complex in *E2f1*$^{-/-}$ MEFs; n = 3. **(Ciii)** ChIP using an E2F1 antibody in *Rb1*$^{+/+}$ and *Rb1*$^{-/-}$ MEFs; n = 3. **P* < 0.05.

heterochromatin. It has been previously reported that binding of pRB to E2F1 can alter the preference of E2F1 for canonical E2F consensus sequences such that its preference for a non-canonical recognition sequence is dependent on pRB (Wells *et al* 2003, Korenjak *et al* 2012, Tao *et al* 1997, Dick and Dyson 2003). Therefore we determined whether the presence of pRB affected the recruitment of E2F1 to pericentromeric DNA. Chromatin immunoprecipitation of E2F1 in $Rb1^{+/+}$ and $Rb1^{-/-}$ MEFs demonstrates that E2F1 localization to pericentromeric heterochromatin was greatly reduced in $Rb1^{-/-}$ MEFs (Fig. 3.7Ciii). This suggests that binding of pRB and E2F1 is maintained at pericentromeric heterochromatin through a co-operative mechanism and likely involves interaction with a non-canonical E2F binding sequence. The Condensin II complex is then recruited to chromatin *via* an interaction with the LXCXE binding cleft of pRB, which is abrogated in $Rb1^{\Delta L/\Delta L}$ MEFs. If any of these interactions are disrupted, there is a loss of Condensin II complex loading at pericentromeric heterochromatin. Therefore pRB, E2F1 and Condensin II form a complex at pericentromeric heterochromatin and prevent the accumulation of DNA damage, which likely occurs during S-phase as difficult to replicate sites, including pericentromeric heterochromatin, are replicated.

3.4.3 DNA damage and recruitment of Condensin II to chromatin is *Rb1* gene dosage-dependent

The implication that stable binding of E2F1 at pericentromeric DNA relies on binding to pRB suggests that the abundance of pRB may be of particular importance in the formation of complexes at this genomic location (Fig. 3.7Ciii). To determine the effect of *Rb1* heterozygosity we first transduced $Rb1^{+/-}$ MEFs with H2BGFP to visualize the cells as they progressed through mitosis. $Rb1^{+/-}$ MEFs exhibited both chromosome congression and condensation defects as they took significantly longer to reach the metaphase plate from the onset of chromosome condensation compared with $Rb1^{+/+}$ MEFs (Fig. 3.8A middle, Table 3.1). Moreover, $Rb1^{+/-}$ MEFs presented with a significant increase in the number of cells displaying lagging chromosomes during anaphase compared to controls (Fig. 3.8A middle, Table 3.1). As these same genomic instability phenotypes were previously linked to a defective interaction between the LXCXE binding cleft of pRB and the Condensin II complex, we transduced $Rb1^{\Delta L/+}$

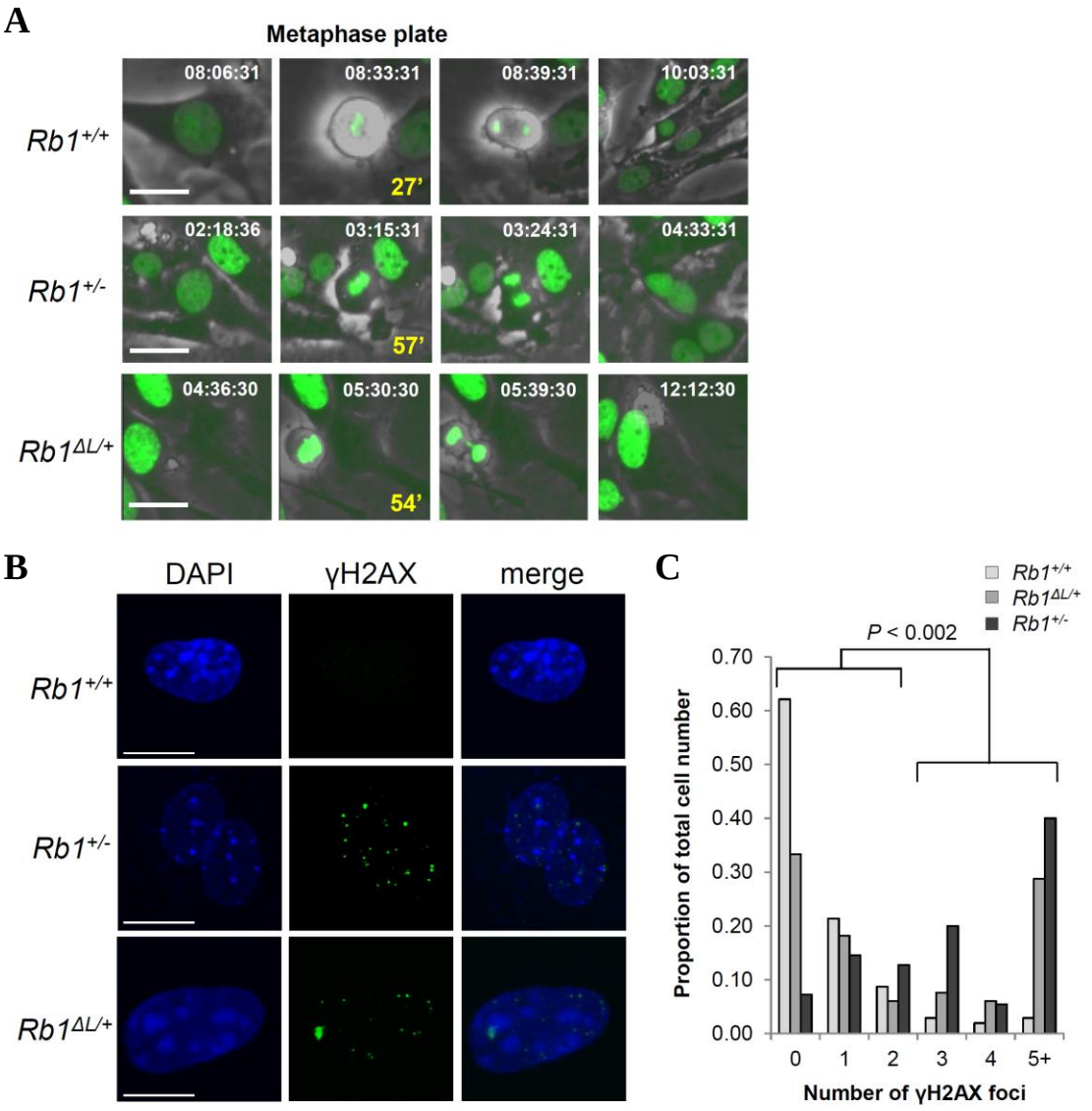

Figure 3.8: *Rb1* heterozygous mutants exhibit mitotic defects.

(A) Video microscopy was performed on MEFs expressing an H2B-GFP reporter by capturing phase contrast and GFP images every three minutes over a 15 hour time course. The images shown begin with the onset of chromatin condensation in prophase as the left most panel. The last image of the metaphase plate before the onset of anaphase is indicated along with the elapsed time since the onset of prophase (in minutes). The right most image shows resolved daughter (or binucleated) cells. Scale bars are 50 µm. **(B)** Immunofluorescence in $Rb1^{+/+}$, $Rb1^{+/-}$, and $Rb1^{\Delta L/+}$ MEFs to detect DNA double strand breaks using γH2AX as representative of damage (green). MEFs were counterstained with DAPI (blue). **(C)** Quantitation of DNA damage foci in MEFs. The number of cells with two or less foci was compared for $Rb1^{+/+}$ controls (n = 103) and $Rb1^{+/-}$ (n = 55) and $Rb1^{\Delta L/+}$ (n = 66) MEFs using a χ^2 test.

Table 3.1. Summary of mitotic phenotypes observed in *Rb1* mutant MEF video microscopy experiments.

Genotype[a]	N-value	Lagging Chromosomes[b]	N-value	Average time from onset of condensation to onset of anaphase (min)
Rb1$^{+/+}$	60	21	47	34.51
Rb1$^{+/-}$	116	67[c]	106	45.55[d]

[a]For all statistical tests *Rb1*$^{+/-}$ is compared with wild type controls.
[b]Includes mitoses where the metaphase plate never visually divided, chromatin decondensed, and cells became tetraploid.
[c]Indicates a difference from controls that is above 95% confidence interval (χ2-test, $P<0.05$).
[d]Above 95% confidence interval (t-test, $P<0.05$).

MEFs with H2BGFP and observed subsequent mitoses (Coschi *et al* 2010). *Rb1*$^{\Delta L/+}$ MEFs also exhibited an increase in the length of time it took to proceed from the onset of chromosome condensation to the metaphase plate, and exhibited a significant increase in the number of mitoses with lagging chromosomes as compared to *Rb1*$^{+/+}$ MEFs (Fig. 3.8A bottom, Table 3.2).

Next, because *Rb1*$^{-/-}$ and *Rb1*$^{\Delta L/\Delta L}$ MEFs exhibit DNA double strand breaks, we investigated whether the ability of pRB to prevent the accumulation of DNA double strand breaks was compromised due to haploinsufficiency. Immunofluorescence of asynchronously cycling *Rb1*$^{+/-}$ and *Rb1*$^{\Delta L/+}$ MEFs revealed that there was a significant increase in the number of cells with three or more γH2AX foci in both heterozygous genotypes compared to the wild type control (Fig. 3.8B, C). Moreover, these double strand breaks were found at pericentromeric heterochromatin in *Rb1*$^{+/-}$ and *Rb1*$^{\Delta L/+}$ MEFs more frequently than in *Rb1*$^{+/+}$ MEFs, as determined by γH2AX foci colocalization with DAPI-rich foci (Fig. 3.9A, B). To further confirm the *Rb1* and *Rb1*$^{\Delta L}$ gene dosage sensitivity of these phenotypes, we performed chromatin immunoprecipitation of the CAP-D3 subunit of the Condensin II complex to determine whether it bound normally at pericentromeric heterochromatin. CAP-D3 was significantly reduced at pericentromeric heterochromatin in both *Rb1*$^{+/-}$ and *Rb1*$^{\Delta L/+}$ MEFs compared to wild type MEFs (Fig. 3.9Ci, Cii).

Finally, to determine whether this accumulated DNA damage likely occurred as a result of both replication stress and the pRB-E2F1-Condensin II complex interaction at pericentromeric DNA, we investigated the amount of DNA damage in *Rb1*$^{\Delta L/+}$ MEFs as a function of their phase in the cell division cycle. Again we observed DNA damage foci in mitosis and, the proportion of cells in G1 with three or more DNA damage foci was significantly increased over other stages of the cell division cycle ($P < 0.05$; Fig. 3.10B, C).

Taken together, these data clearly demonstrate that the retinoblastoma gene, and an *Rb1* gene with a mutation in the LXCXE binding cleft (*Rb1*$^{\Delta L}$), both exhibit haploinsufficiency in their ability to prevent the accumulation of DNA double strand

Table 3.2. Summary of mitotic phenotypes observed in *Rb1*-ΔL mutant MEF video microscopy experiments.

Genotype[a]	N-value	Lagging Chromosomes[b]	N-value	Average time from onset of condensation to onset of anaphase (min)
$Rb1^{+/+}$	42	13	23	66.26
$Rb1^{\Delta L/+}$	73	42[c]	62	89.76[d]

[a]For all statistical tests $Rb1^{\Delta L/+}$ is compared with wild type controls.
[b]Includes mitoses where the metaphase plate never visually divided, chromatin decondensed, and cells became tetraploid.
[c]Indicates a difference from controls that is above 95% confidence interval (χ2-test, $P<0.05$).
[d]Above 93% confidence interval (t-test, $P<0.065$).

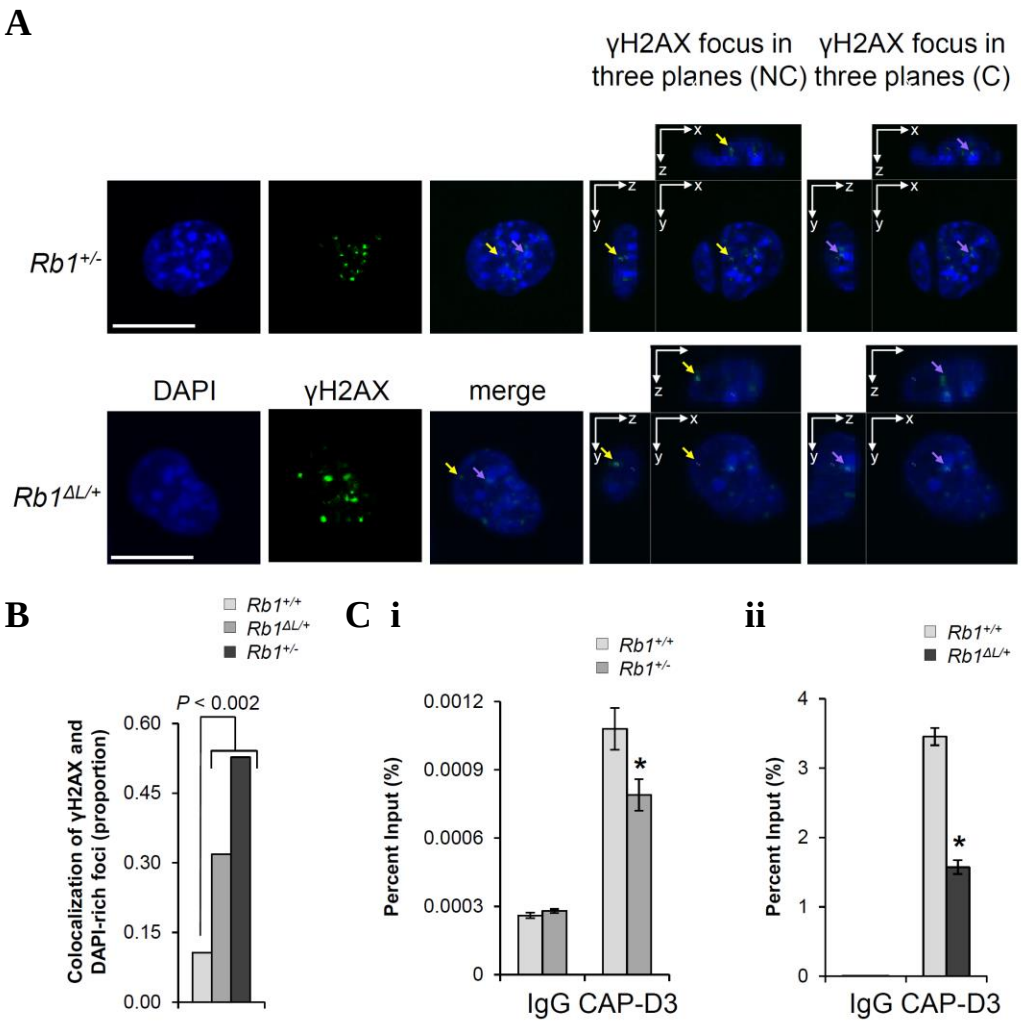

Figure 3.9: DNA damage and recruitment of Condensin II is *Rb1* gene dosage-dependent.

(A) Immunofluorescence of γH2AX foci (green) and DAPI counterstain (blue). 3D rendering of the cells in the two rightmost panels allows visualization of colocalization of DNA damage foci with DAPI-rich foci. Orange arrows- DAPI-rich focus absent of DNA damage; Yellow arrows- DNA damage foci that do not colocalize with DAPI-rich foci; Purple arrows- DNA damage foci colocalizing with DAPI-rich foci. NC- no colocalization. C- colocalization. Scale bars are 10μm. **(B)** The number of cells with DNA damage foci for $Rb1^{+/+}$ controls (n = 103) and $Rb1^{+/-}$ (n = 55) and $Rb1^{\Delta L/+}$ (n = 66) MEFs colocalizing with DAPI-rich foci was compared using a χ^2 test. **(C)** Chromatin immunoprecipitation (ChIP) investigating the *Rb1* gene dosage sensitivity of Condensin II complex recruitment to centromeres. ChIP for CAP-D3 was followed by real time PCR amplification of major satellite repeat DNA. Data are reported as a percent of the chromatin input into the ChIP. **(Ci-ii)** ChIP with a CAP-D3 antibody and IgG control was performed in $Rb1^{+/+}$, $Rb1^{+/-}$ and $Rb1^{\Delta L/+}$ MEFs; n = 3. *****$P < 0.05$ using a t-test.

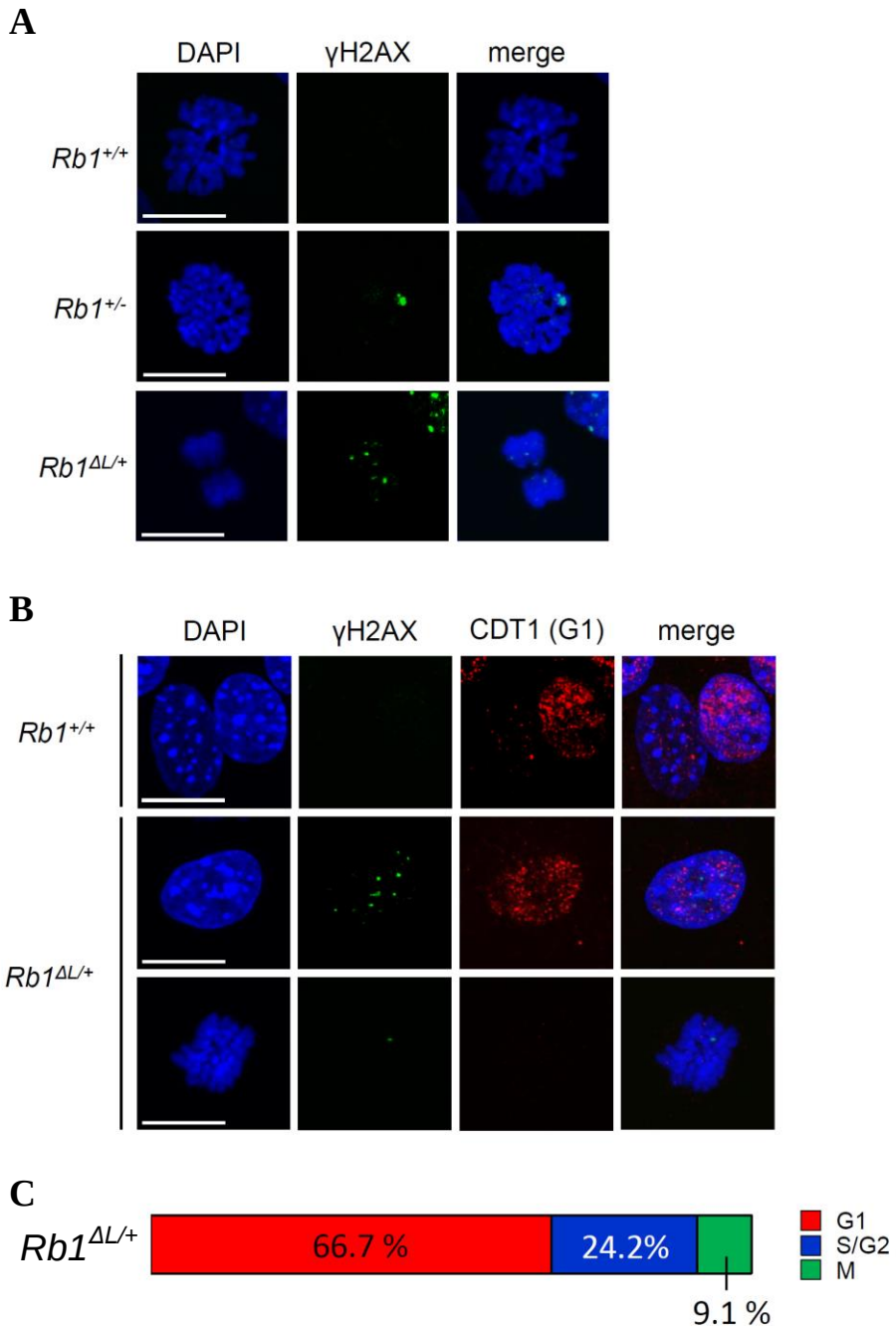

Figure 3.10: *Rb1*$^{\Delta L/+}$ MEFs accumulate DNA damage in G1.

(A) Immunofluorescence of MEFs with the indicated genotypes in various stages of mitosis. DNA damage is marked by γH2AX (green) and DNA is counterstained with DAPI (blue). Scale bars at 10μm. **(B)** Immunofluorescence of MEFs of the indicated genotypes. DNA double strand breaks are marked by γH2AX (green) and cells in G1 are marked by CDT1 expression (red). DNA is counter-strained with DAPI (blue). Scale bars are 10μm. **(C)** Representation of the proportion of cells in G1, S/G2 and M phases of the cell division cycle with three or greater DNA damage foci in *Rb1*$^{\Delta L/+}$ MEFs (n = 84).

breaks. Therefore the accumulation of DNA damage at pericentromeric heterochromatin, and subsequent mitotic errors are *Rb1* gene dosage-dependent.

3.4.4 Human *RB1*$^{+/-}$ cells exhibit DNA double strand breaks, mitotic defects and genomic instability

The kinetics of *RB1* loss in retinoblastoma gave rise to the now famous 'two-hit' hypothesis (Knudson 1971). However, our data on haploinsufficiency in *Rb1* mutant mouse fibroblasts motivated us to determine if a similar phenotype is present in normal fibroblasts from retinoblastoma patients (*RB1*$^{+/-}$). To investigate this possibility, we obtained several patient fibroblast lines (GM_01408, GM_06418, GM_01123) from the Coriell Institute for Medical Research and confirmed their heterozygous status by sequencing (Table 3.3). We compared them with data acquired from three normal fibroblast cell lines (IMR90, BJ, WI38). We first determined whether patient fibroblasts exhibited increased DNA double strand breaks compared to controls. Using γH2AX as a marker of DNA double strand breaks, we concluded that there is a significant increase in the number of patient fibroblasts exhibiting greater than three γH2AX foci compared with pooled data from normal controls (Fig. 3.11A, B). Moreover, DNA damage foci were found in mitosis in *RB1*$^{+/-}$ fibroblasts and so we investigated whether this resulted in subsequent mitotic defects as observed in *Rb1* mutant MEFs (Fig. 3.12A; Fig. 3.8A, Coschi *et al* 2010). We examined patient fibroblasts as they progressed through mitosis by transducing cells with H2BGFP and subjecting them to fluorescence video microscopy. All three patient fibroblast lines exhibited a significant delay in progression to the metaphase plate from the onset of chromosome condensation as compared to pooled normal control data (Fig. 3.12B, Table 3.4). Moreover, patient fibroblasts also showed a significant increase in the number of mitoses exhibiting lagging chromosomes compared to controls (Table 3.4). Taken together, these data demonstrate that as with mice, human cells hemizygous for *RB1* exhibit haploinsufficiency in their ability to prevent the accumulation of DNA double strand breaks, and to prevent mitotic errors.

Given the direct impact of haploinsufficiency for *RB1* on DNA breaks and mitotic errors we sought evidence for the manifestation of these errors in cancer. Using the copy number analysis data available in the Cancer Cell Line Project of the Catalogue Of

Table 3.3. Summary of sequencing results of retinoblastoma patient fibroblasts.

Cell Line	Mutation	Exon	Result of mutation	Wild type sequence	Mutation
GM_01123 DNA Protein	Heterozygous 1333 C > T Arg 445 X	14	Immediate termination codon	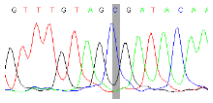	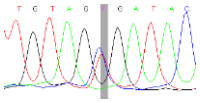
GM_06418 DNA Protein	Heterozygous 1597 G > T Glu 533 X	17	Immediate termination codon	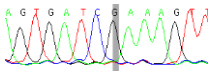	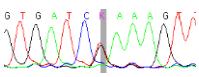
GM_01408 DNA Protein	Heterozygous 1982 G > C Arg 661 Pro	20	Predicted by amino acid conservation analysis and 3D structure as probably damaging (misfolding)	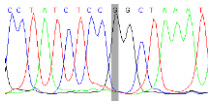	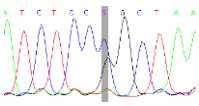
GM_01879B DNA	Heterozygous 1532 dup A	17	Frame-shift leading to termination codon	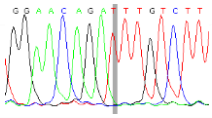	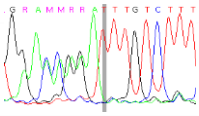
GM_06419A DNA Protein	Heterozygous 1597G > T Glu 533 X	17	Immediate termination codon	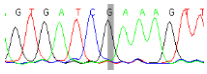	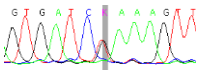

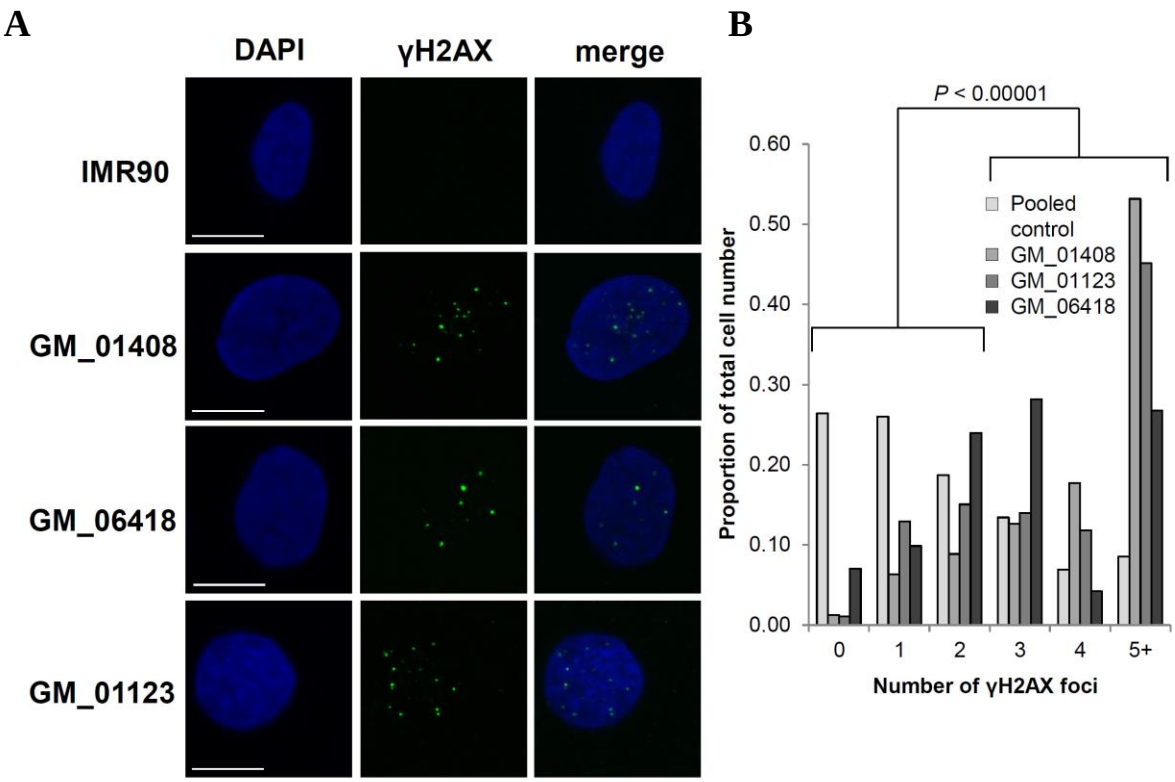

Figure 3.11: Retinoblastoma patient fibroblasts (*RB1*$^{+/-}$) exhibit increased DNA double strand breaks.

(A) Immunofluorescence in control (IMR90) and patient (GM_01408, GM_01123 and GM_06418) fibroblasts to detect DNA damage using γH2AX as representative of damage (green). Fibroblasts were counterstained with DAPI (blue). Scale bars are 10μm. **(B)** Quantitation of DNA damage foci in control and patient fibroblasts. The number of cells with two or less foci was compared for all patient fibroblasts (GM_1408, n = 79; GM_01123, n = 93; GM_06418, n = 71) against pooled control data (IMR90, BJ, WI-38 fibroblasts, n = 246) using a χ^2 test.

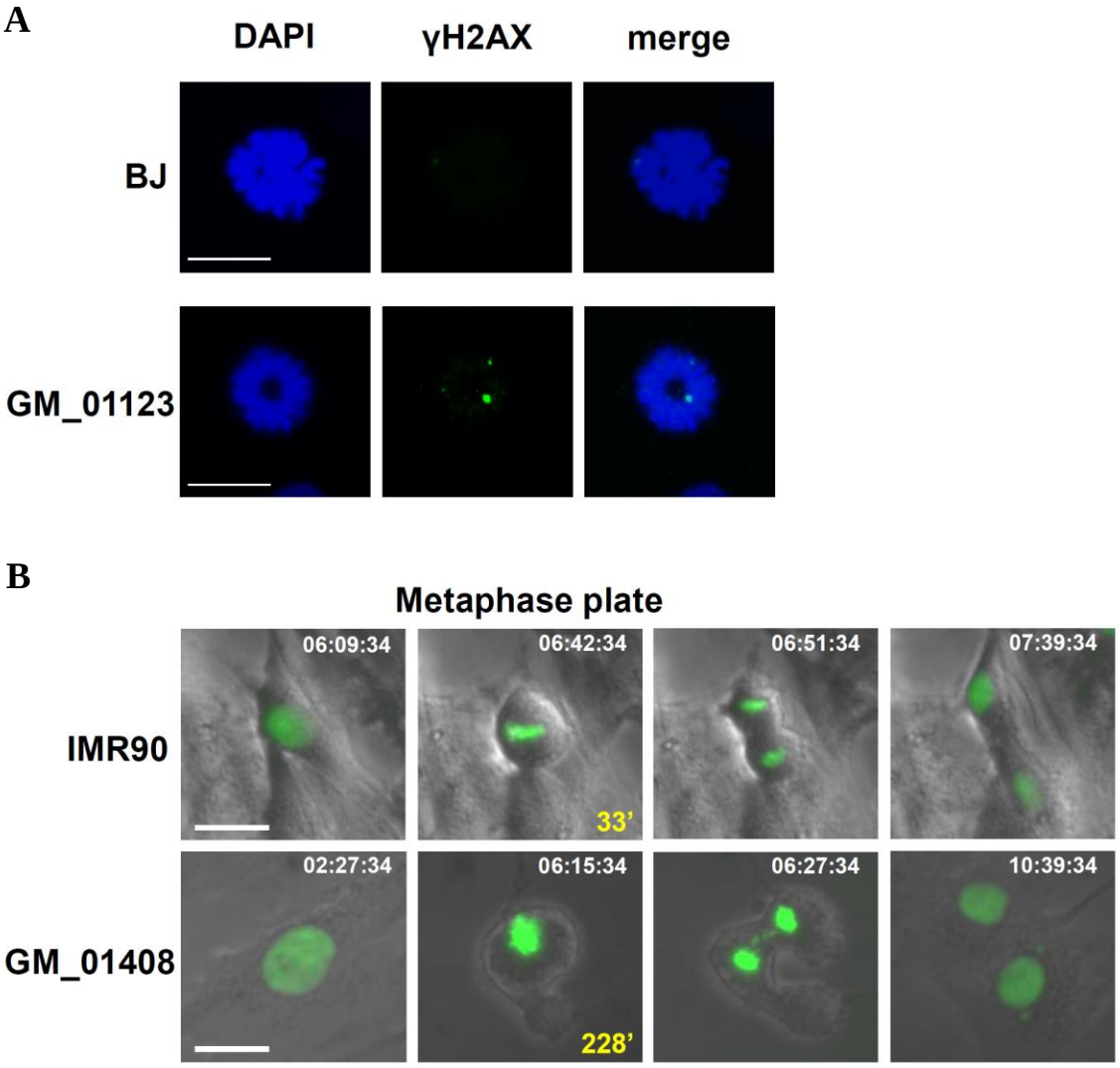

Figure 3.12: Retinoblastoma patient fibroblasts (*RB1*$^{+/-}$) exhibit mitotic defects.

(A) Immunofluorescence of control and Retinoblastoma patient fibroblasts in various stages of mitosis. DNA damage is marked by γH2AX (green) and DNA is counterstained with DAPI (blue). Scale bars at 10μm. **(B)** Control and Retinoblastoma patient fibroblasts were transduced with retroviruses expressing H2B-GFP. Video microscopy was performed by capturing phase contrast and GFP images every three minutes over a 15 hour time course. The images shown begin with the onset of chromatin condensation in prophase as the left most panel. The last image of the metaphase plate before the onset of anaphase is indicated along with the elapsed time since the onset of prophase (in minutes). The right most image shows resolved daughter cells. Scale bars are 50 μm.

Table 3.4. Summary of mitotic phenotypes observed in retinoblastoma patient fibroblast video microscopy experiments.

Genotype[a]	N-value	Lagging Chromosomes[b]	N-value	Average time from onset of condensation to onset of anaphase (min)
IMR90	31	19	13	45
BJ	42	14	17	61
WI38	18	3	3	49
GM_01123	10	9[c]	7	211[d]
GM_01408	31	19[c]	20	85[d]
GM_06418	8	4[c]	6	120[d]

[a]For all statistical tests each patient fibroblast line is compared with pooled control data.
[b]Includes mitoses where the metaphase plate never visually divided, chromatin decondensed, and cells became tetraploid.
[c]Indicates a difference from controls that is above 95% confidence interval (χ2-test, $P<0.05$)
[d]Above 95% confidence interval (t-test, $P<0.05$)

Somatic Mutation In Cancer (COSMIC) database, we asked whether human cancers hemizygous for *RB1* also exhibit increased levels of genomic abnormalities compared to cell lines that are wild type with respect to *RB1* status (COSMIC database). Since Retinoblastoma survivors acquire second primary neoplasms that are generally of mesenchymal origin, the majority of which are sarcomas, we compared the available copy number data from human cancer cell lines of mesenchymal origin for each of $RB1^{+/+}$, $RB1^{+/-}$ and $RB1^{-/-}$ genotypes. We sorted genomic abnormalities into four categories: whole chromosome changes, total genomic segments, total abnormal genomic segments, and chromothriptic regions (Abramson *et al* 1976). Criteria for inclusion in these categories can be found in Figure 3.13A and B. $RB1^{+/-}$ and $RB1^{-/-}$ cancers exhibited significantly more whole chromosome changes than cancers retaining both wild type copies of *RB1* (Fig. 3.14A). Importantly, $RB1^{+/-}$ cancers exhibited as many whole chromosome changes as $RB1^{-/-}$ cancers (Fig. 3.14A). The same trend was observed in the three other measurements of genome stability; $RB1^{+/-}$ and $RB1^{-/-}$ cancers exhibited significantly more genome instability than cancers retaining both wild type copies of *RB1*, though they were no different from each other (Fig. 3.14B, C, D). Select cancer cell lines from those used in the copy number analysis were chosen at random to confirm their *RB1* genotype. Pulldowns using GST-tagged Human Papilloma Virus E7 protein demonstrated functional pRB in $RB1^{+/+}$ and $RB1^{+/-}$ cell lines, and confirmed loss of functional pRB in $RB1^{-/-}$ cell lines (Fig. 3.15A). Real time PCR amplification of the retinoblastoma gene locus compared to an internal control locus confirmed the presence of only a single copy of the *RB1* gene in hemizygous cell lines as compared to two copies in the $RB1^{+/+}$ control (Fig. 3.15B).

From these data it is clear that hemizygosity of *RB1* exhibits haploinsufficiency in humans, namely through the ability of pRB to prevent both the accumulation of DNA double strand breaks and mitotic errors (Fig. 3.11, 3.12). Moreover, this is associated with increased genome instability in human cancers at a level comparable to that found in $RB1^{-/-}$ cancers (Fig. 3.14).

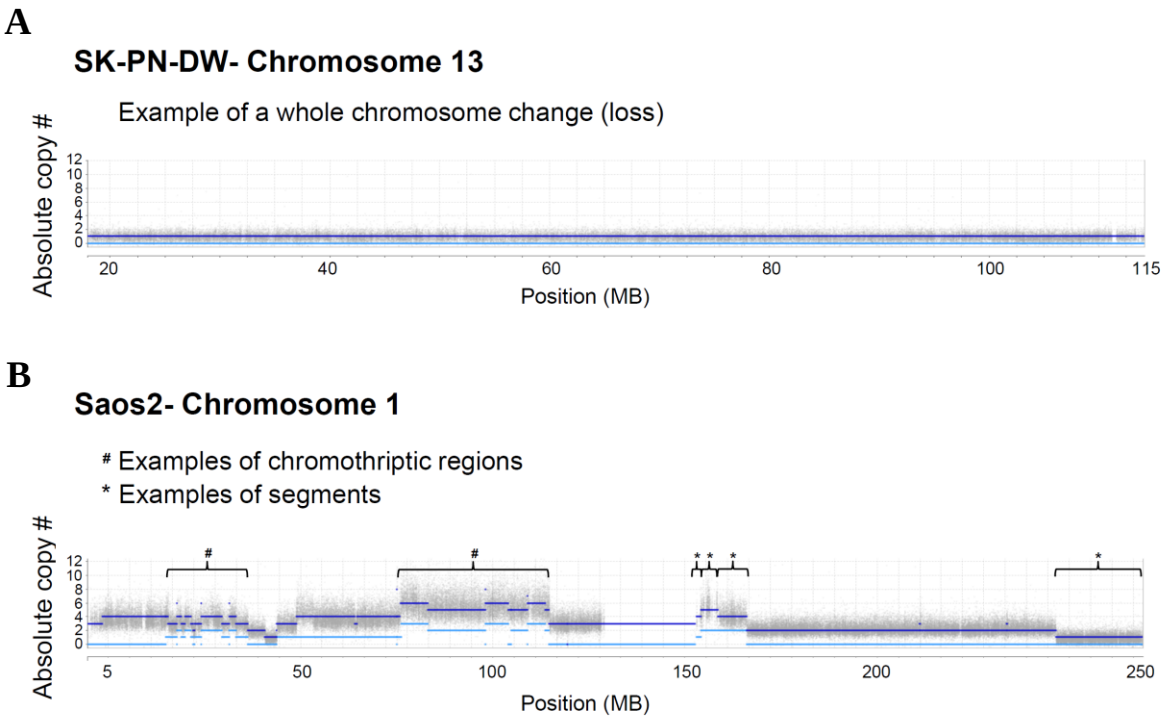

Figure 3.13: Criteria for determining genome instability using copy number data from the COSMIC database.

(A-B) Criteria for determining segmentation, chromothriptic regions and whole chromosome gains or losses using copy number plots from the Catalogue of Somatic Mutations in Cancer (COSMIC) database. The grey data points are normalized copy number data. The dark blue line indicates the total chromosome copy number. The light blue line indicates the predicted copy number of the minor chromosome. Breaks in the blue lines delineate segments of similar copy number status. **(A)** A snapshot of chromosome 13 from the cancer cell line SK-PN-DW demonstrates what was scored as loss of an entire chromosome. **(B)** A snapshot of chromosome 1 from the cancer cell line Saos2 demonstrates what was scored as a segment (*) and which regions were considered as chromothriptic ($^{\#}$). Chromothriptic events are characterized by certain genomic features, some of which can be observed using the copy number data found in the COSMIC database. Stephens *et al*. describe chromothripsis as being marked by rearrangements that are confined to a defined genomic region (Stephens *et al* 2011). Additionally, the copy number profile in these regions typically oscillates between two copy number states (Stephens *et al* 2011). For example, oscillation between copy numbers 1 and 2 are indicative of loss of heterozygosity (LOH) and heterozygosity respectively (Stephens *et al* 2011). These criteria were used to evaluate chromothriptic regions for the cell lines selected from the COSMIC database.

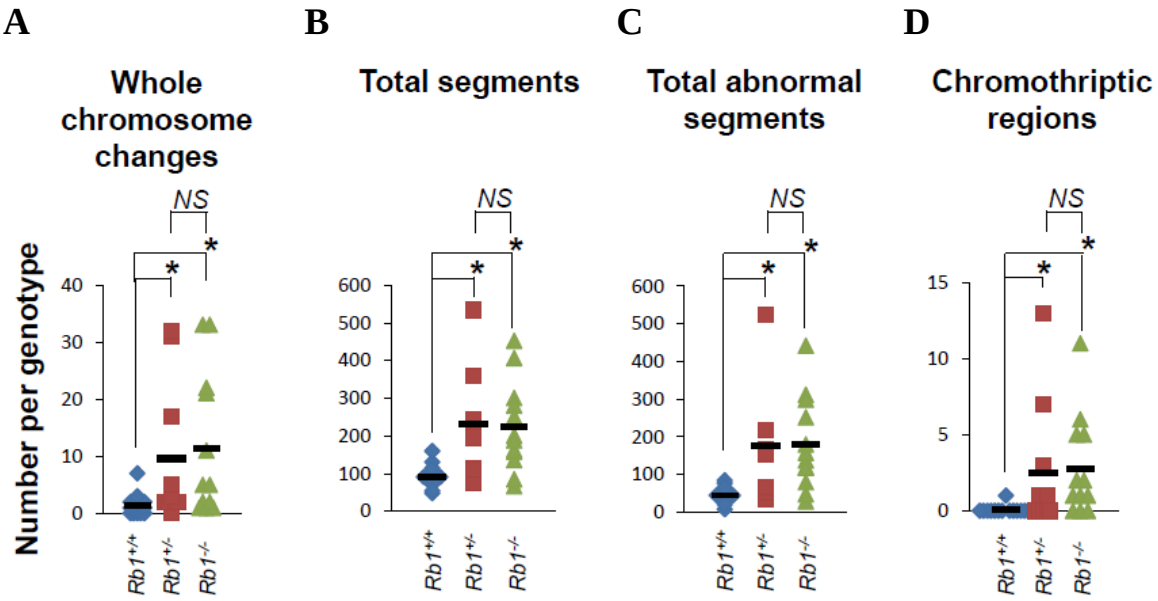

Figure 3.14: *RB1*$^{+/-}$ cancers exhibit as much genome instability as *RB1*$^{-/-}$ cancers.

(A-D) Quantitation of genomic instability in at least ten cancer cell lines that are wild type (n = 15), hemizygous (n = 10) or null (n = 12) for *RB1*. **(A)** Quantitation of the total number of whole chromosome changes per tumor of each genotype was tabulated. These values were plotted and the mean was compared between genotypes using a t-test. **(B)** Quantitation of the total segments per tumor of each genotype was tabulated. These values were plotted and the mean was compared between genotypes using a t-test. **(C)** Quantitation of the total abnormal segments per tumor of each genotype was tabulated. These values were plotted and the mean was compared between genotypes using a t-test. **(D)** Quantitation of the number of chromothriptic regions per tumor of each genotype was tabulated. These values were plotted and the mean was compared between genotypes using a t-test. ***P* < 0.05. *NS*- not significant.

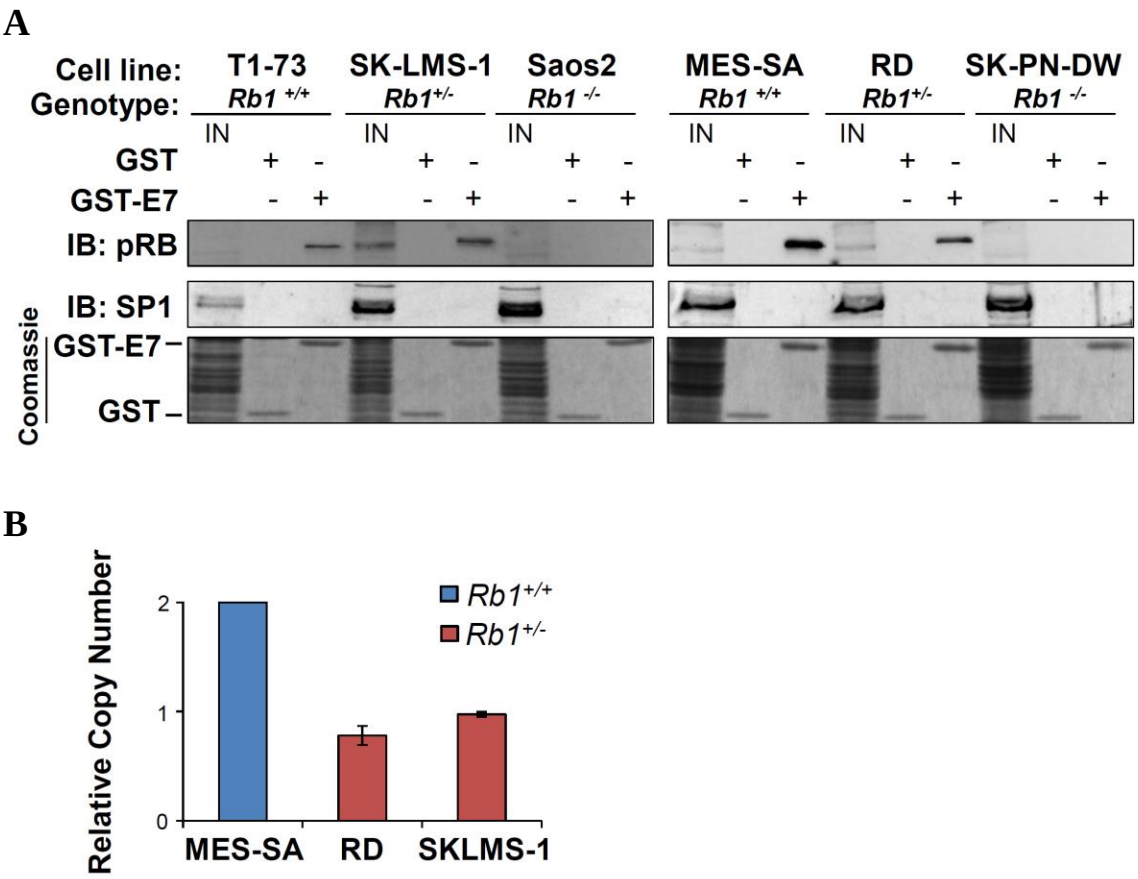

Figure 3.15: Verification of *RB1* genotype and functional pRB in mesenchymal cancer cell lines.

(A) GST-E7 was used to pull down pRB from representative cancer cell lines to demonstrate whether they had functional pRB. Immunoblot of a nuclear transcription factor SP1 was used as a loading control. Coomassie staining reveals levels of GST or GST-E7 used in the experiment. **(B)** Real time PCR amplification of the *RB1* gene locus in *RB1* hemizygous cell lines compared to a $RB1^{+/+}$ cell line. Results are normalized to the copy number of an internal gene locus; n = 3.

3.4.5 Haploinsufficiency of *Rb1* compromises pRB-mediated tumor suppression

The pressing question that remains is whether hemizygosity of the retinoblastoma gene compromises pRB-mediated tumor suppression, and is therefore relevant for the genesis of cancer. As mentioned in the introduction, loss of heterozygosity of the remaining wild type *Rb1* allele is required for the development of pituitary tumors in $Rb1^{+/-}$ mice however $Rb1^{-/-}$ mice are not viable as a comparison (Jacks *et al* 1992, Wu *et al* 2003, Clarke *et al* 1992, Lee *et al* 1992). However, $Rb1^{\Delta L/\Delta L}$ mice are viable and can therefore be utilized to study whether haploinsufficiency of the LXCXE binding cleft of the retinoblastoma protein, as a surrogate for *Rb1* haploinsufficiency itself, compromises pRB-mediated tumor suppression.

We crossed $Rb1^{\Delta L/+}$ mice with $Trp53^{-/-}$ tumor prone mice as previously reported (Coschi *et al* 2010). $Rb1^{\Delta L/+}$; $Trp53^{-/-}$ mice exhibited a significantly decreased survival compared to $Trp53^{-/-}$ controls, with a median of 147 days, which was not significantly different from $Rb1^{\Delta L/\Delta L}$; $Trp53^{-/-}$ mice (139 days) (Fig. 3.16A; Coschi *et al* 2010). PCR amplification of the wild type and knock-in *Rb1* alleles in tumor and corresponding control tail DNA from $Rb1^{\Delta L/+}$; $Trp53^{-/-}$ mice showed retention of the wild type allele in all tumors tested (Fig. 3.16B). Thymic lymphomas from $Rb1^{\Delta L/+}$; $Trp53^{-/-}$ mice demonstrate a more aggressive tumor phenotype compared to $Trp53^{-/-}$ controls as evidenced by smaller cells with large nuclei (Fig. 3.16E-H and D respectively), similar to the histology from $Rb1^{\Delta L/\Delta L}$; $Trp53^{-/-}$ thymic lymphomas (Fig. 3.16C; Coschi *et al* 2010). Furthermore as with $Rb1^{\Delta L/\Delta L}$; $Trp53^{-/-}$ mice, $Rb1^{\Delta L/+}$; $Trp53^{-/-}$ mice exhibit a significant shift in their acquired tumor spectrum from thymic lymphoma commonly reported in $Trp53^{-/-}$ mice, towards sarcoma (Table 3.5; Coschi *et al* 2010). We then investigated whether thymic lymphomas from these mice exhibit increased genomic instability. DNA from thymic lymphomas of twelve $Rb1^{\Delta L/+}$; $Trp53^{-/-}$ mice were subjected to array comparative genomic hybridization (aCGH), and DNA copy number status in tumors was evaluated as previously described (Coschi *et al* 2010). Figure 3.17A shows representative Log_2 ratio plots from a male versus female control hybridization and select $Rb1^{\Delta L/+}$; $Trp53^{-/-}$ tumors hybridized against same sex control DNA. Our analysis revealed a significant increase in the number of whole autosome gains and losses in

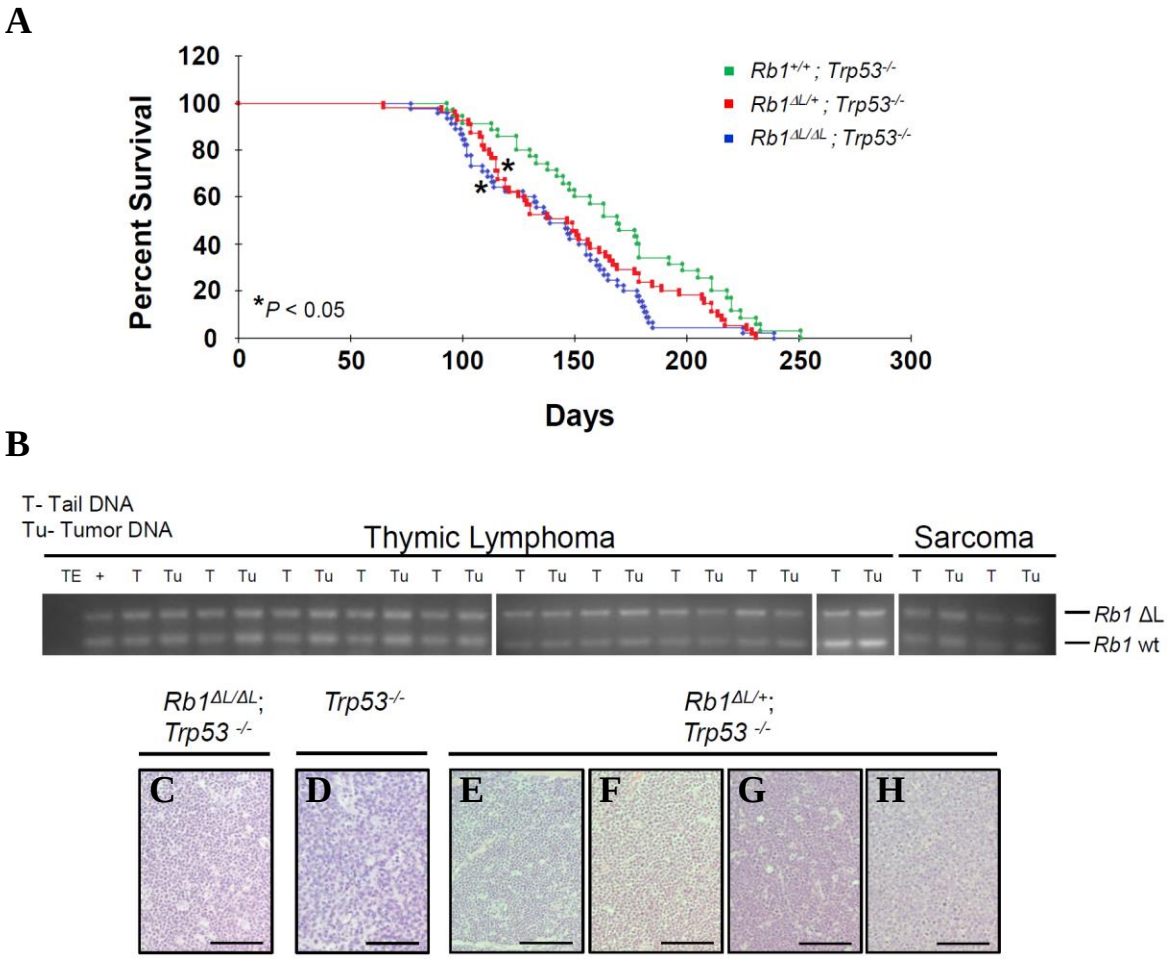

Figure 3.16: Haploinsufficiency compromises pRB-mediated tumor suppression.

(A) Kaplan-Meier survival proportions are shown for *Rb1*$^{\Delta L/+}$; *Trp53*$^{-/-}$ mice (n=52). Data shown for *Rb1*$^{\Delta L/\Delta L}$; *Trp53*$^{-/-}$ and *Trp53*$^{-/-}$ mice has been previously reported by Coschi *et al*, 2010, and is included as a comparison. **(B)** *Rb1* wild type and ΔL alleles from tail and the indicated tumor DNA from *Rb1*$^{\Delta L/+}$; *Trp53*$^{-/-}$ mice were PCR amplified as described (see Methods). **(C-H)** Representative images of cancers found in *Trp53*$^{-/-}$ control, *Rb1*$^{\Delta L/\Delta L}$; *Trp53*$^{-/-}$ and *Rb1*$^{\Delta L/+}$; *Trp53*$^{-/-}$ compound mutants. **(C)** H&E staining of a thymic lymphoma from a *Trp53*$^{-/-}$ mouse. **(D)** H&E staining of a thymic lymphoma from a *Rb1*$^{\Delta L/\Delta L}$; *Trp53*$^{-/-}$ mouse. **(E-H)** H&E staining of thymic lymphomas from *Rb1*$^{\Delta L/+}$; *Trp53*$^{-/-}$ mice. Scale bars in C-H are 100 µm.

Table 3.5. Summary of pathology from mice used in this study.

Genotype	Lymphoma[a]	Sarcoma	Carcinoma	Multiple types[b]	Metastases	N-value
Trp53$^{-/-}$	33	3	0	1	7	35
Rb1$^{\Delta L/\Delta L}$*;Trp53*$^{-/-}$	31	27[c]	3	15[c]	18[d]	45
Rb1$^{\Delta L/+}$*;Trp53*$^{-/-}$	37	18[c]	1	8	7	55

[a]Includes thymic lymphoma among others.
[b]This indicates that a single mouse had more than one tumor from the categories on the left.
[c]Indicates a difference from controls that is above 95% confidence interval (χ2-test, P=0.0019)
[d]Above 90% confidence interval (χ2-test, P=0.094)

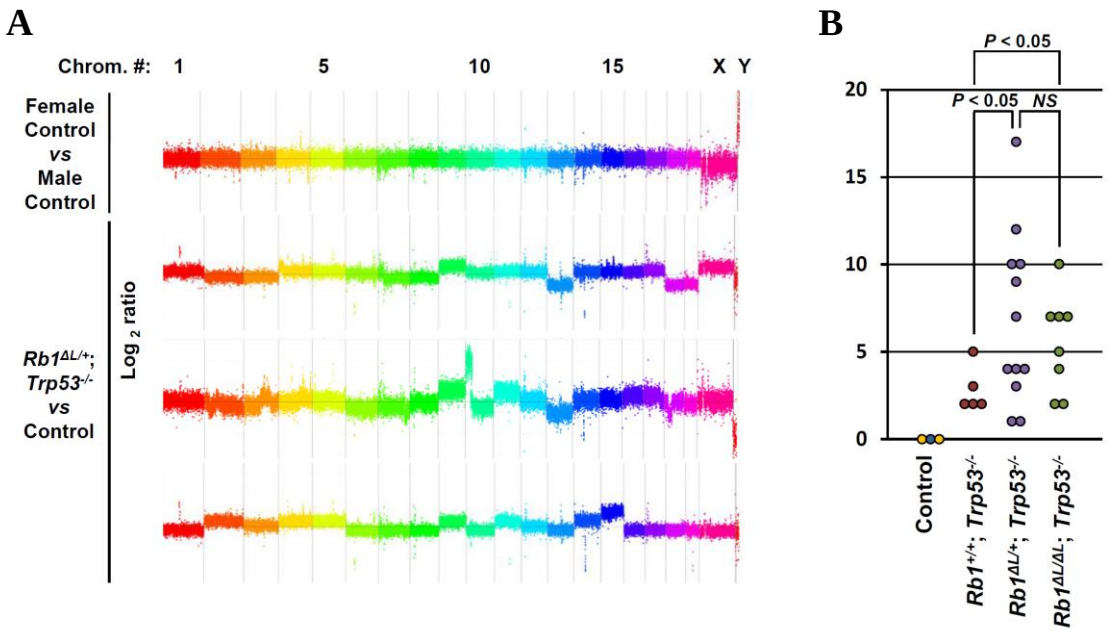

Figure 3.17: Tumors from *Rb1*$^{\Delta L/+}$; *Trp53*$^{-/-}$ mice exhibit genomic instability.

(A) Control, or tumor DNA, was used for hybridization to whole genome arrays to determine regions of gain or loss in thymic lymphoma samples. Representative graphs depicting Log_2 ratio values plotted against chromosome number are shown. Data points from individual chromosomes are shown in different colors. **(B)** Whole chromosome gains and losses were inferred by differences in an entire chromosome and compared with controls. The number of whole chromosome changes for each tumor is plotted against their genotypes. Control, *Trp53*$^{-/-}$ and *Rb1*$^{\Delta L/\Delta L}$; *Trp53*$^{-/-}$ data have been previously reported by Coschi *et al*. 2010, and are presented as a comparison for *Rb1*$^{\Delta L/+}$; *Trp53*$^{-/-}$ data. The control male versus control male hybridization is shown in blue, the male versus female hybridizations are shown in yellow, and *Trp53*$^{-/-}$ and *Rb1*$^{\Delta L/\Delta L}$; *Trp53*$^{-/-}$ samples are denoted by red and green respectively. The analysis of autosomes alone is shown. The mean number of changes was compared between genotypes using a t-test.

thymic lymphomas from *Rb1*$^{\Delta L/+}$; *Trp53*$^{-/-}$ mice compared to *Trp53*$^{-/-}$ controls and most notably, this instability was no less than in *Rb1*$^{\Delta L/\Delta L}$; *Trp53*$^{-/-}$ tumors (Fig. 3.17B; t-test, $P < 0.05$).

Taken together, these data clearly demonstrate that loss of one functional LXCXE binding cleft of pRB results in haploinsufficiency and is enough to compromise pRB-mediated tumor suppression. Furthermore, this compromise occurs through the same mechanism as in *Rb1*$^{\Delta L/\Delta L}$; *Trp53*$^{-/-}$ mice- compromised genome stability.

3.5 Discussion

In this study we report a novel pRB-E2F1-Condensin II complex interaction at pericentromeric heterochromatin that exhibits *Rb1* dose sensitivity. Loss of this complex leads to the accumulation of DNA double strand breaks and mitotic errors which is highly suggestive of replication stress. Recently, replication stress was demonstrated to result in genomic instability associated with tumorigenesis (Burrell *et al* 2013). While the chromosomal abnormalities associated with replication stress are well characterized, the mechanism by which this might occur is still unknown. Therefore understanding the mechanism(s) by which replication stress is mitigated represents a key opportunity for the development of novel therapeutics.

Two key findings will now be highlighted from this report. The first is that we provide strong evidence to question the extrapolation of Knudson's hypothesis, that both copies of *RB1* must be lost to initiate tumorigenesis, to all contexts of *RB1* loss in cancer (Knudson 1971). The sole tumor suppressive role of the retinoblastoma protein has traditionally been attributed to its negative regulation of E2F transcription factors, thereby preventing cell cycle progression (Dyson 1998). Studies using the *Rb1*$^{\Delta L/\Delta L}$ mouse however, have revealed an unappreciated role of pRB-mediated tumor suppression- the maintenance of genome stability. Using *Rb1*$^{\Delta L/\Delta L}$ mice as a comparison, we demonstrate that haploinsufficiency of the LXCXE binding cleft functionally contributes to pRB-mediated tumor suppression. In humans, Retinoblastoma survivors acquire early-onset second primary neoplasms with a penetrance increased over the

general population (Abramson *et al* 1976). Thus it is interesting to speculate that the underlying genomic instability we observe in *RB1*$^{+/-}$ patient fibroblasts could contribute to this increased penetrance. These second primary neoplasms often occur in cells of mesenchymal origin (Abramson *et al* 1976, Friend *et al* 1987). Furthermore, like both the MEFs and patient fibroblasts used in our studies, the thymic lymphomas and sarcomas acquired in our mouse models of cancer also arise from cells of mesenchymal origin. Accordingly, copy number change data from the COSMIC database for several tumors of mesenchymal origin found that *RB1*$^{+/-}$ tumors exhibit as much genome instability as *RB1*$^{-/-}$ tumors across multiple criteria, both of which are significantly increased over tumors with wild type *RB1*. This suggests that haploinsufficiency of *RB1* is particularly important in the pathogenesis of mesenchymal cancers.

It is notable that other studies have implicated heterozygosity of *Rb1* in compromising full pRB-function, though a mechanism to explain the observed haploinsufficiency and its contribution to pRB-mediated tumor suppression has been lacking (Zheng *et al* 2002, Williams *et al* 1994). The second key finding in this report is therefore that we provide strong evidence implicating an *Rb1* gene dosage sensitive complex of pRB, E2F1 and Condensin II in mitigating replication stress to maintain genome stability. In turn, this novel mechanism contributes to pRB-mediated tumor suppression. Replication stress typically occurs at fragile sites or repetitive regions of the genome and is marked by DNA double strand breaks in the ensuing G1 phase, and mitotic errors such as lagging chromosomes. We observe these defects in *Rb1*$^{+/-}$, *Rb1*$^{-/-}$, *Rb1*$^{\Delta L/+}$ and *Rb1*$^{\Delta L/\Delta L}$ MEFs at repetitive pericentromeric heterochromatin, which is particularly difficult to replicate (Zaratiegui *et al* 2011a, Zaratiegui *et al* 2011b). The Condensin II complex has recently been shown to play an important role in DNA replication by helping to resolve sister chromatids (Ide *et al* 2010, Akai *et al* 2011, Ono *et al* 2013). It is also enriched at centromeres, suggesting a unique requirement for its function there (Moore *et al* 2005, Hagstrom *et al* 2002, Ono *et al* 2004). In more than one species, pRB and E2F1 have been found together throughout the genome in S-phase, including at repetitive DNA and sites of replication (Wells *et al* 2003, Korenjak *et al* 2012, Pickering and Kowalik 2006, Mendoza-Maldonado *et al* 2010, Barbie *et al* 2004). Moreover, there are multiple studies demonstrating that binding to pRB promotes E2F1's

preference for non-canonical consensus sequences (Tao *et al* 1997, Dick and Dyson 2003). Taken together, our data is highly suggestive that loss of a pRB-E2F1-Condensin II complex leads to replication stress. Future experiments to definitively demonstrate that replication stress is indeed occurring, such as demonstrating the accumulation of replication protein A (RPA) indicating stalled replication forks, are needed.

Our data brings seemingly disparate concepts together and proposes an *Rb1* gene dosage sensitive role for pRB, E2F1 and the Condensin II complex in DNA replication. $RB1^{+/-}$ patient fibroblasts are haploinsufficient in their ability to prevent the accumulation of DNA double strand breaks and mitotic errors, suggesting that *RB1* haploinsufficiency functionally contributes to tumorigenesis in humans. The retinoblastoma protein is functionally lost in the majority of human cancers (Sherr 1996). Therefore pRB's dosage dependent role in the maintenance of genome stability offers new opportunities to better classify patients who, based on their *RB1* status, may exhibit a superior response to therapies exploiting genomic instability.

3.6 References

Abramson, D. H., Ellsworth, R. M., Zimmerman, L. E. 1976. Nonocular cancer in retinoblastoma survivors. *Transactions. Section on Ophthalmology. American Academy of Ophthalmology and Otolaryngology* **81**(3 Pt 1): 454-57.

Aguilera, A., Gomez-Gonzalez, B. 2008. Genome instability: a mechanistic view of its causes and consequences. *Nature Reviews Genetics* **9**(3): 204-17.

Akai, Y., Kurokawa, Y. Nakazawa, N., Tonami-Murakami, Y. Suzuki, Y., Yoshimura, S. H., Iwasaki, H., Shiroiwa, Y., Nakamura, T., Shibata, E., Yanagida, M. 2011. Opposing role of condensin hinge against replication protein A in mitosis and interphase through promoting DNA annealing. *Open Biology* **1**:110023.

Avni, D., Yang, H., Martelli, F., Hofmann, F., El Shamy, W. M., Ganesan, S., Scully, R., Livingston, D. M. 2003. Active localization of the retinoblastoma protein in chromatin and its response to S phase DNA damage. *Molecular Cell* **12**(3): 735-46.

Barbie, D. A., Kudlow, B. A., Frock, R., Zhao, J. Y., Johnson, B. R., Dyson, N., Harlow, E., Kennedy, B. K. 2004. Nuclear reorganization of mammalian DNA synthesis prior to cell cycle exit. *Molecular and Cellular Biology* **24**(2): 595-607.

Burrell, R. A., McClelland, S. E., Endesfelder, D., Groth, P., Weller, M. C., Shaikh, N., Domingo, E., Kanu, N., Dewhurst, S. M., Gronroos, E., Chew, S. K., Rowan, A. J., Schenk, A., Sheffer, M., Howell, M., Kschischo, M., Behrens, A., Helleday, T., Bartek, J., Tomlinson, I. P., Swanton, C. 2013. Replication stress links structural and numerical cancer chromosomal instability. *Nature* **494**(7438): 492-96.

Cecchini, M. J., Dick, F. A. 2011. The biochemical basis of CDK phosphorylation-independent regulation of E2F1 by the retinoblastoma protein. *Biochemical Journal* **434**(Part 2): 297-308.

Clarke, A. R., Maandag, E. R., Vanroon, M., Vanderlugt, N. M. T., Vandervalk, M., Hooper, M. L., Berns, A., Riele, H. T. 1992. Requirement for a functional RB-1 gene in murine development. *Nature* **359**(6393): 328-30.

Clemente-Blanco, A., Mayan-Santos, M., Schneider, D. A., Machin, F., Jarmuz, A., Tschochner, H., Aragon, L. 2009. Cdc14 inhibits transcription by RNA polymerase I during anaphase. *Nature* **458**(7235): 219-22.

Coschi, C. H., Martens, A. L., Ritchie, K., Francis, S. M., Chakrabarti, S., Bérubé, N. G., Dick, F. A. 2010. Mitotic chromosome condensation mediated by the retinoblastoma protein is tumor-suppressive. *Genes & Development* **24**(13): 1351-63.

Dick, F. A., Dyson, N. 2003. pRB contains an E2F1-specific binding domain that allows E2F1-induced apoptosis to be regulated separately from other E2F activities. *Molecular Cell* **12**(3): 639-49.

Dick, F. A., Sailhamer, E., Dyson, N. J. 2000. Mutagenesis of the pRB pocket reveals that cell cycle arrest functions are separable from binding to viral oncoproteins. *Molecular and Cellular Biology* **20**(10): 3715-27.

Dulev, S., de Renty, C., Mehta, R., Minkov, I., Schwob, E., Strunnikov, A. 2009. Essential global role of CDC14 in DNA synthesis revealed by chromosome underreplication unrecognized by checkpoints in cdc14 mutants. *PNAS USA* **106**(34): 14466-71.

Dyson, N. 1998. The regulation of E2F by pRB-family proteins. *Genes & Development* **12**(15): 2245-62.

Fero, M. L., Randel, E., Gurley, K. E., Roberts, J. M., Kemp, C. J. 1998. The murine gene p27(Kip1) is haploinsufficient for tumor suppression. *Nature* **396**(6707): 177-80.

Friend, S. H., Horowitz, J. M., Gerber, M. R., Wang, X. F., Bogenmann, E., Li, F. P., Weinberg, R. A. 1987. Deletions of a DNA sequence in retinoblastomas and mesenchymal tumors: organization of the sequence and its encoded protein. *PNAS USA* **84**(24): 9059-63.

Hagstrom, K. A., Holmes, V. F., Cozzarelli, N. R., Meyer, B. J. 2002. C-elegans condensin promotes mitotic chromosome architecture, centromere organization, and

sister chromatid segregation during mitosis and meiosis. *Genes & Development* **16**(6):729-42.

Harbour, J. W., Lai, S. L., Whangpeng, J., Gazdar, A. F., Minna, J. D., Kaye, F. J. 1988. Abnormalities in structure and expression of the human retinoblastoma gene in SCLC. *Science* **241**(4863): 353-57.

Hensel, C. H., Hsieh, C. L., Gazdar, A. F., Johnson, B. E., Sakaguchi, A. Y., Naylor, S. L., Lee, W. H., Lee, E. Y. H. P. 1990. Altered structure and expression of the human retinoblastoma susceptibility gene in small-cell lung-cancer. *Cancer Research* **50**(10): 3067-72.

Hernando, E., Nahle, Z., Juan, G., Diaz-Rodriguez, E., Alaminos, M., Hemann, M., Michel, L., Mittal, V., Gerald, W., Benezra, R., Lowe, S. W., Cordon-Cardo, C. 2004. Rb inactivation promotes genomic instability by uncoupling cell cycle progression from mitotic control. *Nature* **430**(7001): 797-802.

Hirota, T., Gerlich, D., Koch, B., Ellenberg, J., Peters, J. M. 2004. Distinct functions of condensin I and II in mitotic chromosome assembly. *Journal of Cell Science* **117**(26): 6435-45.

Hurford, R., Cobrinik, D., Lee, M-H., Dyson, N. 1997. pRB and p107/p130 are required for the regulated expression of different sets of E2F responsive genes. *Genes & Development* **11**(11): 1447-63.

Ide, S., Miyazaki, T., Maki, H., Kobayashi, T. 2010. Abundance of Ribosomal RNA Gene Copies Maintains Genome Integrity. *Science* **327**(5966): 693-96.

Isaac, C. E., Francis, S. M., Martens, A. L., Julian, L. M., Seifried, L. A., Erdmann, N., Binne, U. K., Harrington, L., Sicinski, P., Bérubé, N. G., Dyson, N. J., Dick, F. A. 2006. The retinoblastoma protein regulates pericentric heterochromatin. *Molecular and Cellular Biology* **26**(9): 3659-71.

Jacks. T., Fazeli, A., Schmitt, E. M., Bronson, R. T., Goodell, M. A., Weinberg, R. A. 1992. Effects of an Rb mutation in the mouse. *Nature* **359**(6393): 295-300.

Johzuka, K., Horiuchi, T. 2007. RNA polymerase I transcription obstructs condensin association with 35S rRNA coding regions and can cause contraction of long repeat in Saccharomyces cerevisiae. *Genes to Cells* **12**(6): 759-71.

Johzuka, K., Terasawa, M., Ogawa, H., Ogawa, T., Horiuchi, T. 2006. Condensin loaded onto the replication fork barrier site in the rRNA gene repeats during S phase in a FOB1-dependent fashion to prevent contraction of a long repetitive array in Saccharomyces cerevisiae. *Molecular and Cellular Biology* **26**(6): 2226-36.

Knudsen, K. E., Booth, D., Naderi, S., Sever-Chroneos, Z., Fribourg, A. F., Hunton, I. C., Feramisco, J. R., Wang, J. Y., Knudsen E. S. 2000. RB-dependent S-phase response to DNA damage. *Molecular and Cellular Biology* **20**(20): 7751-63.

Knudson, A. G. 1971. Mutation and cancer- Statistical study of retinoblastoma. *PNAS USA* **68**(4): 820-23.

Korenjak, M., Anderssen, E., Ramaswamy, S., Whetstine, J. R., Dyson, N. J. 2012. RBF Binding to both Canonial E2F Targets and Noncanonical Targets Depends on Functional dE2F/dDP complexes. *Molecular and Cellular Biology* **32**(21): 4375-87.

Lee, E. Y. H. P., Chang, C. Y., Hu, N. P., Wang, Y. C. J., Lai, C. C., Herrup, K., Lee, W. H., Bradley, A. 1992. *Nature* **359**(6393): 288-94.

Longworth, M. S., Herr, A., Ji, J. Y., Dyson, N. J. 2008. RBF1 promotes chromatin condensation through a conserved interaction with the Condensin II protein dCAP-D3. *Genes & Development* **22**(8): 1011-1024.

Losada, A., Hirano, T. 2005. Dynamic molecular linkers of the genome: the first decade of SMC proteins. *Genes & Development* **19**(11): 1269-87.

Lukas, C., Savic, V., Bekker-Jensen, S., Doil, C., Neumann, B., Pedersen, R. S., Grøfte, M., Chan, K. L., Hickson, I. D., Bartek, J., Lukas, J. 2011. 53BP1 nuclear bodies form around DNA lesions generated by mitotic transmission of chromosomes under replication stress. *Nature Cell Biology* **13**(3): 243-53.

Manning, A. L., Longworth, M. S., Dyson, N. J. 2010. Loss of pRB causes centromere dysfunction and chromosomal instability. *Genes & Development* **24**(13): 1364-76.

Margottin-Goguet, F., Hsu, J. K., Loktev, A., Hsieh, H. M., Reiman, J. D., Jackson, P. K. 2003. Prophase destruction of Emi1 by the SCF(betaTrCP/Slimb) ubiquitin ligase activates the anaphase promoting complex to allow progression beyond prometaphase. *Developmental Cell* **4**(6): 813-26.

Mayhew, C. N., Bosco, E. E., Fox, S. R., Okaya, T., Tarapore, P., Schwemberger, S. J., Babcock, G. F., Lentsch, A. B., Fukasawa, K., Knudsen, E. S. 2005. Liver-specific pRB loss results in ectopic cell cycle entry and aberrant ploidy. *Cancer Research* **65**(11): 4568-77.

Mendoza- Maldonado, R., Paolinelli, R., Galbiati, L., Giadrossi, S., Giacca, M. 2010. Interaction of the Retinonblastoma Protein with Orc 1 and Its Recruitment to Human Origins of DNA Replication. *PLOS ONE* **5**(11): e13720.

Moore, L. L., Stanvitch, G., Roth, M. B., Rosen, D. 2005. HCP-4/CENP-C promotes the prophase timing of centromere resolution by enabling the centromere association of HCP-6 in Caenorhabditis elegans. *Molecular and Cellular bIology* **25**(7): 2583-92.

Nicolay, B. N., Gameiro, P. A., Tschop, K., Korenjak, M., Heilmann, A. M., Asara, J. M., Stephanopoulos, G., Iliopoulos, O., Dyson, N. J. 2013. Loss of RBF1 changes glutamine catabolism. *Genes & Development* **27**(2): 182-96.

Niculescu, A. B. III., Chen, X., Smeets, M., Hengst, L., Prives, C., Reed, S. I. 1998. Effects of p21 Cip1/Waf1 at both the G1/S and G2/M cell cycle transitions: pRB is a critical determinant in blocking DNA replication and in preventing endoreduplication. *Molecular and Cellular Biology* **18**(1): 629-43.

Olshen, A. B., Venkatraman, E. S., Lucito, R., Wigler, M. 2004. Circular binary segmentation for the analysis of array-based DNA copy number data. *Biostatistics* **5**(4): 557-72.

Ono, T., Fang, Y., Spector, D. L., Hirano, T. 2004. Spatial and temporal regulation of condensin I and II in mitotic chromosome assembly in human cells. *Molecular Biology of the Cell* **15**(7): 3296-3308.

Ono, T., Yamashita, D., Hirano, T. 2013. Condensin II initiates sister chromatid resolution during S phase. *Journal of Cell Biology* **200**(4): 429-41.

Pear, W. S., Nolan, G. P., Scott, M. L., Baltimore, D. 1993. Production of high-titre helper-free retroviuses by transient transfection. *PNAS USA* **90**(18): 8392-96.

Pickering, M. T., Kowalik, T. F. 2006. Rb inactivation leads to E2F1-mediated DNA double-strand break accumulation. *Oncogene* **25**(5): 746-55.

Retinoblastoma Solutions- www.retinoblastomasolutions.org

Reynolds, M. R., Lane, A. N., Robertson, B., Kemp, S., Lie, Y., Hill, B. G., Dean, D. C., Clem, B. F. 2013. Control of glutamine metabolism by the tumor suppressor Rb. *Oncogene* (E-pub ahead of Print. doi:10.1038)

Samoshkin, A., Arnaoutov, A., Jansen, L. E. T., Ouspenski, I., Dye, L., Karpova, T., McNally, J., Dasso, M., Cleveland, D. W. Strunnikov, A. 2009. Human Condensin Function Is Essential for Centromeric Chromatin Assembly and Proper Sister Kinetochore Orientation. *PLOS ONE* **4**(8): e6831.

Savvidou, E., Cobbe N. Steffensen, S., Cotterill, S., Heck, M. M. S. 2005. Drosophila CAP-D2 is required for condensin complex stability and resolution of sister chromatids. *Journal of Cell Science* **118**(11): 2529-43.

Sever-Chroneos, Z., Angus, S. P., Fribourg, A. F., Wan, H., Todorov, I., Knudsen, K. E., Knudsen, E. S. 2001. Retinoblastoma tumor suppressor protein signals through inhibition of cyclin-dependent kinase 2 activity to disrupt PCNA function in S-phase. *Molecular and Cellular Biology* **21**(12): 4032-45.

Sherr. C. J. 1996. Cancer cell cycles. *Science* **274**(5293): 1672-77.

Shintomi, K., Hirano, T. 2011. The relative ratio of condensin I to II determines chromosome shapes. *Genes & Development* **25**(14): 1464-69.

Srinivasan, S. V., Mayhew, C. N., Schwemberger, S., Zagorski, W., Knudsen, E. S. 2007. RB loss promotes aberrant ploidy by deregulating levels and activity of DNA replication factors. *Journal of Biological Chemistry* **282**(33): 23867-77.

Stear, J. H., Roth, M. B. 2002. Characterization of HCP-6, a C-elegans protein required to prevent chromosome twisting and merotelic attachment. *Genes & Development* **16**(12): 1498-1508.

Stephens, P. J., Greenman, C. D., Fu, B., Yang, F., Bignell, G. R., Mudie, L. J., Pleasance, E. D., Lau, K. W., Beare, D., Stebbings, L. A., McLaren, S., Lin, M. L., McBride, D. J., Varela, I., Nik-Zainal, S., Leroy, C., Jia, M. M., Menzies, A., Butler, A. P., Teague, J. W., Quail, M. A., Burton, J., Swerdlow, H., Carter, N. P., Morsberger, L. A., Iacobuzio-Donahue, C., Follows, G. A., Green, A. R., Flanagan, A. M., Futreal, P. A., Campell, P. J. 2011. Massive genomic rearrangement acquired in a single catastrophic event during cancer development. *Cell* **144**(1): 27-40.

Tao, Y. X., Kassatly, R. F., Cress, WD., Horowitz, J. M. 1997. Subunit composition determines E2F DNA-binding site specificity. *Molecular and Cellular Biology* **17**(12): 6994-7007.

The Catalogue Of Somatic Mutations In Cancer (COSMIC) database- www.sanger.ac.uk/genetics/CGP/cosmic

Thillainadesan, G., Isovic, M., Loney, E., Andrews, J., Tini, M., Torchia, J. 2008. Genome analysis identifies the p15(ink4b) tumor suppressor as a direct target of the ZNF217/CoREST complex. *Molecular and Cellular Biology* **28**(19): 6066-77.

Torres-Rosell, J., De Piccoli, G., Cordon-Preciado, V., Farmer, S., Jamuz, A., Machin, F., Pasero, P., Lisby, M., Haber, J. E., Aragon, L. 2007. Anaphase onset before complete DNA replication with intact checkpoint responses. *Science* **315**(5817):1411-15.

Wang, B. D., Eyre, D., Basrai, M. Lichten, M., Strunnikov, A. 2005. Condensin binding at distinct and specific chromosomal sites in the Saccharomyes cerevisiae genome. *Molecualr and Cellular Biology* **25**(16): 7216-25.

Wells, J., Yan, P. S., Cechvala, M., Huang, T., Farnham, P. J. 2003. Identification of novel pRB binding sites using CpG microarrays suggests that E2F recruits pRB to specific genomic sites during S-phase. *Oncogene* **22**(10): 1445-60.

Williams, B. O., Schmitt, E. M., Remington, L., Bronson, R. T., Albert, D. M., Weinberg, R. A., Jacks, T. 1994. Extensive contribution of Rb-deficient cells to adult chimeric mice with limited histopathological consequences. *EMBO Journal* **13**(18): 4251-49.

Wood, J. L., Liang, Y. L., Li, K. Y., Chen, J. J. 2008. Microcephalin/MCPH1 Associates with the Condensin II Complex to Function in Homologous Recombination Repair. *Journal of Biological Chemistry* **283**(43): 29586-92.

Wu. L. Z., de Bruin, A., Saavedra, H. I., Starovic, M., Trimboli, A., Yang, Y., Opavska, J., Wilson, O., Thompson, J. C., Ostrowski, M. C., Rosol, T. J., Woollett, L. A., Weinstein M., Cross, J. C., Robinson, M. L., Leone, G. 2003. Extra-embryonic function of Rb is essential for embryonic development and viability. *Nature* **421**(6926): 942-47.

Zaratiegui, M., Castel, S. E., Irvine, D. V., Kloc, A., Ren, J., de Castro, E., Marin, L., Chang, A. Y., Goto, D., Cande, W. Z., Anteguera, F., Arcangioli, B., Martienssen, R. A. 2011b. RNAi promotes heterochromatic silencing through replication-coupled release of RNA Poll III. *Nature* **479**(7371): 135-38.

Zaratiegui, M., Vaughn, M. W., Irvine, D. V., Goto, D., Watt, S., Bahler, J., Arcangioli, B., Martienssen R. A. 2011a. CENP-B preserves genome integrity at replication forks paused by retrotransposon LTR. *Nature* **469**(7328): 112-15.

Zheng, L., Flesken-Nikitin, A., Chen, P. L., Lee, W. H. 2002. Deficiency of Retinoblastoma gene in mouse embryonic stem cells leads to genetic instability. *Cancer Research* **62**(9): 2498-2502.

Chapter 4

4 Discussion

4.1 A new model for pRB-mediated tumor suppression

In addition to its well characterized role in the maintenance of proliferative control, the retinoblastoma protein has been found on chromatin beyond G1 of the cell division cycle where its role is less well defined. Its location on chromatin coincides with E2F1 and together, pRB and E2F1 have been implicated in the regulation of replication (Wells *et al* 2003, Korenjak *et al* 2012, Mendoza-Maldonado *et al* 2010, Pickering and Kowalik 2006, Knudsen *et al* 2000, Sever-Chroneos *et al* 2001, Avni *et al* 2003). The Condensin II complex has also been implicated in facilitating DNA replication (Stear and Roth 2002, Ono *et al* 2004, Ide *et al* 2010, Akai *et al* 2011, Ono *et al* 2013). Though an interaction between the retinoblastoma protein and E2F1 has been previously described, a common mechanism linking this interaction to a role for pRB beyond G1 of the cell division cycle has been lacking (Longworth *et al* 2008).

The data presented in Chapter 2 implicate the retinoblastoma protein in a role separate from the repression of E2F target gene expression and subsequent regulation of the G1 to S-phase transition. This role depends on an interaction between the Condensin II complex and the LXCXE binding cleft and also contributes to pRB-mediated tumor suppression. In Chapter 3, I build upon data reported in Chapter 2 and propose a mechanism whereby the retinoblastoma protein maintains genome stability. This is achieved by a novel E2F1-pRB-Condensin II complex that localizes to repetitive pericentromeric heterochromatin. As pericentromeric repeats are difficult to replicate and may have a special requirement for this complex, this may explain the *Rb1* gene dosage sensitivity of this complex (Zaratiegui *et al* 2011a, Zaratiegui *et al* 2011b). Furthermore, experiments reported in Chapter 3 suggest that this complex maintains genome stability by mitigating replication stress, as we observe DNA damage persisting in mitosis and accumulating in the ensuing G1 phase of the cell division cycle.

Therefore I have added to our current model of pRB-mediated tumor suppression, suggesting that there are in fact multiple mechanisms by which pRB can be tumor suppressive. Specifically, the LXCXE binding cleft of pRB also contributes to pRB-mediated tumor suppression through the maintenance of genome stability. Moreover, I have delineated a mechanism that brings together two seemingly disparate pathways, uniting the roles for both pRB and E2F1 with Condensin II in the maintenance of genome stability.

4.2 Revisiting *RB1* haploinsufficiency

Based on his studies of the childhood cancer retinoblastoma, Knudson proposed that loss of one *RB1* allele did not hasten the loss of the second *RB1* allele and that therefore, the pRB tumor suppressor did not exhibit haploinsufficiency (Knudson 1971). This conclusion became widely known as the "two hit" hypothesis, which is the litmus test for the discovery of new tumor suppressors. While Knudson demonstrates this principle for the childhood cancer retinoblastoma, data presented in this thesis questions the applicability this "two hit" hypothesis to all tumorigenic contexts.

In recent years, genomic instability has transitioned from being viewed as a by-product of tumorigenesis to being causative through enabling the persistence and accumulation of mutations that favour malignancy (Hanahan and Weinberg 2011). Therefore our observation that patient fibroblasts ($RB1^{+/-}$) exhibit haploinsufficiency in their ability to properly maintain genome stability suggests that pRB could be haploinsufficient specifically in the context of mediating the tumor suppression of second primary neoplasms in retinoblastoma patients. There is evidence in the literature to support this hypothesis. Patients with inherited retinoblastoma are more likely to acquire second primary neoplasms than the general population. For example, a study following survivors of inherited retinoblastoma that had received radiation therapy in the eye reported that patients were diagnosed with osteosarcomas originating in the skull 2000 times more frequently than the general population (Abramson *et al* 1976). Moreover, they were also diagnosed with osteosarcomas arising in their extremities 500 times more

frequently than is expected from the general population. In startling contrast, survivors of non-inherited retinoblastoma, meaning that not all cells of their body are missing one copy of *RB1*, were diagnosed with osteosarcomas at a frequency identical to the general population (Abramson *et al* 1976). Data such as these are strongly suggestive that loss of only one *RB1* allele is in fact predisposing to cancer in certain contexts.

The patient fibroblasts used in our studies are, and the majority of second primary neoplasms arising in survivors of inherited retinoblastoma are, both of mesenchymal cell origin (Abramson *et al* 1976, Friend *et al* 1987). Interestingly, the thymic lymphomas and sarcomas that we observe in our mouse models of cancer are also of mesenchymal origin. Moreover, all of our *in vitro* cell-based experiments were performed in mouse embryonic fibroblasts (MEFs), again of mesenchymal origin. One could therefore propose that the mesenchymal lineage has a unique requirement for the proper dose of *RB1*. This is supported by data in Chapter 3 whereby analysis of copy number data from the COSMIC database showed that $RB1^{+/-}$ human cancer cells of mesenchymal origin exhibit as much genomic instability as those with homozygous loss of *RB1*. If we again use the COSMIC database to look at tumors of various cell origins, and not specifically from retinoblastoma patients, we find that a significant number of tumors retain one wild type copy of *RB1* (COSMIC database). In light of these findings, it is tempting to speculate that we have delineated both the appropriate context and the mechanism by which hemizygosity of *RB1* exhibits haploinsufficiency of pRB-mediated tumor suppression.

4.3 Impact on human cancer and cancer therapies

Over 90% of all human cancers have inactivated the retinoblastoma pathway (Sherr 1996). Traditionally, reconstituting cells with wild type pRB, or reactivating the pRB pathway (depending on tumor-specific mutations) has been considered the only way to restore pRB-mediated cell cycle control and thereby stop cancer cell growth. This is based on experiments which showed that reconstituting cancer cells with wild type pRB was enough to restore cell cycle control (Takahashi *et al* 1991, Bookstein *et al* 1990,

Huang *et al* 1988). However, this is not feasible for the many cancers where cyclin/cdk complexes are constitutively activated. If such cancer cells were reconstituted with wild type pRB, the protein would become hyperphosphorylated and remain unable to re-establish cell cycle control.

In light of the work presented in this thesis, I propose that instead of attempting to restore pRB function in cancer cells, their increased genomic instability could be exploited therapeutically. Based on the fact that $RB1^{+/-}$ cells exhibit haploinsufficiency in mediating genome stability, this type of therapy would apply to cancers that have lost either one or both copies of *RB1*. Therefore cancers lacking the wild type dose of *RB1* may respond better to combinations of chemotherapeutic agents or other targeted strategies that enhance genomic instability or inhibit DNA damage repair. In theory, these cancer cells will be more sensitive to the increased burden of DNA damage and will therefore be sent into genomic catastrophe and subsequent apoptosis. There is precedence for the success of such a therapy schema. For example, PARP inhibitors are used to treat breast cancers with *BRCA1/2* mutations (Lord and Ashworth 2008, Rios and Puhalla 2011). BRCA1/2 protein facilitates DNA double strand break repair and when mutated, cells rely solely on PARP to mediate DNA damage repair (Huen *et al* 2010, Stolz *et al* 2010). When these cells are treated with PARP inhibitors, a synthetic lethality is created that compromises DNA repair pathways (Lord and Ashworth 2008, Rios and Puhalla 2011). In turn, cancer cells are unable to recover and undergo apoptosis (Lord and Ashworth 2008, Rios and Puhalla 2011).

Conversely, exploiting the role for pRB in the maintenance of genome stability with combinations of chemotherapies or targeted agents may represent a novel mechanism to treat cancers which appear "addicted" to pRB expression. Colon cancer is unique in that *RB1* has been shown to play an oncogenic role and E2F1 a tumor suppressive role (Yang *et al* 2009, Bramis *et al* 2004). It has been shown that loss of pRB and activation of E2F1 induces apoptosis in colon cancer cells, and this is supported by evidence that the interaction between E2F1 and the C-terminus of pRB serves to inhibit E2F1-induced apoptosis in certain contexts (Carnevale *et al* 2012, Dick and Dyson 2003, Elliot *et al* 2001, Elliot *et al* 2002, Kitagawa *et al* 2008). Therefore,

disruption of the interaction between E2F1 and the C-terminus of pRB in colon cancer with a targeted therapy would serve a two-fold purpose- to increase genomic instability by preventing pRB from recruiting Condensin II to chromatin, and to induce E2F1-mediated apoptosis. If such a targeted therapy were combined with a chemotherapeutic causing DNA damage, exacerbation of genomic instability may be synergistic in leading to cancer cell death.

Other cancers, such as ovarian cancer and non-small cell lung cancer, also retain expression of pRB (Kommoss *et al* 2007, du Bois *et al* 2003, Knudsen and Knudsen 2008). This has been shown to inversely correlate with the induction of cancer cell death in response to DNA damaging chemotherapies and overall survival (Kommoss *et al* 2007, du Bois *et al* 2003, Knudsen and Knudsen 2008). Therefore these subpopulations of patients whose cancers retain pRB expression may benefit from therapies disrupting the specific E2F1-pRB interaction as it represents two potentially synergistic approaches to inducing widespread apoptosis in cancer cells.

4.4 Remaining questions

Though we have begun to delineate the way in which the LXCXE binding cleft mediates tumor suppression, there are still several questions to be answered. For example, though this E2F1-pRB-Condensin II complex acts beyond G1 of the cell division cycle, we do not know whether the pRB in this complex is hyperphosphorylated and whether hyperphosphorylation represents an activating signal for this role, or whether a subset of pRB is protected from hyperphosphorylation and becomes part of this complex. There is evidence to support both possibilities. It has been reported that upon DNA damage in S-phase, pRB becomes dephosphorylated and/or acetylated and can bind to and repress E2F transcription factors (Knudsen *et al* 2000, Sever-Chroneos *et al* 2001, Avni *et al* 2003). It is possible that this hypophosphorylated species binds to E2F1 only at loci that have been marked by DNA damage. Alternatively, E2F1 can bind to the C-terminus of hyperphosphorylated pRB, thereby providing a way to separate pRB's inhibition of E2F target gene transcription from its role in the maintenance of genome

stability through post translational modifications (Cecchini and Dick 2011). Additionally, binding of E2F1 to phosphorylated pRB has been proposed to alter the specificity of E2F1 such that it can bind at non-canonical E2F consensus sequences on DNA, which is perhaps a more satisfying rationale than the first (Tao *et al* 1997, Dick and Dyson 2003). Delineating the contexts in which this E2F1-pRB-Condensin II complex can be formed merits further research because it could potentially indicate whether $RB1^{+/+}$ cancers with constitutively active cyclin/cdk complexes, and therefore hyperphosphorylated pRB and deregulated E2F target gene transcription, would respond to therapies that exacerbate genomic instability in a pRB-dependent manner.

Additionally, though we know that E2F1 recruits pRB to chromatin, which in turn recruits the Condensin II complex, we do not know whether Condensin II is recruited through a direct interaction with pRB, or whether this occurs through secondary means. There is data to suggest that different histone modifications can recruit the Condensin II complex to chromatin (Liu *et al* 2010). If so, the inability of chromatin modifying enzymes to bind in pRB's LXCXE binding cleft may result in loss of the deposition of the necessary histone modifications to recruit Condensin II to chromatin in a pRB-dependent manner. However, immunoprecipitation experiments presented in Chapter 2 of this thesis suggest that the interaction could be direct, for example pRB-ΔL cannot immunoprecipitate with CAP-D3 of the Condensin II complex, though wild type pRB is able.

Another open question asks whether this E2F1-pRB-Condensin II complex is important for facilitating DNA replication. Data presented in Chapter 3 is highly suggestive that this is the case and this is supported by data from other labs. For example Condensin II has recently been shown to mediate sister chromatid resolution as DNA is replicated in S-phase (Ono *et al* 2013). Moreover, replication protein A (RPA) has been demonstrated to antagonize Condensins during replication such that when Condensins are disabled, genomic instability occurs (Akai *et al* 2011). Experiments to challenge DNA replication will help delineate the function of this E2F1-pRB-Condensin II complex in S-phase, and also be indicative of the best use of targeted therapies to exploit genomic instability in cancers lacking *RB1*.

Finally, data reported in Chapter 3 of this thesis suggests that the specific interaction of pRB with E2F1 recruits Condensin II to chromatin, specifically at pericentromeric repeats. In yeast, Condensins have been shown to prevent the transcription and expansion of the highly repetitive rDNA sequences (Johzuka *et al* 2006, Clemente-Blanco *et al* 2009, Johzuka and Horiuchi 2007, Ide *et al* 2010). Moreover, Condensins have also been shown to promote clustering of yeast tRNA genes in the nucleolus (Thompson *et al* 2003, Haeusler *et al* 2008). Therefore it is tempting to suggest that while we have so far identified pericentromeric heterochromatin as having a unique requirement for the Condensin II complex, other repetitive sequences in the human genome may also have this same unique requirement.

4.5 Summary of findings

The retinoblastoma protein is known as the prototypical tumor suppressor. The contribution of the retinoblastoma protein to tumor suppression has been largely attributed to its maintenance of proliferative control mediated through binding to and repressing E2F transcription factors (Dyson 1998). As a result, other functions of the retinoblastoma protein that contribute to tumor suppression have been overlooked.

In this thesis I demonstrate that the LXCXE binding cleft of the retinoblastoma protein contributes to pRB-mediated tumor suppression, independent of its regulation of the cell division cycle, through the maintenance of genome stability. Using the $Rb1^{\Delta L/\Delta L}$ mouse model I show that thymic lymphomas from $Rb1^{\Delta L/\Delta L}$; $Trp53^{-/-}$ exhibit increased genomic instability compared to those from $Trp53^{-/-}$ controls. Moreover, $Rb1^{\Delta L/\Delta L}$ MEFs exhibit chromosome and mitotic defects correlating with increased aneuploidy that are attributed to loss of an interaction between pRB-ΔL and the Condensin II complex.

In Chapter 3 I describe the mechanism by which pRB maintains genome stability in more detail. Localization of the Condensin II complex to chromatin at discrete loci depends on pRB, which in turn is dependent upon a specific interaction with E2F1. I have found a defined locus where this interaction is of particular importance, namely

pericentromeric heterochromatin, a non-canonical E2F binding site. Loss of this complex on chromatin leads to increased DNA damage, specifically at dosage-sensitive loci like pericentromeric heterochromatin.

Another important finding from work in Chapter 3 revealed that the *RB1* gene exhibits haploinsufficiency. *RB1*$^{+/-}$ retinoblastoma patient fibroblasts recapitulate the mitotic defects observed in *Rb1*$^{\Delta L/\Delta L}$, *Rb1*$^{\Delta L/+}$ and *Rb1*$^{+/-}$ MEFs. Moreover, human cancer cells hemizygous for *RB1* exhibit as much genomic instability as those with homozygous loss of *RB1*. This data causes us to re-examine our current view of the "two hit" hypothesis stipulating that both copies of *RB1* must be lost in order to compromise pRB-mediated tumor suppression. However, it may provide an explanation for the statistics showing that survivors of familial retinoblastoma are more susceptible to the acquisition of second primary neoplasms than the general population (Abramson *et al* 1976).

References

Abramson, D. H., Ellsworth, R. M., Zimmerman, L. E. 1976. Nonocular cancer in retinoblastoma survivors. *Transactions. Section on Ophthalmology. American Academy of Ophthalmology and Otolaryngology* **81**(3 Pt 1): 454-57.

Akai, Y., Kurokawa, Y. Nakazawa, N., Tonami-Murakami, Y. Suzuki, Y., Yoshimura, S. H., Iwasaki, H., Shiroiwa, Y., Nakamura, T., Shibata, E., Yanagida, M. 2011. Opposing role of condensin hinge against replication protein A in mitosis and interphase through promoting DNA annealing. *Open Biology* **1**:110023.

Avni, D., Yang, H., Martelli, F., Hofmann, F., El Shamy, W. M., Ganesan, S., Scully, R., Livingston, D. M. 2003. Active localization of the retinoblastoma protein in chromatin and its response to S phase DNA damage. *Molecular Cell* **12**(3): 735-46.

Bookstein, R., Shew, J. Y., Chen, P. L., Scully, P., Lee, W. H. 1990. Suppression of tumorigenicity of human prostate carcinoma-cells by replacing a mutated RB gene. *Science* **247**(4943): 712-15.

Bramis, J., Zacharatos, P., Papaconstantinou, I., Kotsinas, A., Sigala, F., Korkolis, D. P., Nikiteas, N., Pazaiti, A., Kittas, C., Bastounis, E., Gorgoulis, V. G. 2004. E2F-1 transcription factor immunoexpression is inversely associated with tumor growth in colon adenocarcinomas. *Anticancer Research* **24**(5A): 3041-47.

Carnevale, J., Palander, O., Seifried, L. A., Dick, F. A. 2012. DNA Damage Signals through Differentially Modified E2F1 Molecules To Induce Apoptosis. *Molecular and Cellular BiologyMolecular and Cellular Biology* **32**(5): 900-12.

Cecchini, M. J., Dick, F. A. 2011. The biochemical basis of CDK phosphorylation-independent regulation of E2F1 by the retinoblastoma protein. *Biochemical Journal* **434**: 297-308.

Clemente-Blanco, A., Mayan-Santos, M., Schneider, D. A., Machin, F., Jarmuz, A., Tschochner, H., Aragon, L. 2009. Cdc14 inhibits transcription by RNA polymerase I during anaphase. *Nature* **458**(7235): 219-22.

Dick, F. A., Dyson, N. 2003. pRB contains an E2F1-specific binding domain that allows E2F1-induced apoptosis to be regulated separately from other E2F activities. *Molecular Cell* **12**(3): 639-49.

du Bois, A., Luck, H. J., Neier, W., Adams, H. P., Mobus, V., Costa, S., Bauknecht, T., Richter, B., Warm, M., Schroder, W., Olbricht, S., Nitz, U., Jackisch, C., Emons, G., Wagner, U., Kuhn, W., Pfisterer, J. 2003. A randomized clinical trial of cisplatin/paclitaxel versus carboplatin/paclitaxel as first-line treatment of ovarian cancer. *Journal of the National Cancer Institute* **95**(17): 1320-30.

Dyson, N. 1998. The regulation of E2F by pRB-family proteins. *Genes & Development* **12**(15): 2245-62.

Elliot, M. J., Stilwell, A., Dong, Y. B., Yang, H. L., Wong, S. L., Wrightson, W. R., Martin, R. C. G., McMasters, K. M. 2002. C-terminal deletion mutant $p21^{WAF1/CIP1}$ enhances E2F-1-mediated apoptosis in colon adenocarcinoma cells. *Cancer Gene Therapy* **9**(5): 453-63.

Elliot, M. J., Yan Bin Dong, Yang, H., McMasters, K. M. 2001. E2F-1 up-regulates c-Myc and $p14^{ARF}$ and induces apoptosis in colon cancer cells. *Clinical Cancer Research* **7**(11): 3590-97.

Friend, S. H., Horowitz, J. M., Gerber, M. R., Wang, X. F., Bogenmann, E., Li, F. P., Weinberg, R. A. 1987. Deletions of a DNA sequence in retinoblastomas and mesenchymal tumors: organization of the sequence and its encoded protein. *PNAS USA* **84**(24): 9059-63.

Haeusler, R. A., Pratt-Hyatt, M., Good, P. D., Gipson, T. A., Engelke, D. R. 2008. Clustering of yeast tRNA genes is mediated by specific association of condensin with tRNA gene transcription complexes. *Genes & Development* **22**(16): 2204-14.

Hanahan, D., Weinberg, R. A. 2011. Hallmarks of cancer: the next generation. *Cell* **144**(5): 646-74.

Huang, H. J. S., Yee, J. K., Shew, J. Y., Chen, P. L., Bookstein, R., Friedmann, T., Lee, E. Y. H. P., Lee, W. H. 1988. Suppression of the neoplastic phenotype by replacement of the RB gene in human cancer-cells. *Science* **242**(4885): 1563-66.

Huen, M. S. Y., Sy, S. M. H., Chen, J. J. 2010. BRCA1 and its toolbox for the maintenance of genome integrity. *Nature Reviews Molecular and Cell Biology* **11**(2): 138-48.

Ide, S., Miyazaki, T., Maki, H., Kobayashi, T. 2010. Abundance of Ribosomal RNA Gene Copies Maintains Genome Integrity. *Science* **327**(5966): 693-96.

Johzuka, K., Horiuchi, T. 2007. RNA polymerase I transcription obstructs condensin association with 35S rRNA coding regions and can cause contraction of long repeat in Saccharomyces cerevisiae. *Genes to Cells* **12**(6): 759-71.

Johzuka, K., Terasawa, M., Ogawa, H., Ogawa, T., Horiuchi, T. 2006. Condensin loaded onto the replication fork barrier site in the rRNA gene repeats during S phase in a FOB1-dependent fashion to prevent contraction of a long repetitive array in Saccharomyces cerevisiae. *Molecular and Cellular Biology* **26**(6): 2226-36.

Kitagawa, M., Aonuma, M., Lee, S. H., Fukutake, S., McCormick, F. 2008. E2F-1 transcriptional activity is a critical determinant of Mdm2 antagonist-induced apoptosis in human tumor cell lines. *Oncogene* **27**(40): 5303-14.

Knudsen, E. S., Knudsen, K. E. 2008. Tailoring to RB: tumor suppressor status and therapeutic response. *Nature Reviews Cancer* **8**(9): 714-24.

Knudsen, K. E., Booth, D., Naderi, S., Sever-Chroneos, Z., Fribourg, A. F., Hunton, I. C., Feramisco, J. R., Wang, J. Y., Knudsen E. S. 2000. RB-dependent S-phase response to DNA damage. *Molecular and Cellular Biology* **20**(20): 7751-63.

Knudson, A. G. 1971. Mutation and cancer- Statistical study of retinoblastoma. *PNAS USA* **68**(4):820-823.

Kommoss, S., du Bois, A., Ridder R., Trunk, M. J., Schmidt, D. Pfisterer, J., Kommoss, F. 2007. Independent prognostic significance of cell cycle regulator proteins p16(INK4a) and pRB in advanced-stage ovarian carcinoma including optimally debulked patients: a translational research subprotocol of a randomised study of the Arbeitsgemeinschaft Gynaekologische Onkologie Ovarian Cancer Study Group. *British Journal of Cancer* **96**(2): 306-13.

Korenjak, M., Anderssen, E., Ramaswamy, S., Whetstine, J. R., Dyson, N. J. 2012. RBF Binding to both Canonial E2F Targets and Noncanonical Targets Depends on Functional dE2F/dDP complexes. *Molecular and Cellular Biology* **32**(21): 4375-87.

Liu, W., Tanasa, B., Tyurina, O. V., Zhou, T. Y., Gassmann, R., Lie, W. T., Ohgi, K. A., Benner, C., Garcia-Bassets, I., Aggarwal, A. K., Desai, A., Dorrestein, P. C., Glass, C. K., Rosenfeld, M. G. 2010. PHF8 mediates histone H4 lysine 20 demethylation events involved in cell cycle progression. *Nature* **466**(7305): 508-12.

Longworth, M. S., Herr, A., Ji, J. Y., Dyson, N. J. 2008. RBF1 promotes chromatin condensation through a conserved interaction with the Condensin II protein dCAP-D3. *Genes & Development* **22**(8): 1011-1024.

Lord, C. J., Ashworth, A. 2008. Targeted therapy for cancer using PARP inhibitors. *Current Opinions in Pharmacology* **8**(4):363-69.

Mendoza- Maldonado, R., Paolinelli, R., Galbiati, L., Giadrossi, S., Giacca, M. 2010. Interaction of the Retinonblastoma Protein with Orc 1 and Its Recruitment to Human Origins of DNA Replication. *PLOS ONE* **5**(11): e13720.

Ono, T., Fang, Y., Spector D. L., Hirano, T. 2004. Spatial and temportal regulation of condensins I and II in mitotic chromosome assembly in human cells. *Molecular Biology of the Cell* **15**(7): 3296-3308.

Ono, T., Yamashita, D., Hirano, T. 2013. Condensin II initiates sister chromatid resolution during S phase. *Journal of Cell Biology* **200**(4): 429-41.

Pickering, M. T., Kowalik, T. F. 2006. Rb inactivation leads to E2F1-mediated DNA double-strand break accumulation. *Oncogene* **25**(5): 746-55.

Rios, J., Puhalla, S. 2011. PARP inhibitors in breast cancer: BRCA and beyond. *Oncology* **25**(11): 1014-25.

Sever-Chroneos, Z., Angus, S. P., Fribourg, A. F., Wan, H., Todorov, I., Knudsen, K. E., Knudsen, E. S. 2001. Retinoblastoma tumor suppressor protein signals through inhibition of cyclin-dependent kinase 2 activity to disrupt PCNA function in S-phase. *Molecular and Cellular Biology* **21**(12): 4032-45.

Sherr, C. J. 1996. Cancer cell cycles. *Science* **274**(5293): 1672-77.

Stear, J. H., Roth, M. B. 2002. Characterization of HCP-6, a C-elegans protein required to prevent chromosome twisting and merotelic attachment. *Genes & Development* **16**(12): 1498-1508.

Stolz, A., Ertych, N., Kienitz, A., Vogel, C., Schneider, V., Fritz, B., Jacob, R., Dittmar, G., Weighert, W., Petersen, I., Bastians, H. 2010. The CHK2-BRCA1 tumor suppressor pathway ensures chromosomal stability in human somatic cells. *Nature Cell Biology* **12**(5): 492-99.

Takahashi, R., Hashimoto, T., Xu, H. J., Hu, S. X., Matsui, T., Miki, T., Bigomarshall, H., Aaronson, S. A., Benedict, W. F. 1991. The Retinoblastoma gene functions as a growth and tumor suppressor in human bladder-carcinoma cells. *PNAS USA* **88**(12): 5257-61.

Tao, Y. X., Kassatly, R. F., Cress, WD., Horowitz, J. M. 1997. Subunit composition determines E2F DNA-binding site specificity. *Molecular and Cellular Biology* **17**(12): 6994-7007.

The Catalogue Of Somatic Mutations In Cancer (COSMIC) database- www.sanger.ac.uk/genetics/CGP/cosmic

Thompson, M., Haeusler, R. A., Good, P. D., Engelke, D. R. 2003. Nucleolar clustering of dispersed tRNA genes. *Science* **302**(5649): 1399-1401.

Wells, J., Yan, P. S., Cechvala, M., Huang, T., Farnham, P. J. 2003. Identification of novel pRB binding sites using CpG microarrays suggests that E2F recruits pRB to specific genomic sites during S-phase. *Oncogene* **22**(10): 1445-60.

Yang. G., Fu, H., Lu, X., Jin, L., Zhang, J., Yao, L., Zifan, L. 2009. E2F1: A colon cancer specific putative tumor suppressor and a valuable therapeutic target. *Bioscience Hypotheses* **2**(5): 313-15.

Zaratiegui, M., Castel, S. E., Irvine, D. V., Kloc, A., Ren, J., de Castro, E., Marin, L., Chang, A. Y., Goto, D., Cande, W. Z., Anteguera, F., Arcangioli, B., Martienssen, R. A. 2011b. RNAi promotes heterochromatic silencing through replication-coupled release of RNA Poll III. *Nature* **479**(7371): 135-38.

Zaratiegui, M., Vaughn, M. W., Irvine, D. V., Goto, D., Watt, S., Bahler, J., Arcangioli, B., Martienssen R. A. 2011a. CENP-B preserves genome integrity at replication forks paused by retrotransposon LTR. *Nature* **469**(7328): 112-15.

Appendix A

Appendix A: Permission for publication by Cellular and Molecular Life Sciences.

Some material in Chapter 1 was excerpted from a review article published in Cellular and Molecular Life Sciences, containing three figures, by Springer and SP Birkhäuser Verlag Basel. Copyright © 2012 by Springer Basel AG.

Coschi CH, and Dick FA. (2012). Chromosome instability and deregulated proliferation: an unavoidable duo. *Cell Mol Life Sci*. **69**(12): 2009-24.

Below, with kind permission from Springer Science+Business Media B. V., is the granted permission for publication in this thesis.

Dear Sir/Madam,

With reference to your request to reprint material in which Springer Science and Business Media control the copyright, our permission is granted free of charge and at the following conditions:

Springer material

- represents original material which does not carry references to other sources (if material in question refers with a credit to another source, authorization from that source is required as well);
- requires full credit [Springer and the original publisher/journal title, volume, year of publication, page, chapter/article title, name(s) of author(s), figure number(s), original copyright notice] to the publication in which the material was originally published, by adding; with kind permission from Springer Science+Business Media B.V.;
- may not be altered in any manner. Abbreviations, additions, deletions and/or any other alterations shall be made only with prior written authorization of the author and/or Springer Science + Business Media.
- may not be republished in Electronic Open Access.

This permission

a. is non-exclusive.
b. includes use in an electronic form: provided it's password protected, or on intranet or university's repository, including UMI (according to the definition at the Sherpa website: http://www.sherpa.ac.uk/romeo/), or CD-Rom/E-book,
c. is subject to a courtesy information to the author (address is given with the article/chapter).
d. is personal to you and may not be sublicensed, assigned, or transferred by you to any other person without Springer's written permission.
e. is valid only when the conditions noted above are met.

Permission free of charge on this occasion does not prejudice any rights we might have to charge for reproduction of our copyrighted material in the future.

Best regards,

Kind regards,

Nel van der Werf (Ms)
Rights and Permissions/Springer

Van Godewijckstraat 30 | P.O. Box 17
3300 AA Dordrecht | The Netherlands
tel +31 (0) 78 6576 298
fax +31 (0)78 65 76-377

Appendix B

Appendix B: Permission for publication by Genes & Development.

Data presented in Chapter 2 is published in Genes & Development; Copyright © 2010 by Cold Spring Harbor Laboratory Press.

Coschi CH, Martens AL, Ritchie K, Francis SM, Chakrabarti S, Bérubé NG, Dick FA. (2010). Mitotic chromosome condensation mediated by the retinoblastoma protein is tumor-suppressive. *Genes Dev*. **24**(13): 1351-63.

Below is permission for publication in this thesis.

Hello,

I published an article in Genes & Development July 1, 2010 as follows: Mitotic chromosome condensation mediated by the retinoblastoma protein is tumor suppressive. Coschi et al. (2010) 24(13): 1351-63.

I am preparing to submit my thesis and defend my PhD and was wondering if I could have a letter of permission from Genes & Development to publish my article in my thesis.

I look forward to hearing from you.
Sincerely,
Courtney Coschi

PhD Candidate
Department of Biochemistry
Western University
London Regional Cancer Program
[redacted]

Permission granted by the copyright owner, contingent upon the consent of the original author, provided complete credit is given to the original source and copyright date.

By [redacted] 9/27/12
Date

COLD SPRING HARBOR LABORATORY PRESS

Appendix C

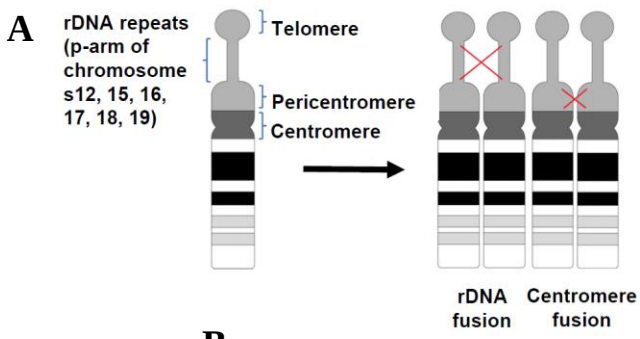

C

Fusions	*Rb1*$^{+/+}$ MEF	*Rb1*$^{\Delta L/\Delta L}$ MEF
Frequency of chromosome interactions involving rDNA (%)	0.435	0.393

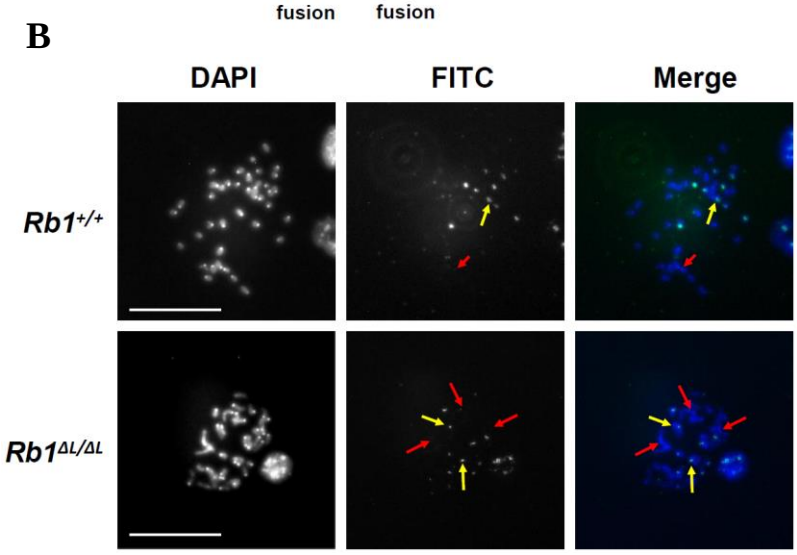

Appendix C: Investigation of chromosome fusions mediated by rDNA repeats.

(A) Pictogram showing the location of rDNA genes on the p-arms of mouse chromosomes 12, 15, 16, 17, 18 and 19. In order to investigate whether centromere fusions also include rDNA repeats, fluorescence *in situ* hybridization using probes specific to rDNA repeats was performed on metaphase spreads from MEFs. **(B)** Metaphase spreads were prepared, hybridized with rDNA probes, and subsequently stained with DAPI. Images of DAPI stained chromosomes (blue) and FITC stained rDNA repeats (green) are shown, as are the corresponding overlaid images. Red arrows indicate chromosome interactions in the absence of rDNA repeats, yellow arrows indicate centromere interactions where one of the chromosomes stains positively for rDNA. **(C)** The total number of adjacent centromeres was counted, as well as the number of interactions involving rDNA-containing chromosomes, in *Rb1*$^{+/+}$ and *Rb1*$^{\Delta L/\Delta L}$ MEFs. The proportion of centromere interactions containing rDNA was compared between both genotypes using the χ2-test for statistical significance and no difference was found. Thus, even though *Rb1*$^{\Delta L/\Delta L}$ metaphase spreads have a greater proportion of interacting chromosomes than wild type, the frequency with which rDNA repeats could be part of this interaction is no more abundant in the mutants than wild type controls.

Appendix D

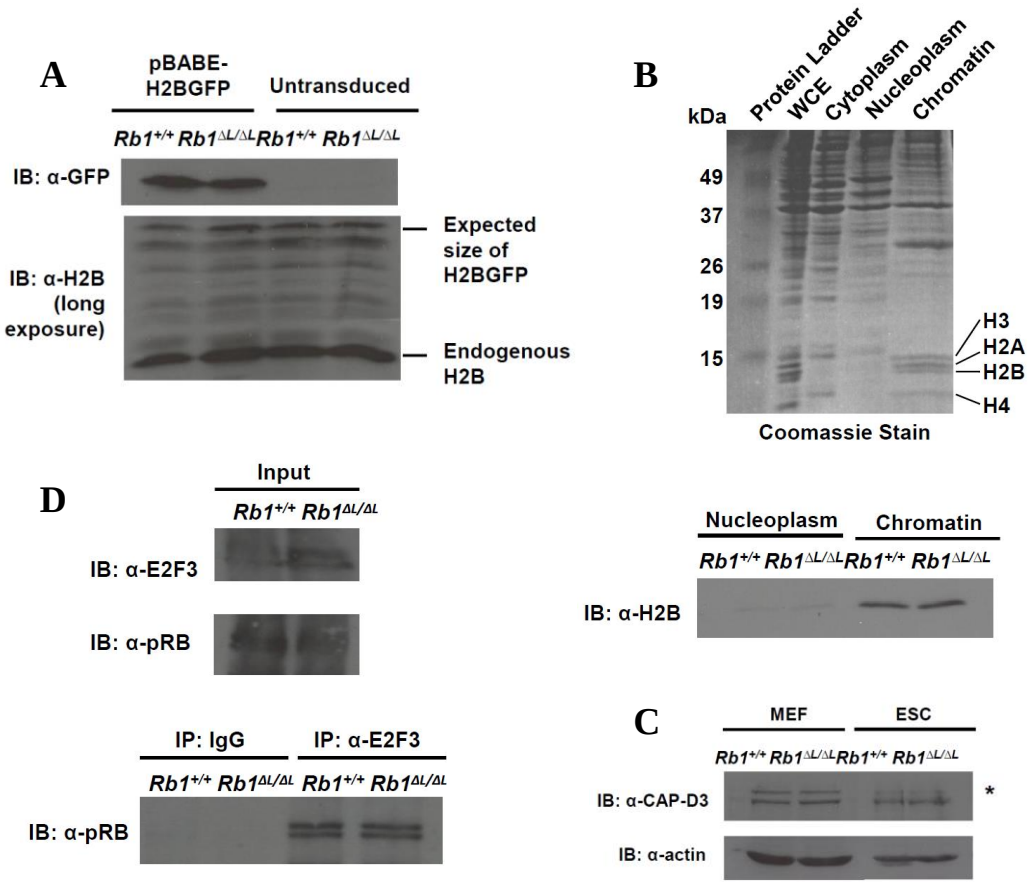

Appendix D: Equivalent, low level expression of H2B-GFP in *Rb1*$^{+/+}$ and *Rb1*$^{\Delta L/\Delta L}$ MEFs.

(A) Western blot analysis of pBABE-H2B-GFP transduced MEFs using an anti-GFP antibody shows equivalent expression in *Rb1*$^{+/+}$ and *Rb1*$^{\Delta L/\Delta L}$ MEFs (upper panel). The lower panel shows a western blot of the same extracts using an anti-H2B antibody. The migration positions for endogenous H2B and the expected position of H2B-GFP are shown. The inability to detect H2B-GFP over background using anti-H2B antibodies reveals that the ratio of H2B-GFP to endogenous H2B is very low. **(B)** Coomassie stain and Western blot analysis of the chromatin fractionation demonstrates clear enrichment of the chromatin fraction with histones, that are absent in the nucleoplasmic fraction. **(C)** Western blot analysis of whole cell extract from both MEFs and ESCs demonstrates that there are normal levels of CAP-D3 protein in *Rb1*$^{\Delta L/\Delta L}$ cells compared to wild type. The asterisk (*) indicates a non-specific band. **(D)** Western blot analysis of whole cell extract reveals the presence of hypophosphorylated pRB in ESCs. Analysis of chromatin fractions reveals enrichment of hypophosphorylated pRB on the chromatin of *Rb1*$^{+/+}$ and *Rb1*$^{\Delta L/\Delta L}$ MEFs and ESCs. Please note that these samples were not normalized for input levels.

Appendix E

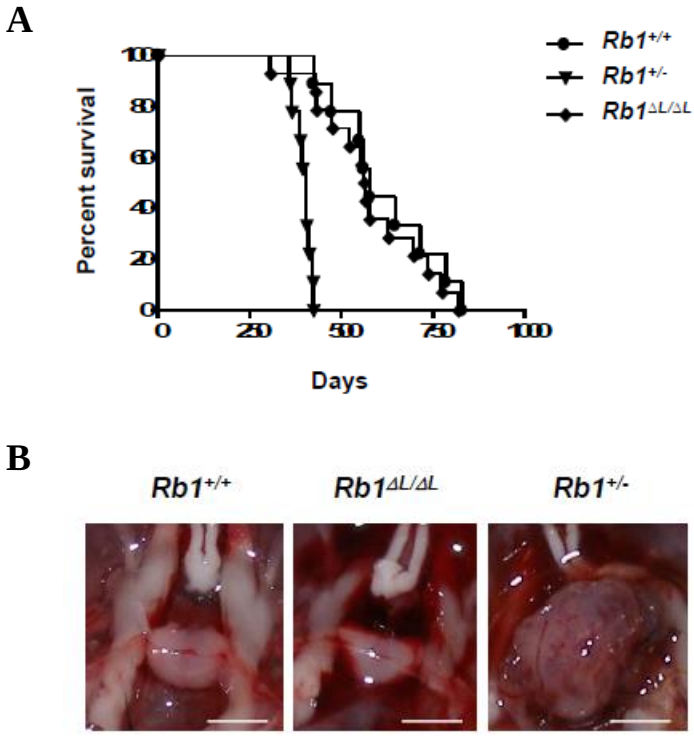

Appendix E: *Rb1*$^{\Delta L/\Delta L}$ mice do not develop spontaneous tumors.

(A) Kaplan-Meier survival proportions for wild type (n=9), *Rb1*$^{+/-}$ (n=9), and *Rb1*$^{\Delta L/\Delta L}$ (n=14) mice. *Rb1*$^{+/-}$ mice most frequently succumb to pituitary tumors, and occasionally to thyroid cancers, at approximately one year of age. Our data is consistent with previous reports for this genotype in a mixed genetic background. From this analysis, *Rb1*$^{\Delta L/\Delta L}$ mutant mice have a similar life expectancy as wild type controls. Furthermore, these animals do not display any distinct pathology at the time of euthanasia. **(B)** Photographs of normal pituitaries in wild type and *Rb1*$^{\Delta L/\Delta L}$ mice at the time of necropsy, a pituitary tumor from a *Rb1*$^{+/-}$ control is shown for comparison. The scale bar is 2 mm.

Appendix F

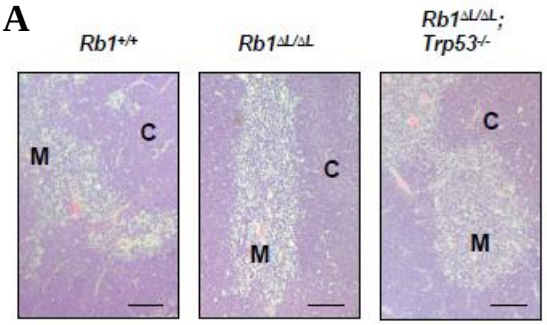

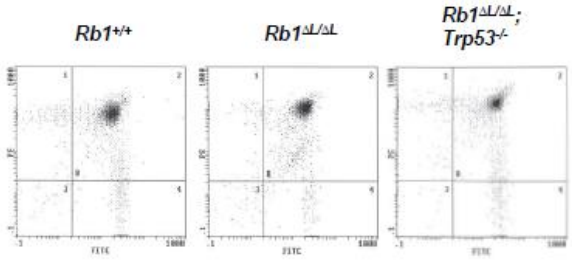

Genotype	*n*	$CD4^-$ $CD8^-$	$CD4^+CD8^+$	$CD4^-CD8^+$	$CD4^+CD8^-$
Rb1 $^{+/+}$	6	3.17 ± 1.44	81.82 ± 5.66	5.60 ± 2.08	9.41 ± 2.59
Rb1 $^{\Delta L/\Delta L}$	5	3.44 ± 2.85	85.18 ± 6.89	3.64 ± 1.05	7.73 ± 3.12
Rb1 $^{\Delta L/\Delta L}$*;Trp53* $^{-/-}$	6	1.64 ± 0.66	84.4 ± 6.11	5.11 ± 2.05	8.84 ± 4.30

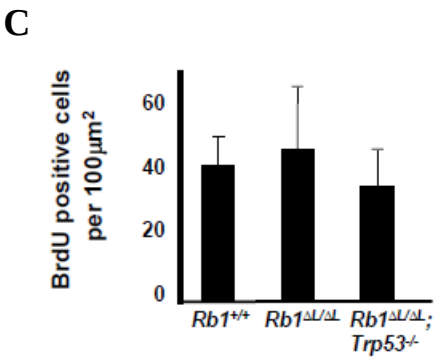

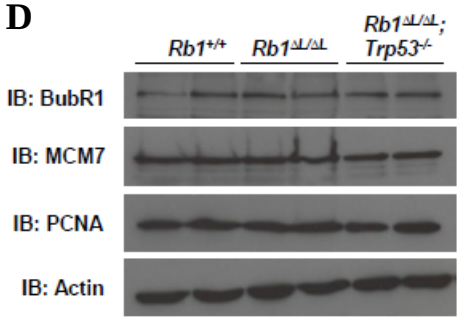

Appendix F: Normal thymic development in *Rb1*$^{\Delta L/\Delta L}$ and *Rb1*$^{\Delta L/\Delta L}$; *Trp53*$^{-/-}$ mice.

(A) H&E staining of tissue sections from developing thymi in mice of the indicated genotypes. Note the normal appearance of the cortex (C) and medullar regions (M) in all genotypes. The scale bar is 50μm. **(B)** Development of T-cells was assessed by staining for CD4 and CD8 cell surface markers and by quantitating positive cells by flow cytometry. Note normal levels of all cell types in scatter plots and the summary table. **(C)** Proliferation was measured by injecting mice with BrdU one hour prior to euthanasia. Cryosections of thymic tissue were stained using anti-BrdU antibodies. The abundance of positively staining nuclei per unit area of tissue was counted and averaged for at least three mice of each genotype. This analysis revealed that there is no difference in proliferation among these genotypes. **(D)** E2F target gene expression, BubR1, MCM7, and PCNA was examined in the thymus of *Rb1*$^{+/+}$, *Rb1*$^{\Delta L/\Delta L}$ and *Rb1*$^{\Delta L/\Delta L}$; *Trp53*$^{-/-}$ mice. In all cases, western blots revealed that protein expression was normal.

Appendix G

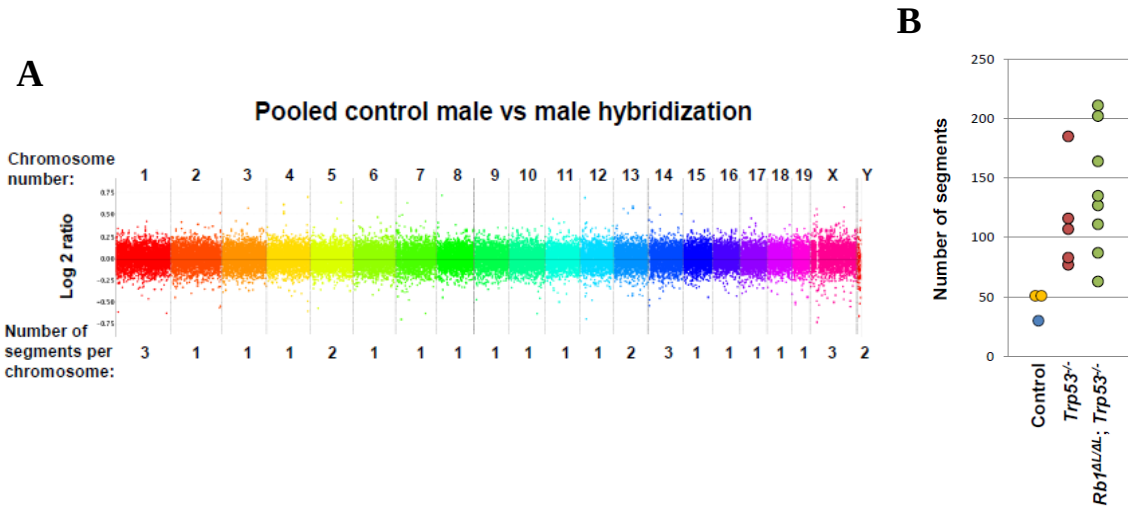

Appendix G: Some *Rb1*$^{\Delta L/\Delta L}$; *Trp53*$^{-/-}$ tumor DNA samples have an increased number of sub-chromosomal segment changes compared to controls.

Control DNA samples, or DNA samples from individual tumors versus controls, were used for hybridization to whole genome arrays as described in materials and methods. The graph shows Log2 ratio values plotted against chromosome number, data points from each chromosome are a different color. In order to examine sub-chromosomal DNA copy number changes in each control and tumor DNA hybridization, a segmentation algorithm was applied to all data sets. Simply put, this algorithm groups data points with similar Log2 ratio values that are adjacent to one another. **(A)** The number of segments found in this control male versus control male hybridization is shown below each respective chromosome. The total number of segments is 30, which is relatively close to the total number of autosomes and sex chromosomes (21) and, as shown, most chromosomes are seen as a single segment by this analysis with only a few slight changes in Log2 ratios being erroneously detected and described as different. This indicates that increased numbers of segments can be related to actual changes in the genome with relatively high confidence. **(B)** The total number of segments for each hybridization experiment was determined and are organized into categories by control or tumor genotype. The blue dot is control male versus control male, the yellow dots are control male versus control female. In the tumor samples, the number of segments vastly exceeds the number of individual chromosomes. This implies that extensive sub-chromosomal rearrangements take place in these cancers. Some *Rb1*$^{\Delta L/\Delta L}$; *Trp53*$^{-/-}$ tumor DNA samples have elevated numbers of segments compared with controls, suggesting that segmental chromosome instability may play a role in the increased aggressiveness of *Rb1*$^{\Delta L/\Delta L}$; *Trp53*$^{-/-}$ tumors.

Appendix H

Appendix H: Histology and necropsy data of *Rb1*$^{\Delta L/\Delta L}$; *Trp53*$^{-/-}$, *Trp53*$^{-/-}$, *Rb1*$^{\Delta L/\Delta L}$; *Trp53*$^{+/-}$ and *Trp53*$^{+/-}$ mice in the Chapter 2 tumor study.

Mouse	Sex	Genotype	# days lived	Histology/Necropsy results
A4021	M	*Rb1*$^{\Delta L/\Delta L}$;*Trp53*$^{-/-}$	132	thymic lymphoma
A4029	M	*Rb1*$^{\Delta L/\Delta L}$;*Trp53*$^{-/-}$	136	thymic lymphoma
A4054	M	*Rb1*$^{\Delta L/\Delta L}$;*Trp53*$^{-/-}$	239	thymic lymphoma, kidney - lymphoma, tumor - sarcoma
A4074	M	*Rb1*$^{\Delta L/\Delta L}$;*Trp53*$^{-/-}$	185	tumor - sarcoma
A4222	M	*Rb1*$^{\Delta L/\Delta L}$;*Trp53*$^{-/-}$	89	tumor - sarcoma
A4246	M	*Rb1*$^{\Delta L/\Delta L}$;*Trp53*$^{-/-}$	119	thymic lymphoma
A4634	M	*Rb1*$^{\Delta L/\Delta L}$;*Trp53*$^{-/-}$	93	tumor - sarcoma
A4636	M	*Rb1*$^{\Delta L/\Delta L}$;*Trp53*$^{-/-}$	102	salivary gland - lymphoma
A4678	M	*Rb1*$^{\Delta L/\Delta L}$;*Trp53*$^{-/-}$	99	thymic lymphoma
A4832	M	*Rb1*$^{\Delta L/\Delta L}$;*Trp53*$^{-/-}$	165	thymic lymphoma
A4850	F	*Rb1*$^{\Delta L/\Delta L}$;*Trp53*$^{-/-}$	111	thymic lymphoma
A4871	M	*Rb1*$^{\Delta L/\Delta L}$;*Trp53*$^{-/-}$	148	thymic lymphoma
A4891	M	*Rb1*$^{\Delta L/\Delta L}$;*Trp53*$^{-/-}$	137	liver & spleen - lymphoma, lung - carcinoma & lymphoma
A4892	F	*Rb1*$^{\Delta L/\Delta L}$;*Trp53*$^{-/-}$	95	thymic lymphoma
A5633	M	*Rb1*$^{\Delta L/\Delta L}$;*Trp53*$^{-/-}$	178	kidneys & lymph nodes - lymphoma
A5667	M	*Rb1*$^{\Delta L/\Delta L}$;*Trp53*$^{-/-}$	146	tumor - high grade sarcoma, thymic lymphoma
A6547	M	*Rb1*$^{\Delta L/\Delta L}$;*Trp53*$^{-/-}$	157	spleen - lymphoma
A6553	F	*Rb1*$^{\Delta L/\Delta L}$;*Trp53*$^{-/-}$	152	tumor - sarcoma
A7568	M	*Rb1*$^{\Delta L/\Delta L}$;*Trp53*$^{-/-}$	104	tumor - sarcoma
A6585	M	*Rb1*$^{\Delta L/\Delta L}$;*Trp53*$^{-/-}$	160	thymic lymphoma, lymph nodes - lymphoma
A6557	M	*Rb1*$^{\Delta L/\Delta L}$;*Trp53*$^{-/-}$	225	liver - adenocarcinoma & lymphoma, lymph nodes - sarcoma, spleen - lymphoma
A7000	M	*Rb1*$^{\Delta L/\Delta L}$;*Trp53*$^{-/-}$	127	tumor - sarcoma with lymphoma infiltration, liver - lymphoma, thymic lymphoma
A7047	M	*Rb1*$^{\Delta L/\Delta L}$;*Trp53*$^{-/-}$	133	tumor - sarcoma
A6946	M	*Rb1*$^{\Delta L/\Delta L}$;*Trp53*$^{-/-}$	101	tumor - sarcoma
A6968	F	*Rb1*$^{\Delta L/\Delta L}$;*Trp53*$^{-/-}$	172	spleen - lymphoma
A6985	M	*Rb1*$^{\Delta L/\Delta L}$;*Trp53*$^{-/-}$	102	thymic lymphoma, lung, kidneys & liver - lymphoma
A7504	M	*Rb1*$^{\Delta L/\Delta L}$;*Trp53*$^{-/-}$	97	thymic lymphoma, kidney, spleen & liver - lymphoma
A7516	F	*Rb1*$^{\Delta L/\Delta L}$;*Trp53*$^{-/-}$	100	tumor - sarcoma
A7540	F	*Rb1*$^{\Delta L/\Delta L}$;*Trp53*$^{-/-}$	147	tumor - squamous cell carcinoma, thymus - sarcoma
A7557	M	*Rb1*$^{\Delta L/\Delta L}$;*Trp53*$^{-/-}$	183	tumor - sarcoma
A7567	M	*Rb1*$^{\Delta L/\Delta L}$;*Trp53*$^{-/-}$	169	thymic lymphoma, thyroid, spleen & liver - lymphoma, tumor - lymphoma & sarcoma
A7568	M	*Rb1*$^{\Delta L/\Delta L}$;*Trp53*$^{-/-}$	104	tumor - sarcoma
A7598	F	*Rb1*$^{\Delta L/\Delta L}$;*Trp53*$^{-/-}$	155	high grade lymphoma throughout lymphatics, lymphoma encapsulating kidney, salivary gland & lymph node - lymphoma
A9714	M	*Rb1*$^{\Delta L/\Delta L}$;*Trp53*$^{-/-}$	182	heart, liver, spleen & lymph node - lymphoma, tumor & lungs - sarcoma & lymphoma
A9728	M	*Rb1*$^{\Delta L/\Delta L}$;*Trp53*$^{-/-}$	180	lymph node, spleen, pancreas & salivary gland - lymphoma, thymic lymphoma, lung- sarcoma, tumor - sarcoma
A9747	M	*Rb1*$^{\Delta L/\Delta L}$;*Trp53*$^{-/-}$	179	large intestine & colon - sarcoma
B2958	M	*Rb1*$^{\Delta L/\Delta L}$;*Trp53*$^{-/-}$	109	large intestine - sarcoma with some lymphoma
B2309	F	*Rb1*$^{\Delta L/\Delta L}$;*Trp53*$^{-/-}$	161	lymph node & spleen - lymphoma, thymus - sarcoma with some lymphoma
B2311	F	*Rb1*$^{\Delta L/\Delta L}$;*Trp53*$^{-/-}$	163	lymph node, salivary gland - lymphoma, tumor - sarcoma,ovary - lymphoma
B2330	F	*Rb1*$^{\Delta L/\Delta L}$;*Trp53*$^{-/-}$	114	liver - lymphoma, thymic lymphoma, spleen - lymphoma, tumor - lymphoma & sarcoma
B2386	M	*Rb1*$^{\Delta L/\Delta L}$;*Trp53*$^{-/-}$	181	tumor - sarcoma
B3854	M	*Rb1*$^{\Delta L/\Delta L}$;*Trp53*$^{-/-}$	155	thymic lymphoma, spleen & liver - lymphoma
B4699	M	*Rb1*$^{\Delta L/\Delta L}$;*Trp53*$^{-/-}$	139	tumor - sarcoma & lymphoma
B4931	F	*Rb1*$^{\Delta L/\Delta L}$;*Trp53*$^{-/-}$	113	tumor - sarcoma, kidney - sarcoma
B4920	F	*Rb1*$^{\Delta L/\Delta L}$;*Trp53*$^{-/-}$	77	liver - sarcoma, spleen - lymphoma, tumor - sarcoma

Appendix H Cont'd

Mouse	Sex	Genotype	# days lived	Histology/Necropsy results
A2986	M	*Trp53*$^{-/-}$	124	thymic lymphoma
A3306	M	*Trp53*$^{-/-}$	133	thymic lymphoma
A3323	F	*Trp53*$^{-/-}$	224	thymic lymphoma
A3328	M	*Trp53*$^{-/-}$	170	thymic lymphoma
A3332	M	*Trp53*$^{-/-}$	205	thymic lymphoma
A3358	M	*Trp53*$^{-/-}$	124	tumor - sarcoma (mesenchymal)
A3359	M	*Trp53*$^{-/-}$	100	thymic lymphoma
A3365	M	*Trp53*$^{-/-}$	142	tumor - sarcoma
A3374	M	*Trp53*$^{-/-}$	138	thymic lymphoma
A3379	M	*Trp53*$^{-/-}$	179	thymic lymphoma
A3381	M	*Trp53*$^{-/-}$	211	thymic lymphoma
A3382	F	*Trp53*$^{-/-}$	198	thymic lymphoma
A3385	M	*Trp53*$^{-/-}$	177	thymic lymphoma
A3387	F	*Trp53*$^{-/-}$	220	thymic lymphoma, ovary - lymphoma
A3388	M	*Trp53*$^{-/-}$	211	thymic lymphoma, spleen - lymphoma
A3392	M	*Trp53*$^{-/-}$	231	thymic lymphoma (poorly differentiated)
A4904	M	*Trp53*$^{-/-}$	218	thymic lymphoma
A4914	M	*Trp53*$^{-/-}$	220	thymic lymphoma, spleen - lymphoma
A4915	M	*Trp53*$^{-/-}$	169	thymic lymphoma, liver, kidney & spleen - lymphoma
A4938	F	*Trp53*$^{-/-}$	150	thymic lymphoma
A4941	F	*Trp53*$^{-/-}$	148	thymic lymphoma
A4948	M	*Trp53*$^{-/-}$	192	thymic lymphoma
A4957	M	*Trp53*$^{-/-}$	145	very aggressive thymic lymphoma
A4959	M	*Trp53*$^{-/-}$	163	thymic lymphoma
A4970	M	*Trp53*$^{-/-}$	130	thymic lymphoma
A4974	M	*Trp53*$^{-/-}$	251	thymic lymphoma
A4982	M	*Trp53*$^{-/-}$	163	tumor - high grade sarcoma & diffuse lymphoma
A4986	M	*Trp53*$^{-/-}$	113	thymic lymphoma
A4992	M	*Trp53*$^{-/-}$	116	thymic lymphoma
A4997	F	*Trp53*$^{-/-}$	179	thymic lymphoma
A8510	M	*Trp53*$^{-/-}$	96	thymic lymphoma, lymph node, spleen, kidney & liver - lymphoma
A8518	M	*Trp53*$^{-/-}$	93	thymic lymphoma, thyroid & salivary gland - lymphoma (poorly differentiated)
B2489	M	*Trp53*$^{-/-}$	233	thymic lymphoma, lung - lymphoma
B2493	M	*Trp53*$^{-/-}$	178	thymic lymphoma
B2495	F	*Trp53*$^{-/-}$	157	thymic lymphoma
A4493	M	*Rb1*$^{\Delta L/\Delta L}$;*Trp53*$^{+/-}$	362	tumor - high grade sarcoma
A4494	M	*Rb1*$^{\Delta L/\Delta L}$;*Trp53*$^{+/-}$	440	small cell lymphoma in lymph node, tumor - sarcoma
A4622	M	*Rb1*$^{\Delta L/\Delta L}$;*Trp53*$^{+/-}$	480	kidney & liver - lymphoma
A5604	M	*Rb1*$^{\Delta L/\Delta L}$;*Trp53*$^{+/-}$	449	lymphoma & sarcoma (poorly differentiated) - lymph node, liver - sarcoma
A5631	M	*Rb1*$^{\Delta L/\Delta L}$;*Trp53*$^{+/-}$	498	tumor - sarcoma
A5656	F	*Rb1*$^{\Delta L/\Delta L}$;*Trp53*$^{+/-}$	531	thymic lymphoma, spleen - lymphoma, tumor - sarcoma
A5674	F	*Rb1*$^{\Delta L/\Delta L}$;*Trp53*$^{+/-}$	233	lymph node & salivary gland - lymphoma
A5700	M	*Rb1*$^{\Delta L/\Delta L}$;*Trp53*$^{+/-}$	361	high grade spindle cell sarcoma, salivary gland - lymphoma
A6531	F	*Rb1*$^{\Delta L/\Delta L}$;*Trp53*$^{+/-}$	236	salivary gland, spleen & liver - sarcoma
A6540	M	*Rb1*$^{\Delta L/\Delta L}$;*Trp53*$^{+/-}$	451	tumor - sarcoma, lung - sarcoma
A6600	M	*Rb1*$^{\Delta L/\Delta L}$;*Trp53*$^{+/-}$	482	tumor - sarcoma, spleen - lymphoma
A6916	F	*Rb1*$^{\Delta L/\Delta L}$;*Trp53*$^{+/-}$	372	tumor - sarcoma, lymph node & spleen - lymphoma
A6999	F	*Rb1*$^{\Delta L/\Delta L}$;*Trp53*$^{+/-}$	398	tumor - sarcoma with some lymphoma
A7046	M	*Rb1*$^{\Delta L/\Delta L}$;*Trp53*$^{+/-}$	332	spindle cell carcinoma from wall of seminal vesicle
A7521	M	*Rb1*$^{\Delta L/\Delta L}$;*Trp53*$^{+/-}$	534	liver & kidney - lymphoma, spleen & lungs - sarcoma & lymphoma
A7528	F	*Rb1*$^{\Delta L/\Delta L}$;*Trp53*$^{+/-}$	414	tumor - sarcoma, colon - sarcoma
A7530	F	*Rb1*$^{\Delta L/\Delta L}$;*Trp53*$^{+/-}$	458	tumor - sarcoma & lymphoma
A7565	M	*Rb1*$^{\Delta L/\Delta L}$;*Trp53*$^{+/-}$	458	intestine - sarcoma with some lymphoma
A7573	M	*Rb1*$^{\Delta L/\Delta L}$;*Trp53*$^{+/-}$	250	salivary gland & lymph node - lymphoma
A7580	F	*Rb1*$^{\Delta L/\Delta L}$;*Trp53*$^{+/-}$	342	liver & spleen - lymphoma
A7581	F	*Rb1*$^{\Delta L/\Delta L}$;*Trp53*$^{+/-}$	184	lymph node - lymphoma
A7583	F	*Rb1*$^{\Delta L/\Delta L}$;*Trp53*$^{+/-}$	342	lymph node - lymphoma & sarcoma, spleen - lymphoma, liver - lymphoma & sarcoma
A8483	M	*Rb1*$^{\Delta L/\Delta L}$;*Trp53*$^{+/-}$	662	liver - sarcoma, spleen - lymphoma (poorly differentiated), tumor - sarcoma with some lymphoma
B4621	M	*Rb1*$^{\Delta L/\Delta L}$;*Trp53*$^{+/-}$	137	tumor - sarcoma, spleen - lymphoma

Appendix H Cont'd

Mouse	Sex	Genotype	# days lived	Histology/Necropsy results
A2936	M	*Trp53*$^{+/-}$	414	tumor - high grade sarcoma
A2941	M	*Trp53*$^{+/-}$	422	spleen - low grade hemangiosarcoma
A3380	M	*Trp53*$^{+/-}$	620	liver - lymphoma
A3384	M	*Trp53*$^{+/-}$	659	tumor - squamous cell carcinoma & lymphoma, seminal vesicles - lymphoma, seminal vesicles & salivary gland - lymphoma
A3398	M	*Trp53*$^{+/-}$	304	thymic lymphoma
A3399	F	*Trp53*$^{+/-}$	342	tumor - sarcoma
A4903	M	*Trp53*$^{+/-}$	389	thymic lymphoma
A4905	M	*Trp53*$^{+/-}$	726	kidney encapsulated with lymphoma, lungs - sarcoma, spleen - sarcoma, liver - sarcoma, seminal vesicles - sarcoma
A4909	F	*Trp53*$^{+/-}$	406	lymphoma (large cell, highly proliferative) in liver & spleen
A4910	F	*Trp53*$^{+/-}$	505	thymic lymphoma with sarcoma, liver, spleen, lymph node & thymus - lymphoma, spleen,liver & thymus - sarcoma
A4911	F	*Trp53*$^{+/-}$	612	tumor - sarcoma
A4918	F	*Trp53*$^{+/-}$	526	tumor - sarcoma with osteoid definition (osteosarcoma)
A4920	F	*Trp53*$^{+/-}$	567	hematopoetic lymphoma (infiltration into muscle, mesenchymal tumor), liver - lymphoma & sarcoma, ovary - sarcoma
A4935	M	*Trp53*$^{+/-}$	600	sarcoma invading pancreas & some lymphoma, lump - sarcoma, spleen - lymphoma, seminal vesicles - sarcoma
A4942	M	*Trp53*$^{+/-}$	408	large cell lymphoma in lymph node
A4943	M	*Trp53*$^{+/-}$	462	hemangiosarcoma in spleen & liver
A4944	M	*Trp53*$^{+/-}$	498	tumor - osteosarcoma
A4947	F	*Trp53*$^{+/-}$	537	spleen & liver - lymphoma
A4971	F	*Trp53*$^{+/-}$	494	tumor - sarcoma
A4980	M	*Trp53*$^{+/-}$	590	liver, kidney & spleen - lymphoma
A4985	F	*Trp53*$^{+/-}$	394	lymph node - lymphoma, spleen - lymphoma, liver - small amount of lymphoma
A4990	M	*Trp53*$^{+/-}$	588	kidney & spleen - lymphoma, liver - sarcoma, seminal vesicles - sarcoma
A4991	M	*Trp53*$^{+/-}$	484	seminal vesicles- sarcoma with lymphoma infiltration, lymph node - lymphoma
A4995	F	*Trp53*$^{+/-}$	137	liver - lymphoma & sarcoma
A4996	F	*Trp53*$^{+/-}$	515	uterus - spindle cell sarcoma, large & small tumor - lymphoma

Appendix I

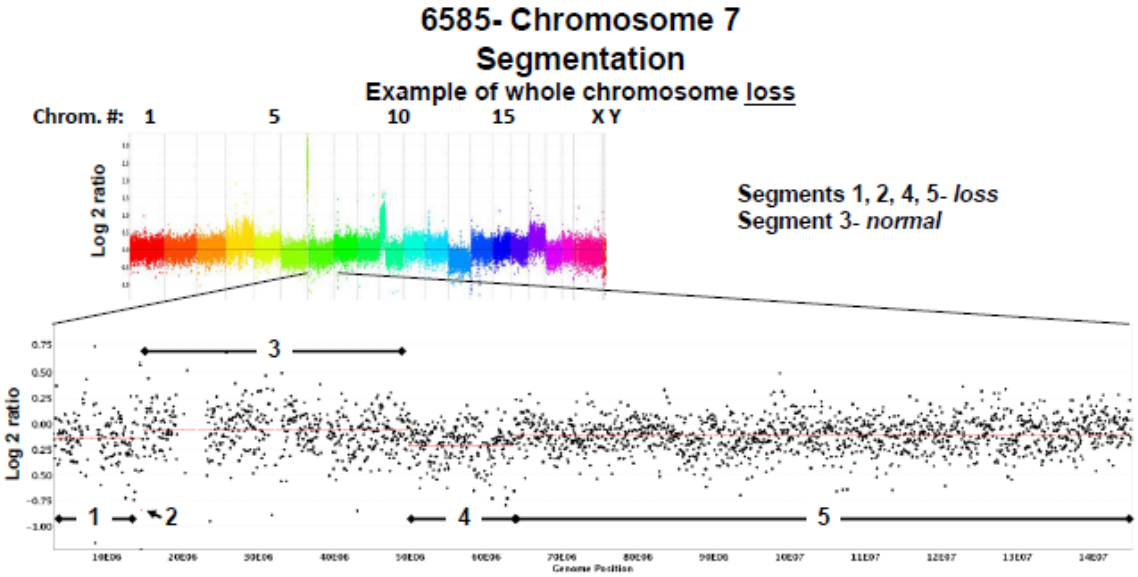

Appendix I: Example of a whole chromosome loss from aCGH data.

The graph depicts the Log2 ratio values versus chromosome number for the entire genome. Data points for each chromosome are a different color. This plot corresponds to the thymic lymphoma from mouse number 6585. The dot plot below is a close up view of the data points (black dots) and the segments they fall into (red lines) for chromosome 7. In some cases, segments are small enough to appear as red dots (see segment #2). After comparing the Log2 ratio values of the segments for chromosome 7 with the normal Log2 ratio range for this chromosome (see materials and methods), it was determined that segments 1, 2, 4 and 5 fell below the normal copy number range. The Log2 ratio value for segment 3 was within the normal range. Because the majority of chromosome 7 fell below the established normal range, and the only normal copy segment was a small internal portion, chromosome 7 from mouse number 6585 was scored as a whole chromosome loss.

Appendix J

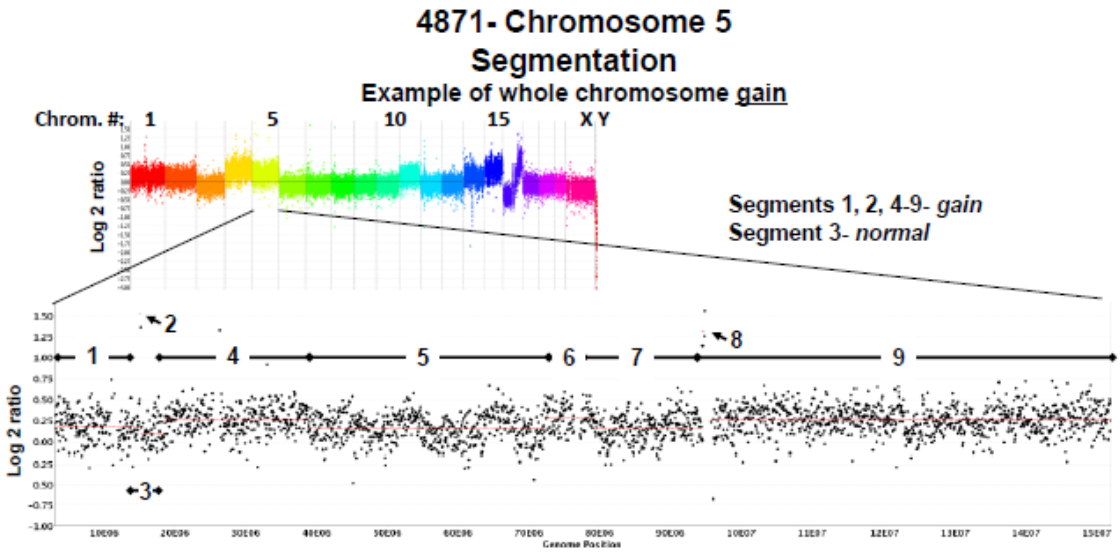

Appendix J: Example of a whole chromosome gain from aCGH data.

The upper graph depicts the Log2 ratio values for the entire genome versus chromosome number for the thymic lymphoma from mouse 4871. The dot plot below depicts the data points (black dots) and the segments they fall into (red lines) for chromosome 5. Again, in some cases, segments are small enough to appear as red dots (see segments #2 and #8). After examining the Log2 ratio values of the segments for chromosome 5, it was determined that segments 1, 2 and 4 -9 were above of the normal copy number range established from the chromosome 5 control hybridization (see materials and methods), while the Log2 ratio value for segment 3 fell within the normal range. Because the majority of chromosome 5 was above the established normal range, and the only segment that was normal was a small internal portion of the chromosome, chromosome 5 from mouse 4871 was scored as a whole chromosome gain.

Appendix K

Appendix K: Histology and necropsy data of *Rb1*$^{\Delta L/+}$; *Trp53*$^{-/-}$ mice in the Chapter 3 tumor study

Mouse	Sex	Genotype	# days lived	Histology/Necropsy Results
A4025	M	*Rb1*$^{\Delta L/+}$;*Trp53*$^{-/-}$	164	thymic lymphoma, tumor- unknown origin, tumor- unknown origin
A4053	M	*Rb1*$^{\Delta L/+}$;*Trp53*$^{-/-}$	116	tumor- unknown origin
A4247	M	*Rb1*$^{\Delta L/+}$;*Trp53*$^{-/-}$	119	thymic lymphoma
A4621	M	*Rb1*$^{\Delta L/+}$;*Trp53*$^{-/-}$	115	tumor- sarcoma
A4652	M	*Rb1*$^{\Delta L/+}$;*Trp53*$^{-/-}$	214	thymic lymphoma, metastasis (pancreas, liver)- lymphoma
A4675	M	*Rb1*$^{\Delta L/+}$;*Trp53*$^{-/-}$	110	tumor- sarcoma
A4679	M	*Rb1*$^{\Delta L/+}$;*Trp53*$^{-/-}$	104	tumor- sarcoma
A4685	M	*Rb1*$^{\Delta L/+}$;*Trp53*$^{-/-}$	231	thymic lymphoma
A4686	M	*Rb1*$^{\Delta L/+}$;*Trp53*$^{-/-}$	115	tumor- sarcoma
A4688	F	*Rb1*$^{\Delta L/+}$;*Trp53*$^{-/-}$	109	thymic lymphoma
A4689	F	*Rb1*$^{\Delta L/+}$;*Trp53*$^{-/-}$	91	thymic lymphoma
A4827	F	*Rb1*$^{\Delta L/+}$;*Trp53*$^{-/-}$	65	enlarged thymus
A4842	F	*Rb1*$^{\Delta L/+}$;*Trp53*$^{-/-}$	119	thymic lymphoma
A4858	M	*Rb1*$^{\Delta L/+}$;*Trp53*$^{-/-}$	166	thymic lymphoma
A4870	M	*Rb1*$^{\Delta L/+}$;*Trp53*$^{-/-}$	103	tumor- sarcoma
A4876	M	*Rb1*$^{\Delta L/+}$;*Trp53*$^{-/-}$	211	thymic lymphoma, tumor- sarcoma
A4877	M	*Rb1*$^{\Delta L/+}$;*Trp53*$^{-/-}$	179	thymic lymphoma
A5216	M	*Rb1*$^{\Delta L/+}$;*Trp53*$^{-/-}$	151	tumor- unknown origin
A5221	M	*Rb1*$^{\Delta L/+}$;*Trp53*$^{-/-}$	128	thymic lymphoma
A5269	M	*Rb1*$^{\Delta L/+}$;*Trp53*$^{-/-}$	156	thymic lymphoma
A5270	M	*Rb1*$^{\Delta L/+}$;*Trp53*$^{-/-}$	157	thymic lymphoma, metastasis (lump around forelimb)- carcinoma
A5601	M	*Rb1*$^{\Delta L/+}$;*Trp53*$^{-/-}$	211	thymic lymphoma, tumor- sarcoma
A5605	M	*Rb1*$^{\Delta L/+}$;*Trp53*$^{-/-}$	112	thymic lymphoma
A5606	M	*Rb1*$^{\Delta L/+}$;*Trp53*$^{-/-}$	138	thymic lymphoma, metastasis (kidney, liver, skin)- lymphoma
A5610	F	*Rb1*$^{\Delta L/+}$;*Trp53*$^{-/-}$	216	tumor- sarcoma
A5618	F	*Rb1*$^{\Delta L/+}$;*Trp53*$^{-/-}$	169	thymic lymphoma
A5651	M	*Rb1*$^{\Delta L/+}$;*Trp53*$^{-/-}$	189	thymic lymphoma
A5662	M	*Rb1*$^{\Delta L/+}$;*Trp53*$^{-/-}$	125	tumor- sarcoma
A5666	M	*Rb1*$^{\Delta L/+}$;*Trp53*$^{-/-}$	97	enlarged thymus
A5683	F	*Rb1*$^{\Delta L/+}$;*Trp53*$^{-/-}$	229	thymic lymphoma
A6502	M	*Rb1*$^{\Delta L/+}$;*Trp53*$^{-/-}$	116	tumor- sarcoma
A6504	F	*Rb1*$^{\Delta L/+}$;*Trp53*$^{-/-}$	161	thymic lymphoma
A6518	M	*Rb1*$^{\Delta L/+}$;*Trp53*$^{-/-}$	109	thymic lymphoma
A6527	M	*Rb1*$^{\Delta L/+}$;*Trp53*$^{-/-}$	115	thymic lymphoma
A6558	M	*Rb1*$^{\Delta L/+}$;*Trp53*$^{-/-}$	130	tumor- sarcoma
A6577	M	*Rb1*$^{\Delta L/+}$;*Trp53*$^{-/-}$	217	thymic lymphoma
A6590	M	*Rb1*$^{\Delta L/+}$;*Trp53*$^{-/-}$	227	thymic lymphoma
A6917	M	*Rb1*$^{\Delta L/+}$;*Trp53*$^{-/-}$	208	tumor- sarcoma
A6926	M	*Rb1*$^{\Delta L/+}$;*Trp53*$^{-/-}$	104	thymic lymphoma
A6927	M	*Rb1*$^{\Delta L/+}$;*Trp53*$^{-/-}$	108	thymic lymphoma
A6930	F	*Rb1*$^{\Delta L/+}$;*Trp53*$^{-/-}$	179	tumor- lymphoma, tumor- sarcoma
A6951	F	*Rb1*$^{\Delta L/+}$;*Trp53*$^{-/-}$	177	metastasis (lump above tail)- lymphoma, tumor- sarcoma
A6958	F	*Rb1*$^{\Delta L/+}$;*Trp53*$^{-/-}$	130	thymic lymphoma, tumor- sarcoma
A6981	F	*Rb1*$^{\Delta L/+}$;*Trp53*$^{-/-}$	224	tumor- unknown origin
A6983	M	*Rb1*$^{\Delta L/+}$;*Trp53*$^{-/-}$	207	tumor- sarcoma
A6988	M	*Rb1*$^{\Delta L/+}$;*Trp53*$^{-/-}$	149	tumor- sarcoma
A6992	F	*Rb1*$^{\Delta L/+}$;*Trp53*$^{-/-}$	197	thymic lymphoma
A7502	M	*Rb1*$^{\Delta L/+}$;*Trp53*$^{-/-}$	152	thymic lymphoma
A7568	M	*Rb1*$^{\Delta L/+}$;*Trp53*$^{-/-}$	104	tumor- sarcoma
A7577	M	*Rb1*$^{\Delta L/+}$;*Trp53*$^{-/-}$	129	metastasis (pancreas)- lymphoma
A7578	M	*Rb1*$^{\Delta L/+}$;*Trp53*$^{-/-}$	121	thymic lymphoma
A9727	M	*Rb1*$^{\Delta L/+}$;*Trp53*$^{-/-}$	149	thymic lymphoma

Appendix K Cont'd

Mouse	Sex	Genotype	# days lived	Histology/Necropsy Results
A9768	F	*Rb1*$^{\Delta L/+}$;*Trp53*$^{-/-}$	147	thymic lymphoma, metastasis (lung)- lymphoma, tumor- sarcoma
A9784	M	*Rb1*$^{\Delta L/+}$;*Trp53*$^{-/-}$	167	thymic lymphoma, metastasis (liver)- lymphoma
B439	F	*Rb1*$^{\Delta L/+}$;*Trp53*$^{-/-}$	98	thymic lymphoma

Appendix L

Appendix L: List of Plasmids.

Plasmid name	Genes encoded	Obtained/ Constructed by	Resistance	Stock #
pBOS-H2BGFP	H2BGFP fusion	BD Pharmingen	Ampicilin, Blasticidin	0448
pBABE-H2BGFP	H2BGFP fusion	Christina Isaac	Ampicillin, Puromycin	0449
pMr100	rDNA genes	Ingrid Grummt	Ampicillin	0664
pMr3'Eco	rDNA genes	Ingrid Grummt	Ampicillin	0665
pMr074	rDNA genes	Ingrid Grummt	Ampicillin	0666
shLuc	H2BGFP, shLuc	Courtney Coschi	Ampicillin	0608
sh63	H2BGFP, sh63	Courtney Coschi	Ampicillin	0607
sh64	H2BGFP, sh64	Courtney Coschi	Ampicillin	0606
sh66	H2BGFP, sh66	Courtney Coschi	Ampicillin	0605
sh67	H2BGFP, sh67	Courtney Coschi	Ampicillin	0604
pLMP	PGK, GFP, shLuc	Mike Golding	Puromycin	0487
pGIPz-V2LMM_91263	sh63	Open Biosystems	Ampicillin, Puromycin, Hygromycin, Zeomycin	0650
pGIPz-V2LMM_91264	sh64	Open Biosystems	Ampicillin, Puromycin, Hygromycin, Zeomycin	0651
pGIPz-V2LMM_91266	sh66	Open Biosystems	Ampicillin, Puromycin, Hygromycin, Zeomycin	0652
pGIPz-V2LMM_91267	sh67	Open Biosystems	Ampicillin, Puromycin, Hygromycin, Zeomycin	0653
pCR2.1-TOPO	LacZα fragment	Invitrogen	Ampicillin, Kanamycin	N/A
pCR2.1-TOPO-Trp53	Trp53	Courtney Coschi	Ampicillin, Kanamycin	0603
psCodon1-GST-RBLP	GST, RB	Fred Dick	Ampicillin	0526
pGST-E7	GST, E7	K. Munger	Ampicillin	0111
FUtdTW	Td Tomato, HIV psi pack	Greg Fonseca	Ampicillin	0654
PAX2	Gag_HIV (variant)	Greg Fonseca	Ampicillin	0655
PMD2G	vsv-G	Greg Fonseca	Ampicillin	0656
FUtdTW-H2BGFP	H2BGFP fusion	Courtney Coschi	Ampicillin	0657

Appendix L Cont'd

Plasmid name	**Genes encoded**	**Obtained/ Constructed by**	**Resistance**	**Stock #**
psCodon-GST-CAP-D3	GST CAP-D3 fusion	Courtney Coschi	Ampicillin	0658
psCodon-GST-CAP-D2	GST CAP-D2 fusion	Courtney Coschi	Ampicillin	0659
psCodon-GST-SMC2	GST SMC2 fusion	Courtney Coschi	Ampicillin	0660
pSTABY1.2	ccdA	Eurogentec	Ampicillin	0509
pHISTEV30a-CAP-D3	His CAP-D3 fusion	Courtney Coschi	Kanamycin	0661
pHISTEV30a-CAP-D2	His CAP-D2 fusion	Courtney Coschi	Kanamycin	0662
pHISTEV30a-SMC2	His SMC2 fusion	Courtney Coschi	Kanamycin	0663

Appendix M

Appendix M: PCR conditions for genotyping.

PCR Conditions- *Rb1*-ΔLXCXE

Master Mix per reaction:
0.5 µL $MgCl_2$
2 µL dNTPs
2 µL 10X PCR Buffer
0.25 µL of 20 µM FD-134 primer
0.25 µL of 20 µM FD-135 primer
12.5 µL water
0.5 µL Taq
2 µL DNA

Reaction Conditions:

Program SL01

94°C for 2:30
94°C for 0:20
60°C for 0:20
70°C for 2:00
Go to step #2, 29 times
72°C for 10:00
12°C until stopped

Expected Results:

Wild type band- 136 bp
Mutant band- 274 bp

PCR Conditions- *Trp53*

Master Mix per reaction:
1 µL $MgCl_2$
2.5 µL dNTPs
2.5 µL 10X PCR Buffer
0.62 µL of 20 µM AM3 primer
0.62 µL of 20 µM AM4 primer
0.27 µL of 20 µM neo-sense primer
0.27 µL of 20 µM neo-antisense primer
16.8 µL water
0.15 µL Taq
2 µL DNA

Reaction Conditions:

Program p53 new

94°C for 2:30
94°C for 0:30
58°C for 0:30
72°C for 1:10
Go to step #2, 29 times
72°C for 10:00
12°C until stopped

Expected Results:

Wild type band- 548 bp
Mutant band- 424 bp

Primers:

FD134- AGCTTCATACAGATAGTTGGG
FD135- CACAAATCCCCATACCTATG
AM3- ATAGGTCGGCGGTTCAT
AM4- CCCGAGTATCTGGAAGACAG
Neo-sense- GGAAGGGACTGGCTGCTATTG
Neo-antisense- CAATATCACGGGTAGCCAACG

Appendix N

Appendix N: List of antibodies.

Antibody name	Protein recognized	Species	Supplier	Category #	Application*
H2B	Histone H2B	Rabbit	Millipore	07-371	WB
GFP	GFP	Goat	Clontech	G095	WB
CAP-H	CAP-H	Rabbit	Gifted by Kyoko Yokomori, University of California at Irvine	N/A	WB
CAP-H2	CAP-H2	Rabbit	Gifted by Tatsuya Hirano, Riken, Japan	N/A	WB
SMC1	SMC1	Rabbit	Bethyl Laboratories	A300-055A	WB
G3-245	pRB	Mouse	BD Pharmingen	G3-245	WB, IP
C-20	BubR1	Goat	Santa Cruz Biotechnology Inc.	sc-16195	WB
PC10	PCNA	Mouse	Santa Cruz Biotechnology Inc.	sc-56	WB
141.2	MCM7	Mouse	Santa Cruz Biotechnology Inc.	sc-9966	WB
C-18	E2F3	Rabbit	Santa Cruz Biotechnology Inc.	sc-878	WB, IP
PG37	E2F3	Mouse	Millipore	05-551	WB, IP
Phospho histone H2A.X Ser 139	Histone variant H2A.X phosphorylated at serine 139	Mouse	Millipore	05-636	IP, IF
Phospho histone H2A.X Ser 139	Histone variant H2A.X phosphorylated at serine 139	Rabbit	Millipore	07-164	IP, IF
Anti-digoxigenin	Digoxigenin	Mouse	Roche	11 333062910	IF
C-20	E2F1	Rabbit	Santa Cruz Biotechnology Inc.	sc-193	IP
Donkey anti-goat HRP-conjugated	Goat IgG	Donkey	Santa Cruz Biotechnology Inc.	sc-2020	WB
Sheep anti-mouse HRP-conjugated	Mouse IgG	Sheep	GE	NA931V	WB
Donkey anti-rabbit HRP-conjugated	Rabbit IgG	Donkey	GE	NA934V	WB
Goat anti-mouse Alexa Fluor 488	Mouse IgG	Goat	Invitrogen	A11029	IF
Goat anti-rabbit Alexa fluor 594	Rabbit IgG	Goat	Invitrogen	A11012	IF

*WB: Western blot, IP: Immunoprecipitation, IF: Immunofluorescence

Appendix N Cont'd

Antibody name	Protein recognized	Species	Supplier	Category #	Application*
CAP-D3	CAP-D3	Rabbit	Courtney Coschi**	N/A	WB, IP
CAP-D2	CAP-D2	Rabbit	Courtney Coschi**	N/A	WB
SMC2	SMC2	Rabbit	Courtney Coschi**	N/A	WB

*WB: Western blot, IP: Immunoprecipitation, IF: Immunofluorescence
**See Appendix O for information on making these antibodies

Appendix O

Appendix O: Instructions for making and purifying anti-CAP-D3, -CAP-D2, -SMC2 antibodies.

GST- or His-tagged proteins (as indicated below) were generated. Rabbits were immunized at PTG Laboratories and immunogenicity was tested by ELISA using His- or GST-tagged proteins respectively. Non-purified test bleeds and production bleeds are stored at -80^{o}C in box 4-6.

Antibodies to **CAP-D3** were raised against a GST fusion protein containing amino acids 1243-1506 of mouse CAP-D3. A His-tagged version was created for ELISA (to test immunogenicity) and purification purposes. The CAP-D3 antibody was immunogenic to a titre of 1:1,000,000.

Antibodies to **CAP-D2** were raised against a GST fusion protein containing amino acids 943-1132 of mouse CAP-D2. A His-tagged version was created for ELISA (to test immunogenicity) and purification purposes. The CAP-D3 antibody was immunogenic to a titre of 1:10,000.

Antibodies to **SMC2** were raised against a His fusion protein containing amino acids 24-308 of mouse SMC2. A GST fusion version was created for ELISA (to test immunogenicity) and purification purposes. The CAP-D3 antibody was immunogenic to a titre of 1:1,000,000.

Antibodies were affinity purified according to the following protocols:

A) Reduce the peptide or protein to be coupled to the SulfoLink® column for antibody purification (Steps 1-5 of the Immobilized TCEP Disulfide Reducing Gel protocol for Reduction in Gravity Flow Columns (> 250µL samples); Cat # 77712 from Pierce).

1. Choose a column size (Poly-Prep® Chromatography Columns Cat# 731-1550 and Two-way stop cock Cat# 7328102 from Bio Rad Laboratories) appropriate for a volume of TCEP Disulfide Reducing Gel that is 2X the volume of the sample you are reducing.

Appendix O Cont'd

2. Ensure the TCEP gel is a homogeneous slurry and pipette the appropriate volume into the column. The slurry is 50% gel so 4X the sample volume gives a gel bed that is 2X the sample volume. **Do not let buffer drain below the top of the gel bed.

1. Wash the gel with two column volumes of water if desired.

2. Apply the peptide/protein to the column (Ex. 1mg peptide/mL gel bed) and allow the buffer to drip out the bottom until the entire sample has entered the gel bed. Incubate the peptide/protein with the gel bed according to criteria outlined in the Immobilized TCEP Disulfide Reducing Gel protocol (Cat # 77712 from Pierce).

3. Elute sample from the column with Coupling Buffer (recipe in the SulfoLink® Coupling Gel protocol; Cat # 20401 from Pierce) and collect fraction volumes appropriate to the column size prepared (Ex. 0.5-1mL fractions from a 2mL column to which 1mL of peptide/protein was applied).

4. Determine which fractions contain protein by checking absorbance at 280nm relative to a buffer blank (which ever buffer the peptide/protein was originally dissolved in).

B) Immobilize the peptide/protein to the SulfoLink® gel (Select steps are highlighted below from the SulfoLink® Coupling Gel protocol; Cat 20401 from Pierce).

1. Follow steps A, B, C and D from the Procedure for Immobilizing a Protein or Peptide Having Free Sulfhydryls in the SlufoLink® Coupling Gel protocol.

2. For step B1, look ahead to determine how much gel slurry you need for the amount of serum you will load (Ex. Loading 5mL of serum requires 5mL of gel bed and therefore 10mL of slurry).

3. For step B8, consider using the BCA or the Bradford assays to measure protein/peptide concentrations.

4. Stop before step D3 if you intend to continue with antibody purification. If you are storing the column for future antibody purification, continue with steps D3-D4. Finish by capping the column and storing it upright at 4^{o}C.

C) Affinity Purification of the Antibody- perform at 4^{o}C

1. If you are using an already coupled SulfoLink® column, follow step "E" of this protocol to regenerate the column for antibody purification. If you are proceeding directly from step "B", continue antibody purification with the following steps:

Appendix O Cont'd

2. Thaw production bleeds of the antibody at 4^{o}C. Centrifuge the serum to clear debris (Ex. SS34 rotor at 10,000 rpm for 10 min at 4^{o}C).

3. Apply 5mL of serum to the affinity column and run the column at 10mL/hr at 4^{o}C. Collect and save the flow through.

4. Wash the column with 20mL of 1X PBS at 20mL/hr.

5. Elute the antibody in two steps. **Ensure the gel bed does not run dry between elutions- after the first 8mLs has reached the top of the gel bed, add the next 8mLs as described in steps 6 and 7 below. After the second 8mLs has reached the top of the gel bed, add 20 mL of 1X PBS and let it flow through at a rate of 20mL/hr.

6. Elute in 8mL of 0.2M glycine-HCl pH 2.5 (150mg glycine, 0.82mL of 1N HCl, 9.2mL H_2O). Collect 1mL fractions into eppendorf tubes already containing 95µL of 1.5M Tris-HCl pH 8.8 to immediately neutralize each fraction to ~ pH 7.3.

7. Elute in another 8mL of 0.2M glycine-HCl pH 1.9 (150mg glycine, 1.58mL of 1N HCl, 8.4mL H_2O). Collect 1mL fractions into eppendorf tubes already containing 160µL of 1.5M Tris-HCl pH 8.8 to immediately neutralize each fraction to ~ pH 7.3.

8. While the 20mL of 1X PBS is flowing through the column (this washed out residual antibody/protein), check the absorbance of each fraction. This can be done by dotting ~ 50µL of Bradford Reagent on a swatch of Parafilm and adding 1-2µL of each eluted fraction to a dot. Fractions with eluted antibody will change the colour of the Bradford Reagent to blue.

9. Pool the fractions containing antibody and dialyze it in 4L of 1X PBS overnight at 4^{o}C. The following morning, determine the protein concentration of the antibody.

10. Store the antibody at 1µg/µL in 1X PBS with 10% glycerol and 0.05% sodium azide.

D) Regenerating and Storing the SulfoLink® Column

1. Wash the column with 20mL of 1X PBS.

2. Equilibrate the column with 10mL of degassed 1X PBS with 0.05% sodium azide (Storage Buffer).

3. Stop the gravity flow and add 2mL of storage buffer to the top of the column and store it upright at 4^{o}C.

Appendix O Cont'd

E) Regenerating the column for Antibody Purification

1. Remove the top cap of the column first to avoid drawing air into the gel bed, remove the bottom cap and allow the excess Storage Buffer to drain until it is level with the gel bed.

2. Equilibrate the column by washing it with 10mL of 1X PBS at 4^{o}C and proceed with step "C" of this protocol.

Curriculum Vitae

Courtney Heather Coschi

Education

PhD The University of Western Ontario Supervisor: Dr. Fred Dick	2013
BMSc; *with distinction* The University of Western Ontario Supervisor: Dr. Victor Han	2007

Fellowships and Awards

CIHR- Canada Graduate Scholarship; PhD	2010-2012
CIHR- Strategic Training Program; PhD	2009-2012
Drs. Madge and Charles Macklin Fellowship	2011
2010 Institute of Cancer Research Publication Prize	2011
Western Graduate Research Scholarship	2008-2012
Ontario Graduate Scholarship; PhD	2009-2010
CIHR- Strategic Training Program; MSc	2008-2009
NSERC- Canada Graduate Scholarship; MSc	2008-2009
Ontario Graduate Scholarship; MSc *declined*	2008-2009
Schulich Graduate Scholarship	2007-2008
Macromolecular Informatics Award	2007
Biochemistry Summer Studentship Award	2006
Continuing Entrance Scholarship	2003-2007
Queen Elizabeth II Aiming for the Top Scholarship	2003-2007

Publications

Coschi CH, Ishak C, Talluri S, Martens AL, Welch I, Dick FA. Haploinsufficiency of a pRB-E2F1-Condensin II complex causes genome instability and contributes to mesenchymal cancers. (*In preparation.*)

Coschi CH, Dick FA. Chromosome instability and deregulated proliferation: an unavoidable duo. (2012) Cell Mol Life Sci. **69(12):** 2009-24.

Coschi CH, Martens AL, Ritchie K, Francis SM, Chakrabarti S, Bérubé NG, Dick FA. Mitotic chromosome condensation mediated by the retinoblastoma protein is tumor suppressive. (2010) Genes Dev. **24(13):** 1351-63.

Reviewed in: *Nature. Aug 2010;* ***466(7310):*** *1051-52*
Nat Rev Cancer. Aug 2010; ***10(8):*** *536*
Nat Rev Mol Cell Biol. Aug 2010; ***11(8):*** *541*
Genes Dev. Jul 2010; ***24(13):*** *1329-33*

Francis SM, Bergsied J, Isaac CE, **Coschi CH**, Martens AL, Hojilla CV, Chakrabarti S, DiMattia GE, Khoka R, Wang JYJ, and Dick FA. A functional connection between pRB and TGF-β in growth inhibition and mammary gland development. (2009) Mol Cell Biol. **29(16):** 4455-66.

Presentations- International meetings (*denotes the presenter)

Mechanisms and Models of Cancer **August 2012**
Coschi CH*, Martens AL, Dick FA. Haploinsufficiency of the retinoblastoma protein compromises genome stability. Cold Spring Harbor Laboratory in NY. *Poster*

ICGEB DNA Tumor Virus Meeting **July 2011**
Coschi CH*. Martens AL. Ritchie K, Francis SM, Chakrabarti S, Bérubé NG, Dick FA. Mitotic chromosome condensation mediated by the retinoblastoma protein is tumor suppressive. *Talk*

Epigenetics, Eh! **May 2011**
Coschi CH*, Martens AL, Ritchie K, Francis SM, Chakrabarti S, Bérubé NG, Dick FA. Mitotic chromosome condensation mediated by the retinoblastoma protein is tumor suppressive. London, Ontario. *Poster*

The Cell Cycle **May 2010**
Coschi CH*, Martens AL, Ritchie K, Francis SM, Chakrabarti S, Bérubé NG, Dick FA. Mitotic chromosome condensation mediated by the retinoblastoma protein is tumor suppressive. Cold Spring Harbor Laboratory in NY. *Poster*

First International RB Meeting **November 2009**
Coschi CH*, Martens AL, Ritchie K, Bérubé NG, Dick FA. Investigating the role of the retinoblastoma protein in regulating heterochromatin and maintaining genome stability. Toronto, Ontario. *Poster*

Mechanisms and Models of Cancer **August 2008**
Francis S*****, **Coschi C**, Isaac C, Hojilla C, Bergsied J, Chakrabarti S, DiMattia G, Khoka R, Wang J, and Dick F. A Unique Connection between pRB and TGFβ in Mammary Gland Development. Cold Spring Harbour Laboratory in NY. *Poster*

Presentations- Institutional meetings (*denotes the presenter)

Oncology Research and Education Day **June 22, 2012**
Coschi CH*, Martens AL, Dick FA. Haploinsufficiency of the retinoblastoma protein compromises RB-mediated genome stability and tumor suppression. Oncology Research and Education Day Conference. *Poster*

Oncology Research and Education Day **June 17, 2011**
Coschi CH*, Martens AL, Ritchie K, Francis SM, Chakrabarti S, Bérubé NG, Dick FA. Mitotic chromosome condensation mediated by the retinoblastoma protein is tumor suppressive. Oncology Research and Education Day Conference. *Poster*

Oncology Research and Education Day **June 18, 2010**
Coschi CH*, Martens AL, Ritchie K, Francis SM, Chakrabarti S, Bérubé NG, Dick FA. Mitotic chromosome condensation mediated by the retinoblastoma protein is tumor suppressive. Oncology Research and Education Day Conference. *Talk*
Awarded- best talk

Margaret Moffat Research Day **March 31, 2010**
Coschi CH*, Martens AL, Ritchie K, Bérubé NG, Dick FA. Investigating the role of the retinoblastoma protein in regulating heterochromatin and maintaining genome stability. Toronto, Ontario. *Poster*
Awarded- best poster in category

Oncology Research and Education Day **June 12, 2009**
Coschi CH*, Martens AL, Dick FA. pRB regulation of pericentric heterochromatin during the cell division cycle. Oncology Research and Education Day Conference. *Poster*

Research and Professional Experience

Attend Gynecological Cancer Disease Site Team Meetings **January 2012 - present**
Victoria Hospital; London Health Sciences Centre. London, ON.

Speaker Selection Committee for the CaRTT program **2010 - 2011**
CaRTT- Cancer Research and Technology Transfer program
Victoria Research Labs.

Honors Thesis Student **September 2006 - April 2007**
The University of Western Ontario, Victoria Research Labs
Supervisor: Dr. Victor Han

Volunteer Undergraduate Student Researcher **September 2005 - August 2006**
The University of Western Ontario
Supervisor: Dr. Chris Brandl